Study on Earthquake Ground Motion Prediction and its Application to Structural Response of Bridge in Vietnam

October 2012

Waseda University

Graduate School of Creative Science and Engineering

Major in Civil and Environmental Engineering, Research on Structural Engineering

TRAN VIET HUNG

WASEDA UNIVERSITY

Study on Earthquake Ground Motion Prediction and its Application to Structural Response of Bridge in Vietnam

DISSERTATION

Submitted in partial fulfillment of the requirements for the degree of
Doctor of Engineering

October 2012

by

TRAN VIET HUNG

Study on Earthquake Ground Motion Prediction and its Application to Structural Response of Bridge in Vietnam

By

TRAN VIET HUNG

ACKNOWLEDGMENT

First of all, I would like to express my deepest appreciation to Professor Osamu Kiyomiya for his enthusiasm, generosity, support and patience with me, who led me to the earthquake engineering. Professor Kiyomiya is not only to teach and share his vast knowledge with me, but also he took cares my life during the course of my studies at Waseda University. It has been a privilege to work under the supervision of Professor Osamu Kiyomiya. It was an honor to be his student, and to be guided and directed by his passion and his wealth of knowledge. I will never forget the experiences interacting and discussing results with him during these past four years. His inspiration will guide me for many years.

I would like to thank the thesis committee members, Professor Masanori Hamada, Professor Teruhiko Yoda and Professor Mitsuyoshi Akiyama, for their carefully reviewing and useful suggestions.

I am extremely grateful to Associate Professor Tongxiang An for his efforts towards making this project a success and his involvement from the beginning of my research work and also for being part of the defense committee. It was an enjoyable experience to write a joint paper with him. I really appreciate his guidance and friendship during these past years.

I am also extremely grateful to all members of the Kiyomiya Laboratory of Waseda University, for a calm academic research environment they provided. I would like to thank Dr. Haiming He, for his kindness help during the first year of my research. I am also grateful to Secretary Mrs. Endo for her helping during these past years. I will always remember the friendship of many past and present students.

Financial support for this research was provided by the Yoshida Scholarship Foundation (YSF). I would like to thank YSF and YSF's staff for their support during in years of my research and has given me the opportunity to study in Japan. This support is gratefully acknowledged.

I would like to thank Professor Cao Dinh Trieu, Professor Nguyen Hong Phuong and Dr. Le Tu Son of the Vietnam Institute of Geophysics for their support regarding the Vietnam earthquake data, which is very important to complete my research. I am grateful to the assistance from all my friends. Besides, I would like to thank all colleagues in Division of

Urban Transport Work and Coastal Engineering, University of Transport and Communications, Vietnam.

Finally, my heartfelt thanks go to my family, especially my parent who forever encourages and supports me in silence, and provided me the opportunities of receiving a good education. A debt of love and gratitude is due to my wife, Phuong, for the long hours spent on this research rather than spending time with her; whose patience and understanding are the essential to the completion of this research program. Besides, I think that my wife also completed a big project, give birth our daughter, Linh, our great happiness. Without her love and constant support, I would not have finished my dissertation this soon.

Study on Earthquake Ground Motion Prediction and its Application to Structural Response of Bridge in Vietnam

By

TRAN VIET HUNG

Tectonically, northern Vietnam is located in the most seismically active region at the boundary between the Indochina and South China plates. Most of the main faults in northern Vietnam are strike-slip faults. This region is tectonically active, as demonstrated by the occurrence of moderate earthquakes in the countryside and adjacent areas. Earthquakes with magnitudes of 5.0 to 6.8 on the Richter scale were recorded during the 20-th century, including the Dien Bien earthquake (1935, M = 6.8 and 2001, M = 5.3), the Luc Yen earthquake (1953, 1954, M = 5.4), and the Tuan Giao earthquake (1983, M = 6.7). These earthquakes have occurred in northern Vietnam, and they are a mostly shallow crustal earthquake type. In 2005, a seismic network consisting of 24 broadband seismographs was deployed in Vietnam in a cooperative effort between the Vietnam Institute of Geophysics (*VIG*) and the Institute of Earth Sciences at Academia Sinica, Taiwan (*IESAS*). However, there are a limited number of ground motion records for strong earthquake events in Vietnam. Time history of ground motion was not mentioned for seismic design of the bridge in Vietnam, and Vietnam had not enough the observed ground motions to apply the seismic response analysis of structures. The characterizations of time histories of earthquake ground motion have considerably in the structural analysis, but it is unlikely those recordings of earthquake ground motion will be available for all sites. Therefore, studies on earthquake engineering are experiencing great challenges due to insufficient observed earthquake records in Vietnam.

Each structure will be most sensitive with frequencies near its natural frequency. Damage to a bridge thus depends on its properties and on the character of an earthquake ground motion, such as peak acceleration and velocity, duration, frequency, etc. Besides, evaluation on dynamic behaviour of bridge structure demands the representation of seismic action in terms of the acceleration time-histories (dynamic analysis) or a response spectrum (push-over analysis). It led to be necessary to reliable input seismic waves. The major goals in this study consist of the ground motion prediction and application to structural dynamic response analysis of bridges under seismic excitation. Therefore, this study addresses the problems of characterizing strong ground motion for computing the dynamic response of bridge structures to earthquakes in Vietnam.

The whole thesis consists of six chapters. In **Chapter 1**, we introduce the aim of this study consists of the literature reviews and a necessary to research. This chapter described a qualitative and quantitative comparative study of seismic design requirements in four specifications for bridge design; these are the specifications in Vietnam (*22TCN 272-05*), American (*AASHTO LRFD 1998* and *LRFESEIS-1, 2009*), Europe (*EC 8*), and Japan (*JRA-2002*). This comparative study includes the applicability and design objective of each code, and the response spectrum specified by each one. It also includes the effects of soil type in situ, the structural system of the bridge, the bridge utilization, and other factors affecting the analysis of seismic actions on bridges. The study discusses the differences and similarities between the codes under consideration. It has also shown that not only *JRA-2002* introduced the static and the dynamic analysis methods in detail, but also proposed seismic waveforms such as Level one and Level two earthquake ground motions (in here, Level one is earthquake ground motion with high probability of occurrence for the bridge service life, Level two is earthquake ground motion by a strong earthquake with low probability of occurrence for the bridge service life) for the different zones and soil conditions. Therefore, study on earthquake ground motion and its application for seismic design is really necessary and important for bridge design in Vietnam.

Chapter 2 introduces the historical earthquake, earthquake activities and records of earthquake in Vietnam. This chapter described that Vietnam lies in a low-to-moderate aseismic region in the world. The high probability of earthquakes almost concentrates in the magnitudes of 4.5 to 5.5 on the Richter scale. The earthquake magnitude with M = 5.8 is computed with 95% confidence interval for the mean. Besides, the previous studies also shown the earthquake occurred with a low probability and maximum earthquake of magnitude of M = 7.0 may occur in Vietnam in the future (e.g., *Phuong, 1991*; *VIG, 2005*; *Trieu et al., 2008; etc)*.

Given the different geology and earthquake activity, establishing a regional attenuation relationship is deemed important for the seismic design of structures. A new PGA attenuation relationship for northern Vietnam is established in **Chapter 3**. The ground motion attenuation relationship, which is used to estimate the ground maximum acceleration values for a seismic design, is very important for probabilistic seismic hazard analysis (*PSHA*). The attenuation of ground motion is represented and modeled using empirical attenuation equations of PGAs. This equation is related to the source/site parameters such as source magnitude, source distance, and site condition. Most of the relationships are developed based on widely distributed magnitudes, peak ground motions, distances, and source mechanisms acquired from many earthquakes. The current attenuation relationships have been developed for many countries and regions. Their relationships are not appropriate for seismic hazard analyses in Vietnam because it does not reflect local conditions. In particular, the relationship currently used does not consider any earthquake records obtained in Vietnam. Thus, this study

constructed a new attenuation relationship that considers Vietnamese conditions. This chapter presents a new equation in place of the relationship currently used in Vietnam for horizontal ground motion based on database sets compiled from strike-slip and shallow crustal earthquakes with magnitudes ranging from $3.0 \leq M_w \leq 6.9$ and source distances of up to 300 km for northern Vietnam. This new equation estimates the ground motion in terms of moment magnitude, distance and site conditions for strike-slip earthquakes. The equation is derived based on a regression analysis of earthquake records; in this study, the database consists of earthquake records from Japan, Vietnam and adjacent areas. This study also assume a few simple relationships, such as the relationship between M_w and M_s, the closest distance to the fault and the effects of shallow site conditions on the average shear-wave velocity in the upper 30 m (V_{s30}) to develop a comparison with existing relationships. The new equation for northern Vietnam corresponds better with other equations for near and far-field distances than the equations currently used for seismic design in Vietnam.

Chapter 4 uses new attenuation relationship in **Chapter 3** to quantify ground motion based on *PSHA*. This method is the most widely used approach for the determination of seismic design loads for engineering structures. The equations generally rely on the basic assumption that ground motion prediction equations (*GMPEs*) have been developed for other regions with similarly tectonic. The accelerograms obtained from small magnitude earthquakes can be used as the basis for predicting ground motions due to the larger magnitude events considered in seismic hazard analysis. Current seismological network is monitoring the earthquake events with magnitudes of more than 3.0 on the Richter scale in Vietnam. The study of tectonic stress field and dynamic-geometric characteristics of the faults is especially the importance for seismic assessment. However, these studies are very limited in Vietnam. The network of broadband seismograph stations has just established in recent years. Even though, the stochastic method was used to predict earthquake ground motion may occur in Vietnam based on continuously collected seismic data by Vietnam Institute of Geophysics (*VIG*) such as an earthquake catalogue from 114 to 2005 an earthquake record of Dien Bien and Tuan Giao earthquakes. When considering some seismic codes around the world, the contents of the seismic design for bridge are compared in order to find limited points in the current specification of bridge design in Vietnam. After that, the simulation of prediction ground motion based on the results from probabilistic seismic hazard analysis in Vietnam following to the Weibull extremely distribution is also discussed.

Chapter 4 also proposes the generation of artificial earthquake motion, which is one of the main objects of this study. Two techniques to predicting earthquake ground motion of physics-based models and stochastic models. Physics-models simulate ground motions by modeling the fault rupture, the resulting wave propagation, and the near-surface site amplification since they require precise information about the earthquake source, wave propagation path, and soil structure. However, that is difficult and computationally expensive

to produce simulations that cover the range of possible future earthquakes. Thus, the stochastic method is to be used to simulate ground motion with various epicenter distances from small earthquake events and insufficient strong earthquake data. *Boore (1983, 2003)*, *Atkinson and Somerville (1994)*, *Atkinson and Boore (2006)* and others have demonstrated the well-known stochastic approach. The studies were based on simple physical models of the earthquake process, wave propagation and are estimated by analyzing many seismograms. In contrast, this method is empirically calibrated approaches that directly simulate the ground motion instead modeling fault rupture, wave propagation, and site amplification. In general, this approach is computationally inexpensive, and is equally applicable to high and low frequencies. However, almost stochastic models are based on modified Gaussian white-noise processes; it is difficult to simulate the coherency in the low-frequency region and frequency non-stationary. Simulated ground motions are sometimes useful as input motions because unlike recorded motions they are not limited in a number and because their properties can be varied systematically to understand the impact of ground motion properties on structural response (*Yamamoto and Baker, 2011*).

Chapter 5 provides a brief generation of artificial ground motion procedures. The simulated waveforms were employed to synthesize seismogram of strong ground motion. The artificial waveforms of the target earthquake were performed based on the stochastic model. This method is very useful for prediction of the strong ground motion in a region without observed seismic waveforms. This purpose of the present work consists in the validation of stochastic method for generating artificial ground motion and determines a ground response spectrum due to moderate magnitude earthquakes from available historical earthquakes in Vietnam. The next step of this study proposes the seismic waves and response spectral acceleration spectrum for seismic design of the bridge that is corresponded to earthquake activities in Vietnam.

Regarding performance-based design, dynamic response analysis of bridges for various types of input ground motions is required. This analysis method using of a selected set of ground motion time-histories is available for nonlinear dynamic analysis of structures subjected to earthquakes. The most reliability method for determining, verifying the response of a designed structure to the design intensity is using on the time-history analysis. In addition, the dynamic response of a structure is predicted by time histories of earthquakes having a specified spectral acceleration at a given period. The prediction is often obtained by selecting ground motions that match a target response spectrum, and using those ground motions as input to dynamic analysis. Therefore, **Chapter 5** describes the dynamic response analysis method of a bridge and comparison of the seismic analysis of the bridge when applying predicted ground motions of this research. In this study, dynamic behaviour of a typical bridge model is investigated in **Chapter 5**.

Finally, **Chapter 6** gets the summary for the thesis, discussion of the results, conclusions,

and recommendations for future required studies. The research works on verification of dynamic response analysis for bridge design based on research on earthquake ground motion has been carried out in this study. The undertaken study has revealed that research on earthquake is necessary and interest to seismic design for bridge design is very important in Vietnam.

The great limitation of study is dataset, because strong earthquakes in Vietnam occurred with low frequency. Moreover, bridges are designed on an unstable ground such as across a fault, near-fault zone on a lateral spreading ground due to liquefaction, etc. It is necessary to research on ground motion within these conditions and to consider the interaction between the ground and the foundation structure. These are essential issues for further research.

This page intentionally left blank

TABLE OF CONTENTS

This page intentionally left blank

LIST OF TABLES

This page intentionally left blank

LIST OF FIGURES

CHAPTER 1

INTRODUCTION

1.1 INTRODUCTION

Bridge is one of the important components of transport infrastructure. When the bridges are located in the earthquake zone, they are necessary special interest. Recent strong earthquakes such as the 1995 Hyogo-Ken Nanbu Earthquake in Japan, the 1999 Chi-Chi Earthquake in Taiwan, the 2008 Sichuan Earthquake in China, the 2010 Chile Earthquake, caused the collapse of many buildings, bridges and other facilities of transport infrastructure. The bridges damage during an earthquake depending on the ground motion, site conditions, overall configuration, and specific details of the bridge. Most of the severe damage to bridge has taken one of the unseating of the superstructure at the in-span hinges or simple supports due to inadequate seat lengths or restraint; column brittle failure due to deficiencies in shear capacity and inadequate ductility; unique failures in complex structures.

Vietnam has not experienced any strong earthquake damages and historical large-scale earthquakes until now; in contrast, many small-scale earthquakes occurred in recent years. The seismic design for bridges was not adopted until former 90s of 20^{th} century through this region is located at a moderate seismic activity region (e.g., *VIG, 2005; Ngo et al., 2008*). Many transport work systems have been constructed, are underway and in planning are making to rapid progress corresponding to development of social and economical in Vietnam. Thus, it is necessary to have a seismic design code which suitable to earthquake activities, ground motion and local conditions in Vietnam.

This chapter reviews some causes of damages to bridge under seismic excitation; compares current seismic codes in case of dynamic analysis method of the bridge in Vietnam, Japan and other countries. Therefore, issues need to study for seismic design for highway bridges in Vietnam is then discussed.

1.1.1 Damages of bridges during earthquake

Lessons learned from the 1989 Loma Prieta earthquake, and 1995 Hyogo-Ken Nanbu (Kobe) earthquake are evident of influence to site conditions on bridges such as Cypress Viaduct in Oakland and Hanshin Expressway, respectively were relatively deep, alluvial

deposits and soft soil deposits amplified the bedrock ground motion. The locations of collapse of the Cypress Street Viaduct nearly coincided with zones of natural and artificial fill where ground shaking was likely to have been the strongest. It shows the significant influence of local site conditions, type of strong ground motion, and the subsequent increased vulnerability of bridges on soft soil sites (see **Fig. 1.1**). In the collapse of Hanshin Expressway, the site was directly above the fault rupture, resulting from ground motions having high horizontal and vertical ground accelerations as well as large velocity pulses. Near-fault ground motions can impose large deformation demands on yielding structures (see **Fig. 1.2**) (*Chen and Duan, 2003-2*). Shear failures of concrete bridge columns have occurred with these bridges. Inelastic state, shear failures may occur after flexural yielding by earthquake ground motion.

The influence of earthquake shaking also can induce superstructure movements that cause, they supported span to unseat. Unseating is very important in the short seating that was used common in the simple span bridges because unseating prevention devices are important to prevent collapse of a bridge system even when destructive damage occurs. These collapses are shown in **Figs. 1.3**, **1.4** and **1.5**.

Figure 1.1 Cypress Street viaduct collapsed during the 1989 Loma Prieta earthquake. (*Source: Wikimedia*)

Figure 1.2 Hanshin Expressway collapsed during the 1995 Kobe earthquake. (*Source: internet*).

Figure 1.3 The bridge collapsed during the 1999 Chi-Chi earthquake.
(*Source: http://whatiscivilengineering.csce.ca/structural_earthquakes.htm*)

Figure 1.4 A bridge collapsed in Santiago during the 2008 Sichuan earthquake.
(*Source: http://www.dailymail.co.uk*).

Figure 1.5 A bridge collapsed in Santiago during the 2010 Chile earthquake.
(*Source: AFP, REUTERS*).

Based on lessons learned from the past earthquakes, the prediction of earthquake magnitudes, ground motions of earthquake and application of them to seismic design for bridge has been improving and advancing. Thus, seismic design for highway bridges became to be regarded as an important problem in Vietnam because the natural disaster is very difficult early warning, especially, that is earthquake disaster.

1.1.2 Current seismic design for highway bridge

1.1.2.1 Introduction

Current specification for bridge design in Vietnam (called as *22TCN 272-05*) is based on the *AASHTO LRFD 1998*. The seismic design is a part of *22TCN 272-05* only. Besides, we have a specification for design of structures for earthquake resistance (called as *TCXDVN 375-2006*), which is based on the *EUROCODE 8*. The map of seismic zones is created in 2005 by the Vietnam Institute of Geophysics (*VIG*). Now, the seismic design specifications for highway bridges have been developed for many countries. These codes are *AASHTO LRFD* (most recently *LRFDSEIS-1*: *Guide Specifications for LRFD Seismic Bridge Design*, 1st edition with 2010 Interim Revisions), *EUROCODE 8* (*EC 8* or *EN1998*), the Japan Specification for Highway Bridge in 2002 (*JRA-2002*) and so on. In this chapter, some major parameters in those seismic codes, including the design seismic forces, the response modification factors, the zone classification, etc. will be introduced in detail. Besides, this chapter is also to review and study various parameters and other requirements to be revise seismic analysis method of bridges in Vietnam.

1.1.2.2 Brief of 22TCN 272-05

1.1.2.2.1 General

In *22TCN 272-05*, the seismic design is adopted. Some objects were modified according to Vietnam conditions. There is the map of an acceleration coefficient (see **Fig 1.6**) [referred to *TCXDVN 375-2006*], the seismic zones (classified into three seismic zones and shown in **Table 1.1**) [referred to *22TCN 272-05*], acceleration coefficients, *A*, (adopted 0.00 to 0.29 g) and so on. However, the concept of the structure analysis and seismic analysis took originally from *AASHTO LRFD 1998*. The methodology for seismic design is described in the *AASHTO LRFD* Specification. It incorporates many of the lessons learned from recent major earthquakes in California and elsewhere. Even though, the seismic maps with presentation of equal level lines of acceleration coefficients cover only the United States and are therefore, not appropriate to Vietnam conditions. This map was created by the Vietnam Institute of Geophysics to incorporate into the specification of bridge design as shown in **Fig 1.6**. The seismic zones are classified by acceleration coefficients (*A*) as shown **Table 1.1**.

1.1.2.2.2 Seismic response and design response spectra

When a structure responds to an applied large-scale earthquake load, the corresponding displacement may be large enough to induce nonlinear deformation. The response spectrum for elastic behavior is fairly different than those for nonlinear behavior. The equations and

provisions specified in the design codes based on entirely on elastic behavior analysis. The earthquake load shall be taken to be horizontal force effects determined by the product of the mass, the response modification factor, and the elastic seismic response coefficient, C_{sm}, for the m^{th} vibration mode. The elastic seismic response coefficient may be normalized using the ground acceleration coefficients (A) (see **Fig 1.7**) and the result plotted against the period of vibration. This coefficient is given as following equations:

$$C_{sm} = \frac{1,2AS}{T_m^{2/3}} \le 2,5A \qquad (T_m \le 4.0 \text{ s}) \qquad (1.1a)$$

$$C_{sm} = \frac{3AS}{T_m^{4/3}} \qquad (T_m > 4.0 \text{ s}) \qquad (1.1b)$$

and soil profiles type III, IV:

$$C_{sm} = A\left(0.8 + 4.0T_m\right) \qquad (T_m < 0.3 \text{ s}) \qquad (1.1c)$$

Where T_m is the period of the m^{th} vibration mode (s); A is the acceleration coefficient and it is determined in accordance with the map of seismic zones and maximum seismic intensity zone of Vietnam (referred to **Fig 1.6**) and, it was given by the Vietnam Institute of Geophysics and provided as contour for return period of 500 years. Maximum probable earthquake with a return period of around 2,500 years has to be considered with the critical bridges. S is the site coefficient as shown in **Table 1.2**.

The structure's period will render the bridge engineer idea obout the performance of the structure through the design response spectra. If the period is large, it is likely fall with the dominant displacement portion of the spectra and displacement of the structure will be large. The current industry practice, due largely the development of computer hardware and software, is to perform a multi-modal response spectrum analysis on the bridges. The displacement demands are then determined directly from the analysis results. It should be recognized that these values will be inherently conservative due to the nature of the design response spectra.

The four descriptive soil types are defined as follows:

+ Type I (S = 1.0): Rock of any characteristic or any stable deposit of sands, gravels, or stiff clays less than 60 m deep and overlying rock.

+ Type II (S = 1.2): Deep cohesion-less soil including any stable deposit of sands, gravels, or stiff clays greater than 60 m deep and overlying rock.

+ Type III (S = 1.5): Soft to medium stiff clay, sand, or other cohesion-less soil generally greater than 9 m deep.

+ Type IV (S = 2.0): Soft clays or silts greater than 12 m in depth.

The part of seismic design for bridge in the *22TCN-272-05* permit the designer to utilize a variety of methods for seismic analysis, from simple equivalent static analysis to complex nonlinear dynamic analysis. Depending on the seismic zone, geometry, and importance of the bridge, the following analysis methods may be used for seismic bridge design: for multi-span bridges, the minimum analysis requirements shall be as specified in **Table 1.3**.

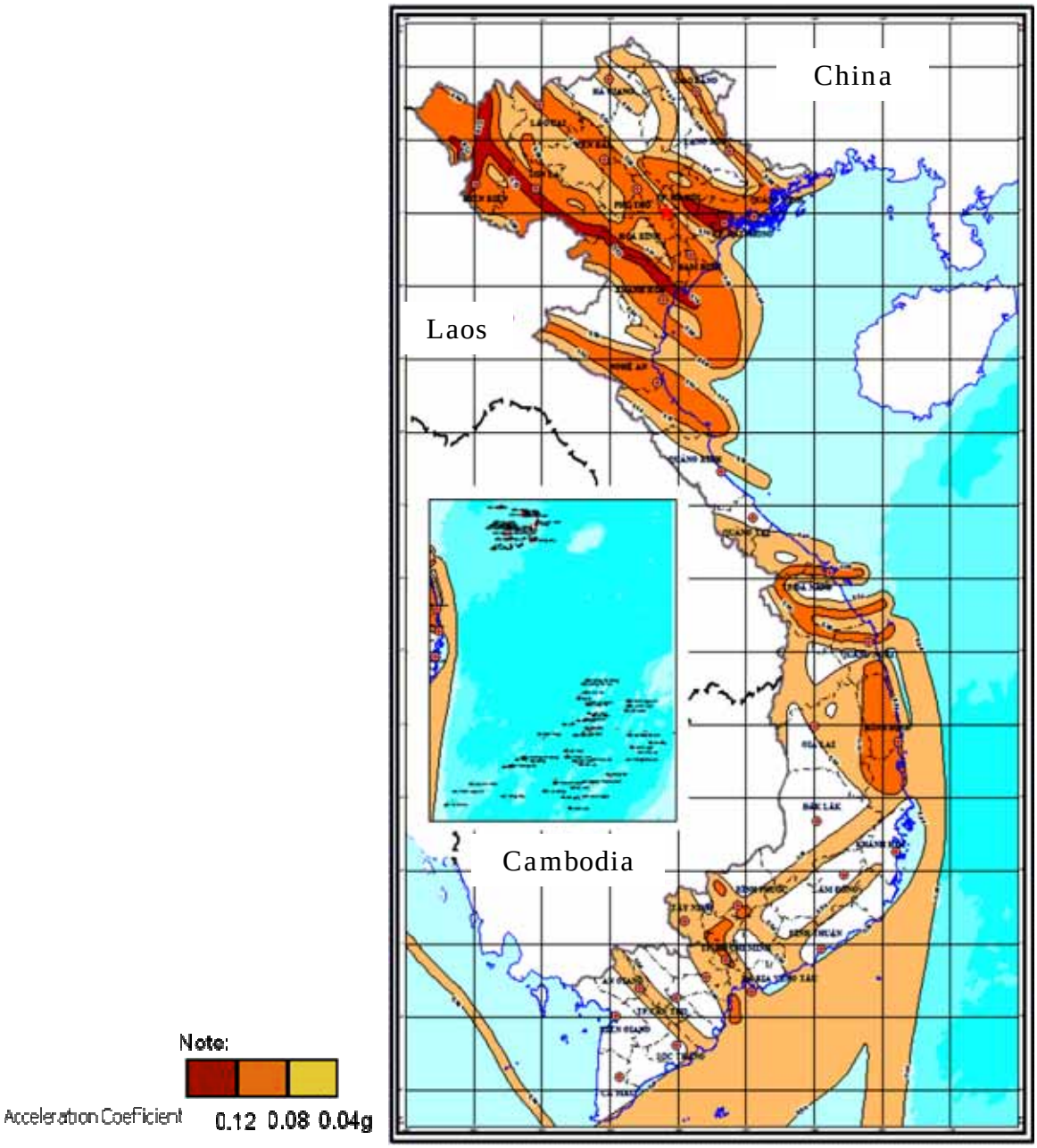

Figure 1.6 Ground acceleration zone map of Vietnam with return period about 500 years. (referred to *TCXDVN 375-2006*).

Table 1.1 Seismic zone classification (*22TCN 272-05*).

Acceleration Coefficient	Seismic zone	MSK - 64 class
$A \le 0.09$	1	Class ≤ 6.5
$0.09 < A \le 0.19$	2	6.5 < Class ≤ 7.5
$0.19 < A < 0.29$	3	7.5 < Class ≤ 8

Table 1.2 Site coefficients (*22TCN 272-05*).

Site coefficient	Soil profile type			
	I	II	III	IV
S	1.0	1.2	1.5	2.0

Table 1.3 Minimum analysis requirements for seismic effects (*22TCN 272-05*).

Seismic Zone	Single-Span Bridges	Multi-span Bridges					
		Other Bridges		Essential Bridges		Critical Bridges	
		Regular	Irregular	Regular	Irregular	Regular	Irregular
1	No seismic	*	*	*	*	*	*
2	analysis	SM/ UL	SM	SM/ UL	MM	MM	MM
3	required	SM/ UL	MM	MM	MM	MM	TH

Where: * is no seismic analysis required; UL is uniform load elastic method; SM is single-mode elastic method; MM is multimode elastic method; TH is time history method.

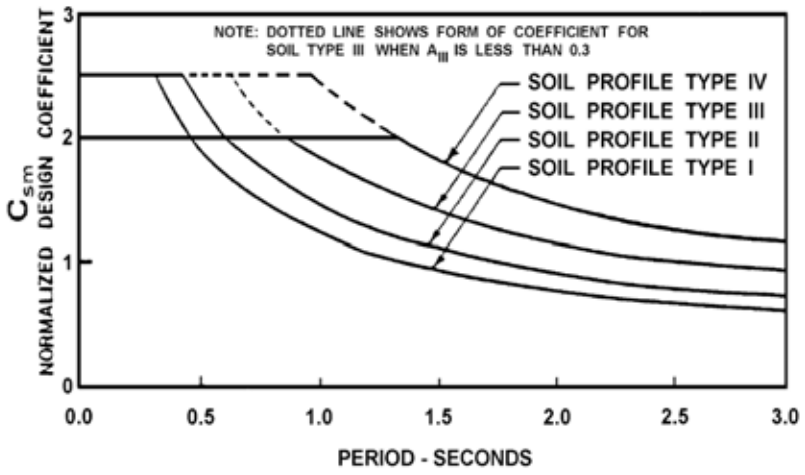

Figure 1.7 Design acceleration response spectra.

1.1.2.2.3 Elastic analysis procedure

When seismic forces are estimated from an elastic analysis, *22TCN 272-05* allow these forces to be reduced by appropriate response modification factors. These reduced forces can be used for design, but only if the substructure units are made ductile enough to undergo plastic hinge without suffering catastrophic failure. The philosophy is that seismic induced forces can only become large enough to produce plastic hinges. Once plastic hinges form, force can no longer be absorbed, but deflections will be large. The response modification factors are applied to forces and not displacements. Since the codes require the seismic analysis and ductile details and allow the use of response modification factors for typical bridge structures with seismicity higher than seismic zone 2 (i.e., acceleration coefficient $A >$ 0.09 g), it is apparent that plastic behavior would be a real possibility in these regions.

In this code has adopted a policy aiming at preventing catastrophic bearing seat loss failure if the elastic limit of the piers is exceeded. This policy requires that bearing seat lengths be constructed long enough to accommodate the maximum displacements obtained from an elastic analysis of the structure or those obtained from the beam seat length (N) shall be taken empirical displacement formula as follows:

$$Minimum\ seat\ width\ = f\ \times N \tag{1.2a}$$

$$N\ =\ \left(200+0.0017L+0.0067H\right)\left(1+0.000125S^2\right) \tag{1.2b}$$

Where f is factor based on seismic performance category and is expressed as a percentage; N is minimum support length measured normal to the centerline of bearing (mm); L is length of the bridge deck to the adjacent expansion joint, or to the end of the bridge deck; for hinges within a span, L shall be the sum of the distances to either side of the hinge; for single-span bridges, L equals the length of the bridge deck (mm); H is average height of columns supporting the bridge deck to the next expansion joint (mm) for columns and/or piers, column, or pier height (mm) for hinges within a span, average height of the adjacent two columns or piers (mm) for single-span bridges (mm); S is skew of support measured from line normal to span (degree).

The **Eq. (1.2b)** is taken originally from *AASHTO LRFD 1998* and it can often give displacement several times larger than those obtain from an elastic analysis.

1.1.2.3 Comparison between 22TCN-272-05 and some seismic design codes

1.1.2.3.1 Basis of seismic performance design

The *AASHTO LRFD 1998* classified seismic performance for two levels of a medium earthquake and a large earthquake. The effects of earthquake consider an only extreme event

limit state; the seismic performance required has interpreted as this limit state. The *AASHTO* has adopted two levels of design seismic force, but it is not clear to the engineers, whether or not, in practice. This extreme event limit state verified for both medium and large earthquake.

The first edition of AASHTO Guide Specifications for LRFD Seismic Bridge Design (called as *LRFDSEIS-1, 2009*) are intended to achieve minimal damage to bridges during moderate earthquake ground motions and to prevent collapse during a rare earthquake that results in high levels of ground shaking at the bridge site. A bridge designed to a performance level of no collapse can be expected to be unusable after liquefaction, for example, and geometric constraints would have no influence. However, because life safety is at the heart of the no collapse requirement, jurisdictions may consider establishing some geometric displacement limits for this performance level for important bridges or those with high average daily traffic.

The *EUROCODE 8* mentions to traffic functions after an earthquake. The limit states based on service limit state and ultimate limit state. This code applies these two limit states to post-earthquake service and post-earthquake safety respectively, with the former verified based on displacement and the latter verified based on the strength of a structure.

The *JRA-2002* required according to the importance of a bridge as a basis of seismic. Judging from bridge importance, two seismic performances, post-earthquake service and post-earthquake restoration (for a case of class B bridges), and post-earthquake service and post-earthquake safety (for a case of class A bridges) are combined with Level 1 and Level 2 earthquake motion, respectively. The two level ground motion as the moderate ground motions induced in the earthquakes with high probability to occur (Level 1 earthquake), and the intensive ground motions induced n the earthquakes with low probability to occur (Level 2 earthquake). The Level 1 earthquake provides the ground motions induced by the moderate earthquakes, and the ground motion considered in the elastic design method in the past for a long time is employed. For the Level 2 earthquake, two types of ground motions are considered. The first is the ground motion (called as Type I) which is induced in the inter plate-type earthquakes with the magnitude approximately 8.0. The second is the ground motion (called as Type II) developed in earthquakes with magnitude approximately 7.0 at very short distance.

The most important issue of the performance-based design code concept is that clear specifications of the requirements, which the designers are not allowed to select other methods, and the acceptable solutions, which the designers can select other methods with the necessary verification. The code structure of the Part V: Seismic Deign is shown in **Fig 1.8**. The both static and dynamic verification methods of the seismic performance as well as the evaluation methods of the strength and ductility capacity of the bridge members are placed as the verification methods and the acceptable solutions, which can be modified by the designers with the necessary verifications.

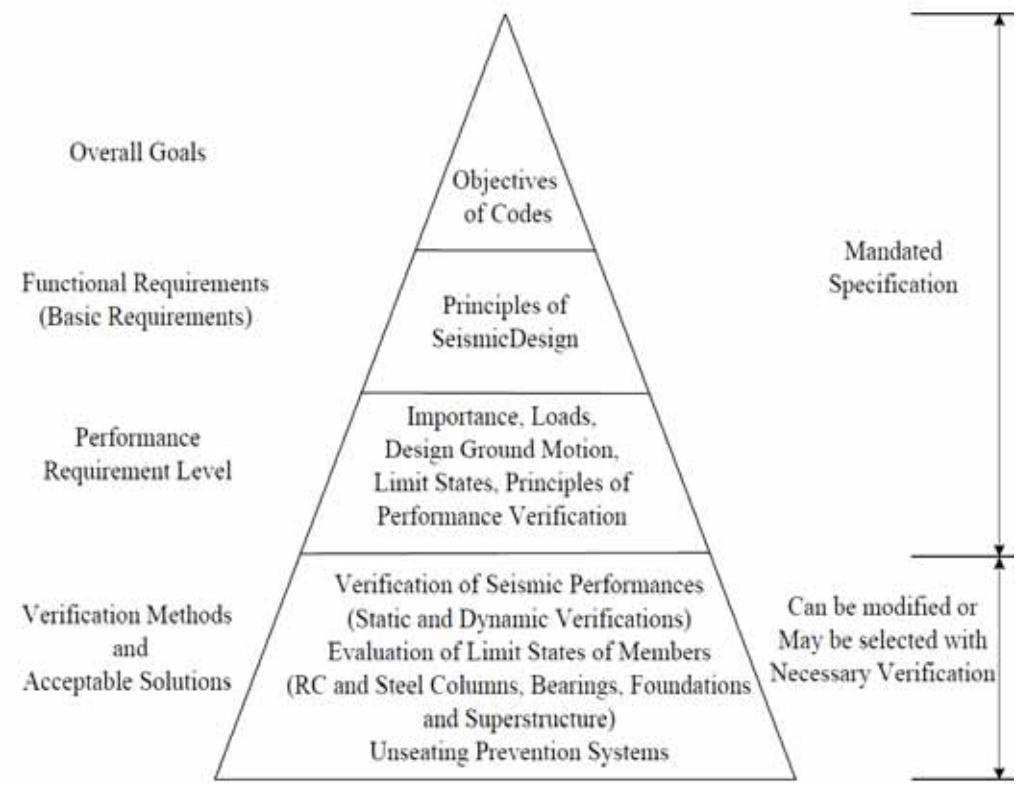

Figure 1.8 Code structure of *JRA-2002*, Part V: Seismic Design.
(*Kawashima and Unjoh,2004*).

1.1.2.3.2 Seismic performance zones

In *AASHTO LRFD 1998*, the *A*-acceleration coefficients for the construction sites based on the hazard map of the return period of 475 years are adopted (10% probability of exceedance during service life of 50 years). The seismic zone has been set as the classes from 1 to 4 based on the *A*-coefficients (the *22TCN 272-05* has been set as the classes from 1 to 3). The zone factors have been used to distinguish differences in the analysis methods, which have been provided on details of design method for bridge piers, abutments and foundations.

The seismic hazard is used in *LRFDSEIS-1 (2009)* corresponds to a 7 % probability of exceedance in 75 years. The precise definition used in the development of the ground shaking hazard maps is a 5 % probability of exceedance in 50 years. Thus, the return period used in development of the hazard maps is actually 975 years compared to that of a 7 % probability of exceedance in 75 years of 1,033 years. The *LRFDSEIS-1, 2009* is classified following to seismic design categories by the value of the design spectra acceleration coefficient at 1.0 second period (S_{D1}), that is the seismic hazard level is defined as a function of the magnitude of the ground surface shaking, and the factor of seismic design categories (*SDC*).

The *EUROCODE 8* has not set specific zone factors, but the design ground acceleration a_g

reflects the degree of earthquake risk in each nation. The *JRA-2002* has set the modifications factor C_Z is provided at value of 1.0, 0.85 and 0.7 according to the three zones categories.

1.1.2.3.3 Design earthquake motion and response spectrum

The *AASHTO LRFD 1998* has set two design earthquake levels. For medium earthquake, it is based on the *A*-coefficients for the return period of 475 years (10% probability of exceedance during design service life of 50 years). For a large earthquake, the maximum credible earthquake is considered to be an earthquake with the return period longer than the design earthquake: an earthquake with the return period of 2,500 years, for example.

In *LRFDSEIS-1 (2009)* the spectral response parameters shall be determined using the USGS/AASHTO Seismic hazard maps, produced by the U.S. Geological survey depicting the probabilistic ground motion and spectral response for a 7% probability of exceedance in 75 years. The seismic zone is provided by the site coefficients for the peak ground acceleration F_{pga}, short-period range F_a, and for the long-period range F_v. These values of F_{pga}, S_s, and S_1 depend on the peak ground acceleration (PGA), the spectral acceleration coefficient at 0.2 s obtained from the ground motion maps (S_s), and the spectral acceleration coefficient at 1.0 s obtained from the ground motion maps (S_1), respectively.

The *EUROCODE 8* defines a large earthquake as an earthquake with the return period of 475 years, but regarding a medium earthquake. It simply stipulates earthquake activity with an appropriate return period shall be evaluated.

The *JRA-2002* defines a medium and large design earthquake motion as earthquake motion with a high probability of occurring during the service life of a bridge and strong one with a low probability of occurring respectively, but does not stipulate specific return periods. *JRA-2002* do not use the acceleration coefficients, *A*, the response spectral acceleration base on acceleration strong motion records actually obtained at the ground surface such as the 1923 Kanto earthquake and the 1995 Hyogo-ken Nanbu earthquake. However, the earthquake ground motion shall be considered if the ground motion can be appropriately estimated based on the information on the historical earthquake, the location and detailed condition of the active faults, ground conditions, including the condition from the faults to the construction sites.

The response spectrum of these codes based on equation for the elastic response spectrums.

1.1.2.3.4 Ground classification

Ground classification in *AASHTO* and *EC 8* is the same depending on V_{S30}-value (the average shear-velocity down to 30 m). Ground types in *JRA-2002* shall be classified according with the ground characteristic value, T_G.

1.1.2.3.5 Load reduction factor

The *AASHTO LRFD 1998* and *EUROCODE 8* established reduction factor *R* or *q* based on the importance of a bridge and the type of a substructure as ways to reduce the elastic seismic force accounting for the non-linear response of ductile members.

The *LRFDSEIS-1, 2009* has not mentioned.

Regarding to *JRA-2002*, the force reduction factor (C_S) shall be determined with considerations of mechanical properties of structural members. The force reduction factor is obtained by modifying the design horizontal seismic coefficient with a modification factor when the structure system consisting of a single substructure and its supporting superstructure part is replaced by a single mass point vibration system in order to obtain the approximate non-linear response value based on the property of energy conservation.

1.1.2.3.6 Analytical procedures

For the *AASHTO LRFD 1998*, the analysis method requirements are the uniform loads elastic method, single-mode elastic method, multimode elastic method and time history method.

For the *EUROCODE 8*, the reference method of analysis is the modal response spectrum analysis. Lateral force static analysis is considered a simplification permitted when the structure complies with particular simplicity and regularity requirements, and the fundamental mode is expected to be dominant in the response. Nonlinear analysis, whether static pushover or in the time domain, is possible but never compulsory.

For the *LRFDSEIS-1*, 2009 equivalent static analysis and linear elastic dynamic analysis are appropriate analytical tools for estimating the displacement demands for normal bridges. Nonlinear time history should be used for critical or essential.

According to outline of requirements of three codes shows that these codes concentrate almost on static method. However, the *JRA-2002* differs to the above codes. The verification methods are based on the static analysis and dynamic analysis.

The plastic region is expected in the verification of seismic performance in these seismic codes. A simplifying assumption used when calculating plastic deformations of columns is that the plastic curvature is constant over the analytical plastic hinge length, L_p. The plastic displacement of an equivalent member from the point of the maximum moment to the point of contra flexure shall be determined on the basic of the plastic rotation (*LRFDSEIS-1, 2009*). Besides, these codes also required the seating length that prevents catastrophic seating length loss failure if the piers exceed the elastic limit.

1.1.3 Remarks

This section presented the outline of the seismic design specifications in Vietnam, the United States, Japan, and Europe. A summary of the principal items in other codes has been compared in this study as shown in **Table 1.4**. The comparison of everyone has been reviewed in section **1.1.2.3**. An earthquake has researched in detail in the countries which strong earthquake frequently occurred such as earthquake parameters of ground motion, acceleration spectrum, seismic waveforms, etc. Hence, they propose the requirements of seismic design base on design theory, earthquake levels of each country.

The design methods adopted by the codes observed to include LRFD, LSD and PBSD concept. Almost verification methods of seismic design codes are the static methods. But *JRA-2002* revised fully both static and dynamic method. The applicability of the dynamic analysis is much widened, and the detailed verification method for the dynamic analysis is specified, and provided seismic waveforms based on earthquake levels and ground types. Two earthquake level design concept is used and the design earth quake ground motion with high probability to occur and the design earthquake ground motion with high intensity and low probability to occur is adopted in *JRA-2002*. Regarding importance catalogue, the *JRA-2002* reflects importance in differences in seismic performance. But in the other codes, it is referred to differences in the value of design seismic forces.

The *JRA-2002* actually provides for the performance of two design levels while the other codes require verifications against a moderate earthquake and large earthquake. Two level earthquakes design method may more suitable than one level earthquake.

The target point of the *JRA-2002* is to be based on the performance-based design concept and to enhance the durability of bridge structures for a long-term use, as well as the inclusion of the improved knowledge on the bridge design and construction methods. It is expected to have the circumstances to employ the new ideas on the materials, structures and constructions methods to construct safer, more durable and more cost-effective bridges in the future (*Kawashima and Unjoh, 2004*).

Thus, the characteristics of earthquake in Vietnam are important for researching, especially seismic waveforms, acceleration spectrum for considering a dynamic response analysis of the bridge in Vietnam. In the future, seismic design specification of bridge is necessary revised based on the performance-based design code concept for the purpose to respond to the international harmonization of design codes and the flexible employment of new structures and new construction methods. The performance-based design code concept is that the necessary performance requirements and the verification policies are clearly specified.

1.2 GOAL OF RESEARCH

Tectonically, northern Vietnam is located in the most seismically active region at the boundary between the Indochina and South China plates. Most of the main faults in northern Vietnam are strike-slip faults. This region is tectonically active, as demonstrated by the occurrence of moderate earthquakes in the countryside and adjacent areas. Earthquakes with magnitudes of 5.0 to 6.8 on the Richter scale were recorded during the 20th century, including the Dien Bien earthquake (1935, M = 6.8 and 2001, M = 5.3), the Luc Yen earthquake (1953, 1954, M = 5.4), and the Tuan Giao earthquake (1983, M = 6.7). These earthquakes have occurred in northern Vietnam, and they are a mostly shallow crustal earthquake type. In 2005, a seismic network consisting of 24 broadband seismographs was deployed in Vietnam in a cooperative effort between the Vietnam Institute of Geophysics (*VIG*) and the Institute of Earth Sciences at Academia Sinica, Taiwan (*IESAS*). However, there are a limited number of ground motion records for strong earthquake events in Vietnam. Time history of ground motion was not mentioned for seismic design of the bridge in Vietnam, and Vietnam had not enough the observed ground motions to apply the seismic response analysis of structures. The characterizations of time histories of earthquake ground motion have considerably in the structural analysis, but it is unlikely those recordings of earthquake ground motion will be available for all sites. Therefore, studies on earthquake engineering are experiencing great challenges due to insufficient observed earthquake records in Vietnam.

Generally, each structure will be most sensitive with frequencies near its natural frequency. Damage to a bridge thus depends on its properties and on the character of an earthquake ground motion, such as peak acceleration and velocity, duration, frequency, etc. Besides, evaluation on dynamic behaviour of bridge structure demands the representation of seismic action in terms of the acceleration time-histories (dynamic analysis) or a response spectrum (pushover analysis). It led to be necessary to reliable input seismic waves. In order to obtain ground motion for a particular analysis condition, ground motion scaling and spectral matching are used to adjust recorded ground motion and make them with representative of the target analysis condition. This study selected a data set of simulated ground motions, a functional form for the attenuation equation, and then be used to determine regression coefficients for developing a new ground motion attenuation relationship based on actual empirical data from seismically active regions. It also proposes the new ground motion attenuation relationships for given project sites in low seismicity regions use as input to seismic hazard analysis.

This study illustrated the ground motion prediction, which focused on constructing a stochastic ground motion model and application to structural dynamic response analysis of bridges using the resulting simulated ground motions. This simulation based on probabilistic seismic hazard assessments through the development of a new PGA attenuation relationship

for northern Vietnam. It is often necessary to use ground motion simulation approaches, such as the stochastic point-source model. Therefore, this study addresses the problems of characterizing strong ground motion for computing the dynamic response of bridge structures to earthquakes in Vietnam.

This dissertation will address the following issues

① Probabilistic seismic hazard assessment.

- Propose the new attenuation relationship of earthquake ground motion.
- Probabilistic hazard analysis.

② Propose the new response acceleration spectrum.

③ Generate the time-history waves.

④ Application of proposed waves in dynamic response analysis of a bridge to verify the seismic response of a bridge while it was designed by a static method according to the current Vietnam code.

1.3 PROCEDURE FOR RESEARCH

This dissertation is carried out following the next procedure.

① Investigation of the damages of the bridges due to the past earthquakes

Damage to bridge structures occurred in the recent earthquakes. They are evident of influence to site condition, near-fault ground motion, modern of bridge structural, etc. on the damage of bridges. Base on lessons learned from the past earthquake, the prediction of earthquake ground motions and application of them to seismic design for bridge is necessary.

② Review of current seismic design for highway bridge

The specifications in Vietnam (*22TCN 272-05*), America (*AASHTO LRFD 1998* and *LRFESEIS-1, 2009*), Europe (*EC 8*), and Japan (*JRA-2002*) are reviewed and compared. It has also shown that not only *JRA-2002* introduced both the static and dynamic analysis method in detail, but also proposed seismic waveforms such as *Level one* and *Level two* earthquake ground motions (in here, *Level one* is earthquake ground motion with high probability of occurrence for the bridge service life, *Level two* is earthquake ground motion by a strong earthquake with low probability of occurrence for the bridge service life) for the different zones and soil conditions. Therefore, it is necessary to research on earthquake ground motion and application for seismic design of the bridge in Vietnam.

③ Introduction of historical earthquake activities

The records of earthquake have shown Vietnam lies in a low-to-moderate aseismic region in the world. The high probability of earthquakes almost concentrates in magnitudes of 4.5 to

5.5. The earthquake magnitude of M = 5.8 is computed with 95% confidence interval for the mean. Besides, the previous studies also shown the earthquake occurred with a low probability and maximum earthquake of magnitude of M = 7.0 may occur in Vietnam in the future (e.g., *Phuong 1991; VIG, 2005; Trieu et al., 2008)*.

④ Proposing the new PGA attenuation relationship

The relationships have been developing with widely distributed magnitudes, strong ground motions, distance and source mechanism acquired from many strong earthquakes for many countries and regions in the world, but the developments of current attenuation relationships are not appropriate for using of seismic hazard analysis in Vietnam because the characteristics of earthquakes in Vietnam do not reflect in these current relationships. Especially, no earthquake records obtained in Vietnam were considered in these current relationships. To solve these problems, this study needs to rebuild the attenuation relationship considered various Vietnam conditions. This study has derived the PGA attenuation relationship for northern Vietnam using data set from Japan, Vietnam and adjacent regions in place of old current relationship in Vietnam. The new relation is developed for shallow strike-slip earthquake by a regression technique with the range of magnitudes of $3.0 \leq M_w \leq 6.9$ and source distances up to 300 km. In this relationship, V_{s30} is adopted to estimate of ground motion with linear site effects.

⑤ Probabilistic seismic hazard assessment (*PSHA*)

PSHA is the most widely used approach for the determination of seismic design loads for engineering structures. The probabilistic seismic hazard haves analyzed by the Weibull extremely distribution. The new PGA attenuation relationship is used.

⑥ Generation of artificial earthquake ground motion

A stochastic method is to be used to simulate ground motion with various epicenter distances from small earthquake events and insufficient strong earthquake data as in Vietnam. This approach is in general computationally inexpensive, and is equally applicable to high and low frequencies. This study provided a brief generation of artificial ground motion procedures. The simulated waveforms were employed to synthesize seismogram of strong ground motion. The artificial waveforms of the target earthquake were performed based on the stochastic model. This purpose of the present work consists in the validation of stochastic method for generating artificial earthquake ground motions and determines a ground response spectrum due to moderate magnitude earthquakes from available historical earthquakes in Vietnam.

⑦ Verification of the applicability of the proposed earthquake ground motion to frame PC bridge

This study described the dynamic response analysis method of a bridge and comparison of

the seismic analysis of the bridge when applying predicted ground motions of this research. In this study, dynamic behaviour of the bridge is investigated.

⑧ Summary and conclusions

The research findings and recommendations are described.

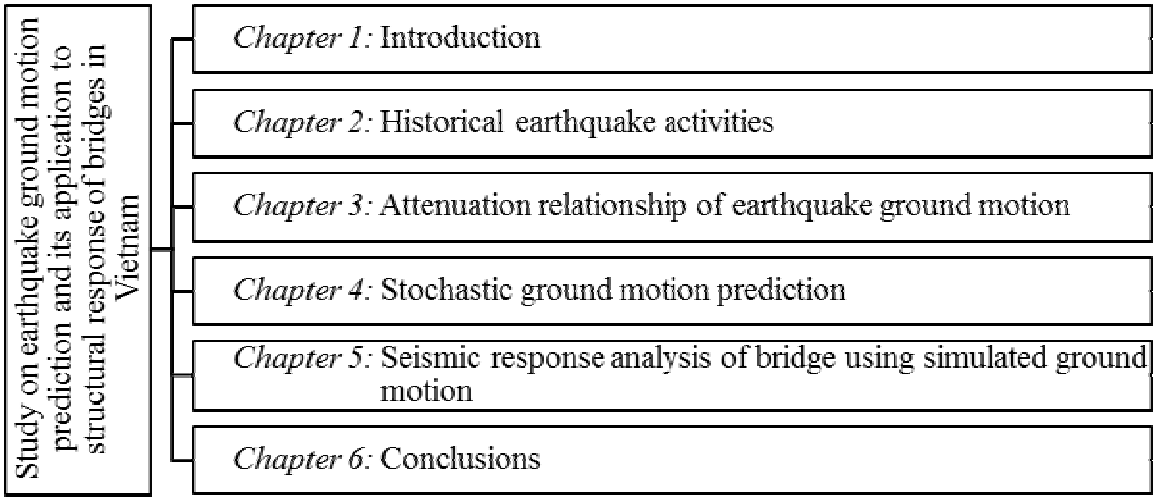

Figure 1.9 The major chapters of this dissertation.

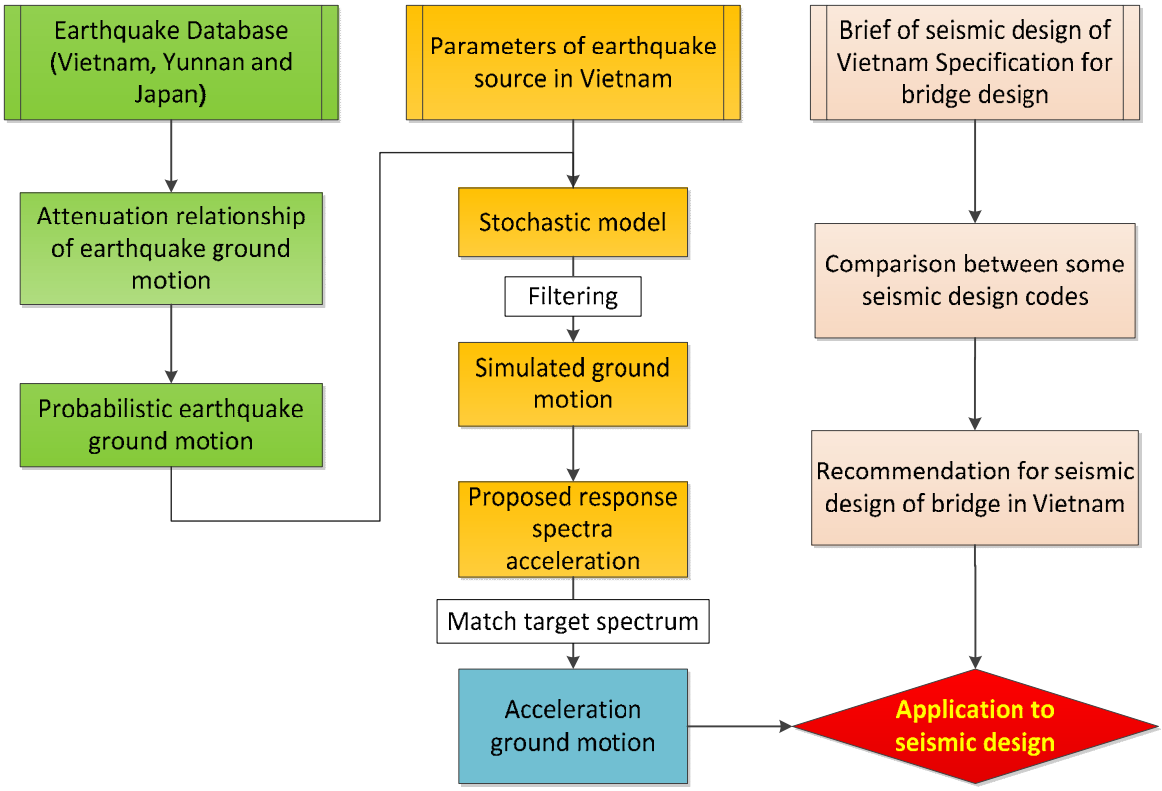

Figure 1.10 Outline diagram of this research.

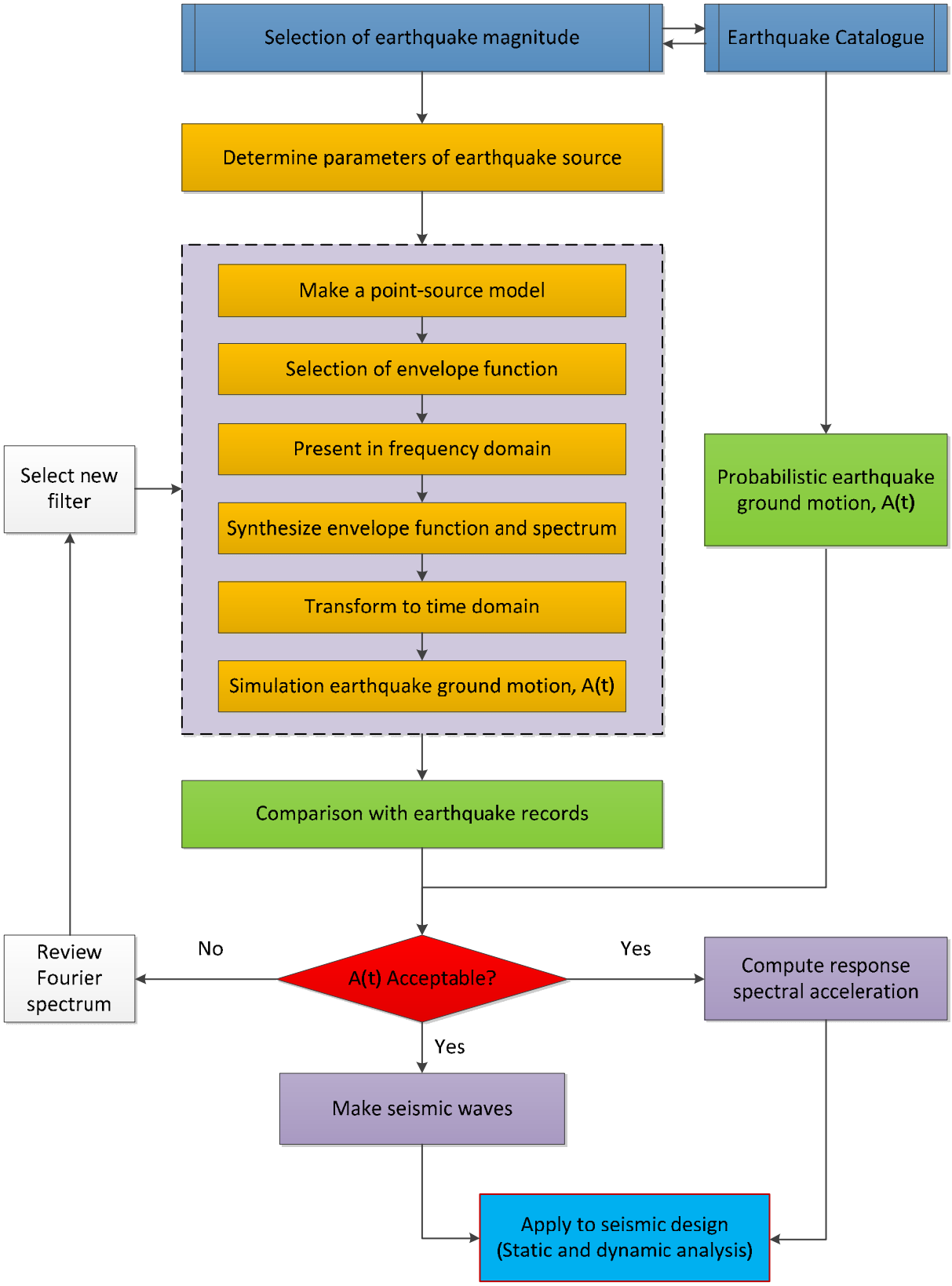

Figure 1.11 A flow chart for simulation of earthquake ground motion.

Table 1.4 Comparison of seismic performance for bridge in various countries.

No.	Code	AASHTO LRFD 1998	LRFDSEIS-1, 2009	22TCN272-05	EUROCODE 8	JRA-2002
1	Name of code	AASHTO LRFD Bridge design Specification (1998, 2nd Edition)	AASHTO Guide Specification for LRFD Seismic Bridge Design (2009, 1nd Edition)	Specification for Bridge design (2005, 1nd Edition)	Design of structures for earthquake resistance Part 1: General rules, seismic actions and rules for buildings Part 2: Seismic design of bridges	Japan Road Association, 2002 (JRA-2002), Specifications for highway bridges, Part V: Seismic design
2	Structure category	Highway bridge	Highway bridge	Highway bridge	Civil engineering and building engineering	Highway bridge
3	Design method	LRFD: Load resistance factor design	LRFD: Load resistance factor design	LRFD: Load resistance factor design	LSD: Limit state design	PBSD: Performance based seismic design code concept
4	Basis of seismic design	For medium earthquake: it shall remain undamaged by resisting within the elastic range of members. For large earthquake: all or parts of a bridge shall not fail. Locations forecast to be damaged shall be ones whose damage can be detected, can be easily approached, and can be easily inspected and repaired	These bridges are seismically designed so that inelastic deformation (damage) intentionally occurs in columns in order that the damage can be readily inspected and repaired after an earthquake. Capacity design procedures are used to prevent damage from occurring in foundations and beams of bents and in the connections of columns to foundations and columns to the superstructure.	Same as the AASHTO LRFD 1998	The design philosophy requires general requirements that emergency vehicles can drive on the bridge with stipulated reliability after design earthquake.	Depending on the importance factors such as road class, bridge functions and structural characteristics, bridges are categorized into two groups depending on their importance; standard bridges (Type-A bridges) and important bridges (Type-B bridges).
5	Seismic	Extreme event limit state:	These guide specifications are	Same as the AASHTO	[1] Minimization of	Seismic performance

No.	Code	AASHTO LRFD 1998	LRFDSEIS-1, 2009	22TCN272-05	EUROCODE 8	JRA-2002
	performance	The survival of the structure of a bridge shall be guarantee against earthquake, flood, or impact by a ship.	intended to achieve minimal damage to bridges during moderate earthquake ground motions and to prevent collapse during rare earthquakes that results in high levels of ground shaking at the bridge site. Life safety for the design event shall be taken to imply that the bridge ha a low probability of collapse but may suffer significant damage and that significant disruption to service is possible.	LRFD 1998	damage = Service limit state (evaluated by displacement) [2] Unseating prevention provisions = Ultimate limit state (evaluate by bearing capacity and ductility)	level (SPL) depends on the importance of bridges. For the moderate ground motions induced in the earthquakes with high probability to occur, both A and B bridges should behave in an elastic manner without essential structural damage (SPL-1). For the extreme ground motions induced in the earthquakes with low probability to occur, the Type-A bridges should prevent critical failure (SPL-3), while the Type-B bridges should perform with limited damage (SPL-2).
6	Importance	Bridges are classified as critical, essential or other for seismic design. It is treated as one of the factors that is part of the load conversion constant η_i in the equation used to calculate the design load Q ($Q = \sum \eta_i \gamma_i Q_i \le \varphi R_n$), and the factor η_i for the importance is stipulated	Bridges are required to be open to all traffic once inspected after the design earthquake and be usable by emergency vehicles and for security, defense, economical, or secondary life safety purposes immediately after the design earthquake. Bridges that should, as a minimum, is open to	Same as the AASHTO LRFD 1998	Three kinds of importance factor γ_i are following: [1] Greater than average (γ_i =1.30). [2] Average (γ_i =1.00). [3] Less than average (γ_i =0.70). where: γ_i is multiplied by design seismic load AED.	There are class A bridges and class B bridges. Differences in importance of bridges must be reflected in differences in the seismic performance and in differences in the seismic performance and in differences in the safety factor for Type I

No.	Code	AASHTO LRFD 1998	LRFDSEIS-1, 2009	22TCN272-05	EUROCODE 8	JRA-2002
		at (= 0.95 to 1.05)	emergency vehicles and for security, defense, or economical purposes after the design earthquake and open to all traffic within days after that event. Bridges that are formally designated as critical for a defined local emergency plan.			and Type II earthquake motion of each bridge.
7	Ground classification	The soil types are categorized as four types: to set a site constant (*S*) at I, II, III and IV.	The site shall be classified following to the shear wave velocity of soil. There are class A, B, C, D, E and F.	Same as the AASHTO LRFD 1998.	There are 3 sub-soil classes: A, B and C.	Three categories: I, II and III.
8	Zone classification	It is categorized in four categories from 1 to 4 according to the acceleration coefficient (*A*).	It is classified following to seismic design categories from A to D base on the value of the design spectra acceleration coefficient at 1.0 second period (S_{D1}).	It is categorized in four categories from 1 to 3 according to the acceleration coefficient (*A*) and MSK-64 class.	It is set from 0.6 to 1.2 as zone factor *Z*.	The modification factor C_Z is provided at values of 1.0, 0.85 and 0.7 according to the 3 zone categories.
9	Design seismic force	Medium earthquake (design earthquake): Earthquake with return period of 475 years (design service life: 50 years, exceedance probability 10%). Large earthquake: Earthquake longer than the return period the of design earthquake. An earthquake with return period of approximately	The seismic hazard used in this code corresponds to a 7 percent probability of exceedance in 75 years.	Not clearly.	Medium earthquake: Earthquake motion during appropriate return period is evaluated. Large earthquake: Return period of 475 years.	The two level ground motion as the moderate ground motions induced in the earthquakes with high probability to occur (Level 1 Earthquake) and the intensive ground motions induced n the earthquakes with low probability to occur (Level 2 Earthquake). There is no concept of return period.

No.	Code	AASHTO LRFD 1998	LRFDSEIS-1, 2009	22TCN272-05	EUROCODE 8	JRA-2002
		2,500 years is called the maximum probable earthquake.				
10	Elastic response spectrum	$C_{sm} = 1.2AS / T_m^{2/3} \leqq 2.5A$ where: T_m is the period of the mth vibration mode (s); A is the acceleration coefficient. S is the site coefficient.	$S(T) = \begin{pmatrix} F_{pga},\ PGA\ F_a,\ F_v, \\ S_s,\ S_1,\ T,\ T_o,\ T_s \end{pmatrix}$ where: These values of F_{pga}, S_s, and S_1 depend on the peak ground acceleration (PGA), the spectral acceleration coefficient at 0.2s obtained from the ground motion maps (S_s), and the spectral acceleration coefficient at 1.0s obtained from the ground motion maps (S_1), respectively. T is period of vibration	Same as the AASHTO LRFD 1998	$S_e(T) = \begin{pmatrix} a_g,\ S,\ T,\ \eta, \\ \beta_0,\ k_1,\ k_2 \end{pmatrix}$ where: a_g is design ground acceleration accounting for reference return period. S is ground parameter. T is natural period of a single degree of freedom system. η is modification factor for damping. β_0 is response multiplier of a structure. k_1, k_2 is correction factor of spectrum curve	[1] Earthquake motion with a high probability of occurring during a bridge's service life. $k_h = C_Z k_{ho}$ [2] Large earthquake motion with a low probability of occurring during a bridge's service life (Type I and Type II). $k_{hc} = C_Z k_{hco}$
11	Load reduction factor	The R-value (response modification factor) (1.5 to 5.0) is selected, according to a substructure type and a bridge's importance.	Not mentioned	Same as the AASHTO LRFD 1998	The q-value (behavior factor) (1.0 to 3.5) is selected, according to substructure type and required ductility of members.	Force reduction factor (C_S) shall be appropriately determined with considerations of mechanical properties of structure member, including their plastic characters. Force reduction factor depend on allowable ductility ratio (μ_a) of a bridge

No.	Code	AASHTO LRFD 1998	LRFDSEIS-1, 2009	22TCN272-05	EUROCODE 8	JRA-2002
						pier. $C_S = \frac{1}{\sqrt{2\mu_a - 1}}$
12	Analysis method	Static analysis	Static analysis	Same as AASHTO LRFD 1998	Static analysis	Static and dynamic analysis

1.4 REFERENCES

[1]. 22TCN 272-05 (2005). *Specification for Bridge Design, Ministry of Transport of Vietnam*, Vietnam.

[2]. AASHTO LRFD 1998. *Load and resistance factor design (LRFD) specifications for highway bridges*, Washington (DC): American Association of State Highway and Transportation Officials (AASHTO).

[3]. Eurocode 8. *Design of structures for earthquake Resistance-Part 1: general rules, seismic actions, and rules for buildings*. EN 1998-1: 2004.

[4]. JRA-2002, *Specification for Japanese Highway Bridges, part V: seismic design*, Japan Road Association, 2002.

[5]. JTG/T B02-01-2008. *Guidelines for Seismic Design of Highway Bridge*, Ministry of Communications and transport, China.

[6]. LRFDSEIS-1 (2009). *Guide Specifications for LRFD Seismic Bridge Design, 1st Edition with 2010 Interim Revisions*. ISBN: 1-56051-396-4, 258 pages, U.S.

[7]. TCXDVN 375-2006. *Design of Structures for Earthquake Resistance*, Vietnam Ministry of Construction, Vietnam.

[8]. An, T.X (2006). *Study on Oscillation behavior and aseismicity of bridges with seismic isolation foundation system*. Doctor dissertation, Waseda University, 152 pages, Japan.

[9]. Atkinson, G.M. and Boore, D.M. (2006). *Earthquake ground-motion prediction equations for eastern North America*. Bulletin of the Seismological Society of America 96(6): 2181–2205.

[10]. Atkinson, G.M. and Somerville, P.G. (1994). *Calibration of time history simulation methods*. Bulletin of the Seismological Society of America 84(2): 400 - 414.

[11]. Boore, D.M. (1983). *Stochastic simulation of high-frequency ground motions based on seismological models of the radiated spectra*. Bulletin of the Seismological Society of America 73(6): 1865-1894.

[12]. Boore, D.M. (2003). *Simulation of ground motion using the stochastic method*. Pure and Applied Geophysics 160(3-4): 635-676, DOI: 10.1007/PL00012553.

[13]. Chen, W.F and Lui, E.M. [Editors] (2006). Chapter 4: Seismic Design of Bridges, *Earthquake engineering for structural design*, ed., L. Duan, M. Reno, W.F. Chen, and S. Unjoh, CRC Press, Boca Raton, FL, 2006.

[14]. Chen, W.F. and Duan, L. (2003-2). "Bridge Engineering", Seismic Design, *Chapter 2. Earthquake Damage to Bridges* (Moehle J.P. and Eberhard M.O.), CRC Press 2003.

[15]. Clough, R.W. and Penzien, J. (2003), *Dynamics of Structures*, Third Edition, Computers & Structures, Inc.

[16]. Kawashima, K. and Unjoh, S. (2004). *Seismic design of highway bridges*. Journal of Japan Association for Earthquake Engineering, Vol.4, No.3 (Special Issue), pp. 174–183.

[17]. Ngo, T.D., Nguyen, M.D. and Nguyen, D.B. (2008). *A review of the Current Vietnamese Earthquake Design Code*, Special Issue of the Electronic Journal of Structural Engineering (EJSE): Earthquake Engineering in the low and moderate seismic regions of Southeast Asia and Australia, pp. 32-41.

[18]. Okahara, M., Fukui, J., Nishitani, M. and Matsui, K. (2001). *Comparison of performance required by bridge design codes in various countries*. Proceedings of the

joint meeting of the U.S. - Japan cooperative program in natural resources panel on wind and seismic effects, Vol.32, pp. 297-312.

[19]. Phuong, N.H. (1991). *Probabilistic assessment of earthquake hazard in Vietnam based on seismotectonic regionalization*. Tectonophysics, Vol. 198(1), pp. 81-93.

[20]. Trieu, C.D., Panza, G.F., Peresan, A., Vaccari, F., Romanelli, F., Tuyen, N.H., Hung, P.N., Dung, L.V., Bach, M.X., Tuan, T.A. and Trong, C.D. (2008). *Seismic hazard assessment of Vietnam territory on the basis of deterministic approach*. Vietnam Journal of Geology, Series B, No. 31-32/2008, p 220-230.
(website: http://www.idm.gov.vn/nguon_luc/Xuat_ban/2008/b31-32/b220.htm)

[21]. VIG. (2005). *Research and Forecasting Earthquakes and Ground Movements in Vietnam* (Researched by Vietnam Institute of Geophysics - Chairman is Prof. Nguyen Dinh Xuyen), Hanoi, Vietnam (in Vietnamese).

[22]. Yamamoto, Y. and Baker, J. (2011). Report No.176, *Stochastic model for earthquake ground motion using wave packets*. Department of Civil and Environmental Engineering. Stanford University.

This page intentionally left blank

CHAPTER 2

HISTORICAL EARTHQUAKE ACTIVITY

2.1 INTRODUCTION

The historical earthquake in Vietnam has occurred events of large magnitudes from 5.0 to 6.8 of on the Richter scale during the 20th Century. Following the results of a research project of the Vietnam Institute of Geophysics (*VIG*) entitled "Research and Forecasting Earthquakes and Ground Movements in Vietnam" (*VIG, 2005*), showed that from 114 AD to 2003 AD Vietnam, either by measurement or by studying the historical archives, recorded 1645 earthquakes with magnitudes (*M*) of 3.0 to 6.8 on the Richter scale. Any strong earthquakes have occurred in the North of Vietnam including the Dien Bien earthquake (1935), the Tuan Giao earthquake (1983), and the Dien Bien earthquake (2001). The earthquake events were occurred in the North of Vietnam, Yunnan province (China) and Laos' boundary. The longest Red River fault is running through the north of Vietnam as shown in **Fig 2.1**. This map is modified from map that was published by Goddard space flight center (website: *http://core2.gsfc.nasa.gov*). Almost main faults in northern Vietnam are strike-slip faults. The deep-level NW–SE-trending strike-slip fault system in North Vietnam is more active than its perpendicular NE–SW-trending fault system (*Huang et al., 2009*).

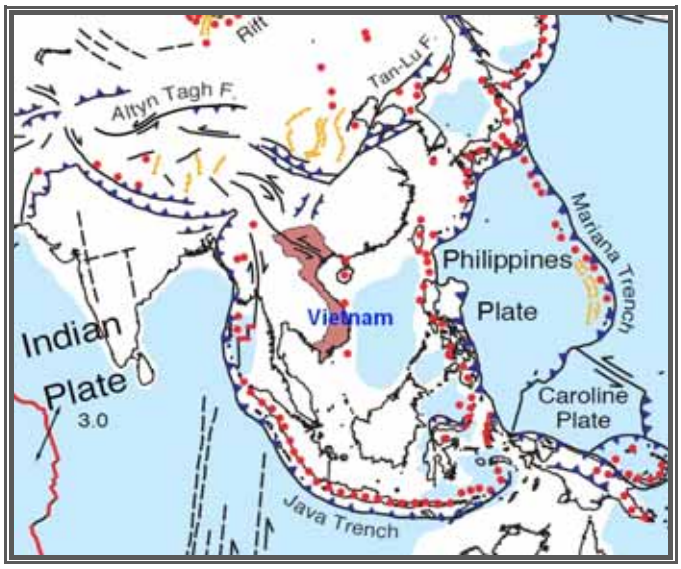

Figure 2.1 Tectonic map.

2.2 SEISMIC ACTIVITIES IN VIETNAM

2.2.1 Earthquake catalogue

According to the earthquake catalogue compiled by *VIG (2005)*, 90% of earthquakes were located in northwestern Vietnam during the 20th century, including two earthquakes with intensity I_0 = 8 ÷ 9 (MSK-64) and magnitude (M) of 6.5 ÷ 7.0 on the Richter scale, 15 earthquakes with I_0 = 7 and M = 5 ÷ 5.9, and more than 100 earthquakes with I_0 = 6 ÷ 7 and M = 4.5 ÷ 4.9. This research is illustrated 30 earthquake active areas with the magnitudes of 5.5 to 6.8 in Vietnam as shown in **Table 2.1** (This information can be obtained from *website: http://english.vietnamnet.vn/news/2005/02/372239/*). The maximum earthquakes can be rising with magnitudes of 6.5 to 7.0 in Vietnam. Vietnam recorded more than 1650 earthquakes that have magnitudes of 3.0 to 7.0 on the Richter scale from 114 to 2005. In the period of the year from 1900 to 2005, more than 350 earthquakes with $4.0 \leq M_S \leq 7$, two earthquakes with intensity (I_0) of 8 to 9 grades, magnitudes (M) of 6.7 to 6.8 on the Richter scale and more than 50 earthquakes with intensity $I_0 \geq 7$, $M_S \geq 5.0$, occurred in the territory of Vietnam. Earthquake events with magnitudes of 6.0 to 6.5 occurred in northeastern Vietnam within the Ca River- Rao Nay and Nam Con Son faults. Earthquake magnitudes of 5.0 to 6.8 have occurred in the Ha Noi area and the other areas in Vietnam. Two strongest earthquakes of the Dien Bien earthquake (1935, M = 6.8) and Tuan Giao earthquake (1983, M = 6.7) were occurred in the main land territory of Vietnam.

The earthquakes have classified into three catalogues according to *Trieu et al. (2008)*. Catalogues are established based on three data sources such as the catalogue earthquakes up to the year 1900. Catalogues seismic data investigated in public documentation (from the year 1900 to 1976) and the earthquake events recorded from seismic network of Vietnam (since the year 1963). The database is using in Vietnam could be considered as reliable as achieved only after 1976 (*Peresan et al., 2009*). *Huang et al. (2009)* displayed faults and epicenters (see **Fig 2.2**). **Fig 2.3** shows the number of earthquake that recorded in each century. In this study, the earthquake catalogue used covers an area between latitudes $3^0$26’ N to $25^0$54’ N, and between longitudes 100^0 E to 118^0 E from 1903 to 2005 consisting of more than 1500 events. Herein, the earthquakes during the period from 1903 to 2003 and from 2004 to 2005 have been collected, which were published from *VIG* and *Thuc (2007)*, respectively. **Fig 2.4** has shown the number of earthquakes during the period from 1900 to 2005. This figure is divided catalogue into six magnitude classes within 10 years as shown in **Fig 2.4**.

Vietnam is regarded as a low-seismicity region; however, it remains tectonically active, as indicated by the occurrence of moderate earthquakes in the country and adjacent areas. Recently, not only the earthquakes occurs in northern Vietnam but also occurs in southern Vietnam. For example, the earthquakes are recently occorred in Nghe An, Thanh Hoa, Vung Tau and Phan Thiet Province.

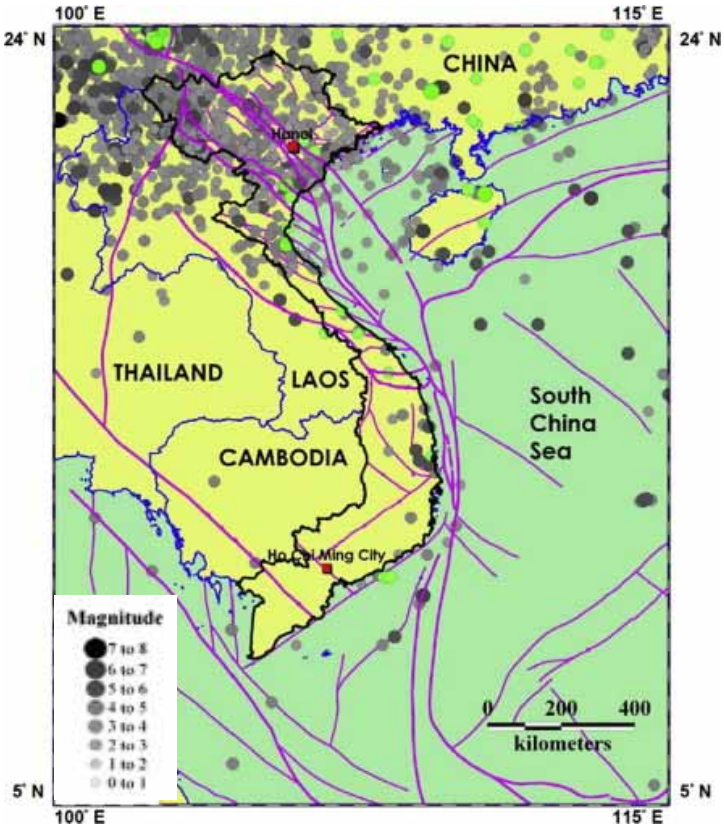

Figure 2.2 Faults and epicenters.

Table 2.1 Areas of the strong earthquakes in Vietnam.

No.	Region	Mag.	No.	Region	Mag.
1	Son La	6.8	16	Song Ma-Fumaytun	6.5
2	Dong Trieu	6.0	17	Red River-Chay River	6.0
3	Song Ca-Khe Bo	6	18	Rao Nay	5.5
4	Cao Bang-Tien Yen	5.5	19	Hanoi's Northeastern sunken area	5.5
5	Cam Pha	5.5	20	Lo River	5.5
6	Phong Tho-Than Uyen Muong La-Cho Bo	5.5	21	Da River	5.5
7	Muong Nhe	5.5	22	Ma River's lower section	5.5
8	Hieu River	5.5	23	Khe Giua-Vinh Linh	5.5
9	Tra Bong	5.5	23	Hue	5.5
10	Da Nang	5.5	25	Tam Ky-Phuoc Son	5.5
11	Poco River	5.5	26	Ba River	5.5
12	Ba To-Cung Son	5.5	27	109.5 meridian	5.5
13	Tuy Hoa-Cu Chi	5.5	28	Thuan Hai-Minh Hai	5.5
14	Vung Tau-Ton Le Sap	5.5	29	Hau River	5.5
15	Phu Quy 1	5.5	30	Phu Quy 2	5.5

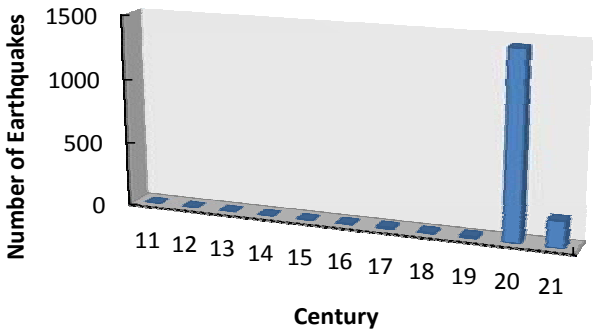

Figure 2.3 Number of earthquakes recorded in each century.

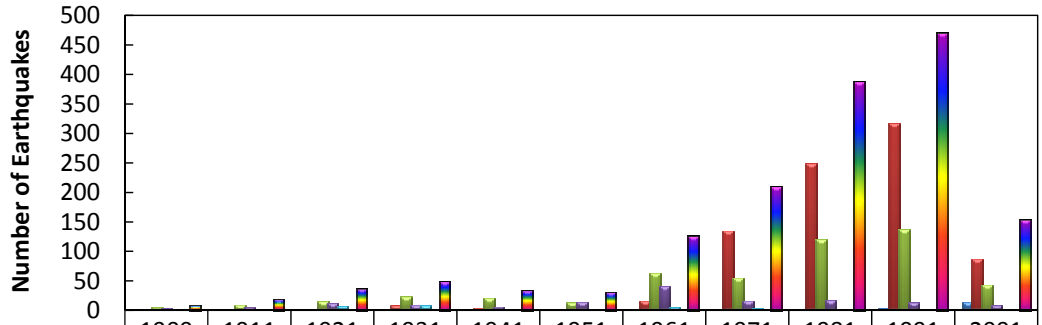

Period / Ms	1900 ~ 1910	1911 ~ 1920	1921 ~ 1930	1931 ~ 1940	1941 ~ 1950	1951 ~ 1960	1961 ~ 1970	1971 ~ 1980	1981 ~ 1990	1991 ~ 2000	2001 ~ 2005
2.0 - 2.9	0	0	0	0	0	0	0	0	0	3	14
3.0 - 3.9	0	1	2	8	4	2	16	135	249	317	87
4.0 - 4.9	5	9	15	23	21	13	63	55	120	137	43
5.0 - 5.9	3	5	12	9	6	14	41	16	17	13	8
6.0 - 6.9	0	2	7	8	1	1	5	3	1	0	1
7.0 - 8.0	0	1	0	0	1	0	0	0	0	0	0
Total	8	18	36	48	33	30	125	209	387	470	153

Figure 2.4 Annual distribution of earthquakes recorded from 1900 to 2005.

2.2.2 Active faults and earthquake record

The previous studies found that Vietnam lies in a low-to-moderate earthquake zone (*Trieu et al., 2008*). These studies illustrated a number of obvious faults in northern Vietnam including thoes in Cao Bang-Tien Yen, Dong Trieu, Lo River, Chay River, Red River, Son La, Ma River, Da River, Muong La, Ca River and Lai Chau-Dien Bien as shown in **Fig 2.5**. The longest fault zone is the Red River fault zone. This fault is most likely to be active in the present day as a right-lateral strike slip fault (*Duong and Feigl, 1999*).

The Red River strike-slip fault plays an important role in recent tectonic activity in North Vietnam. This fault is divided into two parts. The northern segment of the Red River fault is located in China and the southern segment crosses into northern Vietnam. The two segments

show contrasting seismic activities; the northern segment exhibits a higher level of vigorous earthquake activity, whereas the southern segment gives less vigorous activity and is influenced by the tectonic evolution of the northern Vietnam zone, which has the highest seismic activity in the Indochina Peninsula. Furthermore, the activities of earthquakes along the fault zone are inconsistent. For example, a part of the Son La fault from Tuan Giao to Thuan Chau generates strong earthquakes, such as the Tuan Giao earthquake (1983). For the Dien Bien-Sam Nua fault, Phi Cao-Nam Khun had strong earthquake activity as exemplified by the Dien Bien earthquake (1935). In contrast, earthquake activity generated by the Chay River fault has been concentrated in the area of Luc Yen, Yen Bai (*Trieu et al., 2008*).

Fig 2.6 illustrates the major Cenozonic fault systems and large-scale strike-slip movement along the Red river fault accommodating the eastward extrusion of Indochina in response to northward penetration by India (*Fenton et al., 2003*). The faults are expressed arising earthquakes in Vietnam with $M_{max} \geq 5$ as shown in **Fig 2.5** (after *Trieu, 2008*).

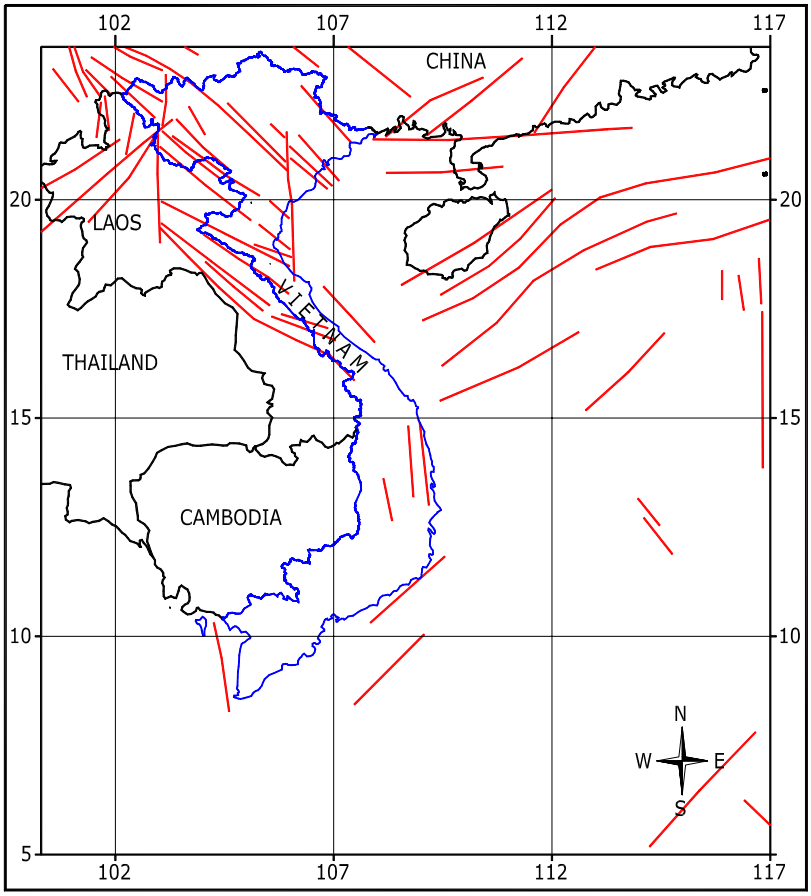

Figure 2.5 Faults arising earthquake $M_{max} \geq 5$.

Table 2.2 Main active faults in the North of Vietnam.

No.	Fault zone	Active fault data					
		Fault type [a)]	L (km)	W (km)	S (mm/yr)	M_{max}	H (km)
1	Cao Bang-Tien Yen	S	300	15	0.002	5.5	12
2	Dien Bien Phu	S, N	160	10	2.00	6.8	12
3	Dong Trieu	S, N	187		0.07	5.9	22
4	Ca River	S	380	25	0.01	6.1	17
5	Chay River	S, N	430	15	2.00	6.1	17
6	Da River	S	46		0.007	5.5	12
7	Ma River	R	460	30	0.5	6.8	22
8	Muong La	S	240	15		5.5	12
9	Red River	S, N	400	20	5.00	6.1	17
10	Lo River	S	340	10		5.5	12
11	Son La	N	175	40	0.7	6.8	22

Where L is surface rupture length (km), W is surface rupture width (km), M_{max} is maximum possible earthquake magnitude, M_{min} is the minimum magnitude, S is slip rate (mm/year), [a)] Fault type: S = strike-slip fault, N = normal fault, R = reverse fault.

(Referred to [*Duong and Feigl, 1999*], [*Jin and Aki., 1988*], [*Lam et al., 2000*], [*Phuong et al., 2007*], [*Lap, 1991*], [*Cuong and Zuchiewicz, 2001*], [*Thuc, 2007*], [*Qin et al., 1997*], [*Mak et al., 2004*], [*Yun et al., 2007*], and [*Wong et al., 2002*]).

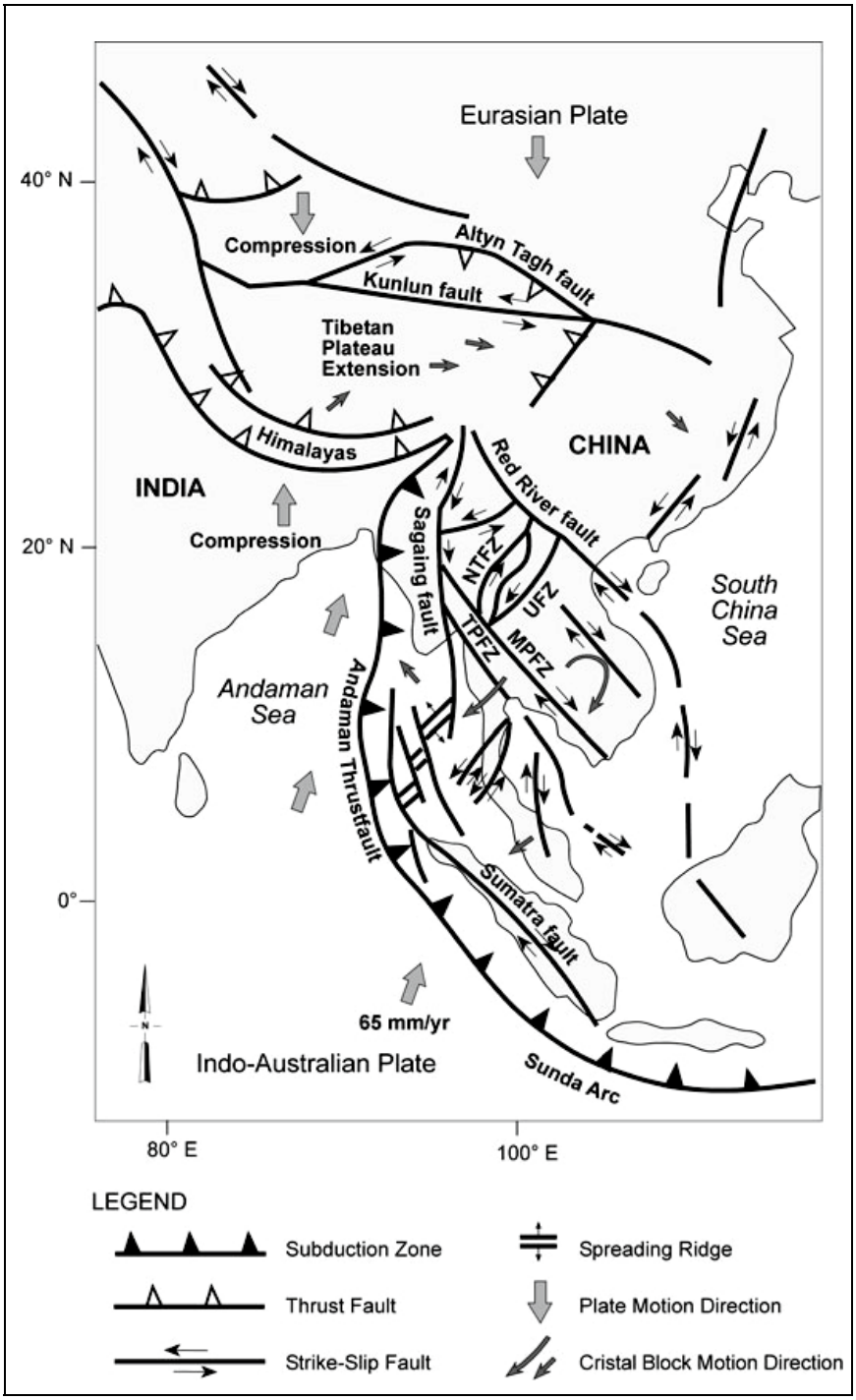

Figure 2.6 Major tectonics in Southeast Asia and Southern China. Arrows show relative directions of motion of crustal blocks during the Late Cenozoic. MPFZ-Mae Ping Fault Zone; NTFZ-Northern Thailand Fault Zone; TPFZ-Three Pagodas Fault Zone; UFZ-Uttaradit Fault Zone.

Table 2.3 Mainshock and aftershocks of the Tuan Giao earthquake in 1983 (*Trieu, 2002*).

No	Time of occurrence		Coordinates		Depth, H (km)	Magnitude, M_S (Richter)	Intensity (I_0)
	dd/mm/yy	Time (GMT)	Latitude	Longitude			
1**	24/06/1983	07h18'22,3"	21,71	103,43	18	6,7	9
2*	24/06/1983	15h43'40,3"	21,81	103,37	12	4,5	
3*	24/06/1983	21h25'11,6"	21,69	103,40	12	4,7	
4*	24/06/1983	22h45'05,8"	21,60	103,50	09	4,0	
5*	25/06/1983	10h52'07,0"	21,61	103,33	07	4,6	
6*	25/06/1983	15h18'23,0"	21,70	103,31	03	4,0	
7*	25/06/1983	19h55'23,3"	21,50	103,41	09	4,2	
8*	25/06/1983	20h16'19,7"	21,62	103,32	06	4,2	

** Main shock; * After shock

Table 2.4 Mainshock and aftershock ($M > 4$) recorded from the Dien Bien earthquake (2001).

No.	Name	dd/mm/yy	Time (GMT)	Latitude	Longitude	M_S (Richter)	Max. of Acc. (cm/s^2)		
							N-S	U-D	E-W
1**	DBIEN001	19/02/2001	15h51'34"	21,34	103,85	5.3	108.97	90.53	107.06
2*	DBIEN005	19/02/2001	16h40'17"	21,42	102,90	4.2	14,90	19,70	21,76
3*	DBIEN006	19/02/2001	19h02'49"	21,40	102,88	4.8	61,70	42,45	74,60
4*	DBIEN012	24/02/2001	22h14'31"	21,36	102,92	4.2	28,26	21,26	27,15
5*	DBIEN013	04/03/2001	20h18'49"	21,39	102,86	4.7	21,14	4,00	42,60

** Main shock; * After shock

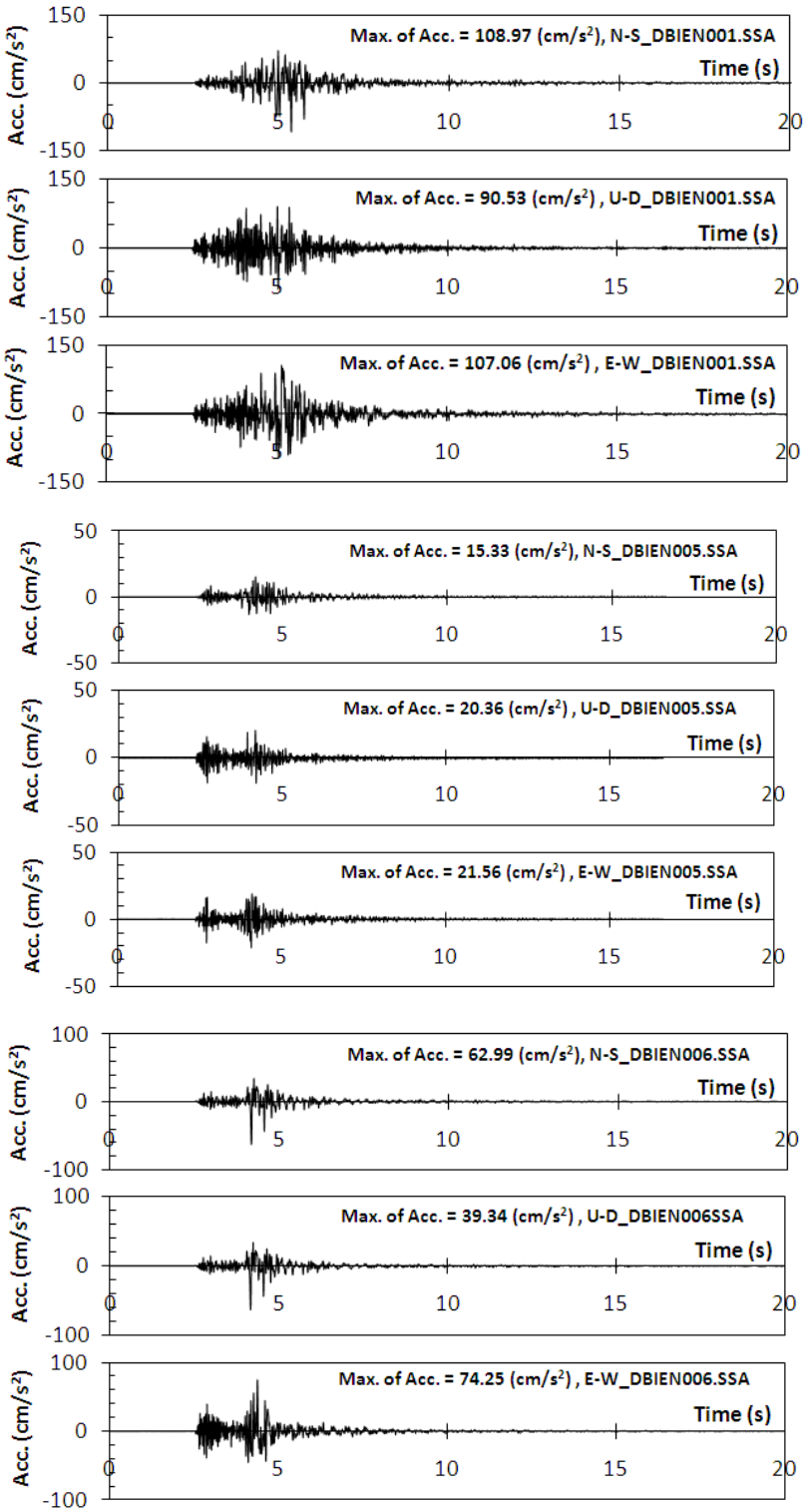

Figure 2.7a The main shock and aftershock from the Dien Bien earthquake (2001) at Dien Bien station (DBV-21°23.38'N, 103°01.10'E).

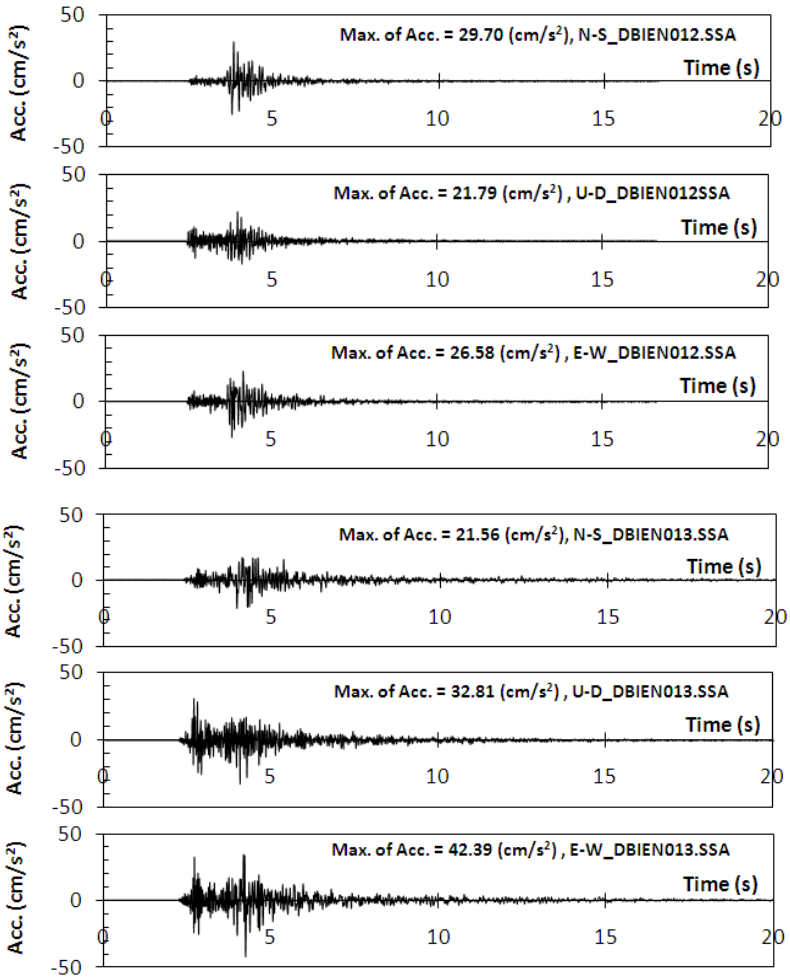

Figure 2.7a Continued.

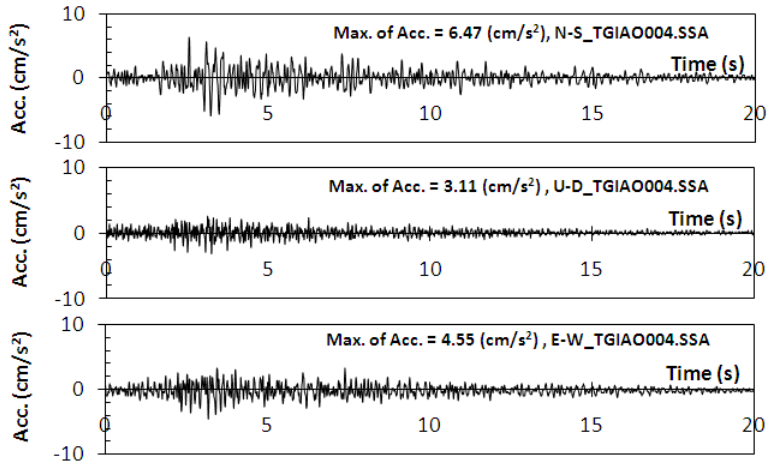

Figure 2.7b The main shock and aftershock of the Dien Bien earthquake (2001) at Tuan Giao station (TGV-21^{o}25.39'N, 103^{o}25.09'E).

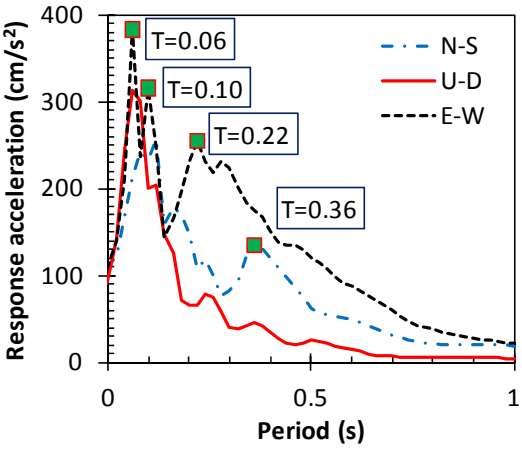

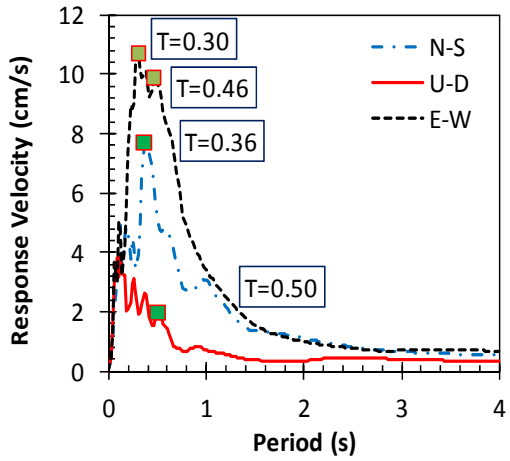

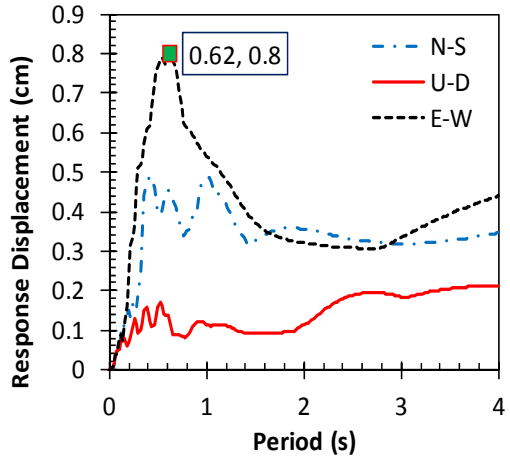

Figure 2.8 Spectra of the main shock of the Dien Bien earthquake record at Dien Bien station.

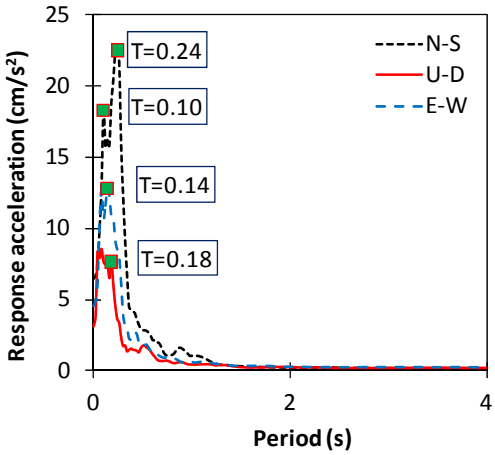

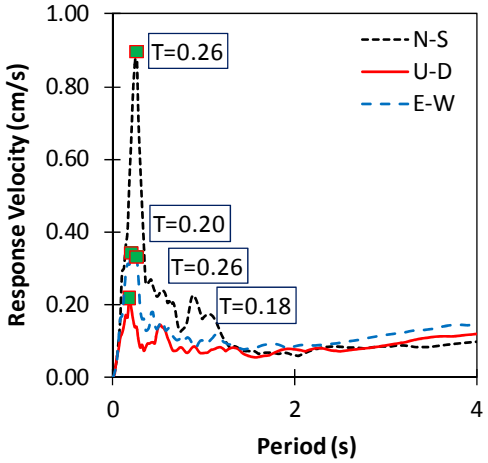

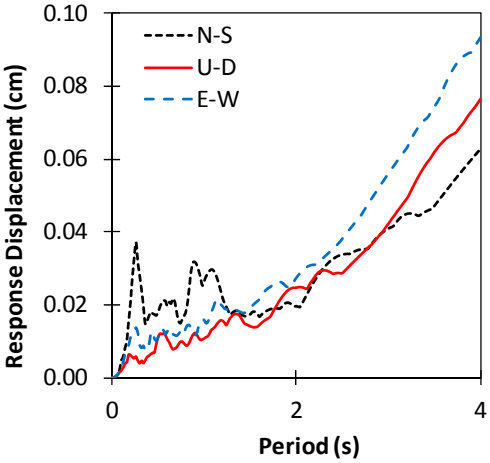

Figure 2.9 Spectra of the main shock of the Dien Bien earthquake record at Tuan Giao station.

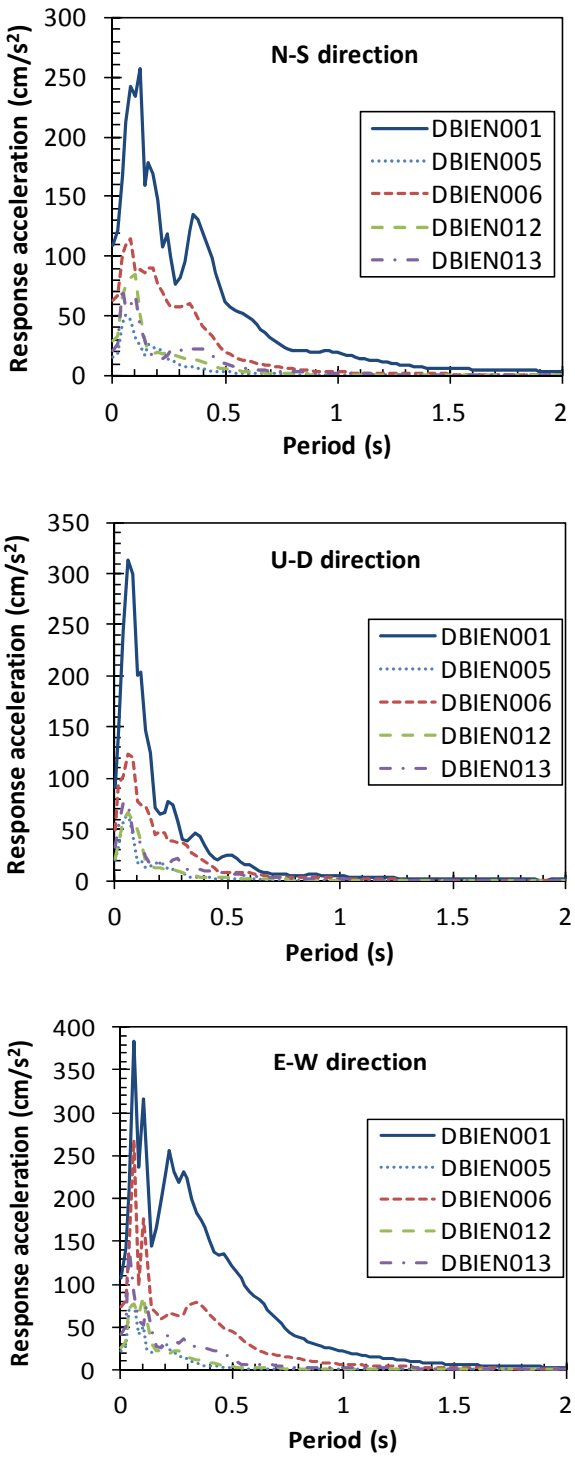

Figure 2.10 Response acceleration of mainshock and four aftershock recorded ($M_S \geq 4.0$) from the Dien Bien earthquake (2001) at Dien Bien station.

Thuc (2007) investigated and descripted the Tuan Giao earthquake (1983) with the earthquake magnitude of M = 6.7 on the Richter scale; the fault-source is stretching in

Northwest-Southeast direction, with a normal, right lateral strike slip mechanism with direction of dip is Northeast with a dip angle of $\gamma = 75^0$; epicenter coordinates are latitude of $21^0$71'N, longitude of $103^0$43'E and seismic moment $M_0 = 3.5\times10^{25}$ dyne·cm; length of fault L = 23 km; wide of fault W = 22 km; duration t_0 = 12 s; average displacement D_0 = 28 cm; seismic energy $E_S = 1.1\times10^{20}$ erg; rupture velocity V_R = 2 km/s; density of soil ρ_s = 2.7 g/cm^3; velocity of S-wave V_S = 3.4 km/s.

No strong earthquake ground motion was observed before 2000. The first earthquake ground motion was recorded during the Dien Bien earthquake (Feb. 19, 2001; 21.33 N, 103.85 E), but only a few earthquake stations obtained earthquake records (see **Figs. 2.7a** and **2.7b**. The seismic stations were arranged at among the Hoa Binh, Son La, Dien Bien, Tuan Giao and Sa Pa by Vietnam Institute of Geophysics. This earthquake recorded a main shock of M = 5.3 and five other events ranging from M = 4.0 – 4.9. Since 2005, 24 broadband seismographs have been installed in northern Vietnam, but strong ground motion data were not available until now. The accelerograms were recorded at seismic stations in Dien Bien, Tuan Giao which is placed on rock clay, siltstone. **Figs 2.8**, **2.9** and **2.10** illustrate the peak spectrum at a period of approximately 0.1 sec, cut down from 0.1 to 0.4 sec and quickly reduced from 0.3 to 1.0 sec. The energies of the main earthquake shock and the aftershock arose from the same mechanism as the Dien Bien earthquake, which had a relatively short period of 0.1 to 0.4 sec.

2.3 EARTHQUAKE MAGNITUDE RECURRENCE RELATIONS

In this section, the earthquake catalogue in the North of Vietnam covers an area between latitudes 18^0N and 24^0N and between longitudes 102^0E and 108^0E for the database of more than 350 seismic events with $M_S \geq 4$ on the Richter scale during the year 1900 to 2005. The frequency of magnitude occurrence relationship helps to characterize the activity of each source. The occurrence rate of events in a given region, the random magnitude and spatial distribution of the epicenter given the occurrence in time can be used to model the temporal and spatial randomness of future events. The rate of earthquake recurrence on a seismic source is assumed to follow the Gutenberg Richter law. Annual occurrence rate (λ_m) of the earthquakes with a magnitude (M) greater than m is calculated by next equations.

$$Log(\lambda_m) = a - b\,m \tag{2.1}$$

$$\lambda_m = N_m / T \tag{2.1a}$$

$$Log(N_m) = a - b\,m \tag{2.1b}$$

Where N_m is the number of earthquakes with magnitudes greater than m, T is the period in year. a and b are the coefficients determined by the regression analysis using the value of λ_m and N_m (see **Figs 2.11** and **2.12**).

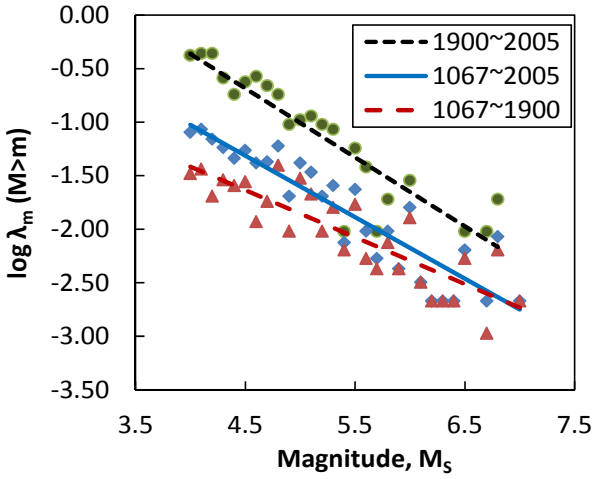

Period	*a*	*b*
1900~2005	2.21	0.64
1067~2005	1.27	0.57
1067~1900	0.34	0.44

Figure 2.11 Annual earthquake occurrence rate, λ_m.

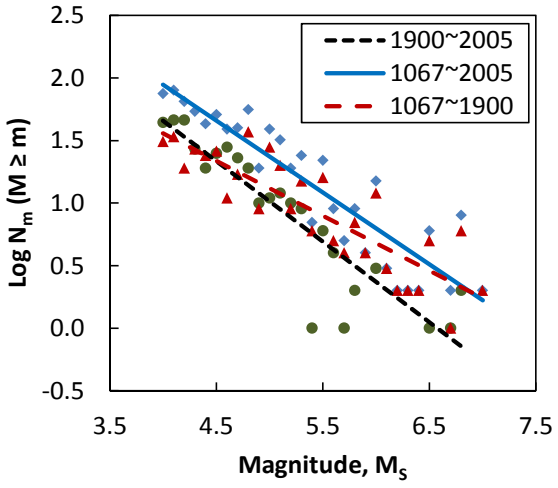

Period	*a*	*b*
1900~2005	4.24	0.64
1067~2005	4.24	0.57
1067~1900	3.31	0.44

Figure 2.12 Earthquake recurrence rate, N_m.

Fig 2.11 shows earthquake occurrence (λ_m) for three different periods. This figure shows that the λ_m for the period of the years 1067~1900 is the lowest and λ_m for the period of the years 1900~2005 is the greatest. Thus, in this study about 350 earthquakes occurred during the period of the years 1900~2005 (105 years) is adopted. **Fig 2.12** also shows the earthquake occurrence with low frequency in the North of Vietnam.

For the prediction of maximum earthquake magnitude, earthquakes occurred during the period of the year 1900~2005 are adopted. Probability distribution of maximum earthquake magnitude is first derived for an unspecified probability distribution of earthquake magnitude. To obtain the probability distribution of a maximum earthquake magnitude, the Gutenberg-Richter recurrence relationship is used. The cumulative probability distribution of magnitudes ($m_0 \leq M \leq m_u$) is given by **Eq. (2.2)**.

$$F_M(m) = \frac{1-\exp\left[-\beta\left(m-M_0\right)\right]}{1-\exp\left[-\beta\left(m_U-M_0\right)\right]} \tag{2.2}$$

$$\beta = b \log_e 10 \tag{2.2a}$$

$$b = \frac{\log_{10} e}{\overline{M} - M_{Small}} \tag{2.2b}$$

Where m_U (m_U = 6.8) is the largest magnitude event which can be expected in the region; m_0 (m_0 = 4.0) is the smallest magnitude considered in the model; $\overline{M}$ ($\overline{M}$ = 5.2) is mean magnitude; M_{Small} (M_{Small} = 4.6, $M_{Small} \neq m_0$) is the minimum magnitude when *b*-value of 0.927 is estimated (approached by *Kiureghian and Ang, 1977* and *Izumi, 1994*).

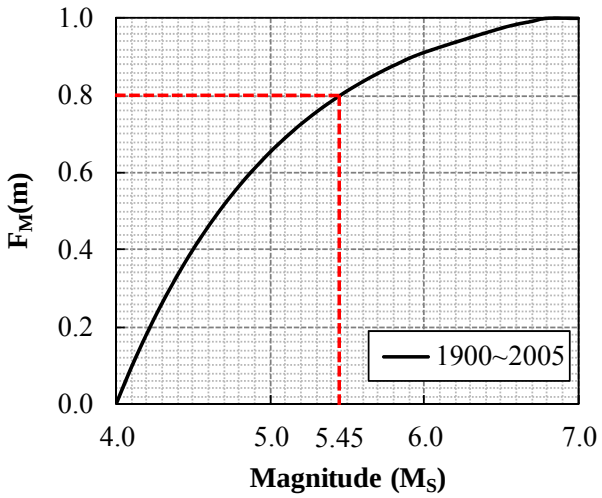

Figure 2.13 Cumulative probability function of magnitude in the North of Vietnam.

The cumulative distribution probability of earthquake magnitude is shown in **Fig 2.13**. Besides, other assumptions are selected to obtain the probability distribution of a maximum earthquake magnitude (see **Fig 2.14**). The high probability of earthquakes almost concentrates in the magnitude ranging of M = 4.5 to 5.5 (see **Fig 2.14**). This probability is estimated approximately equal to 95% confidence interval for the mean of earthquake magnitudes (M = 5.8 with 95% confidence interval for the mean) is shown in **Fig 2.15**. The descriptive statistics in details are shown in **Table 2.5.**

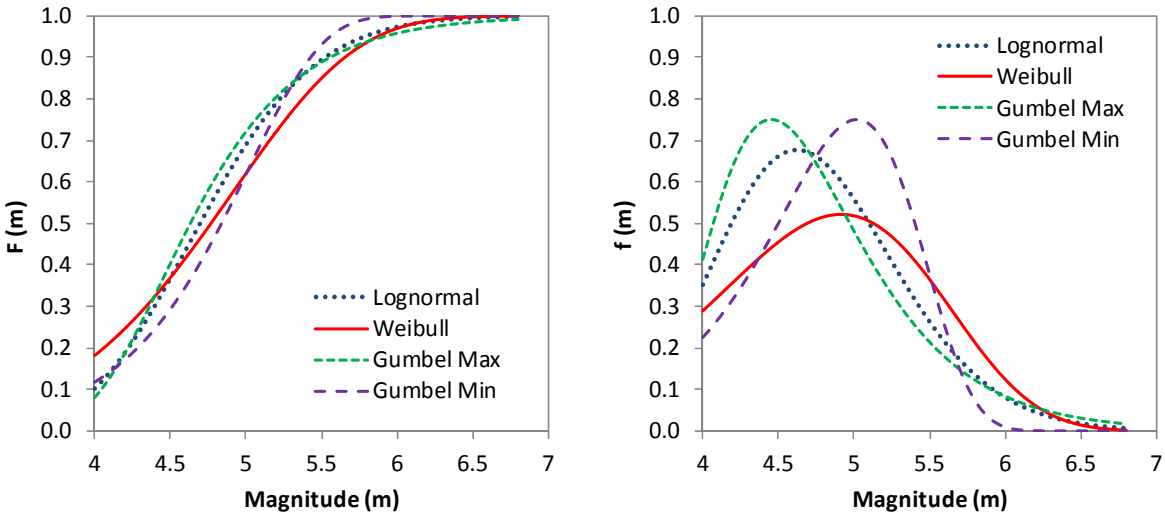

Figure 2.14 Cumulative distribution function and probability density function using other extreme value distributions.

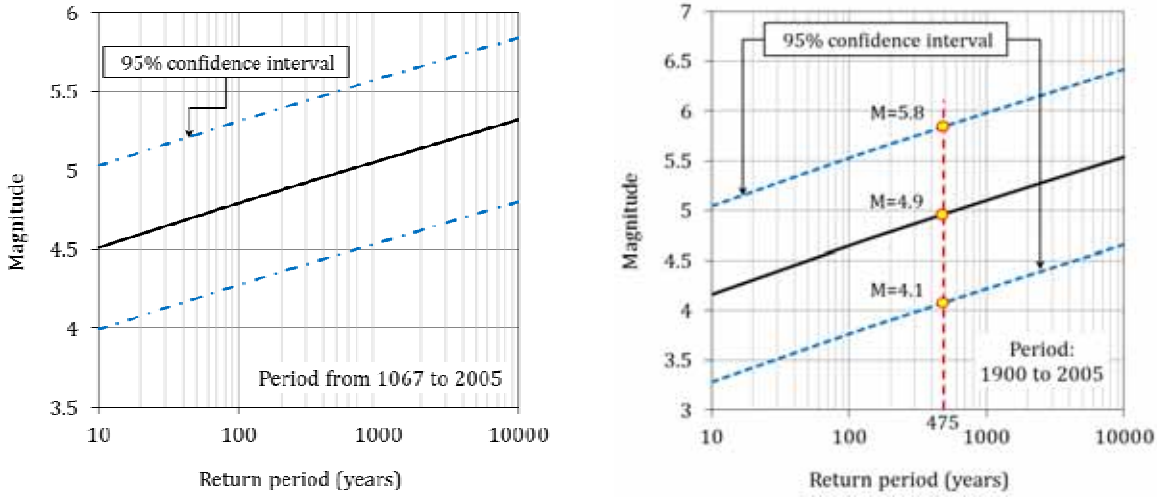

Figure 2.15 A probability of exceedance is estimated by the Weibull distribution.

Table 2.5 Descriptive statistics.

Statistic	Value	Percentile	Value (Magnitude)
Sample Size	23	Min	4
Range	2.8	5%	4
Mean	4.74	10%	4.1
Variance	0.39	25%	4.2
Std. Deviation	0.63	50% (Median)	4.6
Coef. of Variation	0.13	75%	5.1
Std. Error	0.13	90%	5.6
Skewness	1.03	95%	5.8
Excess Kurtosis	0.78	Max	6.8

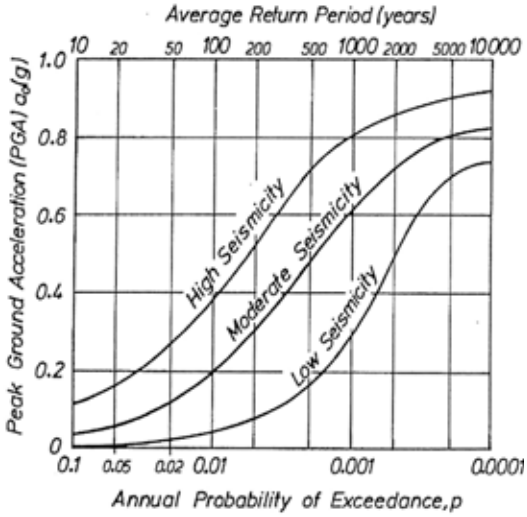

Figure 2.16 Relationship between peak ground acceleration and annual probabilistic of exceedance for different seismic regions.

Following to *Paulay and Priestley (1992)*, at short return periods, expected PGA in moderate to high seismicity regions may be an order of magnitude greater than for low seismicity regions. These trends are included in **Fig 2.16**, which plots PGA against the annual probability of exceedance for three levels of site seismicity. This means the probability of structural collapse is higher in low-to-moderate seismicity regions compared with high seismic regions when subject to an extreme event larger than the design event. On the other hand, the comparison between observed earthquake records and the relationship in **Fig 2.16** shows also earthquakes occur in Vietnam laid in a low to moderate seismic regions. The difference between these return periods is much more significant for low-to-moderate seismicity regions. The highest consequence earthquake events can up to magnitude of M = 7.0 (e.g., *VIG, 2005*; *Trieu et al., 2008; etc.*).

2.4 CONSIDERATION

The analyzing of this chapter is shown that Vietnam lies in a low-to-moderate seismicity. The high probability of earthquakes almost concentrates in the magnitude ranging of M = 4.5 to 5.5. The earthquake magnitude of M = 5.8 is computed with 95% confidence interval for the mean. The large earthquake magnitudes occur with low probability. The highest consequence earthquake events can of up to magnitude of M = 7 (e.g., *VIG, 2005*; *Trieu et al., 2008; etc.*). The historical earthquake activity indicated earthquakes took place frequently with larger magnitude of 6.8 at Dien Bien province (two times during 50 years).

The application of the measures to ensure the seismic safety of the construction is very necessary. Ground motion is still not sufficiently research; this leads to the difficulty in the choice the accelerograms needed for the design of many constructions. Currently, Vietnam has not yet the official regulations on seismic safety and code for bridge design. Thus, the application of seismic analysis for bridges is very limited both input data and knowledge in this field.

This chapter also presents the outline of earthquake records of the previous seismology researches in Vietnam. The necessary to improving the predicted seismic maps and ground motions in the future, especially in Vietnam, achievement of seismic researchers and measure instruments are very limited. To solve this problem, Vietnam needs to be increased seismic stations, improved, assisted with international research institutes, joint researches, exchange of data and experience with other countries, etc.

2.5 REFERENCES

[1]. Cuong, N.Q. and Zuchiewicz, W. (2001). *Morphotectonic properties of the Lo River fault near Tam Dao in North Vietnam*. Natural Hazards and Earth System Sciences, Vol. 1, pp. 15-22.

[2]. Duong, C., and Feigl, K.L. (1999). *Geodetic measurement of horizontal strain across the Red River fault near Thac Ba, Vietnam*, 1963-1994. Journal of Geodesy, Vol. 73, pp. 298-310.

[3]. Fenton, C.H., Charusiri, P. and Wood S.H. (2003). *Recent paleoseismic investigations in Northern and Western Thailand*. Annals of geophysics, Vol. 46, N. 5, pp. 957-981.

[4]. Huang, B.S., Son, L.T., Liu, C.C., Toan, D.V., Huang, W.G., Wu, Y.M., Chen, Y.G. and Chang, W.Y., (2009). *Portable broadband seismic network in Vietnam for investigating tectonic deformation, the Earth's interior, and early-warning systems for earthquakes and tsunamis*. Journal of Asian Earth Sciences, Vol. 36, Iss. 1, pp. 110-118.

[5]. Izumi, M. (1994). *地震動—その合成と波形処理, 鹿島出版会*, 256 pages, 1994 (in Japanese).

[6]. Jin, A. and Aki, K. (1988*). Spatial and temporal correlation between coda Q and seismicity in China*. Bulletin of the Seismological Society of America, Vol. 78, No. 2, pp. 741-769.

[7]. Kiureghian, A.D. and Ang, A.H.S. (1977). *A fault rupture model for seismic risk analysis*. Bulletin of the Seismological Society of America, Vol.67, No. 4, pp. 1173-1194.

[8]. Lam, N.T.K., Wilson, J.L., Chandler, A.M., and Hutchinson, G.L. (2000). *Response spectral relationships for rock sites derived from the component attenuation model*. Earthquake Engineering & Structural Dynamics, Vol. 29, pp. 1457-1489.

[9]. Lap, N.K. (1991). *The sismotectonics of the Indochina peninsula*. Journal of Southeast Asian earth sciences, Vol. 6, No. 2, pp. 55–61.

[10]. Mak, S., Chan, L.S., Chandler, A.M., and Koo, R.C.H. (2004). *Coda Q estimates in the Hong Kong Region.* Journal of Asian Earth Sciences, Vol. 4, Issue 1, pp. 127-136

[11]. Paulay, T. and Priestley, M.J.N. (1992). *Seismic design of reinforced concrete and masonry buildings*. John Wiley and Sons.

[12]. Perasan, A., Trieu, C.D., Bach, M.X., Hung, N.T., Nam, B.A. and Binh, N.X. (2009). *Seismic activity in Vietnam*. Journal of Geology, Series A, No. 314 (9-10), pp. 27–37.

[13]. Phuong, N.H. and et al. (2007). *Application of GIS technology for modeling and assessment of urban risk for Ha Noi City.* Project No. DL/02-2006-2, Ha Noi.

[14]. Qin, J.Z., Liu, Z.Y., Qian, X.D. and Xie Q.Y. (1997). *Estimation of seismic stress drop from the peak velocity of ground motion*. Acta Seismologica Sinica, Vol. 10, Iss. 5, pp. 81-591.

[15]. Thuc, P.V. (2007). *Seismology and Earthquake in Vietnam*. Natural Science and Technology Publisher, Hanoi, Vietnam (Vietnamese).

[16]. Trieu, C.D, Panza, G.F., Peresan, A., Vaccari, F., Romanelli, F., Tuyen, N.H., Hung, P.N., Dung, L.V., Bach, M.X., Tuan, T.A. and Trong, C.D. (2008). Seismic hazard assessment of Vietnam territory on the basis of deterministic approach. Vietnam Journal of Geology, Series B, No. 31-32/2008, p 220-230.
(website: http://www.idm.gov.vn/nguon_luc/Xuat_ban/2008/b31-32/b220.htm)

[17]. Trieu, C.D. (2002). *Some characteristic features of seismotectonic conditions and seismic regime of the Tuan Giao earthquake area*. Journal of Geology, Series B-No. 19-20, pp. 54-68.

[18]. Trieu, C.D. (2008). *Earthquake*. Science and Technology Publisher, Hanoi, Vietnam (Vietnamese).

[19]. VIG (2005). Research and Forecasting Earthquakes and Ground Movements in Vietnam (Researched by Vietnam Institute of Geophysics – Chairman is Prof. Nguyen Dinh Xuyen), Hanoi, Vietnam (in Vietnamese).

[20]. Wong, Y.L., Zheng, S., Liu, J., Kang, Y., Tam, C.M., Leung, Y.K. and Zhao, X. (2002). *Attenuation function of ground motions and source parameters for Guangdong region of Southern China*. International Conference on Advances and New Challenges in Earthquake Engineering Research, Hong Kong, pp. 19-20.

[21]. Yun, S., Lee, W.S., Lee, K., and Noh, M.H. (2007). Spatial Distribution of Coda Q in South Korea. *Bulletin of the Seismological Society of America*, Vol. 97, No. 3, pp. 1012-1018.

CHAPTER 3

ATTENUATION RELATIONSHIP OF EARTHQUAKE GROUND MOTION

3.1 INTRODUCTION

Peak ground acceleration has been used to quantify ground motion in probabilistic seismic hazard analysis (*PSHA*). The ground motion attenuation relationship, which is used to estimate the ground maximum acceleration values for a design earthquake, is very important for PSHA. Thus, the attenuation of ground motion is represented and modeled using the empirical attenuation equations of peak ground accelerations (*PGAs*). These equations are related to the source/site parameters, including source magnitude, source distance and site conditions. Most of the relationships are developed based on widely distributed magnitudes, peak ground motions, distances and source mechanisms acquired from many earthquakes.

Ground motion attenuation relationships have previously been developed for many countries and regions. For example, empirical attenuation relationships have been proposed by *Joyner and Boore (1981)*; *Fukushima and Tanaka (1990)*; *Si and Midorikawa (2000)*; *Abrahamson and Silva (1997)*; *Campbell (1997)*; *Youngs et al., (1997)*; *Kanno et al., (2006)*; *Boore and Atkinson (2008)*; *Lin and Lee (2008)*; *Ghasemi et al., (2010)* and so on. Attenuation relationship have also been studied in regions adjacent to Vietnam (e.g., *Xiang and Gao (1994)*; *Koketsu et al., (2009)*; etc.), including Yunnan, China, which is near northern Vietnam. An attenuation relationship equation has also been presented by *Xuyen and Thanh (1999)* and used for earthquake prediction in Vietnam (*Xuyen et al., 2001*). However, Vietnamese seismologists selected an attenuation function developed by foreign seismologists for other regions, such as Yunnan, China and the United States. Thus, the current ground motion attenuation relationship is not appropriate for seismic hazard analyses in Vietnam because do it does not reflect local conditions. In particular, the relationship currently used does not consider any earthquake records obtained in Vietnam. Thus, this study constructed a new attenuation relationship that considers Vietnamese conditions.

The historical earthquake activity in Vietnam is demonstrated in **Chapter 2**. Tectonically, northern Vietnam is located in the most seismically active region at the boundary between the Indochina and South China plates (*Findlay and Trinh, 1997*). Most of the main faults in

northern Vietnam are strike-slip faults. This region is tectonically active, as demonstrated by the occurrence of moderate earthquakes in the countryside and adjacent areas. These earthquakes caused a significant amount of structural damage to buildings and other structures. Several large earthquakes with magnitudes of greater than 6.0 on the Richter scale have been recorded in locations in northern Vietnam where the active fault zones are located. However, there is a lack of strong ground motion data for these earthquakes. Thus, earthquake studies in Vietnam are challenging due to the lack of data for the region. In 2005, a seismic network consisting of 24 broadband seismographs was deployed in Vietnam in a cooperative effort between the Vietnam Institute of Geophysics and the Institute of Earth Sciences at Academia Sinica in Taiwan (*Huang et al., 2009*). However, there are a limited number of ground motion records for strong earthquake events in Vietnam. Thus, that is difficult to obtain the appropriate attenuation equations for *PGA* from the seismic records of strong earthquakes in the region.

Many researchers have used strong ground motion data from other regions to compensate for the lack of available local records in obtaining a predictive attenuation relationship. For example, *Campbell (1981)* used eight records from outside the United States; *Fukushima and Tanaka (1990)* used records from Japan and the United States; *Xiang and Gao (1994)* used records from Yunnan and the United States; etc. The prediction results are analyzed to investigate the fluctuations of attenuation relationships with magnitude, distance, and regional site effects. In the same manner, we attempt to establish a new set of appropriate attenuation relationships using data from shallow and strike-slip earthquakes in northern Vietnam and other countries for engineering application purposes. The correlation between the proposed relationship in northern Vietnam and other regions in the world is then discussed.

3.2 DATA SET AND ANALYSIS

Ground motion attenuation relationships can be obtained as functions of simple parameters that characterize the earthquake source, the propagation path between the earthquake source and the site and the geologic conditions beneath the site. Obtaining a reliable empirical relationship for peak ground acceleration with insufficient data is challenging. Following the research project of the Vietnam Institute of Geophysics (*VIG*) entitled “Research and forecasting earthquakes and foundation fluctuations in Vietnam,” chaired by Xuyen (*VIG, 2005*), recently concluded that Vietnam is classified as a low-to-moderate seismicity region and the maximum magnitude of earthquakes in Vietnam does not exceed 7.0 on the Richter scale in Vietnam (e.g., *Phuong, 1991*; *Trieu, 1997*; *Thuc, 2007*; etc.,.). According to the earthquake catalogue compiled by VIG, 90% of earthquakes in Vietnam were located in northwestern Vietnam.

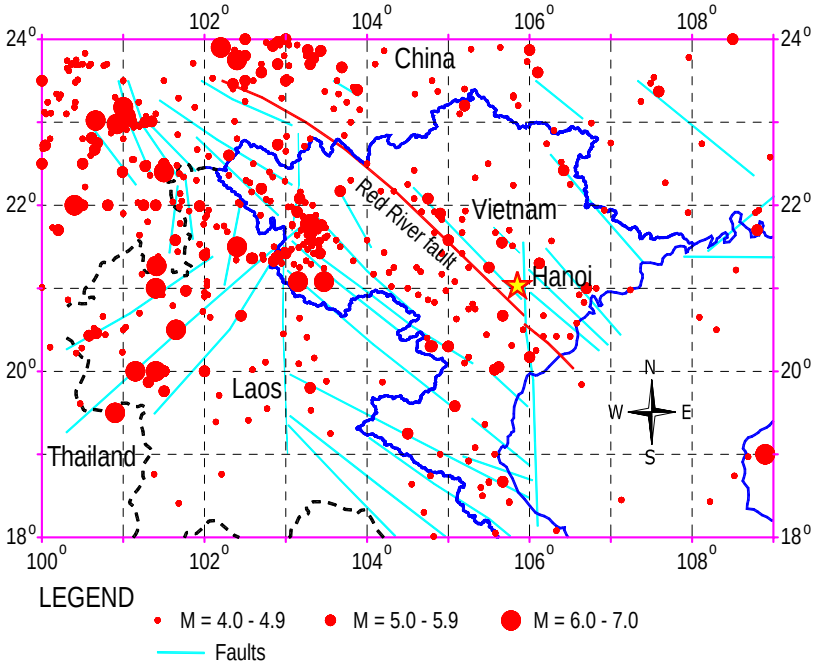

Figure 3.1 Earthquake epicenters and major faults in northern Vietnam and adjacent areas.

The epicenters of typical earthquake in northern Vietnam and adjacent areas with magnitudes of $M > 4$ are shown in **Fig 3.1**.

3.2.1 Database

To compensate for the lack of ground acceleration data in Vietnam, datasets are collected from different source earthquakes in northern Vietnam and other areas. It is important to note that the main faults of regions adjacent to northern Vietnam, such as northern Thailand, Myanmar, Laos and southern China, are also strike-slip faults (e.g., *Lacassin et al., 1998*; *Fenton et al., 2009*; Nielsen *et al., 2004*; *Socquet and Pubellier, 2005*). Therefore, earthquake activities in this region may be similar. Thus, strong motion data from Yunnan (China) is selected. The relevant earthquake parameters used in this analysis are listed in **Table 3.2**. However, these parameters are not sufficient for precise regression analysis for northern Vietnam and adjacent areas. For this reason, foreign ground motion data for shallow and strike-slip earthquakes in Japan have been added from Kyoshin Net (K-NET), which is operated by the National Research Institute for Earth Science and Disaster Prevention in Japan (NIED).

Additional criteria for deciding whether an earthquake should be included are as follows: (1) strike-slip earthquakes; (2) inland-type earthquakes; (3) M_w is not smaller than 3.5 and not larger than 7.0; (4) data were recorded on the ground surface; and (5) data were truncated at

an magnitude-dependent source distance (e.g., *Fukushima and Tanaka, 1990*; *Fukushima, 1997*) such that data from sites without high site amplification factors were also collected. A total of 737 strong motion records are selected from strike-slip earthquakes in Japan, Vietnam and Yunnan. All of the records in the database were obtained from shallow earthquake events in active tectonic regions. However, after applying criteria (5), 469 records are used in this study. The details of these records will be discussed in the following sections.

3.2.2 The selected data set

In this study, we adopted moment magnitude M_W and source distance X as the parameters for the base model. The surface wave magnitudes and moment magnitudes have been taken from the CMT catalogue for events occurring in Vietnam and adjacent areas between latitudes 18^0N to 25^0N and between longitudes 100^0E to 108^0E from 1977–2011 (shown in **Table 3.2**). **Fig 3.2** shows the relation between the moment magnitude (M_W) and surface wave magnitudes (M_S) based on earthquake records with M_S = 4.7 to 6.8 and M_W = 4.8 to 7.0 in Vietnam and adjacent regions. The relationship between M_W and M_S is expressed by **Eq. (3.1)**. Thus, for the earthquake records recorded with a surface wave magnitude of M_S, this magnitude was converted to M_W according to empirical equation **(3.1)**.

$$M_W = 1.0899\, M_S - 0.5332 \qquad (3.1)$$

Numerous records are collected from K-NET, but records with significant distances must be truncated because the signal-to-noise ratios are very small. Thus, we ignored the signal-to-noise ratio, as suggested by *Fukushima and Tanaka (1990)* and *Fukushima (1997)*.

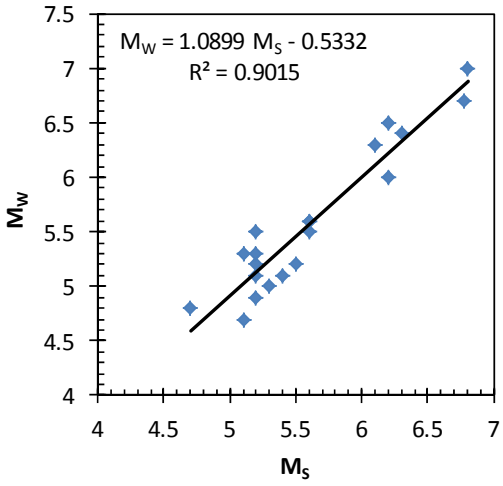

Figure 3.2 The relationship between M_S and M_W.

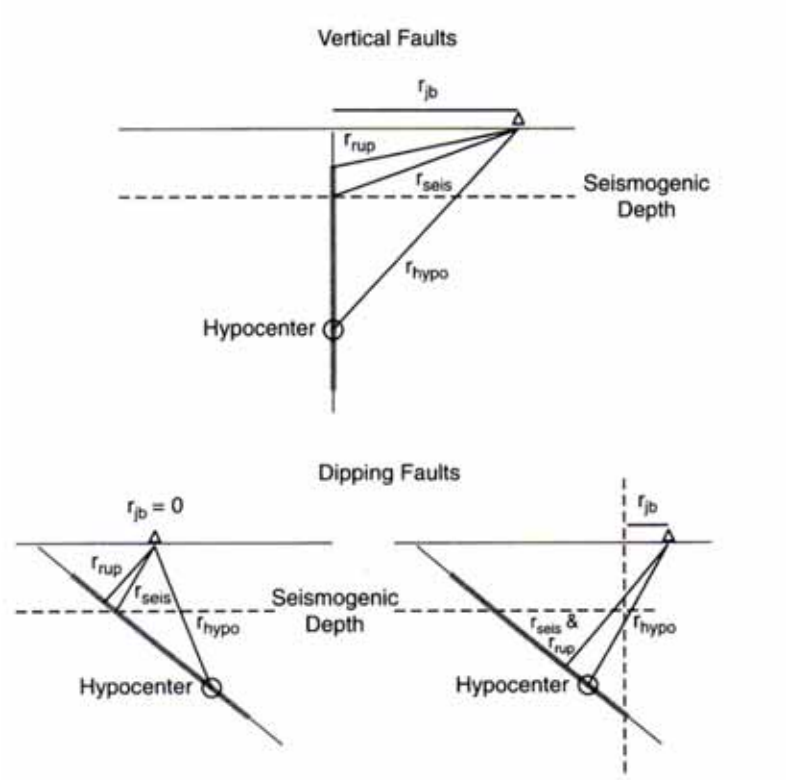

Figure 3.3 Site-to-source distance measures for ground motion attenuation models.

The distance limitation is characterized by the following relationship the between moment magnitude and source distance:

$$a\,M \;-\; \log\,X \;-\; b\,X \;+\; c \;\geq\; \log\,10 \qquad (3.2)$$

Where M is the moment magnitude, X is the source distance. The variables a, b, and c are regression coefficients. The values of the coefficients are shown in **Table 3.4**.

The data used in this analysis represent main shocks (see **Table 3.1)**; a few records from the aftershocks of the Dien Bien earthquake (2001) were included as shown in **Table 3.3** (the original data were obtained from the VIG).

Fig 3.3 illustrates site-to-source distance measures. The distribution of the magnitudes with both hypo-central (R_{HYPO}) and Joyner-Boore distances (R_{JB}) in this data set are shown in **Fig 3.4**. "▲-type" points are events in Vietnam and adjacent areas, "♦-type" points are events in Japan, "□-type" points are full records in Japan and "○-type" points are full records in Vietnam and adjacent areas.

Finally, records with earthquake magnitudes M_w ranging from 3.0 to 6.9 and source distances up to 300 km were used as a data set in this study.

3.2.3 Distance correction

Different researchers use different source-to-site distance measures. Herein, the hypocentral distance is taken by the epicentral distance and focal depth to represent the source-to-site distance. The closest distance to the rupture zone (known as Joyner-Boore distance, R_{JB}, shown in *Joyner and Boore, 1981*) is also used because this distance is smaller than the epicentral distance ($R_{JB} < R_{EPI}$) and recent attenuation relations are used R_{JB} to consider source size (e.g., *Boore and Atkinson, 2007*; *Mandal et al., 2009*; *Sharma et al., 2009*). In this study, we converted R_{EPI} to R_{JB} based on the relationship is suggested by *Montaldo et al. (2005)* as shown in **Eq. 3.3**). This relationship is based on European data and has an extremely high correlation coefficient ($R^2 = 0.95$).

$$R_{JB} = -3.5525 + 0.8845\, R_{EPI} \tag{3.3}$$

3.2.4 Site geology

The effect of geologic and local soil conditions underlying seismographs can significantly influence the characteristics of the ground motion. Ground motion models typically contain a scaling parameter based on site classification (*Boore et al., 1997*) include presented different models for "rock" and "soil" sites (*Campbell, 2003*; *Sadigh et al., 1997*). The widely accepted method for reflecting the effects of geological conditions on ground motion is to classify the recording stations according to their average shear-wave velocities in the upper 30 m (*Graizer and Kailkan, 2007*). V_{s30} was recommended as a means of classifying sites for some codes. It was selected for the NEHRP seismic design provisions, EC8 and LRFD seismic bridge design. The comparison between the seismic codes of the site classification scheme is presented in **Table 3.6**. *Boore (2004)* presented a relationship between V_{s30} and shallower velocities that significantly reduced the bias for shallow models compared to the simple method, which assumed that the lowermost velocity extends to 30 m (shown in **Eq. 3.4**). The shear-wave velocity data set of K-Net does not reach 30 m and instead lies between 10 and 20 m. Thus, these relationships will be used to convert the shallower velocities to V_{s30} according to *Boore (2004)*.

$$\log V_{s30} = a + b \log V_s(d) \tag{3.4}$$

Where $V_s(d)$ is the shear-wave velocity (m/s) at depth d; a and b are the regression coefficients (referring to those of *Boore, 2004*).

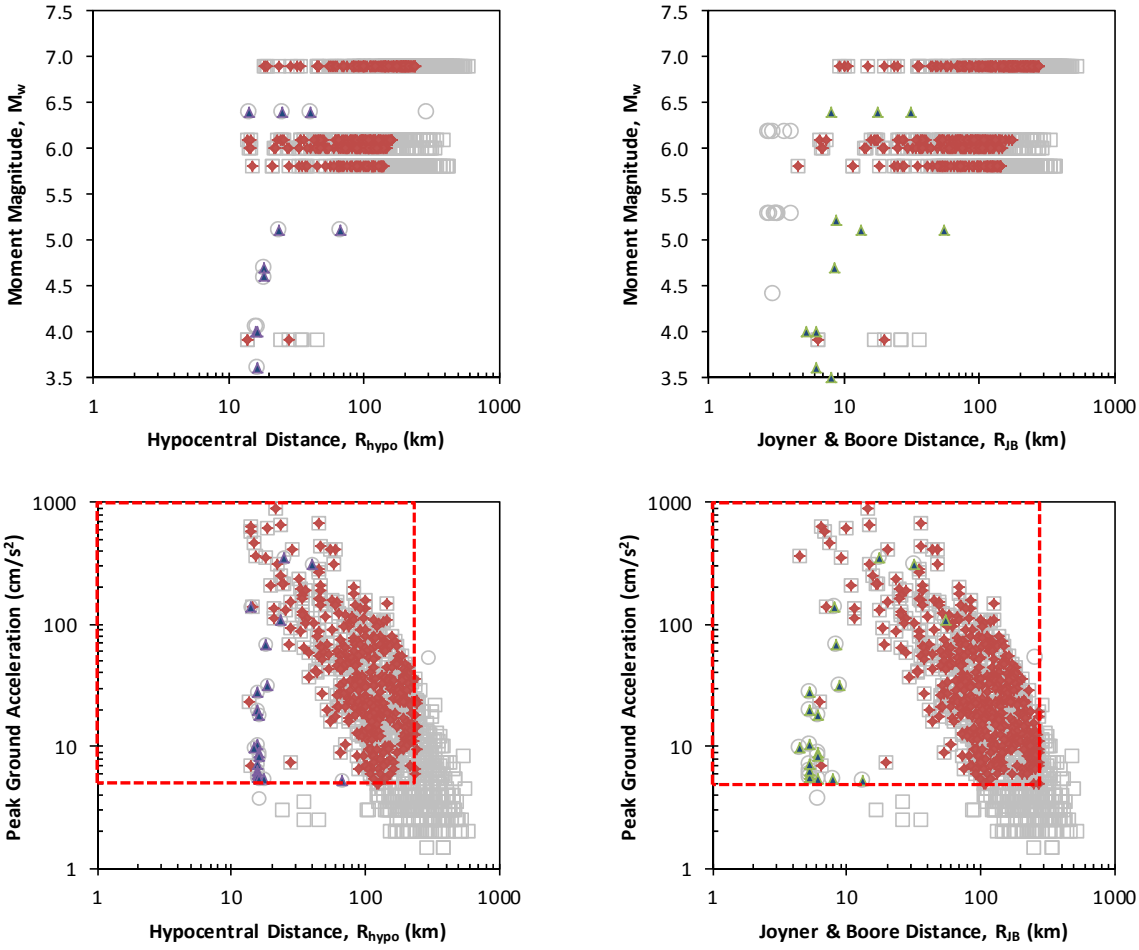

Figure 3.4 Distributions of magnitude with hypocentral (left figure) and Joyner-Boore distances (right figure).

Table 3.1 The events used to develop the attenuation relationship.

No.	Date (yyyy/mm/dd)	Location	Epicenter Coordinates		Magnitude			Depth (km)	Distance Range (km)	Number of Data	PGA Range (cm/s^2)		
			Latitude	Longitude	M_{JMA}	M_s	M_w				N-S	E-W	U-D
1 [8]	1997/03/26	Kagoshima Pref.	32.00	130.40	6.3		6.1 [1]	8	11 ~ 381	122	1 ~ 727	2 ~ 542	1 ~ 246
2 [8]	1997/05/13	Kagoshima Pref.	32.00	130.30	6.2		6.0 [2]	8	11 ~ 333	109	2 ~ 902	2 ~ 901	1 ~ 188
3 [8]	1997/06/25	Yamaguchi Pref.	34.50	131.70	6.1		5.8 [2,3]	12	9 ~ 420	174	2 ~ 421	2 ~ 299	1 ~ 145
4 [8]	1997/06/26	Yamaguchi Pref.	34.40	131.70	3.7		3.9 [3]	8	11 ~ 45	7	3 ~ 29	2 ~ 7	1 ~ 8
5 [8]	2000/10/06	Tottori Pref.	35.30	133.30	7.3		6.9 [4]	11	14 ~ 592	303	2 ~ 528	2 ~ 817	1 ~ 171
6	2001/02/19	Laos-Vietnam border	21.37	102.89		5.3	5.1 [5]	12	19 ~ 66	2	6 ~ 109	4 ~ 106.8	3 ~ 89.97
7 [7]	2007/06/03	Yunnan	23.00	101.06		6.4	6.4 [6]	5	13 ~ 294	4	58 ~ 431	49 ~ 267	23 ~ 157

Note:
[1] Harvard Global CMT
[2] F-Net
[3] Izutani and Kanamori, 2001
[4] USSG
[5] Van, 2006
[6] Xu *et al*., 2009
[7] Zhong *et al., 2008*
[8] K-NET

Table 3.2 Earthquakes used in calculating Equation (3.1).

No.	Events	Location	Lat.	Lon.	M_W	M_S	References
1	2001/02/19	Dien Bien, Vietnam	21.34	102.85		5.3	Trieu (2001)
					5.1		Van (2006)
2	1983/06/24	Tuan Giao, Vietnam	21.71	103.43	6.8	6.7	Thuc (2007)
3	1978/08/02	Southeast Asia	20.26	100.51	5.2	5.2	
4	1979/03/15	Yunnan	23.24	101.61	6.0	6.2	
5	1981/09/19	Yunnan	22.84	101.54	5.3	5.2	
6	1982/06/01	Burma-China border region	21.97	102.36	5.5	5.2	
7	1982/10/27	Yunnan	23.97	105.85	5.2	5.1	
8	1983/06/24	Southeast Asia	21.85	103.67	6.2	6.5	
9	1983/07/15	Southeast Asia	21.93	103.29	5.3	5.0	
10	1988/11/27	Burma-China border region	22.70	100.17	5.5	5.2	
11	1989/06/16	Southeast Asia	20.61	102.61	5.6	5.5	
12	1993/01/26	Yunnan	22.86	100.88	5.6	5.6	
13	1995/04/24	Yunnan	22.88	103.16	5.2	4.9	
14	2000/01/19	Southeast Asia	19.92	101.33	5.4	5.1	
15	2001/07/09	Yunnan	24.89	101.25	5.1	4.7	
16	2007/05/16	Laos	20.52	100.89	6.3	6.4	
17	2007/06/02	Yunnan	23.02	101.13	6.1	6.3	
28	2007/06/23	Myanmar-China border region	21.49	100.00	5.6	5.6	
19	2010/12/30	Laos	20.86	103.42	4.8	4.7	
20	2011/03/24	Myanmar	20.65	100.06	6.8	7.0	

Global CMT Catalog

Table 3.3 A aftershocks of the Dien Bien earthquake (2001; 21°33'N, 102°84'E).

No.	Date (yyyy/mm/dd)	Magnitude		PGA Range (cm/s^2)			Distance (km)	Number of Data
		M_S	M_W	N-S	E-W	U-D		
1	2001/02/19	3.0	2.7	5.314	7.265	6.759	10	1
2	2001/02/19	3.1	2.8	5.92	8.678	6.771	10	1
3	2001/02/19	3.3	3.1	8.311	12.26	11.66	10	1
4	2001/02/19	4.2	4.0	14.82	21.76	19.7	11	1
5	2001/02/19	4.8	4.7	61.68	74.59	42.45	13.5	1
6	2001/02/19	3.0	2.7	3.259	4.16	3.01	11	1
7	2001/02/21	3.8	3.6	7.306	10.49	9.127	11	1
8	2001/02/22	3.4	3.2	18.37	22.09	17.21	10	1
9	2001/02/23	3.2	3.0	6.73	10.28	13.76	11	1
10	2001/02/23	3.1	2.8	3.78	7.19	8.66	11	1
11	2001/02/24	4.2	4.0	28.26	27.15	21.26	10	1
12	2001/03/04	4.7	4.6	21.14	42.6	30.95	14	1
13	2001/03/04	3.4	3.2	5.26	6.13	5.26	10	1
14	2001/03/05	3.5	3.3	4.88	6.89	5.36	10	1
15	2001/03/04	3.2	3.0	7.37	12.44	12.83	9	1
16	2001/03/04	3.7	3.5	5.16	5.836	5.266	13	1

Note: M_S converted to M_w according to the empirical equation (3.1).

Table 3.4 Criterion coefficient in Equation (3.2)

Type of distance		*a*	*b*	*c*
Hypocentral distance	R_{HYPO}	0.401	0.002	1.1
Joyner and Boore distance	R_{JB}	0.379	0.001	1.1

Table 3.5 V_{s30} values with the NEHRP site classification

Site class	A	B	C	D	E
Number of records	8	114	253	83	9
Median category velocities (m/s)	1944	946	525	280	147

Table 3.6 Classification of ground conditions

LRFDSEIS-1, 2009/ NEHRP (U.S.)		EC 8 (Europe)/ TCVN 375-2006 (Vietnam)		AASHTO LRFD 1998/ 22TCN 272-05 (Vietnam)		JRA-2002 (Japan)	
Class	V_{S30} (m/sec)	Class	V_{S30} (m/sec)	Class	V_{S30} (m/sec)	Class	T_g (sec)
A	> 1500	-	-	-	-	-	-
B	760~1500	A	> 800	I	N/A	I	$T_g < 0.2$
C	360~760	B	360~800	II	N/A	II	$0.2 \leq T_g \leq 0.6$
D	180~360	C	180~360	III	N/A	III	$0.6 \leq T_g$
E	< 180	D	< 180	IV	N/A	-	-

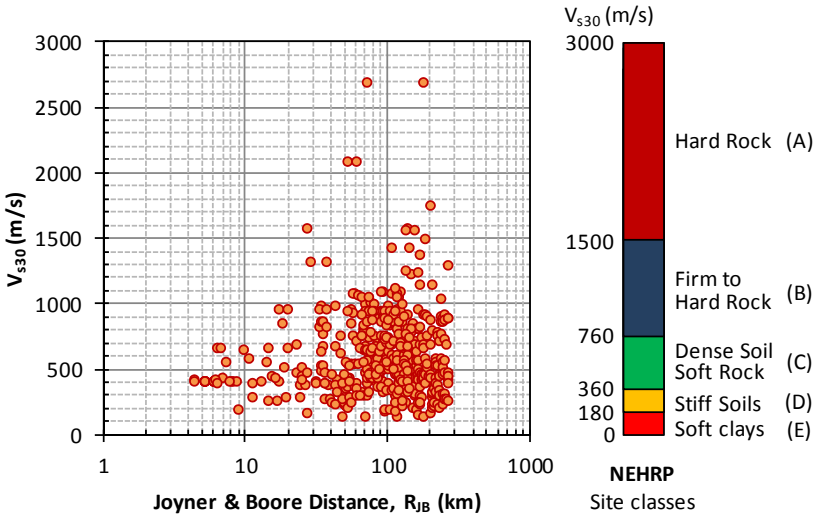

Figure 3.5 Earthquake data distribution with respect to V_{s30} and its compareison with the NEHRP site classes.

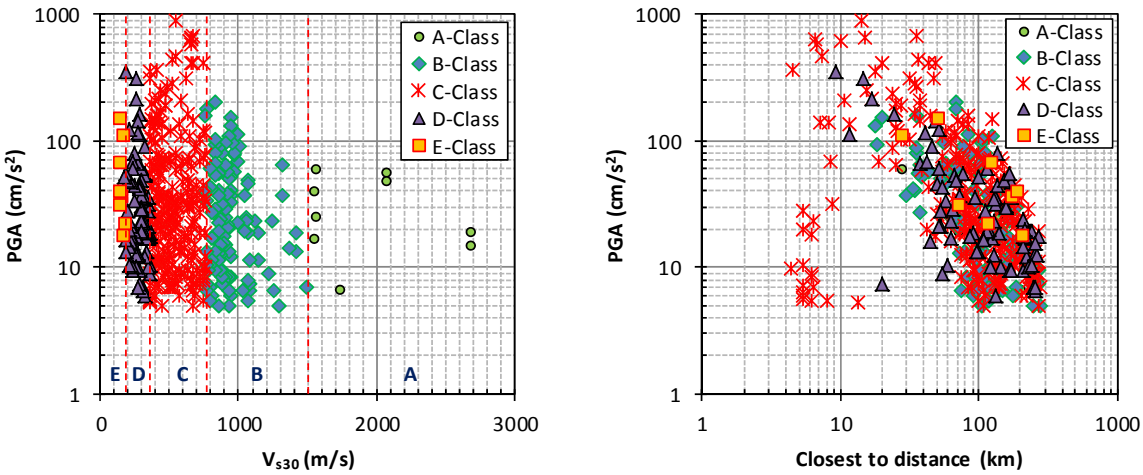

Figure 3.6 Destination of the NEHRP site classes for the data set used in this study.

The shear-wave velocity profiles available at each K-NET recording site were used to classify the sites according to their NEHRP class (**Table 3.6**). The NEHRP site class is based on the shear-wave velocity time averaged over the top 30 m of the soil profile (shown in **Figs 3.5** and **3.6** and **Table 3.5**). For the K-NET sites, soil profiles are typically only available for the top 10 or 20 m. *Boore (2004)* assumed that the velocity obtained at the deepest available level of the profile (10 or 20 m) continues at a constant value to a depth of 30 m. Thus, we used *Boore (2004)*'s relationships to extrapolate the velocity profiles from 10 or 20 m down to 30 m to obtain the appropriate average velocity over 30 m.

3.3 ATTENUATION MODEL AND REGRESSION METHOD

Since the 1970s, peak ground motion attenuation relations have typically been represented by logarithmic empirical equations. In general, a term for the saturation of acceleration amplitude at the short distances must be described as a function of magnitude for shallow earthquake events (e.g., *Trifunac, 1976*; *Campbell, 1981*; *Fukushima and Tanaka, 1990*; *Youngs et al., 1997*; *Abrahamson and Silva, 1997*; *Sadigh et al., 1997*; *Campbell, 2003*; etc.). Recent attenuation relationships have been developed not only shallow earthquake events that consider focal depth (e.g., *Kanno et al., 2006*) but also strike-slip faults (e.g., *Ambraseys et al., 2005*; *Campbell and Bozorgnia, 2007*; *Zhao et al., 2006*; *Graizer and Kalkan, 2007*). Several of the available attenuation relations consider the different source categories. These relationships can typically be separated into three categories, i.e., shallow and crustal earthquakes, subduction interface events and subduction intraplate events, based on their tectonic locations (*Si and Midorikawa, 2000*). *Kanno et al. (2006)* also divided regression models into shallow (a focal depth of 30 km or less) and deep (a focal depth of more than 30

km) events because the ground motion amplitudes from earthquakes with focal depths greater than 30 km were considerably different from those of shallower events. This model may cover a wide data distribution range and is thus selected in this study as shown in **Eq. (3.5)**.

$$\log A = a M_W + b X - \log (X + d \square 10^{eM_W}) + c + \varepsilon \qquad (3.5)$$

Where A is the ground motion parameter (peak ground acceleration [PGA] in cm/s^2), M_w is the moment magnitude; X is the closest distance to the projection of fault in km (here, we have used the approximate values which were converted into R_{JB} from R_{EPI} according to **Eq. (3.3)**, from now called "closest distance"); a, b, and c are the regression coefficients to be determined; ε is the error between observed and predicted values. To make the regression analysis of corrected PGA, e-value of 0.5 was set according to *Si and Midorikawa (2000)*; *Takahashi et al. (2004)*; and *Kanno et al. (2006)*. The style of faulting scaling was not considered in **Eq. (3.5)** because all earthquake records in this study were strike-slip earthquakes type.

3.4 RESULT AND EVALUATION

3.4.1 Results of the regression analysis

To see clearly the influence of earthquake data to the results of the regression analysis, three cases are selected for consideration in this study. Case 1 uses the entire ground motion data, including those from Japan, Vietnam and Yunnan. Case 2 only uses ground motion data from Japan and Case 3 uses ground motion data from Vietnam and Yunnan. The most suitable formula and dataset for predicting PGA in northern Vietnam will then be discussed. In this study, two stage regressions are used. In the first stage, the dependency of magnitude and source distance on the attenuation characteristics was evaluated; in second stage, site effects were incorporated. The coefficients used in the median attenuation equation in the first stage were determined via nonlinear regression analysis. **Table 3.7** lists coefficients a, b, c and e from the regression analysis. **Figs 3.7**, **3.8** and **3.9** illustrate PGA attenuation curves corresponding to the first stage. The residual PGA plots in this stage are presented in these figures for the full data set as functions of the closest distances and magnitudes. These plots illustrate that the predicted values are found with respect to the closest distances and magnitudes, and no significantly different trends are observed. This result may indicate that these parameters are independent of the total residuals.

In this section, we attempted to calculate the attenuation relationships for three cases with the smallest standard error based on the available database. The aim of these cases is to consider the influence of the database on the attenuation models, especially due to the

insufficient data for Vietnam. It is interesting to note that the regression errors obtained in the three cases are not significantly different as shown in **Table 3.7**. The error for case 3 is smaller than those for cases 1 and 2. These regression errors indicate the level of uncertainty related to the database. However, in all three cases, the influence of the variance is small in comparison to the regression error. This conclusion is confirmed in **Fig 3.10**, where the prediction ranges for the three cases are compared. **Fig 3.10** also shows that the predicted PGA of case 3 is smaller than those of cases 1 and 2. All of the relations show stable low residuals, which indicate the strength of our relationships because different relationships are based on different datasets. The consequence of this observation is that the uncertainties related to the strong earthquake data in other regions have a negligible contribution to the errors in the derived relationships. This result demonstrates the validity of the selection assumption made in section **3.2.1**. With the data currently available from Vietnam and adjacent regions, the proposed attenuation relationship in northern Vietnam can be predicted; however, this relationship will not be particularly reliable. Thus, adding strong motion data from Japan is very important for predicting approximate attenuation relations. In this respect, we see that the relationship obtained from the regressions for Vietnam and adjacent regions and Japan for strike- slip earthquakes are similar.

3.4.2 Effect of shallow site conditions

Recent attenuation models for shallow crustal earthquakes use the effects of shallow site conditions based on the V_{s30} using predictive equations (e.g., *Boore and Atkinson, 2007*; *Boore et al., 1997*; *Campbell and Bozorgnia, 2007*; *Chiou and Youngs, 2008*; *Kanno et al., 2006*; *Graizer and Kalkan, 2007*) based on an empirical geotechnical model with linear or nonlinear site effects. In this study, the database consists of five site categories corresponding to classes E, D, C, B and A in the NEHRP site categories. *Choi and Stewart (2005)* indicated that the nonlinearity of amplification factors was significant for $V_{s30} < 180$ m/s and relatively small for $V_{s30} > 300$ m/s. Less than 2% of the stations in our database have $V_{s30} < 180$ m/s; thus, the nonlinearity influence of the amplification factors on the resultant attenuation model would be minimal (*Graizer and Kalkan, 2007*).

Table 3.7 Regression coefficients of Equation (3.5)

Database	*a*	*b*	*d*	*e*	*c*	*ε*
All	0.588	-0.003	0.005	0.5	0.01	0.263
Japan	0.590	-0.003	0.005	0.5	0.01	0.263
Vietnam and Yunnan	0.565	-0.002	0.005	0.5	0.01	0.250

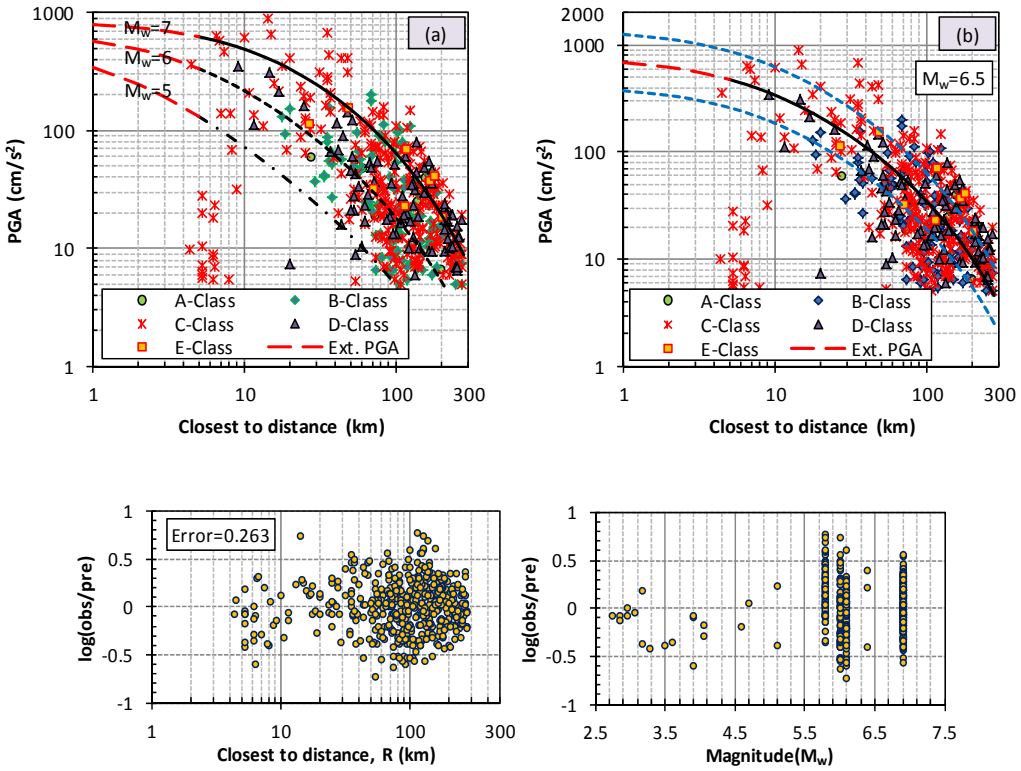

Figure 3.7 Attenuation curves of PGA for Case 1: a) M_w = 5, 6 and 7; b) M_w = 6.5..

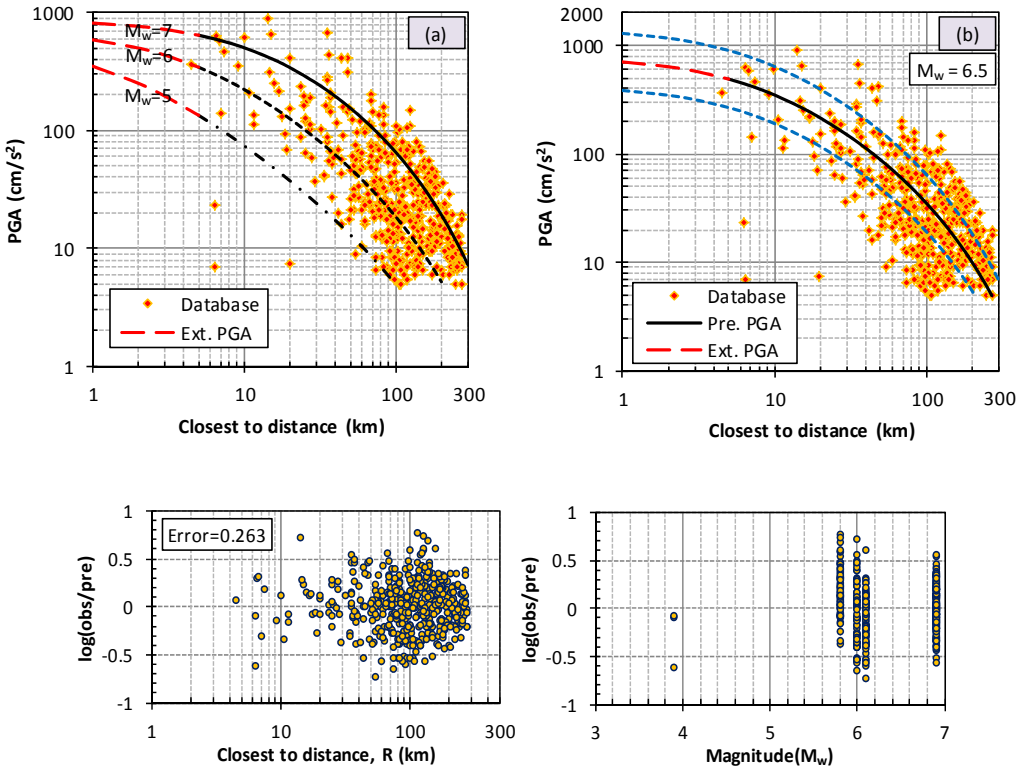

Figure 3.8 Attenuation curves of PGA for Case 2: a) M_w = 5, 6 and 7; b) M_w = 6.5.

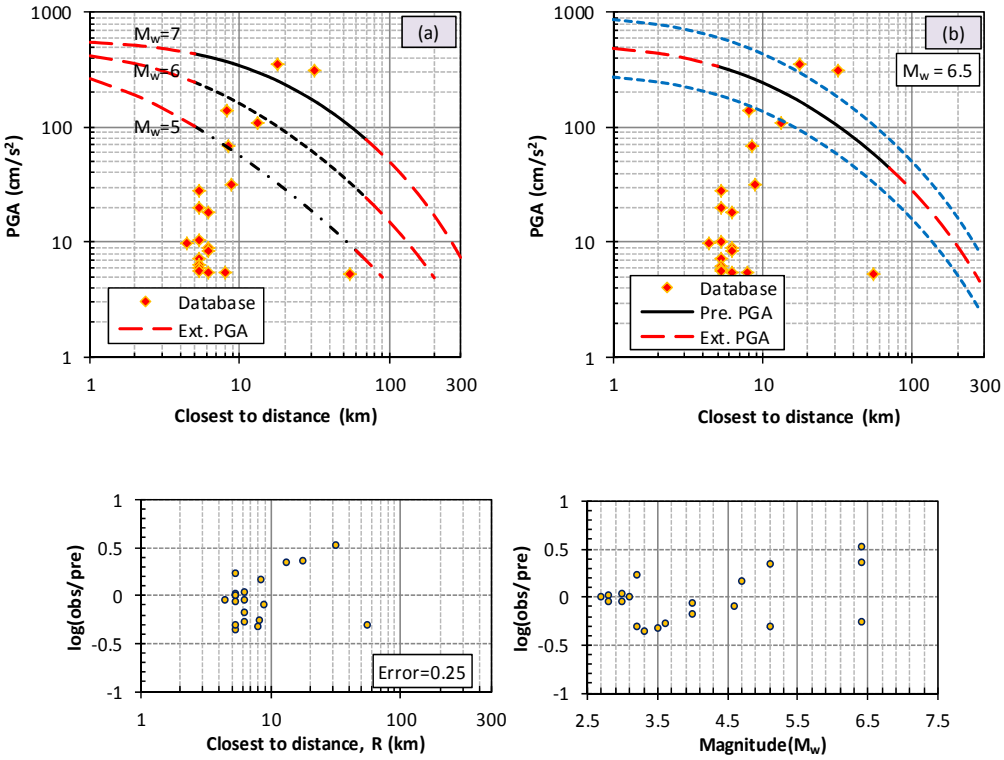

Figure 3.9 Attenuation curves of PGA for Case 3: a) M_w = 5, 6 and 7; b) M_w = 6.5.

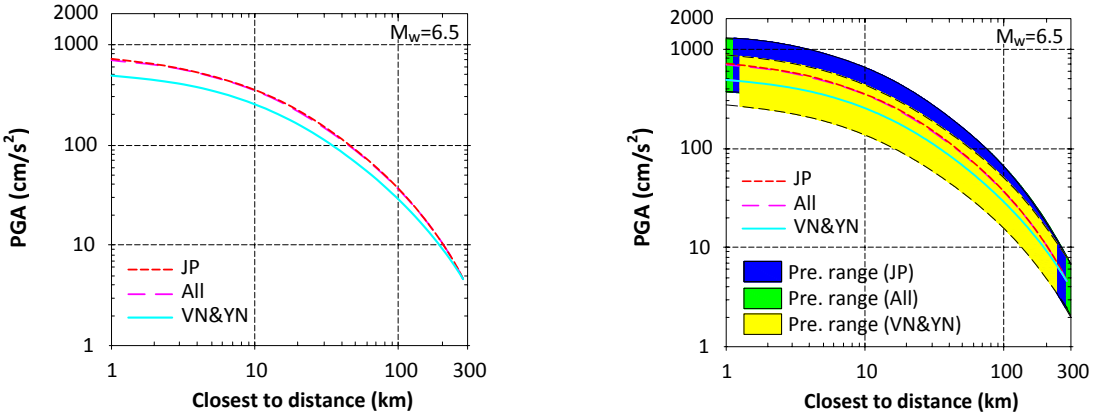

Figure 3.10 Comparison among three cases of attenuation curves (left figure) and comparison of prediction ranges for standard errors (right figure). All is data from Japan, Vietnam and Yunnan; JP is data from only Japan; VN&YN is data from Vietnam and Yunnan.

Therefore in order to calculate the effective site conditions, we decided to use linear scaling for site correction. In this study, we used V_{s30} to characterize site effects using correction formula as follows:

$$G = \log(obs / pre) = p \log V_{s30} + q \qquad (3.6)$$

Equation **(3.6)** can be written as follows:

$$G = p \log\left(V_{s30} / V_{ref}\right) \tag{3.7}$$

where G is the equivalent form of the linear site correction expression provided by *Boore et al. (1997)* and coefficients p and q are derived by using a regression analysis on the residuals averaged at 100-m/s intervals in V_{s30} (*Kanno et al., 2006*). Coefficient V_{ref} is equal to $10^{(-q/p)}$. We determined that the coefficients p and q in **Eq. (3.6)** were -0.209 and 0.559, respectively, as shown in **Fig 3.11**. This figure shows the relationship between averaged residuals and V_{s30}. In the linear site amplification formula suggested by *Boore et al. (1997)*, coefficient p is similar to b_v, and V_{ref} is similar to V_A as shown below.

$$F_{site} = b_v \ln \left(V_{s30} / V_A\right) \tag{3.8}$$

where b_v = -0.371 and V_A = 1396.

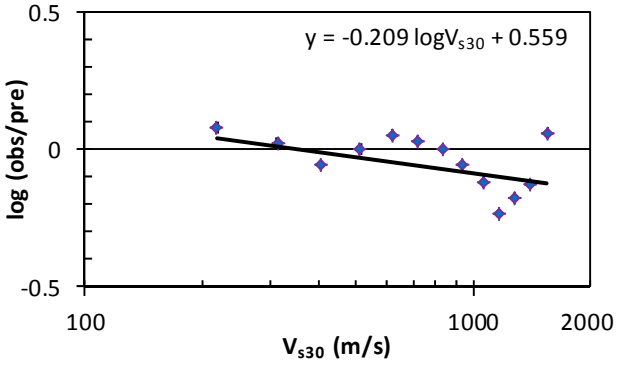

Figure 3.11 The relationship between the residuals and V_{s30}.

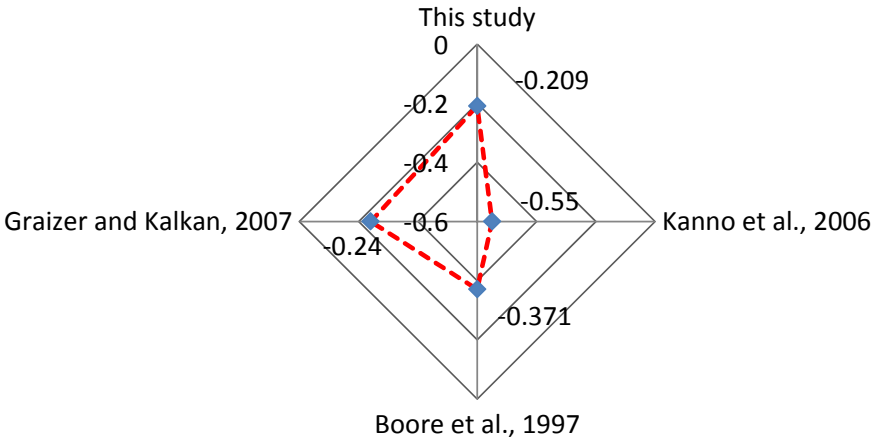

Figure 3.12 Comparison of p (or b_v) coefficients in the site correction.

This study estimated coefficients of -0.209 and 472.8 ($=10^{(-0.559/-0.209)}$); these values are fairly similar to the values of -0.24 and 484.5 obtained by *Graizer and Kalkan (2007)*, possibly because the study of those used a database with shallow earthquakes occurring in strike-slip faults. **Fig 3.12** shows the coefficients of p (or b_v) in some previous studies. The p (or b_v) coefficients in this study is generally lower than those determined by *Boore et al. (1997)* and *Kanno et al. (2006)* (see **Fig 3.12**). This difference is due to the use of different databases or different methods for estimating the the site effects through V_{s30}. The influence of site effect on the resultant attenuation curves is demonstrated in **Fig 3.13**. This figure also compare the predicted PGA attenuations to M_w for V_{s30} = 360 m/s.

The predicted PGA values after applying the site correction can be simply interpreted as follows:

$$\log(PGA) = \log(A) + G \tag{3.9}$$

3.4.3 Final attenuation equation

The final attenuation model is rewritten in **Eq. (3.10)** as a form of **Eq. (3.9)**. Its estimator parameters were found using two-stages of regression on a compiled data set. The standard error of the relationship was calculated to be 0.26. The symbols used in **Eq. (3.10)** have been explained in previous sections.

$$\log(PGA) = 0.59\,M_w - 0.003\,X - \log(X + 0.005\cdot 10^{0.5M_w}) + 0.01 - \\ - 0.209\,\log\left(\frac{V_{s-30}}{472.8}\right) \pm 0.26 \tag{3.10}$$

The resulting PGA attenuation relationships are plotted in **Fig 3.14** for the horizontal component in the stiff soil and the dense soil site with average shear velocities approximately 300 m/s (for soil sites) and 600 m/s (for dense soil sites), respectively. These V_{s30}-values correspond with site conditions in northern Vietnam. The performance of the relationship is also presented in terms of residuals. Residuals plots of PGA in this stage for the full data set as functions of closest distance, magnitude and V_{s30} are presented in **Fig 3.15**; the same remarks apply as for the first stage.

3.4.4 Comparison with previous studies and the recorded data

The estimated PGA attenuation curves from the equation derived in this study were compared with the commonly used attenuation relationships of *Boore et al. (1997), Campbell (1997), Sadigh et al. (1997), Si and Midorikawa (2000), and Ambraseys et al. (2005)*. The available equations of *Xuyen and Thanh (1999)* for Vietnam and *Xiang and Gao (1994)* for

Yunnan, China, which is close to northern Vietnam, are also used for comparison. Similar to this study, these relationships represent a seismically active and shallow crustal tectonic environment. All of the aforementioned relationships are applicable to the stiff soil and dense soil sites. Some of the relationships used the average shear wave velocity in the top 30 m, V_{s30}, as site parameters. These comparisons are plotted in **Fig 3.16**. In these plots, we have used values of 300 m/s and 600 m/s to present generic stiff soil and generic dense soil or soft rock, respectively. Magnitude M_w = 5.1 and 6.5 were used in these cases because this level occur frequently in Vietnam. **Fig 3.16** illustrates several ground motion predictions at the magnitudes of 5.1 and 6.5 from our attenuation relationship and the relationships established for other countries. The predicted PGA attenuation for shallow strike-slip earthquake events based on our study is approximately similar to those predicted by previous studies. The results are slightly less than those of the available relationship for Vietnam (suggested by *Xuyen and Thanh, 1999*) for the distances from 10 to 100 km. Our relationship is more accurate than *Xuyen and Thanh (1999)*'s relationship at distances of less than 10 km and more than 100 km.

The proposed relationship is fairly similar to those of adjacent areas, such as Yunnan, China (suggested by *Xiang and Gao, 1994*), which used most of the Yunnan data from the main event and for aftershocks of the Luquan and Luncang-Gengma earthquakes, the magnitudes of which ranged from 3 to 5 and 10 to 40 km, respectively, for near-field predictions; the relationship used the United States data for far-field predictions.

In comparing our attenuation relationship with those of previous studies, *Si and Midorikawa (2000)*'s form is very close to ours at V_{s30} = 300 m/s and smaller than our relationship at V_{s30} = 600 m/s. The opposite tendencies occurred for the relationship of *Ambraseys et al. (2005)* (see **Figs 3.16a** and **3.16b**). However, these relationships have features that are similar to the predictions made using our relationship. Comparisons with the relationships of *Boore et al. (1997)*, *Campbell (1997)* and *Sadigh et al. (1997)* also reveal that they show similar features. Our relationship is different from the other relationships within the distance range of 10 to 100 km for both soil and dense soil conditions, possible due to the use of different databases, which is expected due to the site effects in our dataset or the different forms of those relationships. **Fig 3.16** also shows that the influence of site effects in our relationship is lower than those in other relationships, such as those of *Si and Midorikawa (2000)*, *Campbell (1997)* and *Sadigh et al. (1997)* because the site category mainly referred to stiff soil. The relationship of *Ambraseys et al. (2005)* used stiff soil ($180 < V_{s30} \leq 360$ m/s) and dense soil or soft rock ($360 < V_{s30} \leq 750$ m/s). The relationships of Xuyen and Thanh (1999) and Xiang and Gao (1994) did not have defined site conditions. Besides, the conversion faulting coefficient between faulting types (e.g. *Sadigh et al., 1997*, *Campbell and Bozorgnia, 2007*, etc.) may also cause differences in the relationships because we only considered the strike-slip fault type.

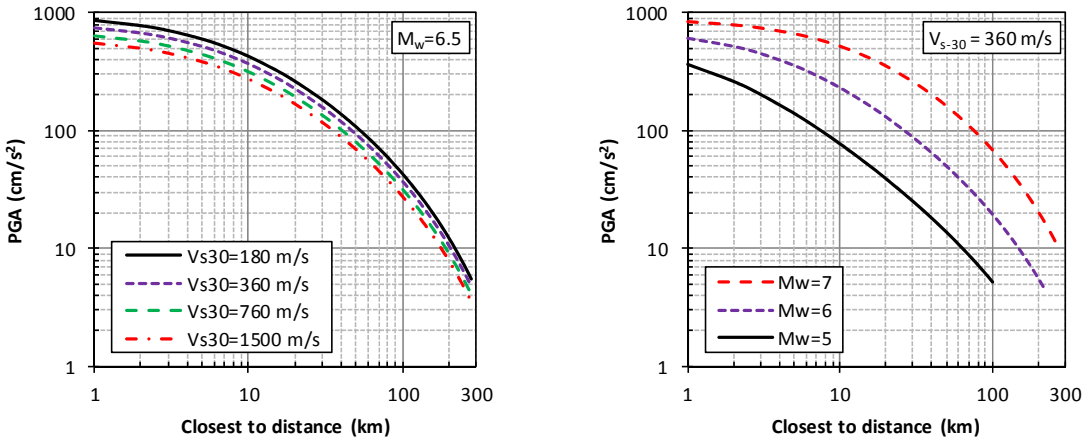

Figure 3.13 Plots of the PGA attenuation characteristics for various V_{s30} with M_w = 6.5 (left figure); comparison of predicted PGA attenuations for V_{s30} = 360 m/s (right figure).

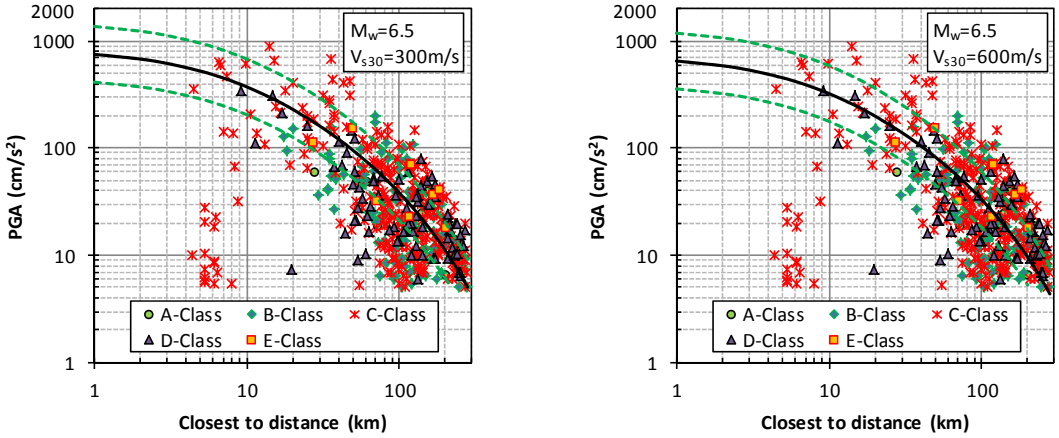

Figure 3.14 Comparison of the PGA attenuation curvers for M_w = 6.5 corresponding to V_{s30} = 300 m/s and V_{s30} = 600 m/s.

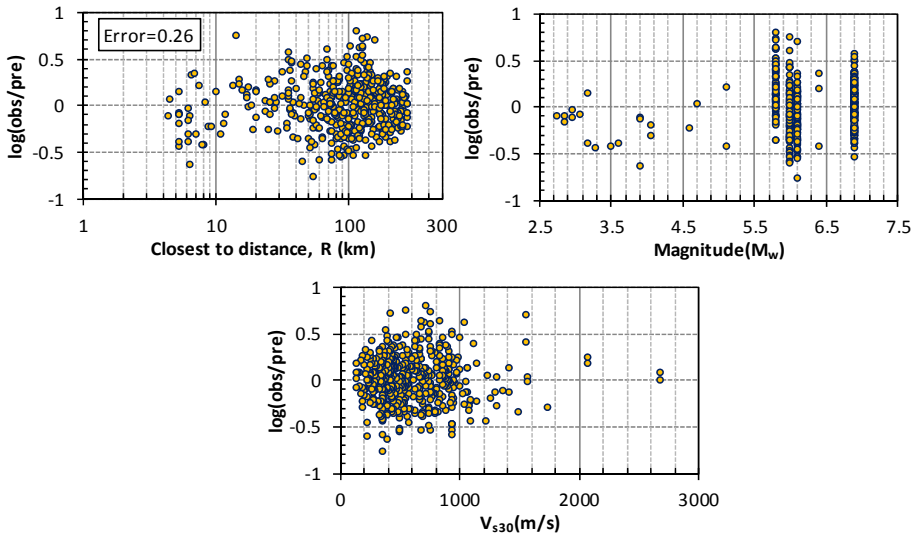

Figure 3.15 Residuals plots of PGA in the final equation.

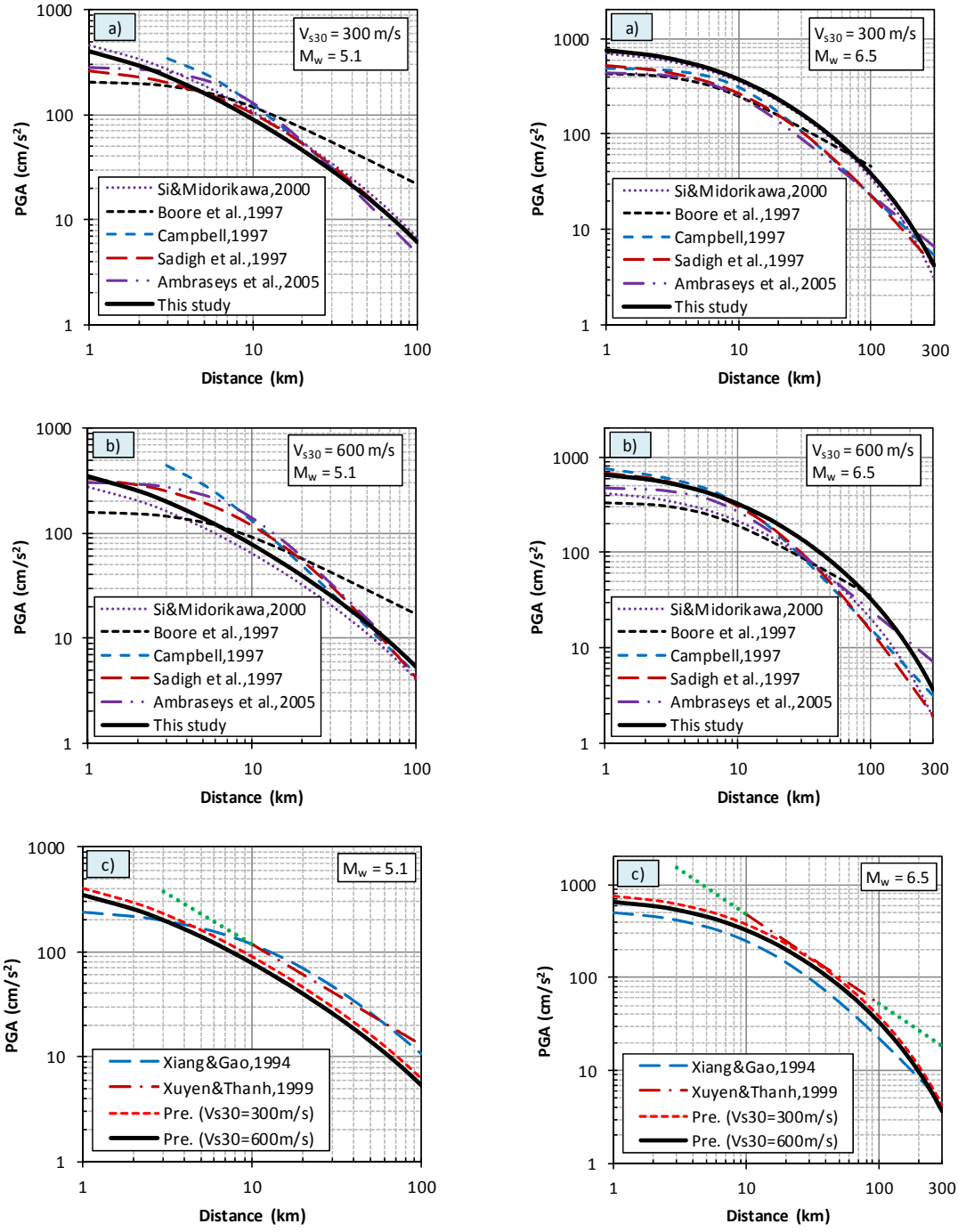

Figure 3.16 Comparison of the PGA attenuation curves for an M_w = 5.1 (left figure) and M_w = 6.5 (right figure) corresponding to V_{s30} = 300 m/s and V_{s30} = 600 m/s.

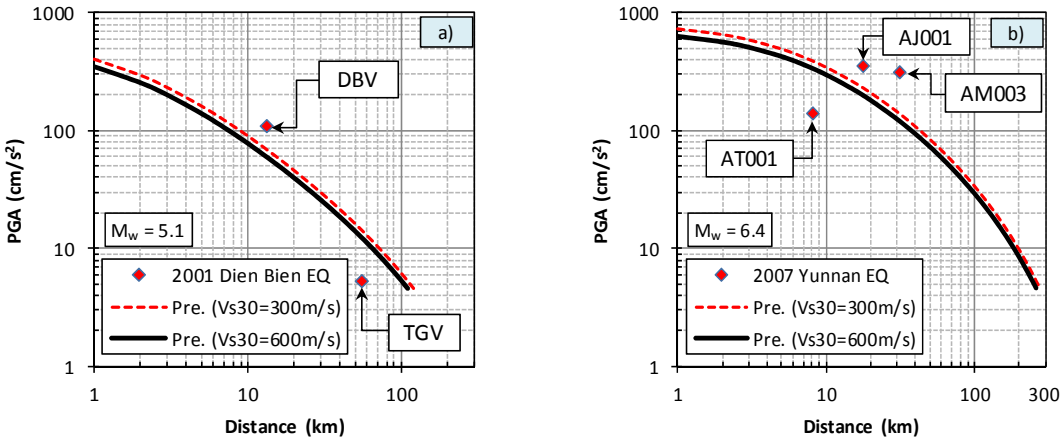

Figure 3.17 Comparison of the actual recorded data with our predictions.

In this comparison, the predicted PGA significantly differs with others, especially in the range of the near-source regions with M_w = 5.1 (see **Fig 3.16**) because the dataset is insufficient at that magnitude. Thus, the number of data for small earthquake evens should be increased, although the prediction of ground motion is less important in these instances. Furthermore, the performance of the proposed attenuation relationship is examined through comparisons with actual recorded data. **Fig 3.17** shows comparisons of our predictions with actual recorded PGA data from events in Vietnam and Yunnan. The left figure represents the Dien Bien earthquake (2001) in Vietnam. DBV and TGV are seismology stations at Dien Bien and Tuan Giao, respectively. The right figure represents the Ninger earthquake (2007) in Yunnan. AJ001, AM003 and AT001 are seismology stations at Dehue, Zhengxing and Mengxian, respectively. The figure also shows that our prediction is fairly consistent. The proposed relationship shows that the expected trend for rock amplitudes is smaller than that for soil amplitudes because ground motions at rock sites are smaller than those at soil sites. The site amplification in soil is higher than that in rock (shown in **Fig 3.16** and **3.17**). This trend is also shown by *Sadigh et al. (1997)*, *Graizer and Kalkan (2007)*, *Ambraseys et al. (2005)*, etc. We also compare our relationship to those of others in terms of residuals averaged at approxi- mately 5-km bins vs. the closest distance in **Fig 3.18**. The left figures represent stiff soil conditions and the right figures represent dense soil or soft rock conditions. The solid and dashed lines are the trends for our predictions and those of previous studies, respectively. Those residuals are then grouped into two categories, one corresponding to dense soil or soft rock conditions (V_{s30} = 600 m/s) and the other corresponding to stiff soil condition (V_{s30} = 300 m/s). We illustrate the trends in the results with linear fitted lines for the data in each category. The trend lines of our relation and those of previous studies are compared. **Fig 3.18** shows that almost all of the relationships are within the median residual range of ± 0.5. The slopes of our relationship differ from those of previous studies because our dataset contains only a small number of earthquake records below M_w = 5.5.

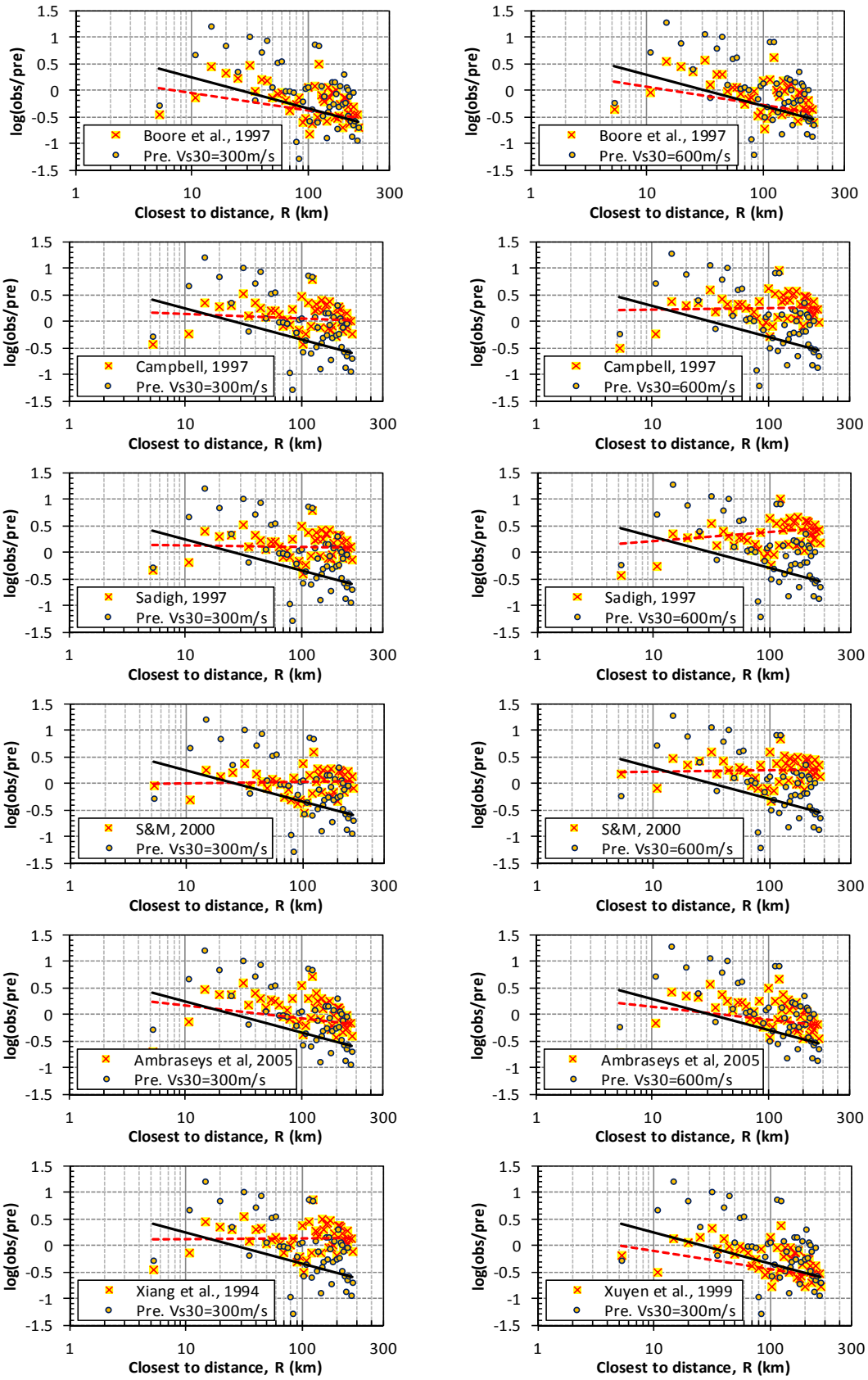

Figure 3.18 Comparison of the residuals averaged over 5-km bins corresponding to V_{s30} = 300 m/s and V_{s30} = 600 m/s.

3.5 CONSIDERATION

In this study, we have derived a new PGA attenuation relationship for northern Vietnam to replace the one currently used for Vietnam. The new relationship is developed for shallow strike-slip earthquakes using a regression technique for earthquakes within a magnitude range of $3.0 \leq M_w \leq 6.9$ and with source distances up to 300 km.

The properties of this new relationship are significantly different from those of the current relationship proposed for Vietnam by *Xuyen and Thanh (1999)* at near-field (less than 10 km) and far-field (more than 100 km) distances. Compared to the previous studies, the proposed relationship shows that estimation is well-defined and stable compared to current some relationships.

In this relationship, V_{s30} is adopted to estimate ground motion with linear site effects. Our relation is significantly different from the relationships by *Boore et al. (1997)* and *Kanno et al. (2006)* in terms of the coefficients for site correction but similar to the relationship by *Graizer and Kalkan (2007)*'s relationship. Furthermore, the attenuation relationships for strike-slip faulting earthquakes in the near and far-source regions are significantly influenced by local site conditions.

The standard error calculated with insufficient data from Vietnam and adjacent regions is close to that obtained using the data from Japan; the standard errors obtained before and after adding the effect of shallow site conditions are similar. Thus, the source parameters obtained using regressions for Vietnam, adjacent regions and Japan are similar for strike-slip earthquakes.

An analysis of the residuals shows that the distributions of the total residuals with respect to distance and magnitude are not biased. The analysis of the residuals within each site condition indicates that site conditions significantly affect ground motion amplitude.

3.6 REFERENCES

[1]. Abrahamson, N.A. and Silva, W.J. (1997). Empirical response spectral attenuation relations for shallow crustal earthquakes. *Seismological Research Letters,* Vol. 68(1), pp. 94-127.

[2]. Ambraseys, N.N., Douglas, J., Sarma, S.K. and Smit, P.M. (2005). Equations for the estimation of strong ground motions from shallow crustal earthquakes using data from Europe and the Middle East: Horizontal peak ground acceleration and spectral acceleration. *Bulletin of Earthquake Engineering*, Vol. 3(1), pp. 1–53.

[3]. Boore, D.M. (2004). Estimating $V_s(30)$ (or NEHRP site classes) from shallow velocity models (depths < 30 m), *Bulletin of the Seismological Society of America,* Vol. 94, pp. 591-597.

[4]. Boore, D.M. and Atkinson, G.M. (2007). Boore-Atkinson NGA Ground Motion Relations for the Geometric Mean Horizontal Component of Peak and Spectral Ground Motion Parameters, *PEER 2007/01*, Pacific Earthquake Engineering Research Center, Berkeley, California, 2007.

[5]. Boore, D.M. and Atkinson, G.M. (2008). Ground-motion prediction equations for the average horizontal component of PGA, PGV, and 5%-damped PSA at spectral periods between 0.01 s and 10.0 s, *Earth. Spec.,* Vol. 24(1), pp. 99-138.

[6]. Boore, D.M., Joyner, W.B. and Fumal, T.E. (1997). Equations for estimating horizontal response spectra and peak acceleration from western North American earthquakes: A summary of recent work, *Seismol. Research Letters*, Vol. 68, pp. 128-153.

[7]. Campbell, K.W. (1981). Near-source attenuation of peak horizontal acceleration. *Bulletin of the Seismological Society of America,* Vol. 71(6), pp. 2039-2070.

[8]. Campbell, K.W. (1997). Empirical near-source attenuation relationships for horizontal and vertical components of peak ground acceleration, peak ground velocity, and pseudo-absolute acceleration response spectra. *Seismol. Research Letters,* Vol. 68(1), pp. 154-179.

[9]. Campbell, K.W. (2003). Strong motion attenuation relationships, in *International Handbook of Earthquake and Engineering Seismology*. W. H. K. Lee, H. Kanamori, P. C. Jennings, and C. Kisslinger (Editors), Vol. 2, Chapter 60, 2003.

[10]. Campbell, K.W. and Bozorgnia, Y. (2007). Campbell-Bozorgnia NGA ground motion relations for the geometric mean horizontal component of peak and spectral ground motion parameters, *PEER Report 2007/02,* Pacific Earthquake Engineering Research Center, College of Engineering, University of California, Berkeley, 2007.

[11]. Chiou, B.S.-J. and Youngs, R.R. (2008). An NGA model for the average horizontal component of peak ground motion and response spectra. *Earthquake Spectra*, Vol. 24(1), pp. 173–215.

[12]. Choi, Y. and Stewart, J.P. (2005). Nonlinear site amplification as function of 30m shear-wave velocity. *Earthquake Spectra*, Vol. 21(1), pp. 1–30.

[13]. Fenton, C.H., Charusiri, P., Wood, S.H. (2009). Recent paleoseismic investigations in northern and western Thailand. *Anna Geophys,* Vol. 46, pp. 957-981.

[14]. Findlay, R.H. and Trinh, P. T. (1997). The Structural Setting of the Song Ma Region, Vietnam and the Indochina-South China Plate Boundary Problem. Gondwana Research, Vol. 1(1), pp. 11-33.

[15]. Fukushima, Y. (1997). Comment on "Ground motion attenuation relations for subduction zones," *Seism. Res. Lett.*, Vol. 68, pp. 947-949.

[16]. Fukushima, Y. and Tanaka, T. (1990). A new attenuation relation for peak horizontal acceleration of strong earthquake ground motion in Japan. *Bulletin of the Seismological Society of America*, Vol. 80(4), pp. 757-783.

[17]. Ghasemi, H., Fukushima. Y., Koketsu, K. and Miyake H. (2010). Ground-Motion Simulation for the 2008 Wenchuan, China, Earthquake Using the Stochastic Finite-Fault Method. *Bulletin of the Seismological Society of America,* Vol. 100(5B), pp. 2476-2490.

[18]. Graizer, V. and Kalkan, E. (2007). Ground motion attenuation model for peak horizontal acceleration from shallow crustal earthquakes. *Earth. Spec.*, Vol. 23 (3), pp. 585–613.

[19]. Huang, B.S, Son, L.T., Liu, C.C., Toan, D.V., Huang, W.G., Wu, Y.M., Chen, Y.G. and Chang, W.Y. (2009). Portable broadband seismic network in Vietnam for investigating tectonic deformation, the Earth's interior, and early-warning systems for earthquakes and tsunamis. *Journal of Asian Earth Sciences*, Vol. 36(1), pp.110-118.

[20]. Izutani, Y. and Kanamori, H. (2001). Scale dependence of seismic energy to moment ratio for strike-slip earthquakes in Japan. *Geophysical Res. Lett.*, Vol. 26 (20), pp. 4007-4010.

[21]. Joyner, W.B and Boore D.M. (1981). Peak horizontal acceleration and velocity from strong-motion records including records from the 1979 Imperial Valley, California, earthquake. *Bulletin of the Seismological Society of America*; Vol. 71(6), pp. 2011-2038.

[22]. Kanno, T., Narita, A., Morikawa, N., Fujiwara, H. and Fukushima, Y. (2006). A new attenuation relation for strong ground motion in Japan based on recorded data, *Bulletin of the Seismological Society of America,* Vol. 96(3), pp. 879–897.

[23]. Koketsu, K., Yokota, Y., Ghasemi, H., Hikima, K., Miyake, H. and Wang, Z. (2009). Source process and ground motions of the 2008 Wenchuan earthquake. *No. 804*. Proceedings of the international conference on earthquake engineering for the 1st anniversary of Wenchuan earthquake, Chengdu, China, 10-12 May 2009.

[24]. Lacassin, R., Replumaz, A. and Hervé Leloup, P. (1998). Hairpin river loops and slip-sense inversion on Southeast Asian strike-slip faults. *Geology,* Vol. 26(8), pp. 703-706.

[25]. Lin, P.S. and Lee, C.T. (2008). Ground-motion attenuation relationships for subduction-zone earthquakes in northeastern Taiwan, *Bulletin of the Seismological Society of America*, Vol. 98(1), pp. 220–240.

[26]. Mandal, P., Kumar, N., Satyamurthy, C. and Raju, I.P. (2009). Ground-motion attenuation relation from strong-motion records of the 2001 Mw 7.7 Bhuj earthquake sequence (2001–2006), Gujarat, India. *Pure and Applied Geophysics*, Vol. 166(3), pp. 451–469.

[27]. Montaldo, V., Faccioli, E., Zonno, G., Akinci, A. and Malagnini, L. (2005). Treatment of ground-motion predictive relationships for the reference seismic hazard map of Italy, *J. Seismology*, Vol. 9, pp. 295-316.

[28]. Nielsen, C., Chamot-Rookea, N. and Rangin, C. (2004): (The ANDAMAN Cruise Team). From partial to full strain partitioning along the Indo-Burmese hyper-oblique subduction. *Marine Geology,* Vol. 209, pp. 303-327.

[29]. Phuong, N.H. (1991). Probabilistic assessment of earthquake hazard in Vietnam based on seismotectonic regionalization. *Tectonophysics,* Vol. 198(1), pp. 81-93.

[30]. Sadigh, K, Chang, C.Y, Egan, J.A., Makdisi, F. and Youngs, R.R. (1997). Attenuation relationships for shallow crustal earthquakes based on California strong motion data. *Seismol. Research Letters,* Vol. 68(1), pp. 180-189.

[31]. Sharma, M.L., Douglas, J., Bungum, H. and Kotadia, J. (2009). Ground-motion prediction equations based on data from the Himalayan and Zagros regions. *Journal of Earthquake Engineering*, Vol. 13(8), pp. 1191–1210.

[32]. Si, H. and Midorikawa, S. (2000). New attenuation relations for peak ground acceleration and velocity considering effects of fault type and site condition. *Paper No.*

0532. Proceedings of 12th World Conference on Earthquake Engineering, Auckland, New Zealand, 30 Jan. - 4 Feb., 2000.

[33]. Socquet, A. and Pubellier M. (2005). Cenozoic deformation in western Yunnan (China–Myanmar border). *Journal of Asian Earth Sciences*, Vol. 24, pp. 495-515.

[34]. Takahashi, T., Asano, A., Okada, H., Saiki, T., Irukura, K., Zhao, J.X., Zang, J., Thio, H.K., Somerville, P.G. and Fukushima Y. (2004). Attenuation relations of strong motion in Japan using site classification based on predominant period, Workshop on seismic input motions, incorporating recent geological studies, Committee on the Safety of Nuclear Installations (CSNI), OECD/NEA, 2004.

[35]. Thuc, P.V. (2007). Seismology and Earthquake in Vietnam. *Natural Science and Technology Publisher*, Hanoi, Vietnam. (Vietnamese).

[36]. Trieu, C.D. (1997). The strong seismogenic zones in Vietnam. *Vietnamese Journal of Geology*, B series, Vol. (9-10), pp. 47-62.

[37]. Trieu, C.D. (2001). Thintoc earthquake (Vietnam-Laos border) Ms = 5.3 on Feb. 19, 2001. *Vietnamese Journal of Geology,* Vol. 264(5-6), pp. 1-14.

[38]. Trieu, C.D. (2008). Earthquake. *Science and Technology Publisher*, Hanoi, Vietnam (Vietnamese).

[39]. Trieu, C.D., Xuan, N.T., Thang, N.C., Dung, L.V. and Tuyen, N.H. (1999). Seismic hazard assessment in North West Vietnam. *Vietnamese Journal of Geology*, B series Vol. (13-14), pp. 163-173.

[40]. Trifunac, M.D. (1976). Preliminary analysis of the peaks of strong earthquake ground motion dependence of peaks on earthquake magnitude, epicentral distance, and recording site conditions. *Bulletin of the Seismological Society of America,* Vol. 66(1), pp. 189-219.

[41]. Van, P.T.K. (2006). The Lai chau-Dien bien neotectonic fault zone and its acting manifestations by moderate local earthquakes. *Vietnamese Journal of Geology,* Vol. 27, pp. 30-39.

[42]. VIG. (2005). Research and Forecasting Earthquakes and Ground Movements in Vietnam, A report conducted by Vietnam Institute of Geophysics (VIG), chaired by Prof. Xuyen ND, Hanoi, Vietnam. (Vietnamese).

[43]. Xiang, J. and Gao, D. (1994). The attenuation law of horizontal peak acceleration on the rock site in Yunnan area. *Earthquake Research in China,* Vol. 8(4), pp. 509-516. (The attenuation relation law is also represented in *research report number: 04-001-SM*, named "Ground motion estimation equations 1964–2003." Imperial College London, John Douglas, 2004).

[44]. Xu, L.S., Chen, U.T., Feng, W.P. and Du, H.L. (2009). Source process of Ms6.4 earthquake in Ning'er, Yunnan in 2007. *Science in China. Series D, Earth sciences (Internet)*, Vol. 52, pp. 180-188.

[45]. Xuyen, N.D. and Thanh, T.T.M. (1999). A formula for estimation of seismic peek ground acceleration in Vietnam. *Vietnamese Journal of Earth Sciences,* Vol. 21(3), pp. 207-213.

[46]. Xuyen, N.D., Thanh T.T.M. and Son, L.T. (2001). Potential Earthquake Disasters in Vietnam And Seismic Hazard in Hanoi city area, *Session 2, Group 3-3*, 4th EqTAP Multilateral Workshop Proceedings, Kamakura, Japan, 2001.

[47]. Youngs, R.R., Chiou, S.J., Silva, W.J. and Humphrey J.R. (1997). Strong ground motion attenuation relationships for subduction zone earthquakes. *Seismological Research Letters,* Vol. 68(1), pp. 58-73.

[48]. Zhao, J.X., Zhang, J., Asano, A., Ohno, Y., Oouchi, T., Takahashi, T., Ogawa, H., Irikura, K., Thio, H.K., Somerville, P. G., Fukushima, Y. and Fukushima, Y. (2006). Attenuation relations of strong ground motion in Japan using site classification based on predominant period. *Bulletin of the Seismological Society of America*, Vol. 96(3), pp. 898–913.

[49]. Zhong, T., Wen, P. and Cong, Z. (2008). Seismic damage analysis on buildings of the Ning'er earthquake with Ms6.4. *Paper No. 01-1089* .The 14th World Conference on Earthquake Engineering, Beijing, China.

This page intentionally left blank

CHAPTER 4

STOCHASTIC GROUND MOTION PREDICTION

4.1 INTRODUCTION

Ongoing economic development means that increasing number of high-rise buildings and large public facilities are being constructed in Vietnam; consequently, seismic hazard analysis and mitigation will be of increasing importance in near future with the aim of design and risk evaluation. The problems are appeared in the study of the earthquake engineering such as require the use of acceleration records for nonlinear analysis, the seismic wave types for calculating dynamic structure and so on. Dynamic response analysis is required to seismic design for important facilities. The prediction of the ground motion for the dynamic response analysis of the structure encounters many difficulties because there is so little actual earthquake data. The dynamic method has been considered, but the seismic wave has not been introduced although Vietnam has been classified as a low-to-moderate seismicity region (*Hung et al., 2009*). *Hung et al. (2009*) is shown that acceleration records in seismic design work from Japan and the United States are not really applicable because earthquake activity in Vietnam is fairly different from those in both countries such as active faults and soil conditions. In Vietnam, the earthquake engineering has been studied by the seismologists, e.g. *Phuong (1991, 2001, 2007a, and 2007b), Thanh (2007), Xuyen et al. (1994, 1999), Trieu (1997a, 1997b, 2002, 2006, 2008a and 2008b), Pereran (2009), Son et al. (2003), Huang et al. (2009), etc.* The research's results shown that the seismic activities and earthquake hazard in Vietnam have occurred mainly in northwestern Vietnam country where has seismically active faults such as Cao Bang-Lang Son, Dien Bien-Lai Chau, Chay River, Ma River, Da River, Dong Trieu-Cam Pha, Son La (*Trieu, 1997a*). Thus, the study of the ground motion prediction is very important in Vietnam, especially, in the region of active faults and on a continental shelf of the country, which indicates that they may occur during 20^{th} century.

This Chapter simulates the ground motion from earthquake data in Vietnam using the stochastic approach (*Boore, 1983 and 2003*) and the ground motion prediction through attenuation relations of PGA, PGV and response spectrum of ground motions of recurrence specifications in this study. The results show the response spectral acceleration and seismic waves were simulated by using earthquake records in Vietnam and adjacent areas. Its application to seismic design in Vietnam is then discussed.

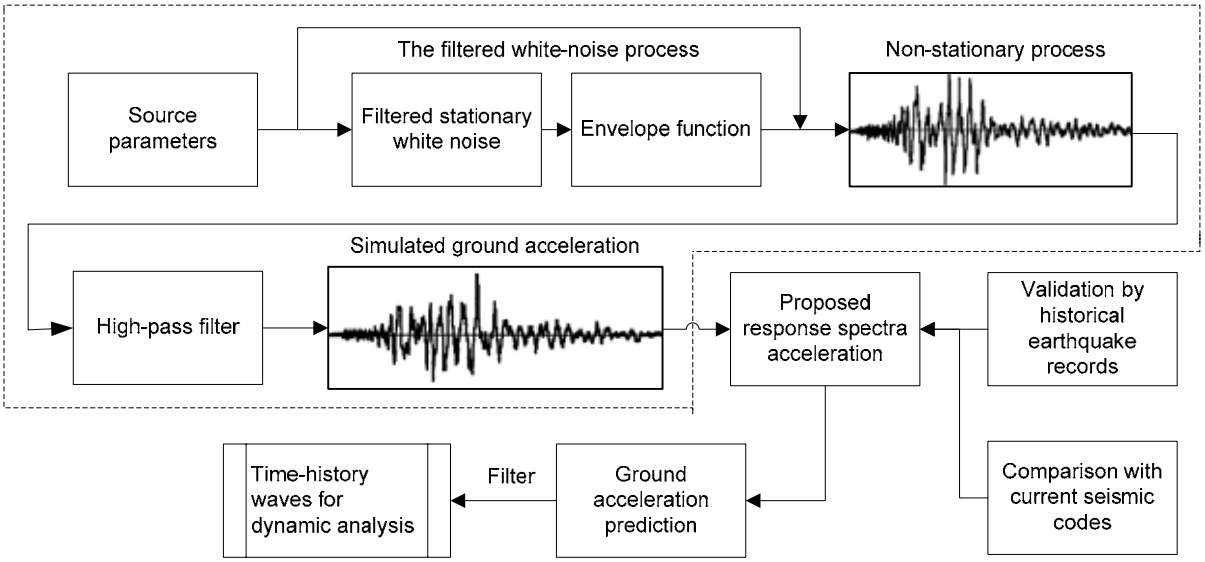

Figure 4.1 Processes for stochastic ground motion simulation (dash line area) and procedure for ground motion prediction.

4.2 MOTIVATION OF EARTHQUAKE GROUND MOTIONS

Performance based design is the seismic design methodology of the future. Recently, some design codes have followed the performance based design such as in Japan and the United States. A bridge shall be designed to achieve the required seismic performance in accordance with the level of design ground motion and the importance of the bridge. The nonlinear analysis is performed to verify the seismic performance. In principle, the earthquake ground motion used for seismic performance verification should be expressed as the time history waveform of acceleration at the construction site. It is necessary to perform a nonlinear dynamic response analysis using a time history waveform of an earthquake ground motion for precise evaluation of the safety of a bridge structure during an earthquake.

As described in **Chapter 1**, the design earthquake ground motions including Level 1 and Level 2 are adopted in *JRA-2002*, which are determined considering the magnitude of the earthquake, source characteristics, structure of the local stratum between the epicenter and construction site, propagation characteristics and distance between the epicenter and the construction site, and topographical, geological and ground conditions of the construction site. The two level ground motion as the moderate ground motions induced in the earthquakes with high probability to occur (Level 1 earthquake motion), and the intensive ground motions induced n the earthquakes with low probability to occur (Level 2 earthquake motion). The Level 1 earthquake provides the ground motions induced by the moderate earthquakes and the ground motion considered in the elastic design method. The Level 2 earthquake, two types of ground motions are considered. The first (Type-I) is the ground motions which are induced in

the interplate-type earthquakes with the magnitude of around 8. The ground motion in the 1923 Kanto earthquake is a typical target of this type of ground motion. The second (Type-II) is the ground motion developed in earthquakes with magnitude of around 7 at very short distance. The ground motion in the Hyogo-ken-Nanbu earthquake is a typical target of this type of ground motion. The recurrence period of the Type-II ground motion may be longer than that of the Type-I ground motion, although the estimation is very difficult. In the *JRA-2002*, Level 1 earthquake ground motion is the ground motion whose return period is about 50 years. Level 2 ground motion is a very strong motion whose return period is about 1000 years. It is chosen from the ground motion caused by an inland active fault beneath or close to the site and by the large scale inter-plate earthquake occurring in the neighborhood of land, taking the one that has the larger effect.

In the *22TCN 272-05* and *AASHTO LRFD (1998, 2004)*, the probability that the coefficient will not be exceeded at a given location during a 50-year period is estimated to be about 90%, i.e., a 10% probability of exceedance. The usage of a 50-year interval to characterize this probability is an arbitrary convenience and does not imply that all bridges are thought to have a useful life of 50 years. It can be shown that an event with the above probability of non-exceedance has a return period of about 475 years and is called the design earthquake. Larger earthquakes than those implied by the above acceleration coefficients have a finite probability of occurrence throughout the United States. Those with a return period of around 2,500 years (2% probability of exceedance within 50 yr) are sometimes called maximum probable earthquakes. It can also be shown that if the time interval is lengthened to, say, 75 years, the probability of exceeding an earthquake with a return period of 475 years increases to about 15 percent. However, the current AASHTO code, namely, g*uide Specifications for LRFD seismic bridge design* (is called *LRFDSEI-1, 2009*) shown that an event with a 7% probability of exceedance in 75 years has a return period of about 1000 yr. This earthquake is called the design earthquake. In addition, the ground motion of recent earthquakes in New Zealand (Christchurch earthquake; M = 6.3; 22 Feb. 2011) and Japan (the 2011 Off the Pacific Coast of Tohoku earthquake; M = 9.0; 11 Mar. 2011) show the ground motions exceed the seismic design codes of those countries (e.g., *Giardini, 2011; Yabe, 2011*). *Giardini (2011)* also presented a lesson for Switzerland as consider increasing the level of the seismic design from 475 years to 1,000 years because M = 6.3 events like the Christchurch earthquake are possible and expected in Switzerland every 80 – 100 years.

Comparison with seismic design codes, earthquake events, life-cycle design of 100 years for bridge design in Vietnam, and capacity of occurrence the largest earthquakes within magnitude M = 7.0 in Vietnam, Level 1 ground motion (called as VN L1) can be considered to the moderate ground motions with high probability to occur corresponding with return periods not exceed 475 years (can be chosen 10% probability of exceedance within 50 years); Level 2 ground motion (called as VN L2) can be considered to the large ground motions with

low probability with the highest consequence earthquake events. Level 1 earthquake is called the design earthquake. The Level 1 earthquake provides the ground motions induced by the moderate earthquakes and the ground motion considered in the elastic design method. Thus, the examples of simulated earthquake ground motion waveforms will be presented for Level 1 earthquake ground motion, Level 2 earthquake ground motion.

Table 4.1 Time history record selection criteria (*Little, 2007*).

Items	Description
General records	Records should be free-field. Multiple records should be selected.
Tectonic conditions	Records should be from a similar tectonic setting, e.g. plate boundary region, continental interior, subduction zone. Records should be from earthquakes caused by similar styles of faulting, e.g. strike-slip, thrust or normal. For near-fault conditions (≤ 10 km), records that show directivity effects (e.g. fault fling or directivity) should be considered.
Geologic conditions	Records should be from rock sites or sites with soil conditions comparable to those at the structure site. It is often difficult to find time histories from sites with comparable soil conditions. If records from rock sites are selected, then soil effects can be evaluated using the site-specific soil conditions and properties of the structure site.
Earthquake scenario	Magnitude should be similar to that of design scenario. Distance should be similar to that of design scenario De-aggregation of hazard provides a method for selecting appropriate magnitude/distance scenarios. Duration should be similar to that typically expected for the scenario magnitude.
Basis of hazard de-aggregation	PGA or S_a seismic hazard corresponding to primary vibration mode of the structure.
Comparison of un-scaled spectrum to target spectrum	General response spectrum shape should be similar to that of the target response spectrum. S_a corresponding to primary vibration mode of the structure should be similar to the target S_a at that period.
After time histories have been spectrum-matched	Check the PGV, PGD and the velocity and displacement time histories of the modified records for reasonableness. Check other parameters such as power spectral density to ensure that the energy content and distribution of the modified records is reasonable.

While the study of earthquake ground motion, many parameters of earthquake events need to choose and some key issues need to solve as follow:

- What makes a time history compatible with a target response spectrum?
- How are appropriate earthquake scenarios determined?
- How are appropriate time histories selected?
- How should the selected time histories be modified to achieve a match with the target response spectrum?

Sufficient seismic waves need to be used to enable uncertainties in ground motion parameters to be reflected in the dispersion of resulting response parameters. Thus, time history record selection criteria are very important as shown in **Table 4.1**, and the designer would like to have a suite of representative seismic wave that were recorded at the construct location.

4.3 PROBABILISTIC SEISMIC HAZARD ANALYSIS

In this section, peak ground motions (PGA) are selected to use in the seismic design. The extreme value distribution as Weibull distribution can be used prediction of ground motion PGA with various return periods. Characteristics of the Weibull distribution are given by equations as follow:

$$P = 1 - \exp\left[-\left(\frac{x - B}{A} \right)^{\kappa} \right] \tag{4.1}$$

$$\gamma_{\upsilon} = \frac{x - B}{A} \tag{4.2}$$

in which κ is factor; γ_{υ} is standardized variable.

In **Chapter 3**, we have derived the new PGA attenuation relationship for northern Vietnam using dataset from Japan, Vietnam and adjacent regions in place of old current relationship in Vietnam. The new relation is developed for shallow strike-slip earthquake by a regression technique with the range of magnitudes of $3.0 \leq M_w \leq 6.9$ and source distances up to 300 km. That relationship was presented in **Eq. (3.10)**.

Due to a limitation of this study, the prediction of PGA will be considered as an example for at four locations, where strong earthquakes may occur. These is Tuan Giao seismic station (TGV – 21^o 25.39’ N, 103^o 25.09’ E), Dien Bien seismic station (DBV - 21^o 23.38’ N, 103^o 01.10’ E), Lai Chau seismic station (LCV - 22^o 02.32’ N, 103^o 09.26’ E) and center of Ha Noi (21^o 03’ N, 105^o 85’ E) are shown in **Fig 4.2**. **Fig 4.3** shows overview of average shear-velocity down to 30 m, V_{s30}, in the North of Vietnam. This map can be used for classification of seismic site conditions in the prediction of ground motions. **Table 4.2** is

indicated the different between the PGA values in this study and those values have been published in *TCXDVN 375-2006*. The PGA values in this study have greater values in *TCXDVN 375-2006*. This is due to this study used the new attenuation relationship. This equation is the completely different with that was used to calculate the PGA values in current Vietnam standard. The result of the prediction of peak ground acceleration for different return periods is shown in **Table 4.3** and **Fig 4.4**.

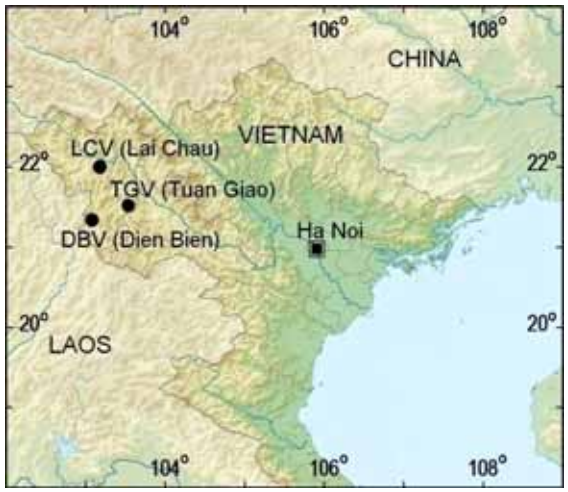

Figure 4.2 Black points indicate the studied locations in this study.

Table 4.2 PGA (cm/s^2) for 475-years return period.

Items	Units	Hanoi	Lai Chau	Tuan Giao	Dien Bien
This study	cm/s^2	124.00	245.84	181.98	150.39
TCXDVN 375-2006	cm/s^2	87.51	145.78	110.26	125.67
Error	%	0.29	0.41	0.39	0.16

Table 4.3 PGA (cm/s^2) for various return periods.

No	Return periods (years)	Hanoi center	Lai Chau	Tuan Giao	Dien Bien
		A (cm/s^2)	A (cm/s^2)	A (cm/s^2)	A (cm/s^2)
1	100	103.35	207.36	158.45	136.32
2	200	112.59	224.56	168.98	142.61
3	500	124.70	247.10	182.78	150.85
4	1,000	133.79	264.01	193.14	157.03
5	2,500	145.71	286.20	206.72	165.15
6	5,000	154.66	302.87	216.92	171.24
7	10,000	163.57	319.45	227.07	177.31
Standard deviation (σ)		22.07	41.08	25.15	15.02

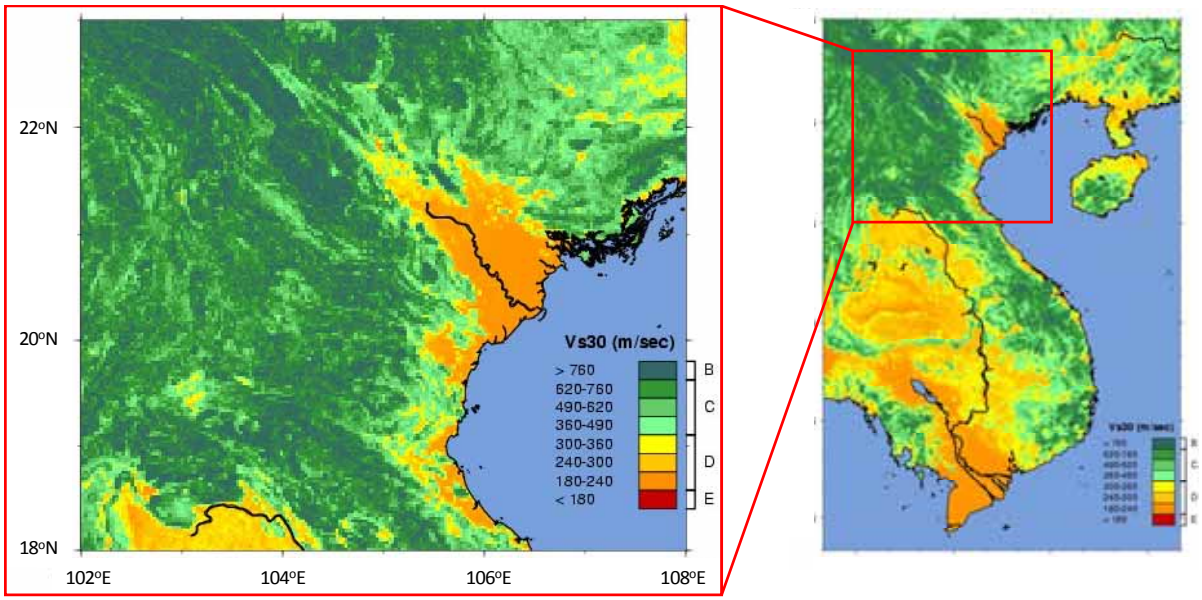

Figure 4.3 V_{S30}-values in the North of Vietnam.
(Created from USGS - *Global V_{S30} map server*).

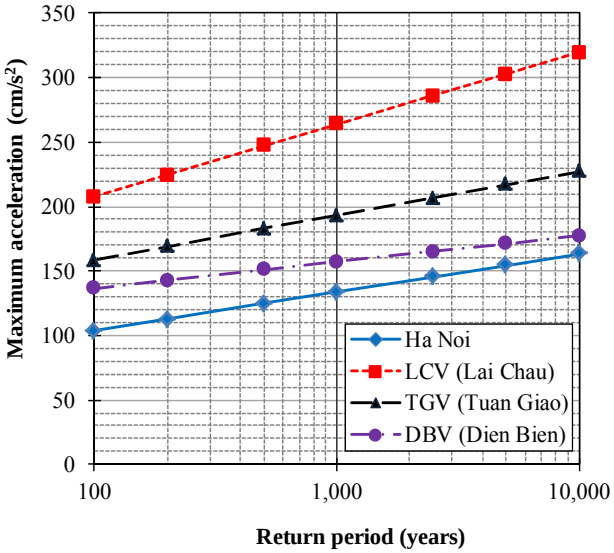

Figure 4.4 Predicted relationships between the maximum acceleration and return periods for some locals in the North of Vietnam.

The international cooperation activities have been carried out on dealing with seismic hazard analysis in region is the "Global Seismic Hazard Assessment Program in Continental Asia - GSHAP" which has been accomplished for the whole Asia Continental region at large scale. Vietnam territory has been roughly studied and estimated the seismic hazard analysis. The GSHAP is almost concerned in the northwest area of Vietnam territory. The remained region of Vietnam mainland is still not covered in details (see **Fig 4.5**). The results of this section showed similarities between them and the results of the GSHAP (see **Table 4.3**).

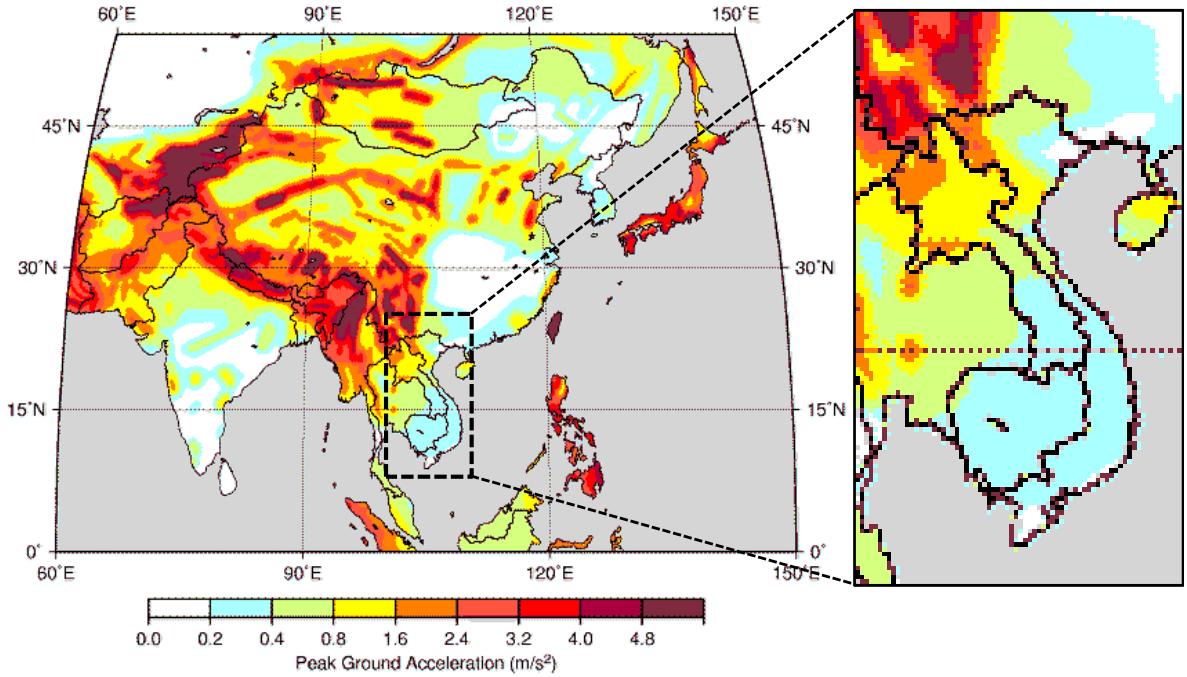

Figure 4.5 Peak ground acceleration was created by the global seismic hazard assessment program. (*website: http://www.seismo.ethz.ch/static/GSHAP/eastasia/*).

4.4 STOCHASTIC GROUND MOTION SIMULATION

The ground motion simulation approach to generating numerical ground motions, which is based on the stochastic simulation method (*SMSIM*), uses regionally determined source and propagation path input parameters. Ground motions are simulated by the point-source simulation using the D-Wave software has been developed by Japanese based on the stochastic method.

4.4.1 Methodology

The stochastic model is a widely used tool to simulate the acceleration time series and to develop the ground-motion prediction equations (e.g., *Hanks and McGuire, 1981*; *Boore, 1983*; *Atkinson and Boore, 1995, 1997 and 1998*; *Toro et al., 1997*; *Atkinson and Silva, 2000*; *Boore, 2003*). The stochastic method begins with the specification of the Fourier spectrum of the ground motion as a function of magnitude and distance. The acceleration spectrum is typically modeled by a spectrum with a ω^2 shape, where ω is angular frequency (e.g., *Aki, 1967*; *Brune, 1970, 1971*; *Boore 1983, 2003*). The stochastic source method assumes that the ground motion can be modeled as band-limited Gaussian white noise and the peak amplitude is approximated using random vibration theory (*Boore, 1983, 2003*). This method assumes that the seismic shear wave energy represented by the Fourier amplitude spectrum is band

limited by the source corner frequency (f_c) at low frequencies and by the site-corner frequency (f_{max}). A point-source stochastic model in the frequency domain assumes that the total Fourier amplitude spectrum of acceleration *A(f)* for horizontal ground motions due to shear waves may be modeled by the general relation. The acceleration of spectrum *A(f)* is represented by **Eq. (4.5)**.

$$A(f) = C \times M_0 \times \frac{(2\pi f)^2}{1+\left(f/f_c\right)^2} \times P(f, f_{\max}) \times \frac{e^{\left(-\frac{\pi f R}{Q(f) V_S}\right)}}{R} \tag{4.5}$$

Where:

- M_0 is the seismic moment (in dyne·cm)
- C is a constant

$$C = \frac{R_{\theta\phi}\ F\ V}{4\pi\ \rho_s\ V_s^3} \times \frac{1}{R_0} \tag{4.5a}$$

where $R_{\theta\phi}$ is the scaling parameter to account for the average shear-wave radiation pattern (= 0.63), F is the free surface effect (F = 2 in almost all applications), V is the partition factor of the horizontal component (=$1/\sqrt{2}$ = 0.71), ρ_S is the soil density (= 2.7 g/cm^3), V_S is the shear wave velocity (= 3.4 km/s) and R_0 is the reference distance, usually set equal to 1 km.

- f is frequency of seismic waves (in Hz)
- f_c is the corner frequency (in Hz)

$$f_c = 4.9 \times 10^6 V_S \left(\frac{\Delta\sigma}{M_o}\right)^{\frac{1}{3}} \tag{4.5b}$$

Herein $\Delta\sigma$ is the stress parameter in bars (Brune stress drop), V_S in km/s.

- Q is the seismic quality factor

$$Q(f) = Q_0 f^{\eta} \tag{4.5c}$$

Herein Q_0, η is correction factor determined by the characteristics of the region.

- Filters are in common use the f_{max} filter. *Boore (1983)* assigned a fourth-order Butterworth filter for $P(f, f_{max})$.

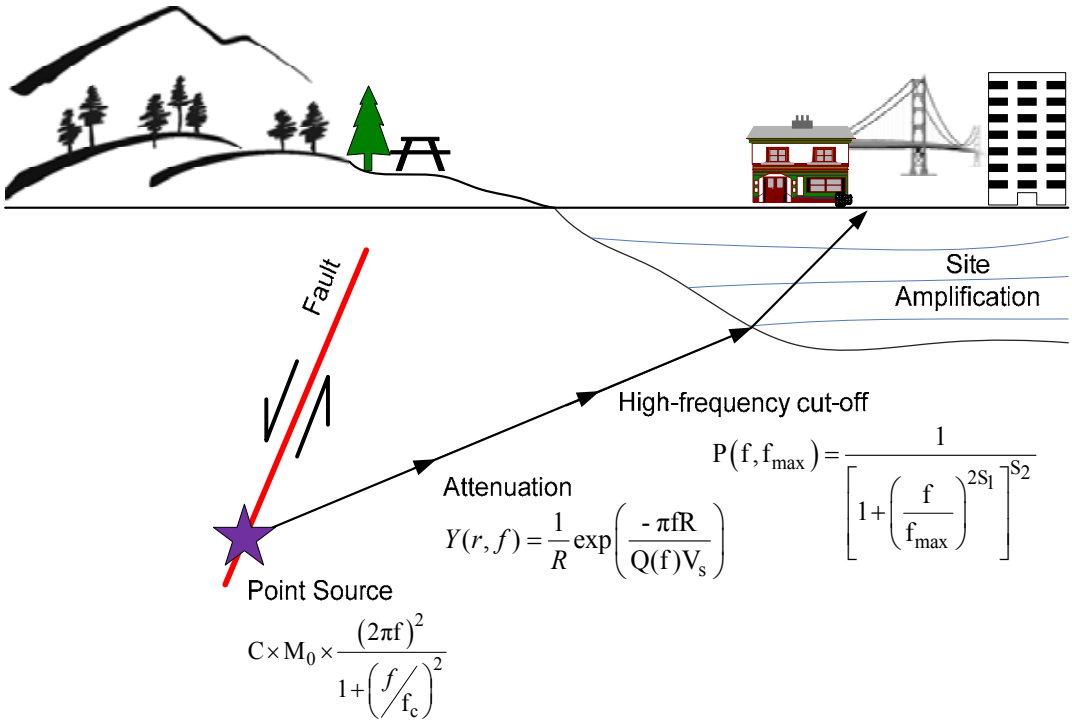

Figure 4.6 Overview of the Fourier amplitude spectrum's elements of the earthquake ground motion modeling.

$$P(f,f_{\max})=\frac{1}{\left[1+(f/f_{\max})^{2S_1}\right]^{S_2}}=\frac{1}{\left[1+(f/f_{\max})^{8}\right]^{1/2}} \tag{4.5d}$$

$$f_{\max}=7.31\times10^{3}M_0^{-0.12} \tag{4.5e}$$

Where P is the high-frequency cutoff of the point-source acceleration spectra for frequencies above f_{max}, f_{max} is the high-cut frequency (in Hz) and S_1 is a constant to control the decay rate of higher frequencies above some high-frequency cut-off, f_{max}. S_1 and S_2 were assigned a value of 4 and 0.5, respectively (*Boore, 1983, 2003*).

- Type of ground motion

$$I(f)=(2\pi f)^p \tag{4.5f}$$

Herein p is 0, 1, and 2 for displacement, velocity and acceleration, respectively.

4.4.2 Analytical procedures

The major objective of this study presents a procedure for generating artificial accelerograms based on stochastic method. The generated accelerograms which has a

response spectrum is used for presenting the proposed new target response spectrum; has a time history wave is used for fitting response spectrum close to new target response spectrum and in the current seismic code. Firstly, the recorded earthquake accelerograms are used for the training of simulation. After that, the accelerogram caused by two-level earthquake ground motions will be simulated by using the stochastic method. **Fig 4.1** illustrates the processes for stochastic ground motion simulation. This method combines the stochastic ground motion technique according to *Boore (1983)*. The source parameters and the cut-off filter originally were introduced for modeling the *S*-wave acceleration spectrum. The major developments and findings to determine the ground motion compatible of this study are summarized in **Fig 4.15**.

For describing the process of earthquake event there exists different kind of mathematical models. Most popular are stochastic models. The common stochastic models are dealing with significant simplifications of the ground acceleration process. The architecture of stochastic method contains three layers (input, hidden and output layer) as shown in **Fig 4.7**.

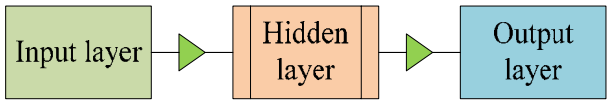

Figure 4.7 The architecture of stochastic method.

4.4.3 Source characterization

4.4.3.1 Duration of ground motion.

Source duration in prediction equations has been developed previously for the bracketed duration, significant duration, and other duration parameters. The significant duration parameters evaluate from the energy integral is denoted as 5 - 95% of the Arias intensity, I_A (*Arias, 1970*). In this study, the significant duration is used because it is relatively stable with respect to the definitions of the beginning and end thresholds (*Bommer and Martinez-pereira, 1999*). The nonzero significant durations can be measured for small-amplitude records that are of little engineering significance. Moreover, the significant duration from the Arias integral has arguably seen the most use in recent engineering practice (*Kempton and Stewart, 2006*).

Thuc (2007) was presented the source duration time of 12 s for the Tuan Giao earthquake (1983) in Vietnam. The observed data of the Dien Bien earthquake (2001) is analyzed, for example, significant durations are shown in **Fig 4.8**, and bracketed durations are shown in **Fig 4.9**. For the Ning'er earthquake (M_S = 6.4), which occurred in Ning'er, Yunnan Province is obtained by inverting the broadband waveform data of 20 global stations. The source time function shows that the duration time of the earthquake is about 14 sec. The most of the

energy releases within the first 11 sec and in 11–14 sec the rupture is weak (*Zhang et al., 2009*). The significant duration is determined based on waveforms from the Dien Bien earthquakes ($3.0 \leq M_S \leq 5.3$) and the earthquakes at the sites of interest. Assuming a linear relationship between significant durations, T_{sd} and surface wave magnitudes, M_s, we obtained the relationship as follows:

$$T_{sd} = 2.23\, M_s - 3.97 \tag{4.6}$$

The duration (T) of an earthquake signal at the hypo-central distance, R, can generally be represented as (*Atkinson and Boore, 1995*):

$$T_d = T_0 + d\, R \tag{4.7}$$

where T_{sd} is the source duration, $T_0 = T_{sd}$; d is the coefficient controlling the increase of duration with distance, $d = 0.05$ (*Atkinson and Silva, 2000*).

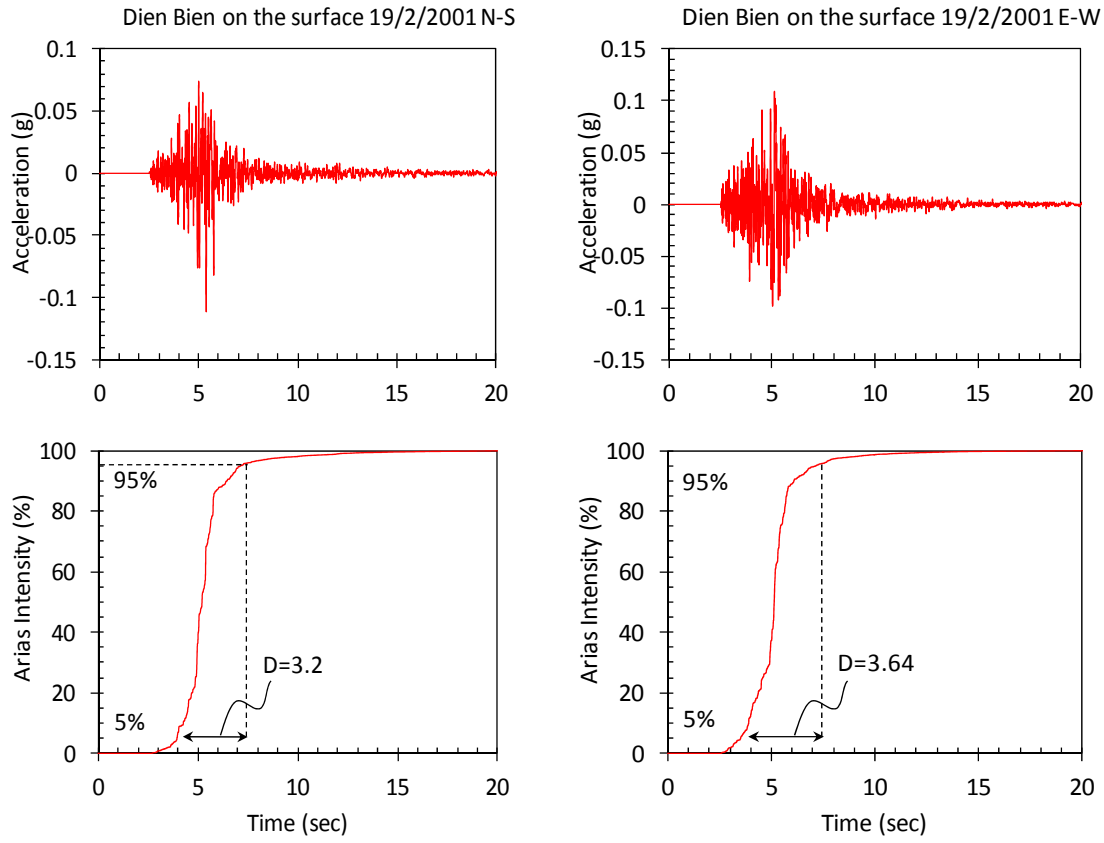

Figure 4.8 The significant duration of main shock at the Dien Bien earthquake (2001).

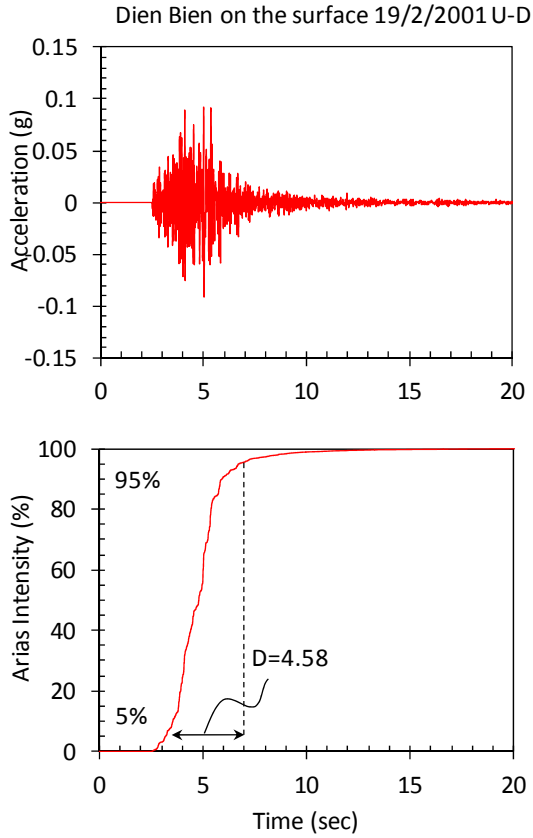

Figure 4.8 Continued.

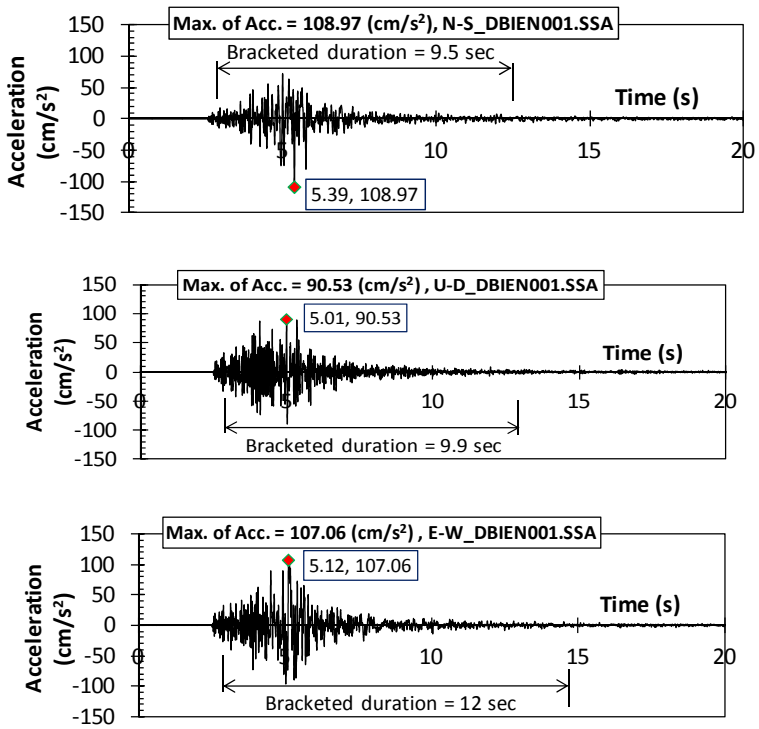

Figure 4.9 The braketed duration of main shock from the Dien Bien earthquake (2001).

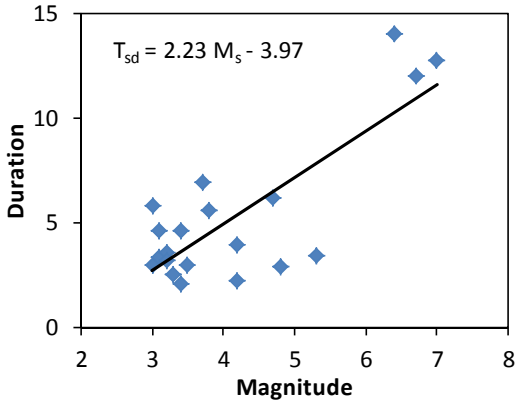

Figure 4.10 The relationship between magnitudes and the significant durations.

4.4.3.2 Seismic moment

Almost main faults of adjacent regions to northern Vietnam, such as northern Thailand, Myanmar, Laos and southern China are also strike-slip faults (e.g., *Lacassin et al., 1998; Fenton et al., 2003*; *Nielsen et al., 2004*; *Socquet and Pubellier, 2005*). Thus, the earthquake activities in these regions may have similarities. The seismic moments and moment magnitudes have been taken from the CMT catalogue for the events that occurred during 1977–2011 in Vietnam and adjacent areas. **Figs 4.11** and **4.12** displays the relationships between the seismic moments (M_0), moment magnitudes (M_W) and surface wave magnitudes (M_S) based on earthquake records with M_S from 4.7 to 7.0 in Vietnam and adjacent regions. This study uses a dataset including the observed earthquakes in Vietnam and the recorded source parameters in the Global CMT catalog from 1978 to 2011 (see **Table 4.4**). The related regression line is depicted with a solid line. The proposed relationship law is different with others because the data and the range of magnitudes used by different authors were slightly different.

The relation between M_0 and M_S is given by **Eq. (4.8a)** as follows:

$$\log(M_0) = 1.12\, M_S + 18.22 \qquad (4.8a)$$

The relation between M_0 and M_W is given by **Eq. (4.8b)** as follows:

$$\log(M_0) = 1.39\, M_W + 16.68 \qquad (4.8b)$$

4.4.3.3 Source dimensions.

Trieu (1999, 2002) has established an empirical formula characterizing the relationship of the length-L (km) and the width-W (km) of the focus with the magnitude of the earthquake in northwestern Vietnam, corrected by the new result of this work as shown in ***Eq. (4.9)***.

$$\begin{aligned} \log L(km) &= 0.60\, M_S - 2.50 \\ \log W(km) &= 0.25\, M_S - 0.35 \end{aligned} \tag{4.9}$$

4.4.3.4 Site amplifications and physical constants.

Thuc (2007) presented the source parameters of the Tuan Giao earthquake occurred on 1983 (21.71, 103.43) as magnitude of M_W = 6.77, M_S = 6.7, seismic moment $M_0 = 3.5\times10^{25}$ dyne·cm, length of fault L = 23 km, wide of fault W = 22 km, duration time of 12 s, average displacement D_0 = 28 cm, seismic energy $E_S = 1.1\times10^{20}$ erg, rupture velocity V_R = 2 km/s, soil density ρ_s = 2.7 g/cm^3, velocity of *S*-wave V_S = 3.4 km/s. These values can be considered as source parameters for the prediction ground motion.

Based on site clasification of USGS by Global V_{S30} map server, the Tuan Giao-Dien Bien-Lai Chau area can be approximately clasified into site class B (Rock site with V_{S30} > 760 m/s), thus, this area corresspond to site class A (Rock site with V_{S30} > 800 m/s) according to *TCXDVN 375-2006*. Therefore, this simulated ground motion base on source parameters in this area can be considered to rock site.

4.4.3.5 Quality Factor.

Quality factor has not been considered in Vietnam. However, several researchers have shown the quality factor at the different regions around Vietnam as shown in **Table 4.5**. Recently, *Xu et al. (2010)* collected records in the seismically active regions of the Yunnan and southern Sichuan provinces of China and also corrected for an elastic attenuation using the relation $Q = 180 f^{0.5}$ and a stress drop of 3 MPa (30 bars) using recordings of 474 small earthquakes with local magnitudes between 3.0 and 5.5 in the 0.3–12 Hz frequency range in those regions. This value has not been estimated for earthquake records occurred in Vietnam.

Therefore, the most recent research and the condition is close to Vietnam will be used to simulate ground motion. Specifically, the relationship of seismic attenuation quality factors was published by *Xu et al. (2010)* ($Q = 180 f^{0.5}$) will be used in this study.

4.4.3.6 Stress Drop.

One of the most important parameters for simulation of the strong ground motion using the stochastic method proposed by *Boore (1983)* is the stress drop. Commonly, Brune stress drop that estimated for the dynamic stress drop that can be determined from the zero-frequency level, Ω_0, and the corner frequency, f_0, of the far-field displacement amplitude spectrum (*Brune, 1970, 1971*).

A simple rupture model is used for the stress drop as relationship between M_S and L, as shown in **Eq. 4.10** (*Bagher et al., 2001*).

$$M_S = 2 \log L + 1.33 \log \Delta\sigma + 1.66 \quad (4.10)$$

Where M_S is surface wave magnitude, L is rupture length (km) and $\Delta\sigma$ is stress drop (bars).

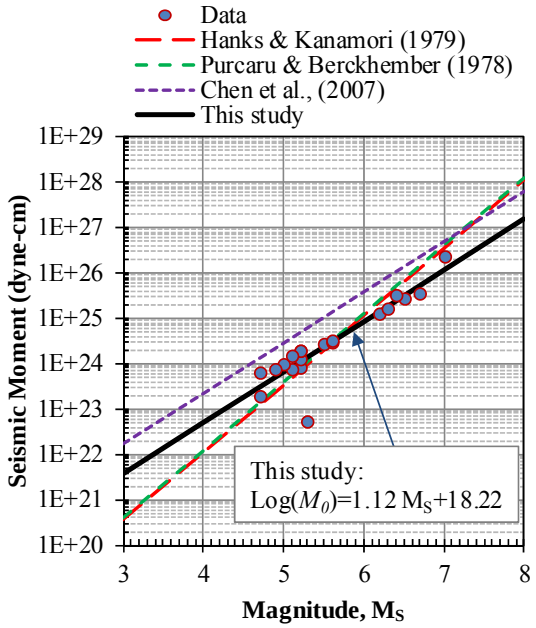

Figure 4.11 The relationship between surface wave magnitudes and seismic moments.

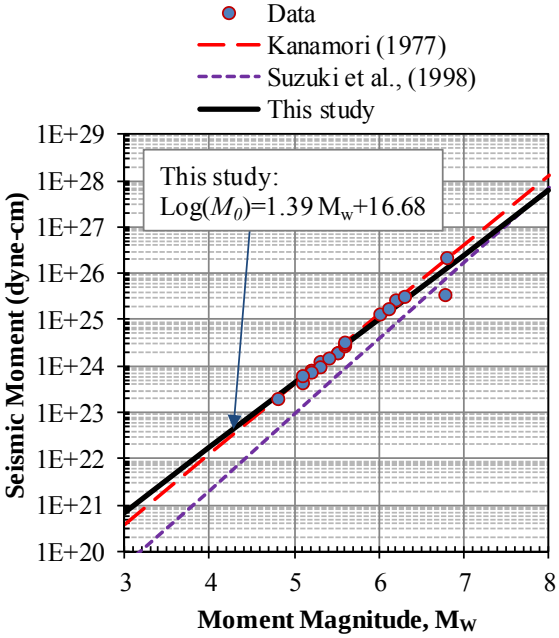

Figure 4.12 The relationship between moment magnitudes and seismic moments.

Table 4.4 Earthquakes used in this study

Events	Location	Lat.	Lon.	M_w	M_s	M_0 (Dyne·cm)	Refer.
2001/02/19	Dien Bien, Vietnam	21.34	102.85		5.3	5.57E+22	Thanh (2007)
				5.1		4.29E+23	Van (2006)
1983/06/24	Tuan Giao, Vietnam	21.71	103.43	6.8	6.7	3.50E+25	Thuc (2007)
1978/08/02	Southeast Asia	20.26	100.51	5.2	5.2	8.29E+23	
1978/09/09	Yunnan	23.20	101.03	5.3		1.19E+24	
1979/03/15	Yunnan	23.24	101.61	6.0	6.2	1.33E+25	
1981/09/19	Yunnan	22.84	101.54	5.3	5.2	1.33E+24	
1982/06/01	Burma-China border region	21.97	102.36	5.5	5.2	1.94E+24	
1982/10/27	Yunnan	23.97	105.85	5.2	5.1	7.93E+23	
1983/06/24	Southeast Asia	21.85	103.67	6.2	6.5	2.84E+25	
1983/07/15	Southeast Asia	21.93	103.29	5.3	5.0	1.00E+24	
1988/11/27	Burma-China border region	22.70	100.17	5.5	5.2	1.93E+24	
1989/06/16	Southeast Asia	20.61	102.61	5.6	5.5	2.85E+24	
1993/01/26	Yunnan	22.86	100.88	5.6	5.6	3.07E+24	
1995/04/24	Yunnan	22.88	103.16	5.2	4.9	7.85E+23	
2000/01/19	Southeast Asia	19.92	101.33	5.4	5.1	1.58E+24	
2001/07/09	Yunnan	24.89	101.25	5.1	4.7	6.41E+23	
2007/05/16	Laos	20.52	100.89	6.3	6.4	3.35E+25	
2007/06/02	Yunnan	23.02	101.13	6.1	6.3	1.73E+25	
2007/06/03	Yunnan	22.93	101.12	4.9		2.65E+23	
2007/06/23	Myanmar-China border region	21.49	100.00	5.6	5.6	3.31E+24	
2010/12/30	Laos	20.86	103.42	4.8	4.7	1.99E+23	
2011/03/24	Myanmar	20.65	100.06	6.8	7.0	2.28E+26	

Global CMT Catalog

Table 4.5 Seismic attenuation quality factors at the different regions around Vietnam

Region	$Q(f)$ relationship	Reference
Yun-nan Province	$200 f^{0.3}$	*Cong et al. (2003)*
Taiwan	$250 f^{0.54}$	*Lam et al. (2000)*
Hong Kong	$256 f^{0.7}$	*Mak et al. (2004)*
South Korea	$80 \text{ to } 300 f^{0.4 \text{ to } 1.1}$	*Yun et al. (2007)*
Southeast China	$481.5 f^{0.31}$	*Wong et al. (2002)*
Haifeng, Guangdong, China	$370 f^{0.4}$	*Jin and Aki (1988)*
Xingfenziang, Guangdong, China	$240 f^{0.3}$	*Jin and Aki (1988)*
Ningxia, China	$104 f^{0.83}$	*Zhao et al. (2000)*
Guangdong province, China	$428 f^{0.31}$	*Wong et al. (2002)*
Yunnan and southern Sichuan provinces	$180 f^{0.5}$	*Xu et al. (2010)*

An example of the source parameter of Tuan Giao earthquake (M_S = 6.7; 1983) have a length of L = 23 km, focal depth of 18 km (*Thuc, 2007*). According to **Eq. (4.10)**, the stress drop $\Delta\sigma$ = 55 bars.

In traditional, for rectangular strike-slip fault, stress drop is determined as follows:

$$\Delta\sigma = \frac{2}{\pi}\frac{M_o}{W^2 L} \tag{4.11}$$

4.4.4 Simulation of the Dien Bien earthquake (2001; *Ms* = 5.3)

A typical example is shown in **Figs 4.13** and **4.14** for a soft site synthetic accelerogram with *Ms* = 5.3. The median estimations of empirical models are computed using the same randomly generated seismological parameter set that is utilized in point-source ground-motion simulations. In this study, the simulations have been performed using the D-wave software. **Figs 4.13** and **4.14** shows an example of the predicted seismic waves of the 2001 Dien Bien earthquake by observed and possible accepted source parameters.

The stress drop generally varies between 50 and 150 bars (*Durukal and Erdik, 2003*). The stress drop of the Dien Bien earthquake is 22 bars, which calculated with **Eq. 4.10**. Therefore, the stress drop ranging 20 to 150 bars is investigated in this study. However, comparison on waveforms and response spectral accelerations between observed and simulated ground motion to look for the most sensible source parameters are performed with stress drop of 100 bars. These results can be seen that they are in good agreement, but using adjusting the stress drop to 100 bars to provide an approximate match to observed ground motion of the Dien Bien earthquake (2001). Based on these results, for the upper limit on the stress drop, we set a value of 100 bars even though the selection of this value is completely arbitrary; there may be some higher or lower values depending on source dimensions.

Table 4.6 Model parameters for the ground motions of the Dien Bien earthquake (2001)

No.	Parameters	Dien Bien earthquake (2001; M = 5.3)
1	$R_{\theta\phi}$, F, V, R_0	0.63, 2, 0.71, 1 km
2	Crustal density, ρ_s	2.7 g/cm^3
3	Crustal shear-wave velocity, V_s	3.4 km/s
4	Seismic moment, M_0	1.43×10^{24} dyne·cm
5	Duration, T_d	7.85 + 0.05 R
6	Rupture velocity	0.8 V_S
7	Elastic attenuation	Q = 180 $f^{0.5}$
8	W x L	9.5 x 4.8 km
9	Stress drop, $\Delta\sigma$	20 – 150 bars

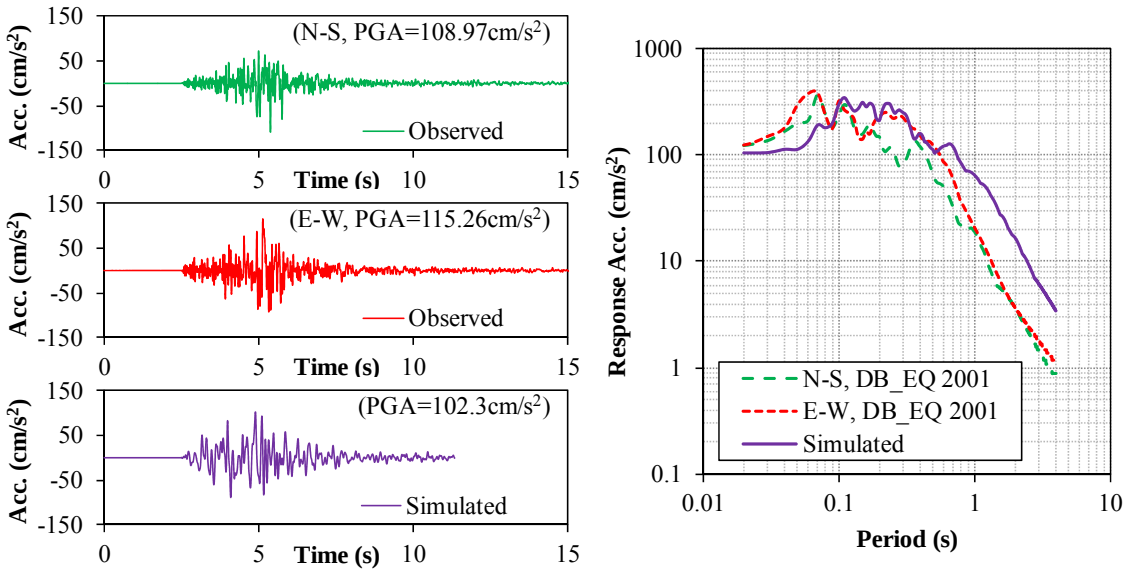

Figure 4.13 Comparison of the observed waveforms (dashed lines) with the simulated median waveform (solid line) corresponding to waveforms at Dien Bien station (Epicenter distance is 19 km). The geometric mean for 90 simulations is shown in each case.

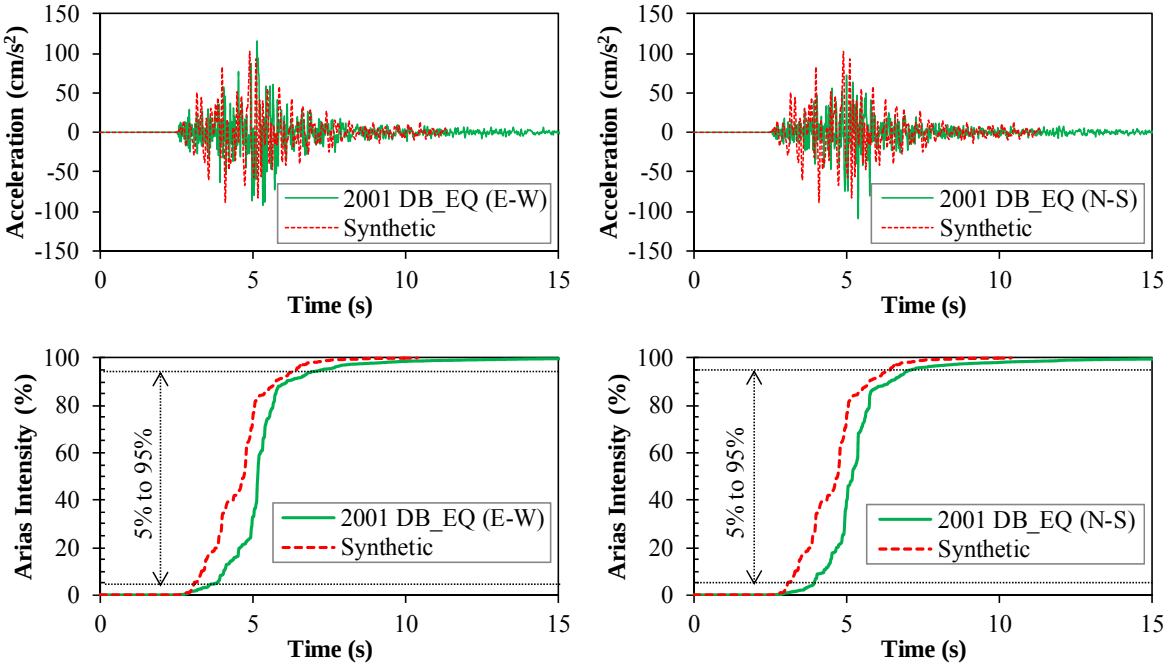

Figure 4.14 Comparison of significant duration between the observed waveforms (solid lines) and the simulated median waveform (dashed line) corresponding to waveforms at Dien Bien station (Epicenter distance is 19 km).

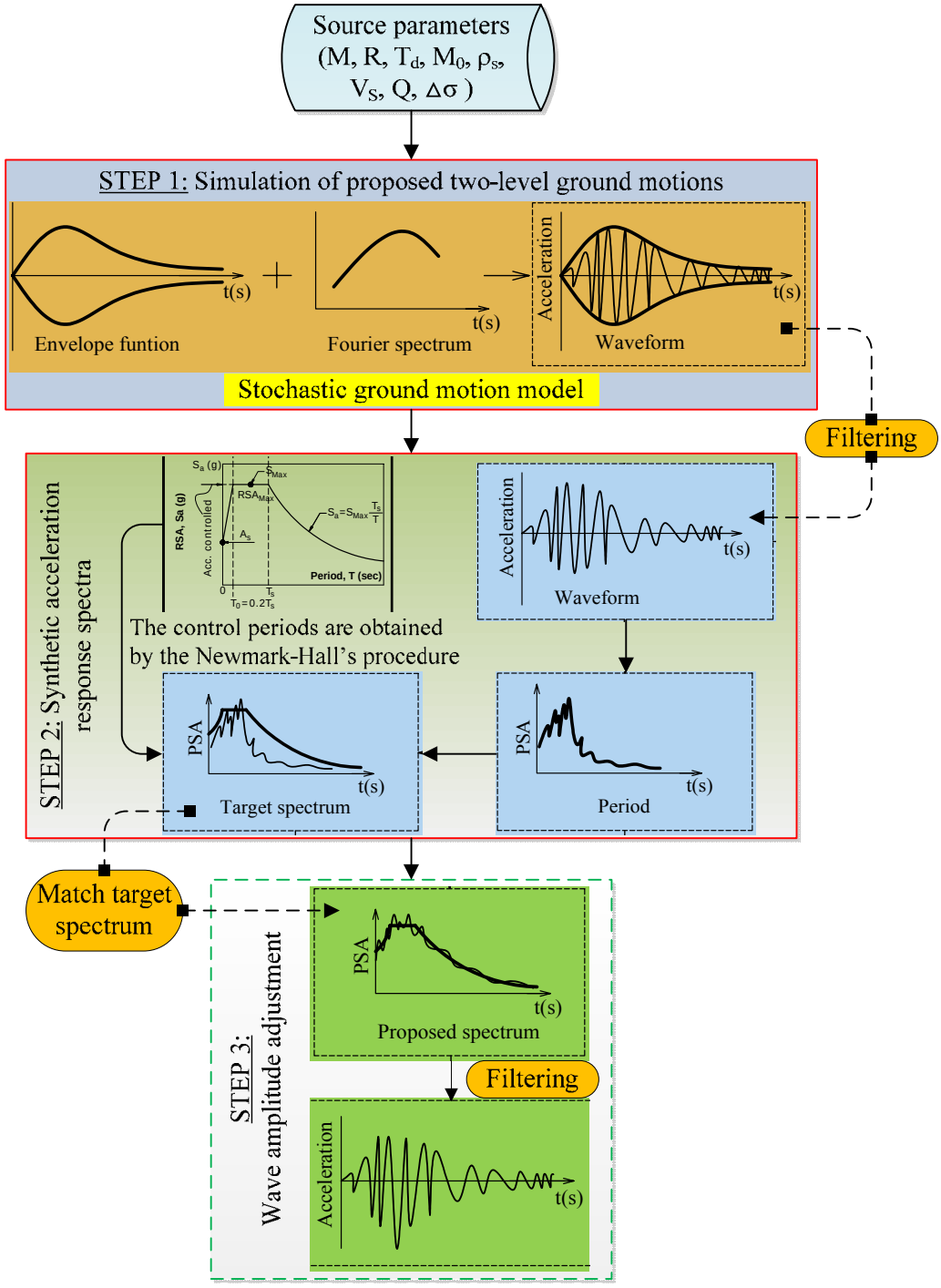

Figure 4.15 Schematic representation of the stochastic ground motion simulation

4.4.5 Step 1: Simulation of proposed two-level ground motions

The earthquake ground motions are calculated by stochastic model according to investigation results on the active faults and earthquake parameters. The objective of this study was to develop a response spectrum, time-histories waves. The Level 1 and Level 2 earthquake ground motion for Vietnam is presented may correspond with Vietnam's condition, namely, VNL1 and VNL2 within a low moderate seismic zone in Vietnam, respectively. Two levels of earthquake performance also proposed corresponding to high and low probability of occurrence in Vietnam. Two earthquake levels may be more suitable for seismic design according to the design conditions, seismic performances and economic requirements of the projects. Seismic scenarios are generated for maximum earthquakes assumed from the high and low probabilistic earthquakes. Comparison between the results of the response spectrum of the simulated seismic waveforms and target spectrum is performed.

The two main objectives proposed are fulfilled:

(1) Acceleration response spectra;

(2) time-history waves for dynamic analysis.

The stochastic algorithm is used, thus, the response spectrum of the generated signal matches the target response spectrum. On the other hand, filter technologies are employed to remove unwanted frequency components from a given signal. In this study, high-pass filter is used because high-pass filtering allows frequencies that are higher than the cut-off frequency to pass through.

The comparison between the simulated response spectrum and response spectrum in *22TCN272-05* and *JRA-2002* is performed as shown in **Figs 4.16** and **4.17**. Almost simulated maximum response spectrum lay in a short-period (less than 0.35 s for VNL1 ground motion and 0.4 s for VNL2 ground motion) and they are rapidly decreased after that period.

Table 4.7 Model parameters for the predicted ground motions (VNL1 and VNL2 ground motions).

No.	Parameters	VNL1 (M = 5.8)	VNL2 (M = 7.0)
1	$R_{\theta\phi}$, F, V, R_0	0.63, 2, 0.71, 1 km	0.63, 2, 0.71, 1 km
2	Crustal density, ρ_s	2.7 g/cm^3	2.7 g/cm^3
3	Crustal shear-wave velocity, V_s	3.4 km/s	3.4 km/s
4	Seismic moment, M_0	5.20×10^{24} dyne·cm	1.15×10^{26} dyne·cm
5	Duration, T_d	9.50 s	12.50 s
6	Rupture velocity	0.8 V_S	0.8 V_S
7	Elastic attenuation	$Q = 180f^{0.5}$	$Q = 180f^{0.5}$
8	Stress drop	50, 100 and 150 bars	50, 100 and 150 bars

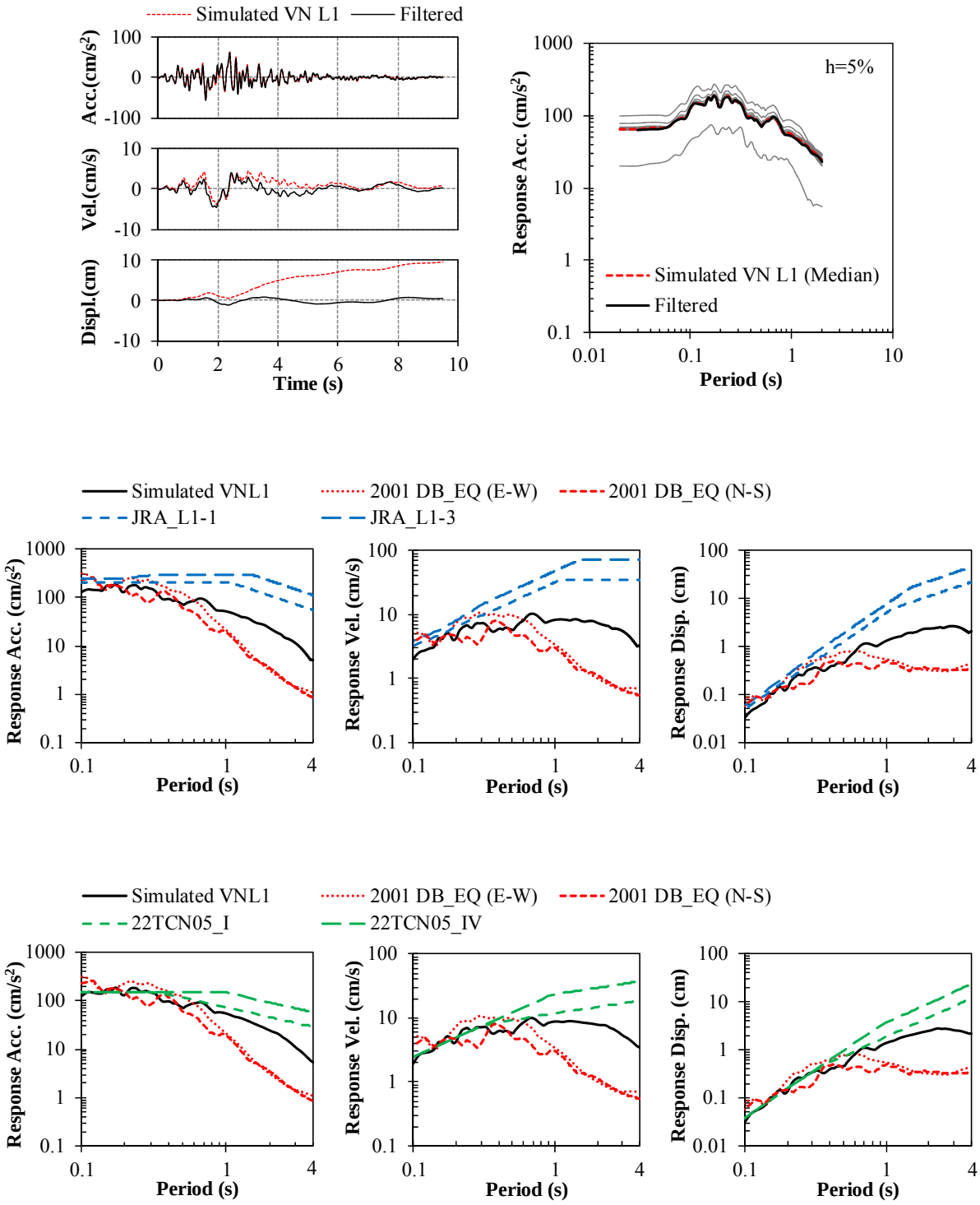

Figure 4.16a Comparison of the observed, simulated level 1 ground motion (case of 50 bar) and other codes (DB_EQ is the 2001 Diendien earthquake; JRA_L1-1 and JRA_L1-3 is level 1 with soil type 1 and 1 type 3 according to JRA-2002; 22TCN05_I and 22TCN05_IV is soil type I and IV according to 22TCN 272-05).

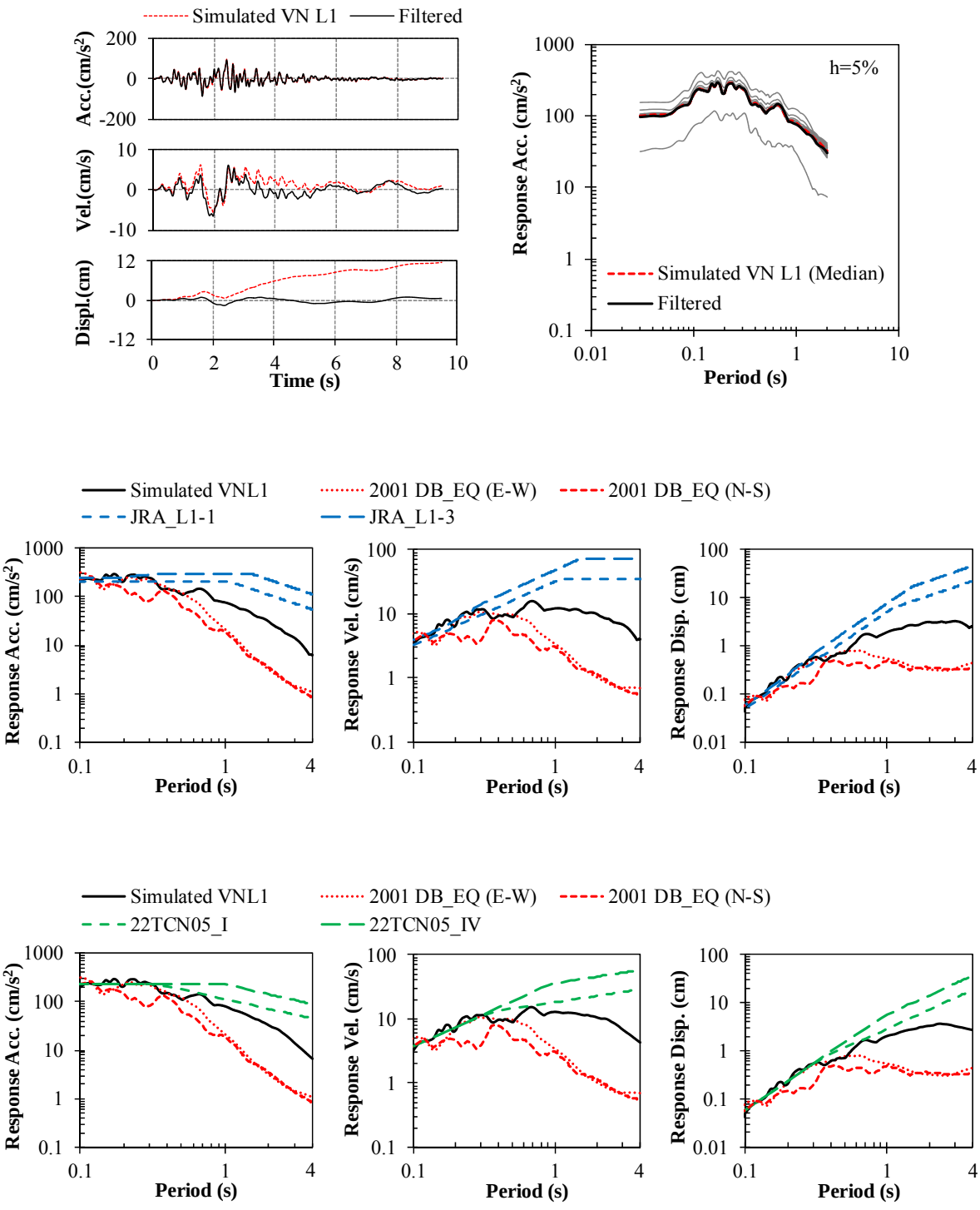

Figure 4.16b Comparison of the observed, simulated level 1 ground motion (case of 100 bar) and other codes (DB_EQ is the 2001 Diendien earthquake; JRA_L1-1 and JRA_L1-3 is level 1 with soil type 1 and 1 type 3 according to JRA-2002; 22TCN05_I and 22TCN05_IV is soil type I and IV according to 22TCN 272-05).

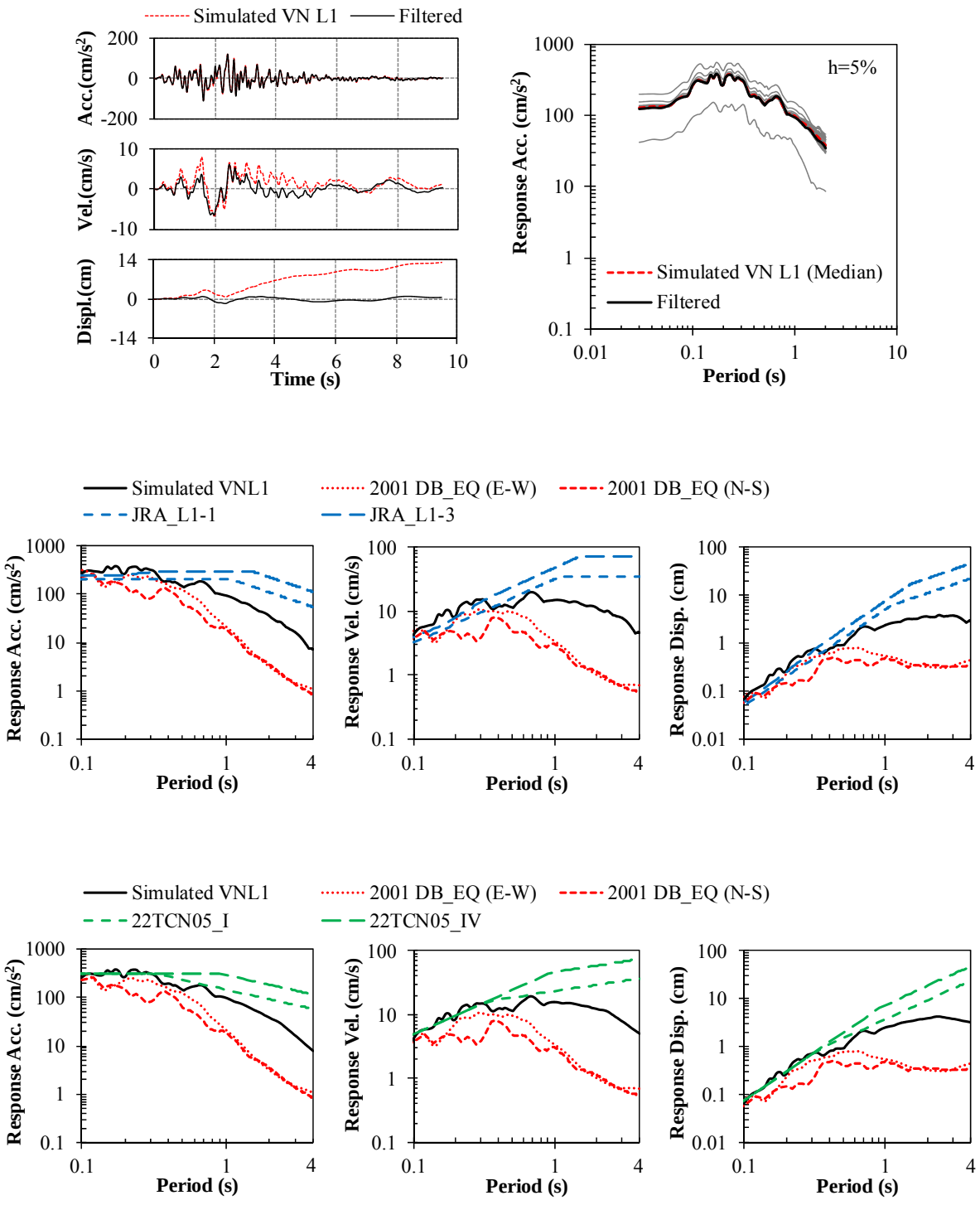

Figure 4.16c Comparison of the observed, simulated level 1 ground motion (case of 150 bar) and other codes (DB_EQ is the 2001 Diendien earthquake; JRA_L1-1 and JRA_L1-3 is level 1 with soil type 1 and 1 type 3 according to JRA-2002; 22TCN05_I and 22TCN05_IV is soil type I and IV according to 22TCN 272-05).

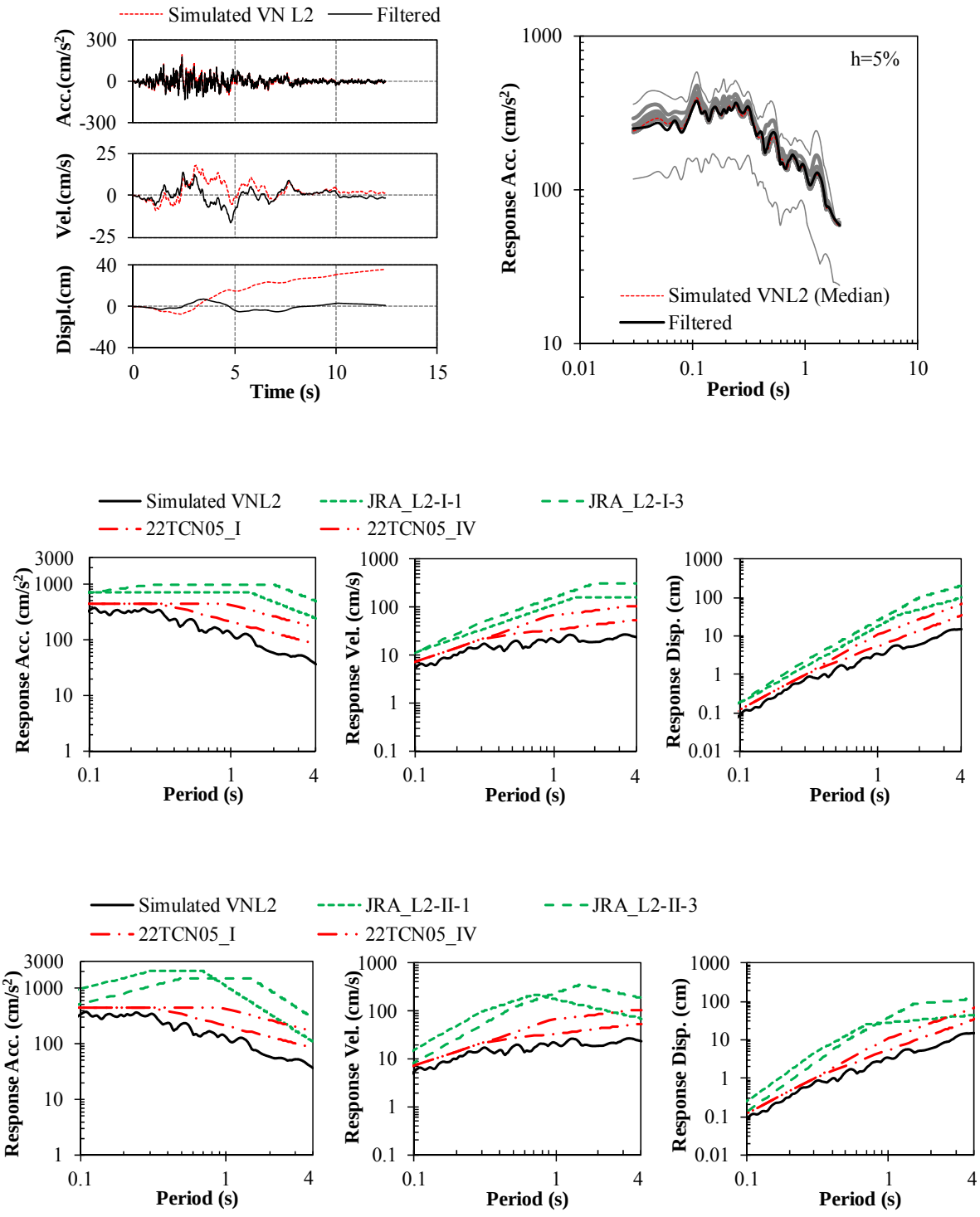

Figure 4.17a Comparison of the observed, simulated level 2 ground motion (case of 50 bar) and other codes (JRA_L2-I-1 and JRA_L2-II-1 is level 2 of type 1 and type 2 with soil type 1 according to in JRA-2002, respectively).

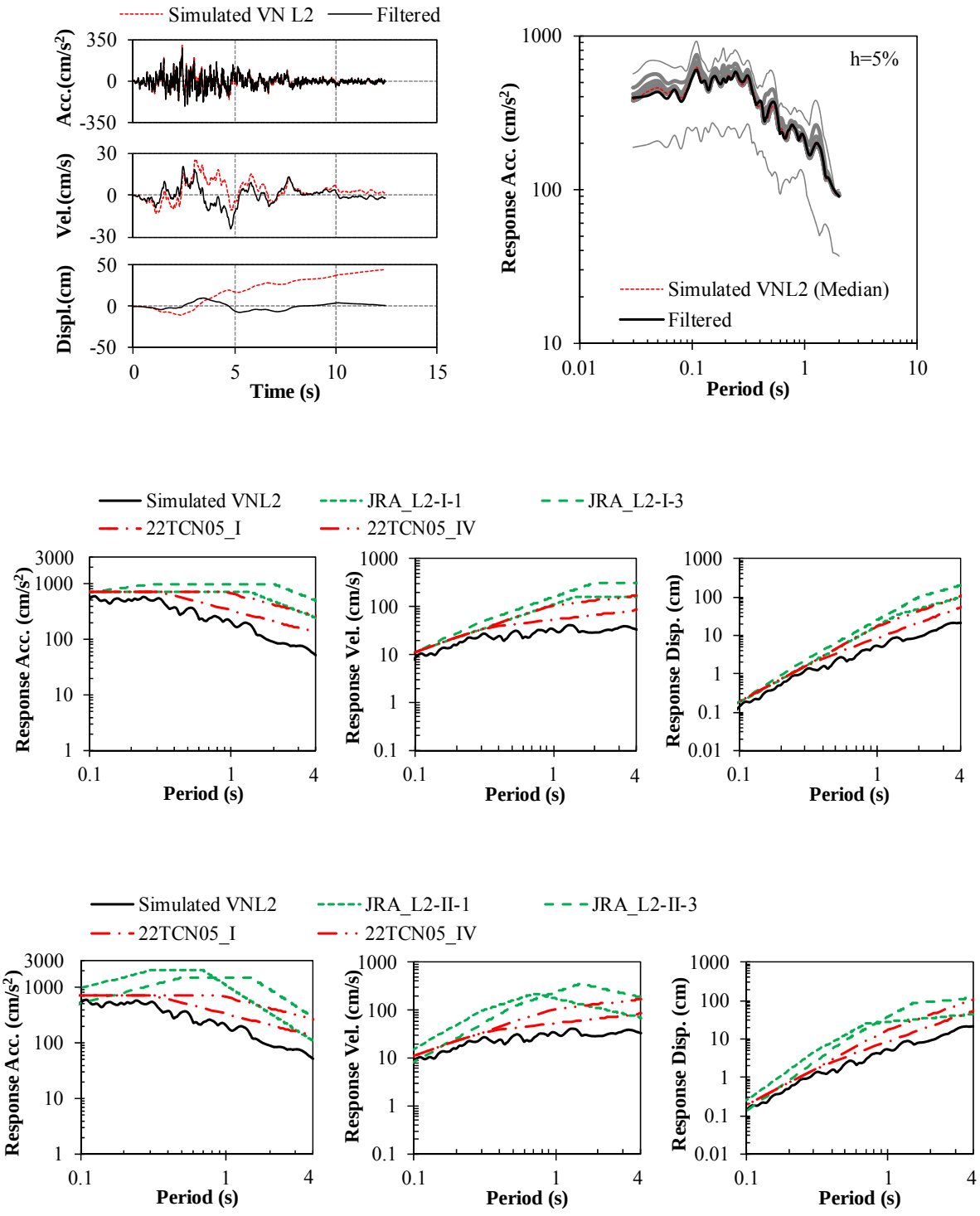

Figure 4.17b Comparison of the observed, simulated level 2 ground motion (case of 100 bar) and other codes (JRA_L2-I-1 and JRA_L2-II-1 is level 2 of type 1 and type 2 with soil type 1 according to in JRA-2002, respectively).

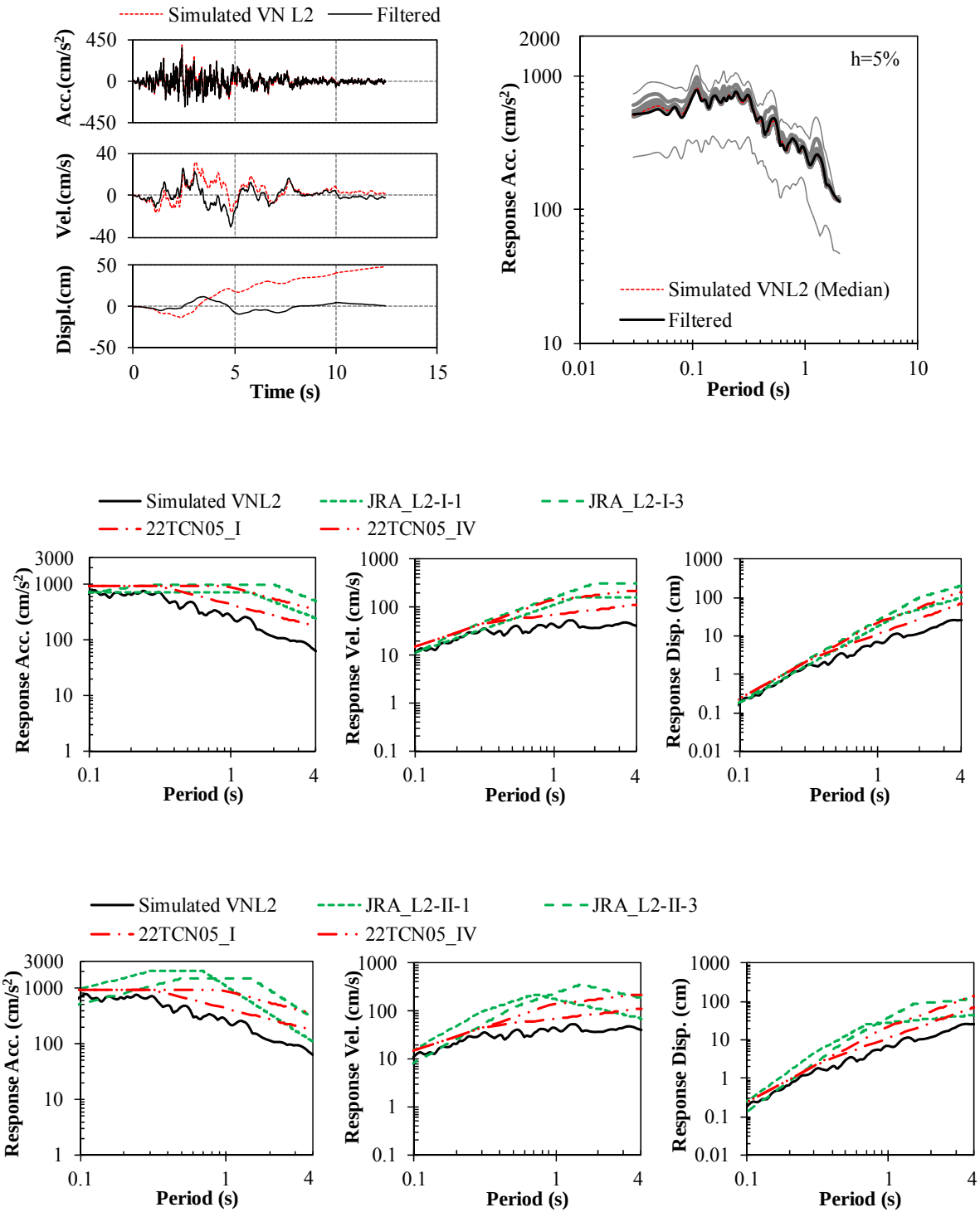

Figure 4.17c Comparison of the observed, simulated level 2 ground motion (case of 150 bar) and other codes (JRA_L2-I-1 and JRA_L2-II-1 is level 2 of type 1 and type 2 with soil type 1 according to in JRA-2002, respectively).

4.4.6 Step 2: Synthetic acceleration response spectra

4.4.6.1 Target spectral accelerations

The target spectrum (proposed spectral acceleration) is proposed in this step. The response spectrum acceleration is generated with earthquake of occurrence based on the historical earthquake parameters and observed earthquake records. The outline of equations for calculation of the acceleration spectrum is shown in **Table 4.9**. The skeleton pattern of the response spectrum is to be compared with current seismic codes in Vietnam.

Figs 4.16 and **4.17** shows the comparisons of the response spectrum associated with the observed, predicted ground motion and other seismic codes by logarithm format in good agreement. These results are accurate for predicting the maximum credible ground motion with the earthquake level in Vietnam. According to *NEHRP (2003)* and *UBC 1997* (*ICC 1997*), the control period that marks the start of the constant-acceleration plateau, T_B, could be calculated as a fraction of the value of T_C as follows:

$$T_0 \left(or\ T_B \right) = 0.2\ T_C \left(or\ 0.2\ T_S \right) \tag{4.12}$$

The final control period, T_D, is clearly a function of earthquake magnitude, and hence could be mapped by performing disaggregation of the UHS at a selected return period, and then estimating the value of T_D from the value of the dominant magnitude, M, using an equation such as that from HAZUS (*FEMA, 2003*):

$$T_D = 10^{(M-5)/2} \tag{4.13}$$

The flat part of the spectrum ($T < T_0$) is defined from acceleration coefficient, A_S ($A_S = S \times PGA$) to maximum response spectral acceleration, S_A ($S_A = 2.5\ A_S$). The part of spectrum ($T_0 < T < T_S$) is defined as the period of the constant response spectral acceleration. Besides, the recent *ASCE [2002]*, *IBC [2003]* and *LRFDSEI-1 (2009)* presented the first corner period $T_0 = 0.2 \cdot T_S$. The second corner control is defined as follows:

$$T_S = \left(S_{D1} / S_{DS} \right) \cdot 1 \text{ sec} \tag{4.14}$$

The control period can be also obtained by the simple relationship from PGD, PGV and PGA according to *Malhotra (2006)* by **Eqs. (4.15)** and **(4.16)**. This procedure is similar to the Newmark-Hall's procedure.

$$T_0 = T_S / 2.5$$
$$T_S = 2\pi \times \left(\frac{PGV \cdot \alpha_V}{PGA \cdot \alpha_A} \right) \tag{4.15}$$
$$T_D = 2\pi \times \left(\frac{PGD \cdot \alpha_D}{PGV \cdot \alpha_V} \right)$$

$$S_A = \alpha_A \cdot PGA$$
$$S_V = \alpha_V \cdot PGV \tag{4.16}$$
$$S_D = \alpha_D \cdot PGD$$

In which amplification factor α_D, α_V and α_A is 2.17, 1.35 and 1.96 corresponding to 5% damping ratio, respectively (published by *Malhotra, 2006*).

Malhotra (2006) shows the different ratio of 0.2 (T_0/T_S = 0.2 in the code spectrum) and 0.4 (T_0/T_S = 1/2.5 = 0.4). That is due to the code spectrum is conservative, and it is a composite of several seismic events. In this section, the effective soil profile is not considered. The period should be considered to earthquake spectral response acceleration at short periods. In this analysis, maximum of response spectral acceleration is about 0.4 sec for the both VNL1 and VNL2. Thus, the upper limit of the period of the constant spectral acceleration branch, T_S = 0.4 is chosen. T_S is larger than the soil type-I of the *22TCN 272-05* but smaller than all cases of the JRA-2002. T_S = 0.4 correspond to soil type-A, and site coefficient (S = 1) in *TCXDVN 375-2006* and in *EC8*. This value will be used as the lower limit of the period of the constant spectral acceleration branch in this study.

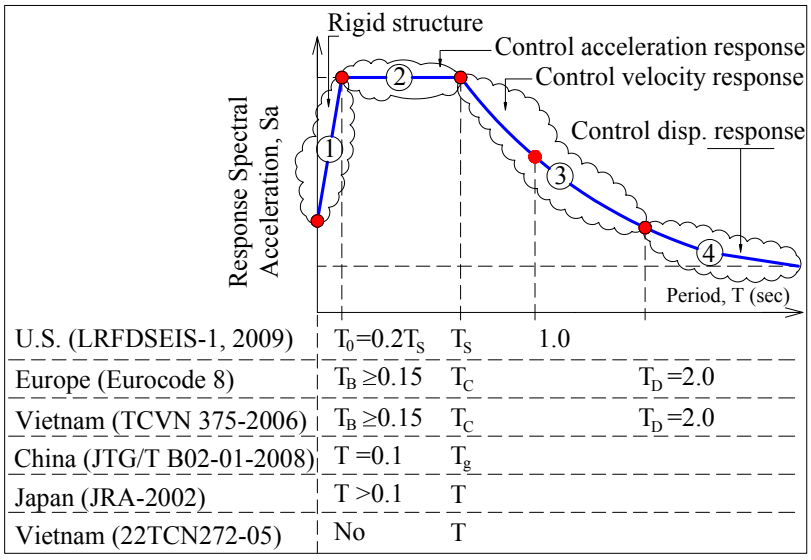

Figure 4.18 Diagrammatic sketch of seismic amplification factors in other seismic codes and classification of control zones in the acceleration response spectra.

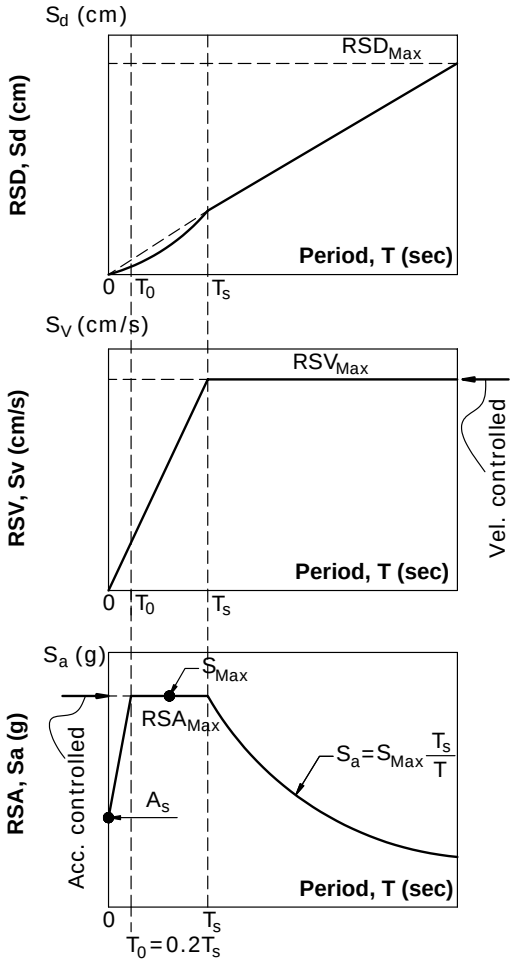

Figure 4.19 Format of the target response spectrum.

Table 4.8 Compute the control periods.

Control periods	Dien Bien Earthquake on the year 2002		Simulated ground motion					
			VN L1			VN L2		
	N-S	E-W	50 bars	100 bars	150 bars	50 bars	100 bars	150 bars
T_0	0.02	0.03	0.06	0.04	0.05	0.08	0.07	0.07
T_S	0.10	0.17	0.32	0.21	0.23	0.40	0.37	0.36
T_D	1.03	0.67	2.50	2.50	2.47	4.50	4.25	4.07

4.4.6.2 The selected spectral accelerations

Almost seismic codes rely on the concept of the elastic ground acceleration response spectrum because it is widely used in the force-based seismic design approach. The elastic response spectrum is usually established to a single ground motion parameter deterministically or probabilistically estimated from the seismicity of the individual region

based on the *PGAs*. In general, the shape of a spectrum is statistically derived from a collection of the numerous spectra representatives of the ground motions recorded in different earthquakes under similar conditions, especially, characterized by local soil conditions). Normally response spectra provide information on the peak elastic response for a specified elastic damping ratio ($\xi = 0.05$), and are plotted against the elastic period but also possible to plot inelastic spectra related to specified displacement ductility levels in case of high peak response acceleration and low peak response displacement.

Design response spectra for seismic design were constructed using the procedures and site factors described in the respective specifications. They were constructed using rock spectral accelerations. The elastic acceleration spectra in the U.S., China and Europe (and Vietnam) are similar each other and the diagrammatic sketch of these spectra in terms of seismic amplification factors is shown in **Fig 4.18**. The formulation to determine the elastic spectral curve in *TCXDVN 375-2006* is Type 1 of *EC 8*. The S_a spectrum is strongly dependent on the site types. The important factors influencing the frequency of a ground motion depend on the site type, epicenter distance and earthquake magnitude. The key points in the response design spectra will be separated the whole spectrum into four zones including the rigid structure region (zone 1), the constant acceleration response region (zone 2), the constant velocity response region (zone 3), and the constant displacement response region (zone 4). The zone 4 only describes in *EC 8* and *TCVN 375-2006*. The constant displacement portion of response spectrum (zone 4) has not been considered for bridge structure in this study.

The proposed response spectrum is assumed for rock site here (i.e. soil class B in *LRFDSEIS-1 (2009)*, soil class A in *EC 8*/*TCVN 375-2006*, soil I type in *AASHTO LRFD 1998*/*22TCN 272-05*). According to the USGS (U.S. Geological Survey) site classification, site class B corresponds to rock and firm sites with average shear wave velocity to a depth of 30 m larger than 750 m/s, and site type E corresponds to soft soil sites with shear wave velocity less than 180 m/s as shown in **Table 3.6**. The characteristic period for everyone ground motion is used to normalize the spectrum before a statistical analysis is carried out. To calculate the elastic spectral acceleration S_a, the characteristic periods, i.e., T_0, T_S is very necessary calculated.

In China, the T_0 value is limited at 0.1 s; the T_g value is 0.35 s, 0.40 s and 0.45 s for zone 1, zone 2 and zone 3, respectively (*JTG/T B02-01-2008*).

In Japan, the T_0 and T_S value of Level 1 is 0.1 s, 0.2 s, 0.33 s and 0.11 s, 0.12 s, 0.13 s for soil of class I, class II, class III, respectively (*JRA-2002*).

In Europe, the characteristic period, T_B value is 0.15 s and 0.20 s for soil classes A, B and C, D, respectively; T_C value is 0.4 s, 0.5 s, 0.6 s and 0.8 s for soil class A, B, C and D, respectively (*EC 8*).

The format of the target response spectrum is selected as shown in **Fig 4.19**. The characteristic periods of the response acceleration spectrum were described in detail in section

4.3.6.1. Besides, based on some earthquake records were recorded in Vietnam. An example of Dien Bien earthquake records have PGA of about 0.11 g, peak response of acceleration of 383.11 cm/s^2 (~ 0.39 g) at a period of 0.06 s and peak response displacement less than 0.8 cm for damping of 5% (described in **Chapter 2**). Finally, the outline of equations for calculation of acceleration spectrum is shown in **Table 4.9**. Peak response region, RSA_{Max}, is equal to 2.5·PGA on almost seismic design codes. RSA_{Max} in *AASHTO LRFD*, *JTG/T B02-01-2008* and *EC 8* was limited by PGA values. Only *JRA-2002* did not uses PGA values when the limit RSA_{Max} value. The comparison between proposed response spectrum and current *22TCN 272-05* are shown in **Fig 4.20**.

Table 4.9 Outline of the target response spectral acceleration.

Period (s)	$T < 0.2T_S$	$0.2T_S \le T \le T_S$	$T_S < T$
Level 1 ground motion	$S_a = (S_{max} - PGA)\frac{T}{T_o} + A_S$ $A_S = S \times PGA$ (S = site coefficient)	$S_a = S_{\max}$ $S_{\max} = 2.5 \times A_S$ $T_S = 0.35$	$S_a = S_{max} \times \left[\frac{T_S}{T}\right]$
Period (s)	$T < 0.2T_S$	$0.2T_S \le T \le T_S$	$T_S < T$
Level 2 ground motion	$S_a = (S_{max} - PGA)\frac{T}{T_o} + A_S$ $A_S = S \times PGA$ (S = site coefficient)	$S_a = S_{\max}$ $S_{\max} = 2.5 \times A_S$ $T_S = 0.4$	$S_a = S_{max} \times \left[\frac{T_S}{T}\right]$

Note:

- ✓ PGA is essentially peak ground acceleration in rock, S is a factor related to the soil class and η is a factor for adjusting to damping values different from 5% of critical.
- ✓ S = 1 for the rock sites.

4.4.7 Step 3: Wave amplitude adjustment

In the third step, the waveform amplitudes will be adjusted, because of when the time-history waves are not close to target spectrum, it is necessary for the wave amplitude adjustment's process. The results of this process were realized as the result of the fitting. On the other hand, the Fourier amplitude should be determined to simulate the design ground motion, such that the associated spectral response acceleration will be compatible with the target spectrum as above proposed. The procedure to simulate a compatible ground motion is illustrated in **Fig 4.15**.

In principle, there were waves in the Dien Bien earthquake should be able to use these waves to match the target spectrum. However, we want to build new common objectives in accordance with earthquakes in Vietnam rather than using the spectrum of foreign standards in this section.

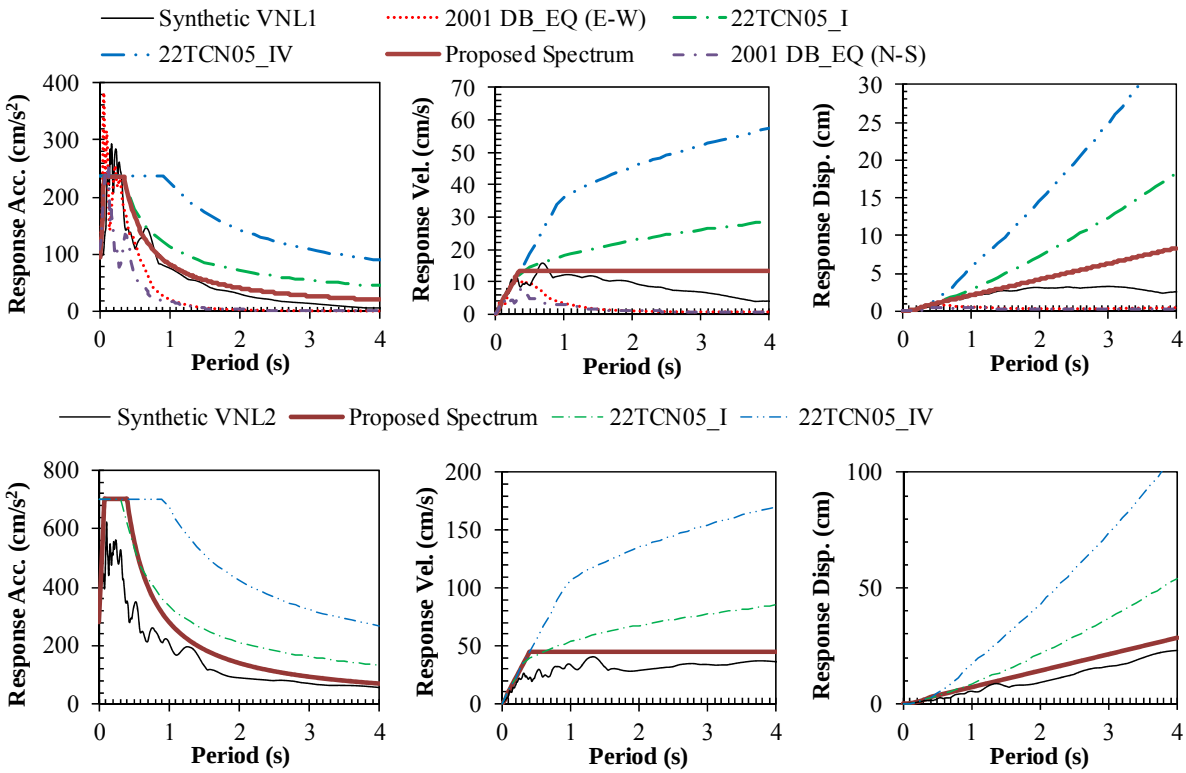

Figure 4.20a Proposed spectral accelerations with level 1 (VNL1) and level 2 (VNL2) ground motions (for case of 100 bars)

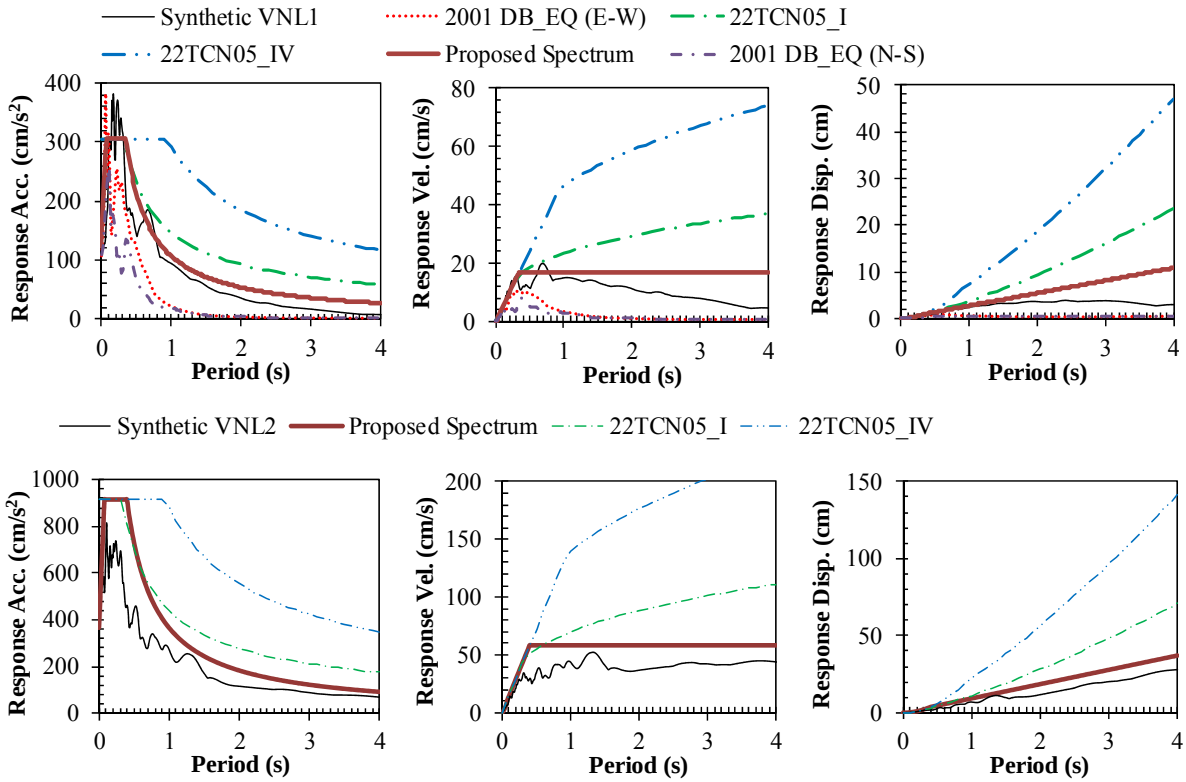

Figure 4.20b Proposed spectral accelerations with level 1 (VNL1) and level 2 (VNL2) ground motions (for case of 150 bars).

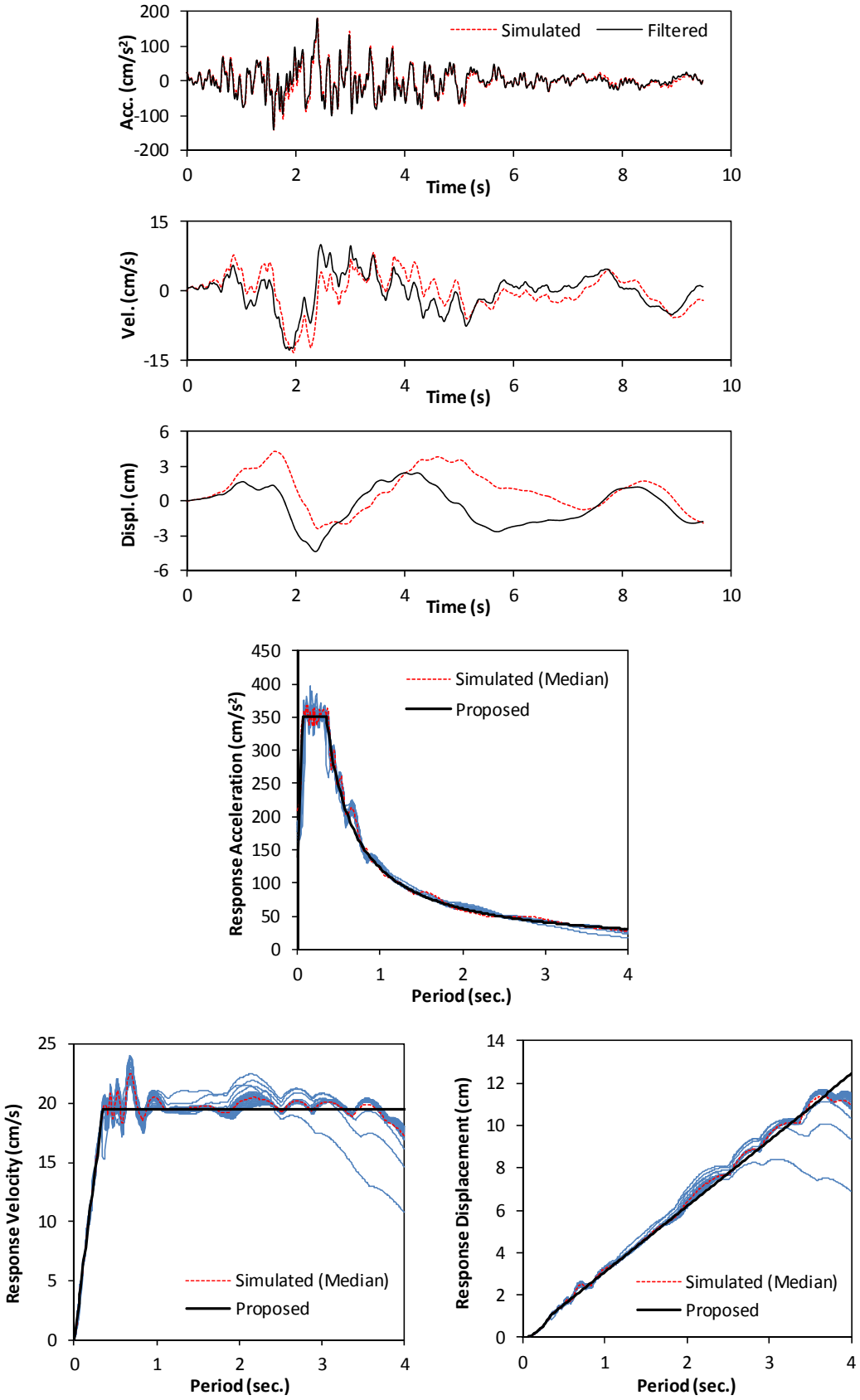

Figure 4.21 Match the target spectrum for VN L1 ground motion (the target spectrum is made by PGA of 140 cm/s^2).

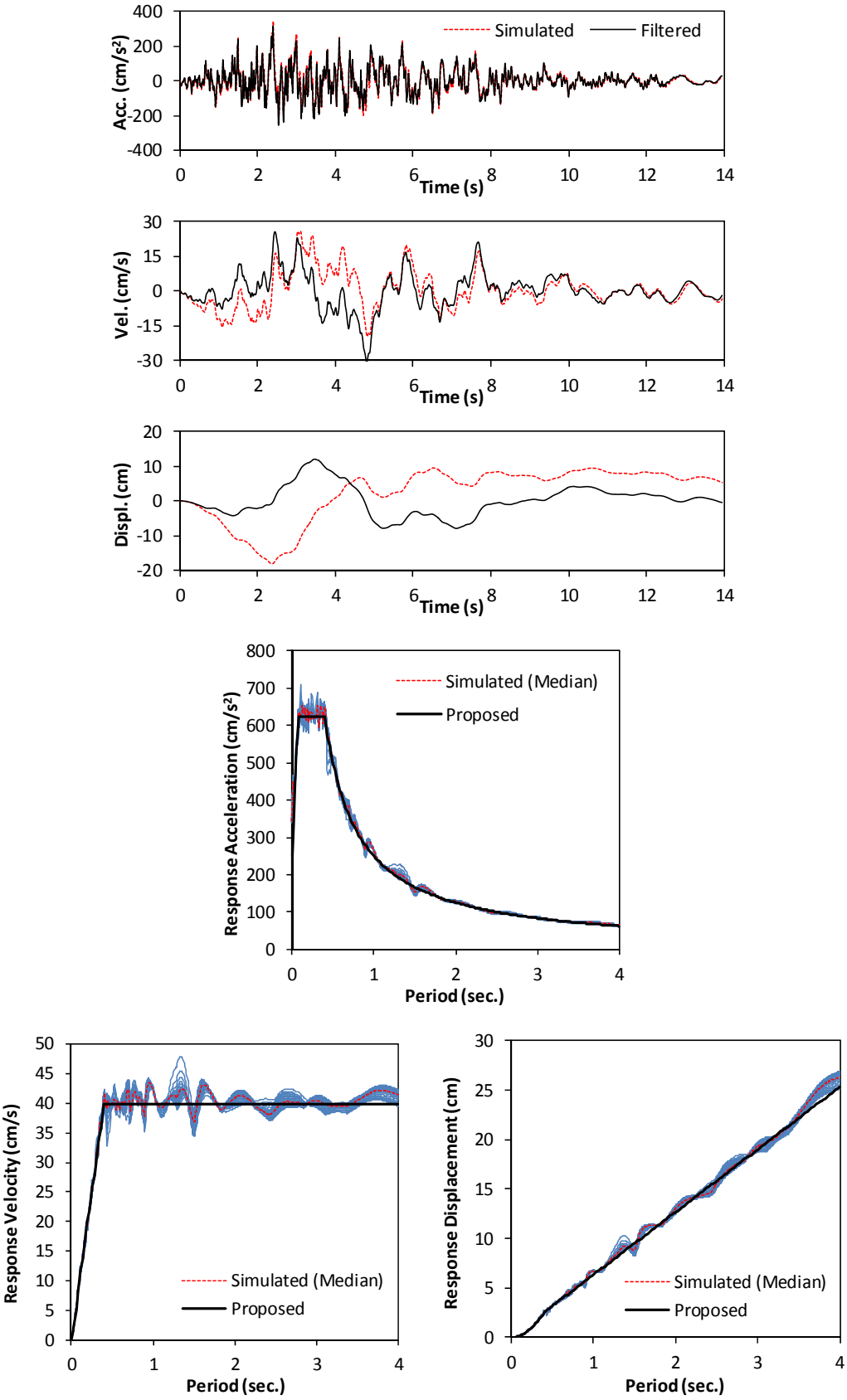

Figure 4.22 Match the target spectrum for VN L2 ground motion (the target spectrum is made by PGA of 250 cm/s^2).

The target response spectral is defined according to simulated ground motions (shown in Step 1). The response acceleration spectrum was generated by those time-histories. However, they tend not to match target response spectral for both VNL1 and VNL2 ground motions. Therefore, these seismic waves are necessary modified to match the target spectrum. **Figs 4.21** and **4.22** show the mean response spectral acceleration obtained from simulated seismic waveforms of VNL1 and VNL2 ground motion after fitting them to match proposed response spectrum. They are performed by using D-wave software. In this section, an example of the PGA of 140 cm/s^2 and 250 cm/s^2 are used to response acceleration spectrum for VNL1 and VNL2 ground motions, respectively.

4.5 CONSIDERATION

The development of the ground motion predictions inevitably depends on the accumulation of the strong ground motion. The results of this chapter can be shown as follows:

Probabilistic seismic hazard analysis is adopted in this chapter. The PGA values in this study have greater values in *TCXDVN 375-2006* (see **Table 4.2**). This is due to this study used the new attenuation relationship which is developed in **Chapter 3**.

The stochastic model is used to determine the target response acceleration spectrum Based on the simulated ground motion, the new response acceleration spectrum is proposed. Two-level (VNL1 and VNL2) ground motions were presented in this Chapter corresponding to the probability of earthquake exceedance with return period of 475 yrs and 2500 yrs. The results of the probabilistic seismic hazard analysis are shown in **Table 4.3**.

After that, the target response spectrum is proposed with a short-period. For the VNL1 ground motion, a horizontal constant spectral acceleration arranged from $T_0 = 0.2\ T_S$ (= 0.07 s) to T_S = 0.35 s. For the VNL2 ground motion, a horizontal constant spectral acceleration arranged from $T_0 = 0.2\ T_S$ (= 0.08 s) to T_S = 0.4 s.

Finally, the waveforms are generated by the processing of the match the target response spectrum (see **Figs 4.21** and **4.22**).

The seismic acceleration achieved from simulated PGA can be used for dynamic analysis of bridge, etc. on the rock site in Vietnam. The selection of seismic waveforms to be used for this requirement is performed.

4.6 REFERENCES

[1]. 22TCN 272-05: *Specification for Bridge Design*, Vietnam Ministry of Transport, 2005.

[2]. Eurocode 8: *Design of structures for earthquake Resistance-Part 1: general rules, seismic actions, and rules for buildings*. EN 1998-1: 2004.
[3]. AASHTO LRFD: *Load and resistance factor design (LRFD) specifications for highway bridges*, Washington (DC): American Association of State Highway and Transportation Officials (AASHTO), 1998.
[4]. JRA-2002, *Specification for Japanese Highway Bridges, part V: seismic design*, Japan Road Association, 2002.
[5]. JTG/T B02-01-2008, *Guidelines for Seismic Design of Highway Bridge*, Ministry of Communications and transport, China, 2008.
[6]. LRFDSEIS-1: Guide Specifications for LRFD Seismic Bridge Design, 1st Edition with 2010 Interim Revisions. ISBN: 1-56051-396-4, 258 pages, 2009.
[7]. TCXDVN 375-2006: *Design of Structures for Earthquake Resistance*, Vietnam Ministry of Construction, 2006.
[8]. Aki, K. (1967). Scaling law of seismic spectrum, J. Geophys. Res., Vol. 72, pp. 1217–1231.
[9]. Arias, A. (1970). A measure of earthquake intensity, in Seismic Design for Nuclear Power Plants, edited by R. Hansen, MIT Press, Cambridge, MA, pp. 438–483.
[10]. Atkinson, G. and Boore, D. (1995). *New ground motion relations for eastern North America*, Bulletin of the Seismological Society of America, Vol. 85, pp. 17–30.
[11]. Atkinson, G. and Boore, D. (1997). Stochastic point-source modeling of ground motions in the Cascadia region, Seism. Res. Lett. 68, 74–85.
[12]. Atkinson, G. and Silva, W. (2000). Stochastic modeling of California ground motions, Bulletin of the Seismological Society of America, Vol. 90, pp. 255–274.
[13]. Atkinson, G. and Boore, D. (1998). Evaluation of models for earthquake source spectra in eastern North America, Bulletin of the Seismological Society of America, Vol. 88, pp. 917–934.
[14]. Bommer, J.J. and Martínez-Pereira, A. (1999). The effective duration of earthquake strong motion. Journal of Earthquake Engineering, Vol. 3, pp. 127-172.
[15]. Boore, D.M. (1983). *Stochastic simulation of high-frequency ground motions based on seismological models of the radiated spectra*, Bulletin of the Seismological Society of America, Vol. 73, No. 6, pp. 1865-1894.
[16]. Boore, D.M. (2003). *Simulation of Ground Motion Using the Stochastic Method*, Pure and Applied Geophysics, Vol. 160, No. 3-4, pp. 635-676.
[17]. Brune, J. (1970). Tectonic stress and the spectra of seismic shear waves from earthquakes, J. Geophys. Res., Vol. 75, pp. 4997–5009.
[18]. Brune, J. (1971). *Correction*, J. Geophys. Res., Vol. 76, 5002.
[19]. Cao, D.T. (2006). *An overview of seismic activity in Vietnam*, The 1st meeting on Seismic Hazard in Asia-The Abdus Salam International Centre for Theoretical Physics, Trieste, Italy.
[20]. Cong, L., Hu, J., Fu, Z., Wen, Y., Kang, G. and Wu, X. (2003). *Distribution of Lg coda Q in the Chinese continent and its adjacent regions.* Science in China Series D: Earth Sciences, Vol. 46, No. 6, pp. 529-539.
[21]. Erdik M. and Durukal E. (2003). *Simulation modeling of strong ground motion*, in Earthquake Engineering Handbook 2003, Chen WF and Scawthorn C (Editors), CRC Press, Boca Raton, Florida, 6-16-67.

[22]. Fenton, C.H., Charusiri, P. and Wood, S.H. (2009). Recent paleoseismic investigations in northern and western Thailand. Anna Geophys, Vol. 46, pp. 957-981.
[23]. Giardini, D. (2011). *The Recent Catastrophic Earthquakes in New Zealand and Japan from a Seismological Perspective*. Published lecture by the Swiss Seismological Service at the ETH Zürich on 17 March 2011.
(Website: http://www.seismo.ethz.ch/Earthquake_Talk_2011_03_17_e).
[24]. Hanks, T. and McGuire, R. (1981). *The character of high-frequency strong ground motion*, Bulletin of the Seismological Society of America, Vol. 71, pp. 2071–2095.
[25]. Hung, T.V., Kiyomiya, O. and An, T.X. (2009). *Evaluation of seismic resistance for a multi-spans bridge in Vietnam by investigation of earthquake activity and dynamic response analysis*. Journal of structural engineering, Vol. 55A, pp. 537-549.
[26]. Jin, A. and Aki, K. (1988). *Spatial and temporal correlation between coda Q and seismicity in China*. Bulletin of the Seismological Society of America, Vol. 78, No. 2, pp. 741-769.
[27]. Kempton, J.J. and Stewart, J.P. (2006). *Prediction equations for significant duration considering site and near-source effects.* Earthquake Spectra, Vol. 22, No. 4, pp. 985–1013, Earthquake Engineering Research Institute, Nov. 2006;
[28]. Lacassin, R., Replumaz, A. and Hervé Leloup, P. (1998). Hairpin river loops and slip-sense inversion on Southeast Asian strike-slip faults. Geology, Vol. 26(8), pp. 703-706.
[29]. Lam, N.T.K., Wilson, J.L., Chandler, A.M. and Hutchinson, G.L. (2000). *Response spectral relationships for rock sites derived from the component attenuation model*. Earthquake Engineering & Structural Dynamics, Vol. 29, pp. 1457-1489.
[30]. Little T. (2007). *Ground motion time-histories matching spectrum*, CSCE, Vancouver, Canada.
(website:http://www.cscevancouver.ca/csce/src/docs/rsseminar07/lect08Slide.pdf).
[31]. Mak, S., Chan, L.S., Chandler, A.M. and Koo, R.C.H. (2004). *Coda Q estimates in the Hong Kong Region.* Journal of Asian Earth Sciences, Vol. 4, Issue 1, pp. 127-136.
[32]. Malhotra, P.K., (2006). *Smooth Spectra of Horizontal and Vertical Ground Motions*, Bulletin of the Seismological Society of America; April 2006; v. 96; no. 2; p. 506-518; DOI: 10.1785/0120050062.
[33]. Mohammadioun, B. and Serva, L. (2001). *Stress Drop, Slip Type, Earthquake Magnitude, and Seismic Hazard*, Bulletin of the Seismological Society of America; August 2001; Vol. 91; No. 4; pp. 694-707; DOI: 10.1785/0120000067.
[34]. Nielsen, C., Chamot-Rookea, N. and Rangin, C. (2004). (The ANDAMAN Cruise Team). From partial to full strain partitioning along the Indo-Burmese hyper-oblique subduction. Marine Geology, Vol. 209, pp. 303-327.
[35]. Perasan, A., Trieu, C.D., Bach, M.X., Hung, N.T., Nam, B.A. and Binh, N.X. (2009). *Seismic activity in Vietnam*. Journal of Geology, Series A, No. 314 (9-10), pp. 27–37.
[36]. Phuong, N.H. (1991). *Probabilistic assessment of earthquake hazard in Vietnam based on seismotectonic regionalization*, Tectonophysics, Vol. 198, Issue 1, pp. 81–93.
[37]. Phuong, N.H. (2001). Probabilistic Seismic Hazard Assessment Along the Southeastern Coast of Vietnam. Natural Hazards. Vol. 24, pp. 53–74.
[38]. Phuong, N.H. and et al. (2007a). *Application of GIS technology for modeling and*

assessment of urban risk for Ha Noi City. Project No. DL/02-2006-2, Ha Noi.
[39]. Phuong, N.H. and Truyen, P.T. (2007b). *Development of a fault-source model for earthquake hazard assessment in Vietnam.* Journal of earth sciences, Vol. 29, No. 3, pp. 228-238.
[40]. Socquet, A. and Pubellier, M., (2005). Cenozoic deformation in western Yunnan (China–Myanmar border). Journal of Asian Earth Sciences, Vol. 24, pp. 495-515.
[41]. Son, L.T. and Dung, N.Q. (2003). The first result of the observed acceleration in Vietnam", Journal of Earth Sciences, Vol. 25(1), pp. 78-85. (Vietnamese).
[42]. Thanh, T.T.M. (2007). Seismic moment of Dien Bien earthquake M = 5.3. Vietnamese Journal of Geology, No. 304 (1-2), pp. 16-20. (Vietnamese)
[43]. Thuc, P.V. (2007). *Seismology and Earthquake in Vietnam*. Natural Science and Technology Publisher, Hanoi, Vietnam, 2007 (Vietnamese).
[44]. Toro, G., Abrahamson, N., and Schneider, J. (1997). *Model of strong ground motion in eastern and central North America: best estimates and uncertainties*, Seism. Res. Lett. 68, 41–57.
[45]. Trieu, C.D. (1997a). *The strong seismogenic zones in Vietnam*, Vietnamese Journal of Geology, Series B, No. 9-10, pp. 47-62.
[46]. Trieu, C.D. (1997b). *Earthquake generation zones on the territory of Vietnam*, ACTA Geophysica, Vol. 45, No. 3, pp. 215-226.
[47]. Trieu, C.D. (2002). *Some characteristic features of seismotectonic conditions and seismic regime of the Tuan Giao earthquake area*. Journal of Geology, Series B-No. 19-20, pp. 54-68.
[48]. Trieu, C.D. (2008). *Earthquake*. Science and Technology Publisher, Hanoi, Vietnam, 2008 (Vietnamese).
[49]. Trieu, C.D., (1999). *Probable approach for long-term earthquake prediction in Vietnam based on the regulation of epicentral distribution*. J. of Geology, A/251, pp. 14-21. Hanoi.
[50]. Trieu, C.D., Panza, G.F., Peresan, A., Vaccari, F., Romanelli, F., Tuyen, N.H., Hung, P.N., Dung, L.V., Bach, M.X., Tuan, T.A. and Trong, C.D. (2008). *Seismic hazard assessment of Vietnam territory on the basis of deterministic approach.* Vietnam Journal of Geology, Series B, No. 31–32, pp. 220-230.
[51]. Van, P.T.K. (2006): The Lai chau-Dien Bien neotectonic fault zone and its acting manifestations by moderate local earthquakes. Vol. 27, pp. 30-39.
[52]. Wong, Y.L., Zheng, S., Liu, J., Kan, Y., Tam, C.M., Leung, Y.K. and Zhao, X. (2002). *Attenuation function of ground motions for Guangdong region of Southern China*. International Conference on Advances and New Challenges in Earthquake Engineering Research, August 15-20, Harbin and Hong Kong, China, pp. 123-130.
[53]. Xu, Y., Herrmann, R.B., Wang, C.Y., and Cai, S. (2010). *Preliminary High-Frequency Ground-Motion Scaling in Yunnan and Southern Sichuan, China*. Bulletin of the Seismological Society of America, Vol. 100, No. 5B, pp. 2508–2517, 2010, doi: 10.1785/0120090196.
[54]. Xuyen, N.D. (1994), *Status of seismic hazard assessment in Vietnam*, Proceedings of Workshop on Implementation of Global Seismic Hazard Assessment Program in Central and Southern Asia, 74-87.

[55]. Xuyen, N.D. and Thanh, T.T.M. (1999). *A formula for estimation of seismic peek ground acceleration in Vietnam*. Journal of Earth Csience, Vol. 21/3, pp. 207-213. (Vietnamese).
[56]. Yabe, M. (2011). 平成 23 年東北地方太平洋沖地震 (地震応答スペクトル). (http://committees.jsce.or.jp/2011quake/system/files/yabe_no1_110321.pdf).
[57]. Yun, S., Lee, W.S., Lee, K. and Noh, M.H. (2007). *Spatial Distribution of Coda Q in South Korea.* Bulletin of the Seismological Society of America, Vol. 97, No. 3, pp. 1012-1018.
[58]. Zhang, Y., Xu, L.S., Chen, Y.T., Feng, W.P. and Du, K.L. (2007), Source process of Ms6.4 earthquake in Ning'er, Yunnan in 2007. Science in China Series D: Earth Sciences. Vol. 52, N. 2, pp. 180-188, DOI: 10.1007/s11430-009-0016-0
[59]. Zhao, W.M., Yang, M.Z., Jin, Y.L., Xu, W.J. and Ren, X.M. (2000). *Characteristics of coda Q-value in the mid-northern part of Ningxia*. ACTA Seismologica Sinica, Vol. 13, No. 3, pp. 265-272.

CHAPTER 5

SEISMIC RESPONSE ANALYSIS OF BRIDGE USING SIMULATED GROUND MOTION

5.1 INTRODUCTION

Linear and non-linear time-history analysis methods are becoming more common in seismic analysis and design of structures. The ground motion (seismic waves) used as input should be representative of the seismo-tectonic environment at the site location, i.e. correspond to earthquake ground motions that have been recorded including magnitudes, epicenter distances, faults and so on at the particular location. In addition to being compatible with a response spectrum constructed from the design spectral acceleration values, these time histories need to have durations and waveforms that will allow the structural model to respond in elastically with sufficient cycles of load reversal or hysteretic model.

According to the analyses of the earthquake records obtained by the seismometers, Vietnam is located at moderated seismic activity area. However seismic design for buildings and bridges become to be regarded as important design and so on in Vietnam. The section **1.1.2.2** described a brief on seismic design for bridge in Vietnamese specification for bridge design (*22TCN 272-05*), determine the seismic response of the pier bridge at the plastic zone in a moderate seismic zone (i.e. acceleration coefficient, $A = 0.09 \div 0.29$g with g being the gravity acceleration), and to make sure that the empirical beam seat formula is appropriate for typical bridge in Vietnam. **Chapter 1** also considered the items of some seismic codes and shown that the only *JRA-2002* considered fully seismic response for bridge by dynamic analysis method while most of the other codes considered by static analysis method. *JRA-2002* recommends a dynamic response analysis to check the structural safety against Level 1 and Level 2 earthquake ground motion because a dynamic response of structure subjected to an earthquake ground motion is a key in evaluating a structural safety against the earthquake. During the analysis of the seismic behavior of a bridge by the dynamic method with Level 1 earthquake ground motion, an analysis model can demonstrate the dynamic properties of the bridge within the elastic range; nonlinear behavior is generally not allowed in a bridge. The Level 2 earthquake ground motion, the plastic deformation and energy absorption of a member are generally considered. It is necessary that an analytical model

which is capable of expressing the dynamic properties of the nonlinear zone of the bridge having considered inelastic hysteretic property of the members such as a pier.

Generally, there are two analytical methods used in dynamic analysis of a bridge. There are the response spectrum method and the time-history response analysis method. The response spectrum analysis most frequently used with simple configurations, and a time history method is not required for ordinary bridges in *22TCN 272-05*. This is approximate dynamic analysis method that gives the maximum response (acceleration, velocity, or displacement) of an SDOF system with the same damping ratio, but with different natural frequencies, responds to a specified seismic excitation. The design is generally based on the maximum earthquake response. Response spectrum analysis is probably the most common method used in design offices to determine the maximum structural response due to transient loading (*Chen and Duan, 2003*). The dynamic analysis may be necessary for some important and complex bridges, however, it is not considered fully in *22TCN 272-05*, this code concentrated only to the response spectrum method. In *JRA-2002*, the dynamic analysis methods can be chosen for the verification of seismic performance for Level 2 earthquake ground motion. Although the time-history response analysis method having used an inelastic hysteretic model is usually selected for a structure member. A basic procedure of dynamic analysis method for bridge structures will be considered in this Chapter.

Besides, **Chapter 4** presented the predicted earthquake ground motion including time-histories and proposed response spectral acceleration with two-level ground motions (Level 1 and Level 2 ground motions). Thus, an example of seismic response analysis of the PC Bridge will be considered in this Chapter.

5.2 DYNAMIC ANALYSIS METHOD OF HIGHWAY BRIDGE

5.2.1 Dynamic analysis method

5.2.1.1 Equation of motion

The dynamic response of a structure depends on its mechanical characteristics and the nature of the induced excitation. Mechanical properties which are efficient to mitigate the structure's response when subjected to certain inputs might have an undesirable effect during other inputs. In a dynamic analysis, the number of displacements required to define the displaced positions of all the masses relative to their original positions is called the number of degrees of freedom (DOF). The equation of motion of an MDOF system is similar to the SDOF system, but the stiffness K, mass M, and damping C are matrices.

The equation of motion to an MDOF system under ground motion can be expressed as (*Chen and Duan, 2003-3*):

$$[M]\{\} + [C]\{\} + [K]\{\} = -[M]\{B\} \tag{5.1}$$

In which, the stiffness matrix [*K*] can be obtained from standard static displacement-based analysis models and may have off-diagonal terms. The mass matrix [*M*] due to the negligible effect of mass coupling can best be expressed in the form of tributary lumped masses to the corresponding displacement degrees of freedom, resulting in a diagonal or uncoupled mass matrix. The damping matrix [*C*] accounts for all the energy-dissipating mechanisms in the structure and may have off diagonal terms. The vector {*B*} is a displacement transformation vector that has values 0 and 1 to define degrees of freedom to which the earthquake loads are applied. Value $\ddot{u}_g$ is ground acceleration.

5.2.1.2 Rayleigh damping

There are advanced research results to identify a general model of damping or the estimation of damping in a random vibrating system. The most common approach is to use viscous damping or Rayleigh damping (see **Fig 5.1**), in which it is assumed that the damping matrix is proportional to the mass [*M*] and stiffness matrices [*K*], or:

$$[C] = \alpha[M] + \beta[K] \tag{5.2}$$

The generalized damping of the ith mode is then given by (*Chen and Duan, 2003-3*):

$$C_i = \alpha M_i + \beta K_i \tag{5.3}$$

$$C_i = \alpha M_i + \beta \omega_i^2 M_i \tag{5.4}$$

$$\xi_i = \frac{1}{2\omega_i}\alpha + \frac{\omega_i}{2}\beta \qquad (i = 1 \text{ to } n) \tag{5.5}$$

Select damping value in two modes, ξ_m and ξ_n ($m < i < n$). Writing **Eq. (5.3)** for each of these two cases and expressing the two equations in matrix (*Clough and Penzien, 2003*):

$$\begin{Bmatrix} \xi_m \\ \xi_n \end{Bmatrix} = \frac{1}{2}\begin{bmatrix} 1/\omega_m & \omega_m \\ 1/\omega_n & \omega_n \end{bmatrix}\begin{Bmatrix} \alpha \\ \beta \end{Bmatrix} \tag{5.6}$$

Rayleigh damping coefficients α and β follows the equation:

$$2\omega_m\xi_m - \beta\omega_m^2 = 4\pi f_m\left(\xi_m - \pi f_m\beta\right) = \frac{4\pi f_m f_n(\xi_m f_m - \xi_n f_n)}{f_m^2 - f_n^2} \tag{5.7}$$

$$\beta = 2\frac{\omega_m\xi_m - \omega_n\xi_n}{\omega_m^2 - \omega_n^2} = \frac{\xi_m f_m - \xi_n f_n}{\pi\left(f_m^2 - f_n^2\right)} \tag{5.8}$$

In matrix form, Rayleigh damping is to be written (*Clough and Penzien, 2003*):

$$\begin{Bmatrix}\alpha\\ \beta\end{Bmatrix} = 2\frac{\omega_m\omega_n}{\omega_n^2 - \omega_m^2}\begin{bmatrix}\omega_n & -\omega_m\\ -1/\omega_n & 1/\omega_m\end{bmatrix}\begin{Bmatrix}\xi_m\\ \xi_n\end{Bmatrix} \tag{5.10}$$

Herein, [C] is damping matrix; [M] is mass matrix; [K] is stiffness matrix; f_m, f_n are normal frequencies of two modes (Hz); ξ_m, ξ_n are damping ratios in each frequency (%); ω_m, ω_n are the angular frequency (rad/s), respectively; and α, β are the Rayleigh damping coefficients.

The damping model uses usually Rayleigh damping in the dynamic analysis of the bridge. The damping of a structure is related to the amount of energy dissipated during its motion. It could be assumed that a portion of the energy is lost due to the deformations, and the damping could be idealized as proportional to the stiffness of the structure.

5.2.1.3 Analytical model

Regarding the purpose of analysis, energy absorbed by inelastic deformation in a structural component may be assumed to be concentrated in plastic hinges and yield lines. The location of these sections may be established by successive approximation to obtain a lower bound solution for the energy absorbed. For these sections, moment-rotation hysteresis curves may be determined by using verified analytic material models. In addition to a linear analysis, it is a common practice to perform a capacity analysis associated with the desired inelastic response in which ductile flexural response occurs at selected plastic hinge on regions within the structure. The regions are detailed to ensure plastic behaviour while inhibiting no ductile failure modes. The hysteresis properties are using the Takeda's model. The Takeda degrading stiffness (see **Fig 5.2**) and bilinear elasto-plastic hysteresis (see **Fig 5.3**) was considered to derive the inelastic spectra. Current trends for the seismic response of bridge structures have embraced the concept of performance-based design as shown in *JRA-2002*. The validity of performance-based design depends on realistic specification of ground motion inputs, realistic models of the bridge structure and realistic boundary conditions of the bridge model.

To investigate the dynamic response behaviour and evaluate the seismic performance of the bridge, nonlinear dynamic response analysis method is adopted in this work. In order to take consideration the nonlinearity of the structural element accurately, the time history nonlinear dynamic analyses are performed by the direct integral calculus, the integration is taken as the Newmark-β method that is used in finite element analysis to model dynamic systems, and the time interval of integration, Δt is 0.01 s. The Newmark-β method is the most widely used in nonlinear dynamic analysis of structures because of its accuracy and stability.

Therefore, the Newmark-β method is adopted here to solve the nonlinear equation of motions of structures. In addition, the Rayleigh damping coefficient type calculated by strain energy damping ratios is used in the dynamic analysis.

5.2.2 Analytical methodology

5.2.2.1 Response spectra analysis

The response spectrum method is a method to obtain the maximum response occurred in the vibration system. The method involves the calculation of only the maximum values of the displacements and member forces in each mode using design spectra that are the average of several earthquake motions. This method has been fully introduced in *22TCN 272-05* and other seismic design codes.

In lieu of a nonlinear time-history dynamic analysis, bridge engineers in recent years have used static push-over analyses as an effective and simple alternative when assessing the performance of existing or new bridge structures under seismic loads. Given the proper conditions, this approximate alternative can be as reliable as the more accurate and complex ones. The primary goal of such an analysis is to determine the displacement or ductility capacity, which is then compared with displacement or ductility demand obtained for most cases from linear dynamic analysis with effective section properties (*Chen and Duan, 2003-4*).

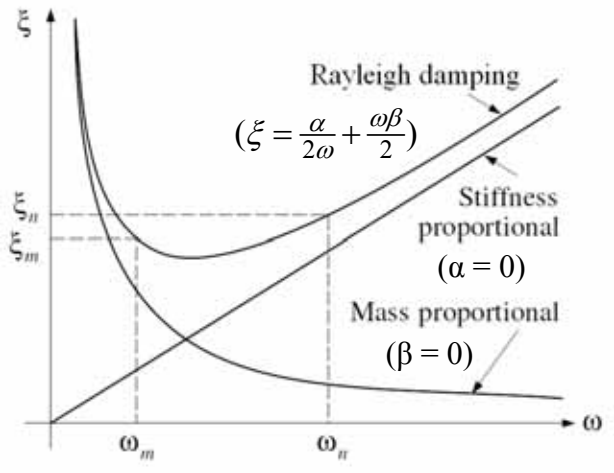

Figure 5.1 Rayleigh damping variation with natural frequency. The coefficients α and β can be determined from specified damping ratios at two independent dominant modes (namely, the m^{th} and n^{th} modes).

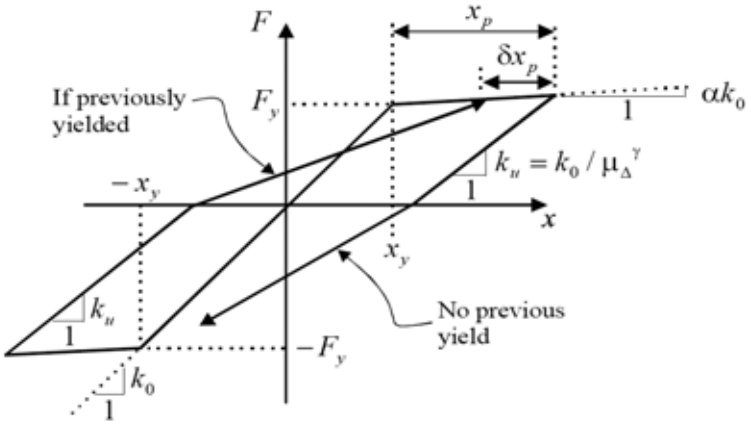

Figure 5.2 Takeda model for RC member.

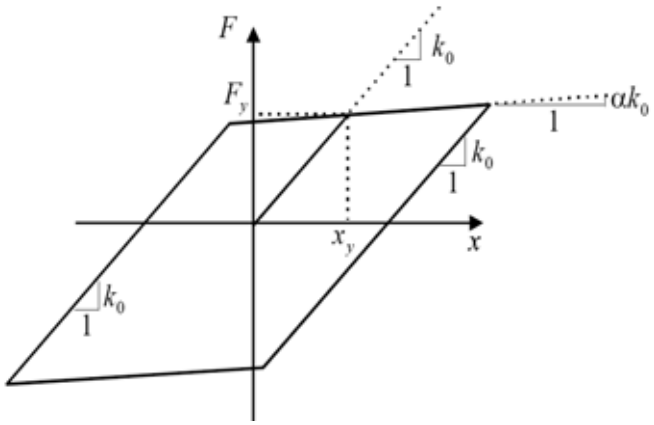

Figure 5.3 Elasto-plastic hysteresis of rubber bearing.

5.2.2.2 Non-linear static (pushover) analysis

The purpose of pushover analysis is to evaluate the expected performance of structural systems by estimating performance of a structural system by estimating its strength and deformation demands in design earthquakes by means of static inelastic analysis, and comparing these demands to available capacities at the performance levels of interest. The inelastic static pushover analysis can be viewed as a method for predicting seismic force and deformation demands, which accounts in an approximate manner for the redistribution of internal forces that no longer can be resisted within the elastic range of structural behavior.

5.2.2.3 Non-linear dynamic (time-history) analysis

In recent years, nonlinear bridge analysis has gained a greater momentum because of the need to assess inelastic structural behavior under seismic loads. Common seismic design

philosophies for ordinary bridges allow some degree of damage without collapse. To control and evaluate damage, a post elastic nonlinear analysis is required. A nonlinear analysis is complex and involves many simplifying assumptions. Engineers must be familiar with those complexities and assumptions to design bridges that are safe and economical (*Chen and Duan, 2003-3*).

In order to capture the essence of the nonlinear behavior, a relatively simple model is used to perform the nonlinear dynamic analysis. This appears quite appropriate in face of various types of approximations, randomness and uncertainty involved in specifying the input ground motion and the structural system. Following to *JRA-2002*, during the analysis of the seismic behavior of a bridge by dynamic method, thoughtful consideration should be made on the factors such as the natural vibration characteristics, damping characteristics and inelastic hysteretic property of the pier. It is necessary to adopt an analysis model being capable of expressing dynamic properties of the bridge in order to calculate the response values during an earthquake. The model used to describe the potentially nonlinear behavior of the piers of the bridges is depicted in **Fig 5.5**. According to this model, a pier is modeled as an elastic column, with a pair of plastic zones of length, L_p, at each end of the column. Each plastic zone is then modeled to consist of a nonlinear rotational spring and a rigid element of length, L_p.

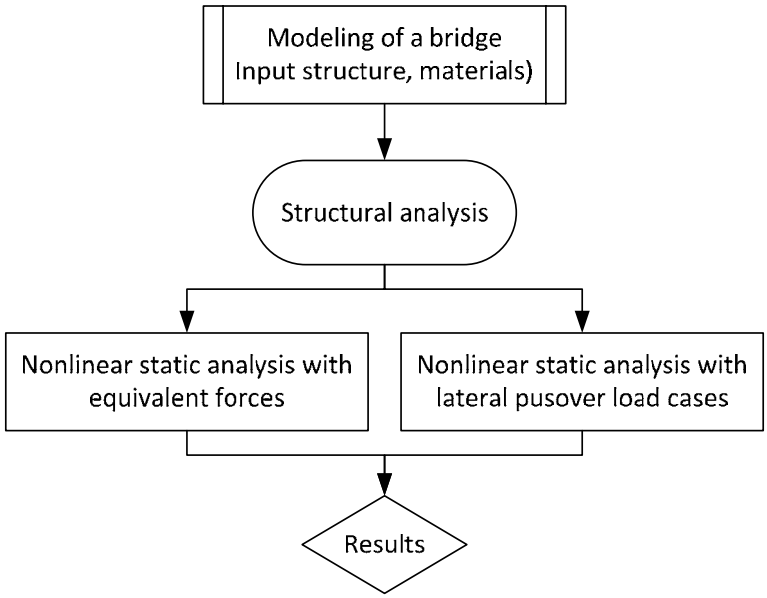

Figure 5.4 Pushover analysis flow chart.

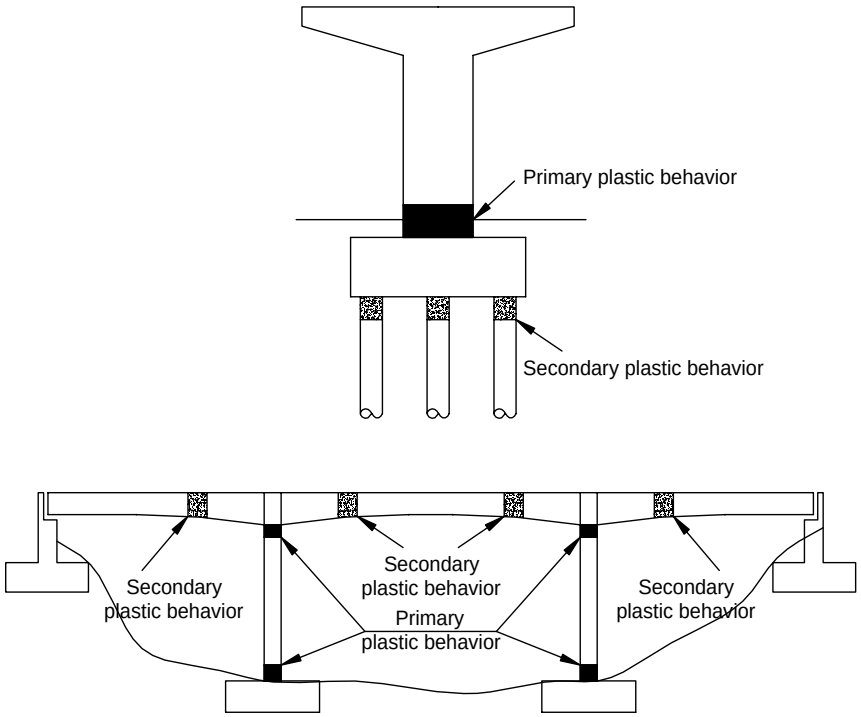

Figure 5.5 The members of bridge structure with consideration of plasticity or nonlinearity (required by *JRA-2002*).

The length of the plastic hinge is calculated according to *JRA-2002* by equation as follows:

$$L_p = 0.2h - 0.1D \tag{5.11a}$$

in which:

$$0.1D \leqq L_p \leqq 0.5D \tag{5.11b}$$

Where L_p is plastic hinge length, h is height of the column pier, and D is section depth.

Currently, the *LRFDSEIS-1 (2009)* uses a hinge property with the idealized bilinear moment-curvature diagram as shown in **Fig 5.6**. These effects are captured in the nonlinear hinge responses. The length of the plastic hinge also is calculated by equation:

$$L_p = 0.08L + 0.15 f_{ye} d_{bl} \geq 0.3 f_{ye} d_{bl} \tag{5.12}$$

Where L is length of column from point of maximum moment to the point of moment contra flexure (in.), f_{ye} is the effective yield strength of the longitudinal reinforcing (ksi), and d_{bl} is the diameter of the longitudinal reinforcing.

5.2.4 Remarks

This section has presented the basic principles and methods of dynamic analysis for the seismic design of a bridge in general and in *JRA-2002*. In *22TCN 272-05* concentrated primarily to response spectrum analysis (the SDOF) for ordinary bridge. Non-linear dynamic time-history analysis may be necessary for important and complex bridges. The response spectrum analysis and pushover analysis are using common for the most bridges and seismic codes in the world. For the time-history analysis, several direct integration schemes have been developed for solving the equations of motion. However, an approach of Newmark-β method is most widely used in the nonlinear dynamic analysis of structures because of its accuracy and stability. Therefore, it is adopted to solve the nonlinear equation of motions of bridge structure in this study.

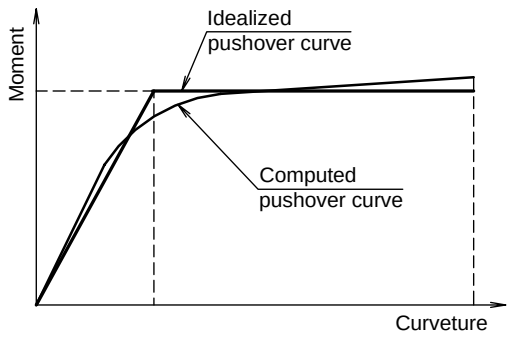

Figure 5.6 Idealized bilinear moment-curvature diagram.

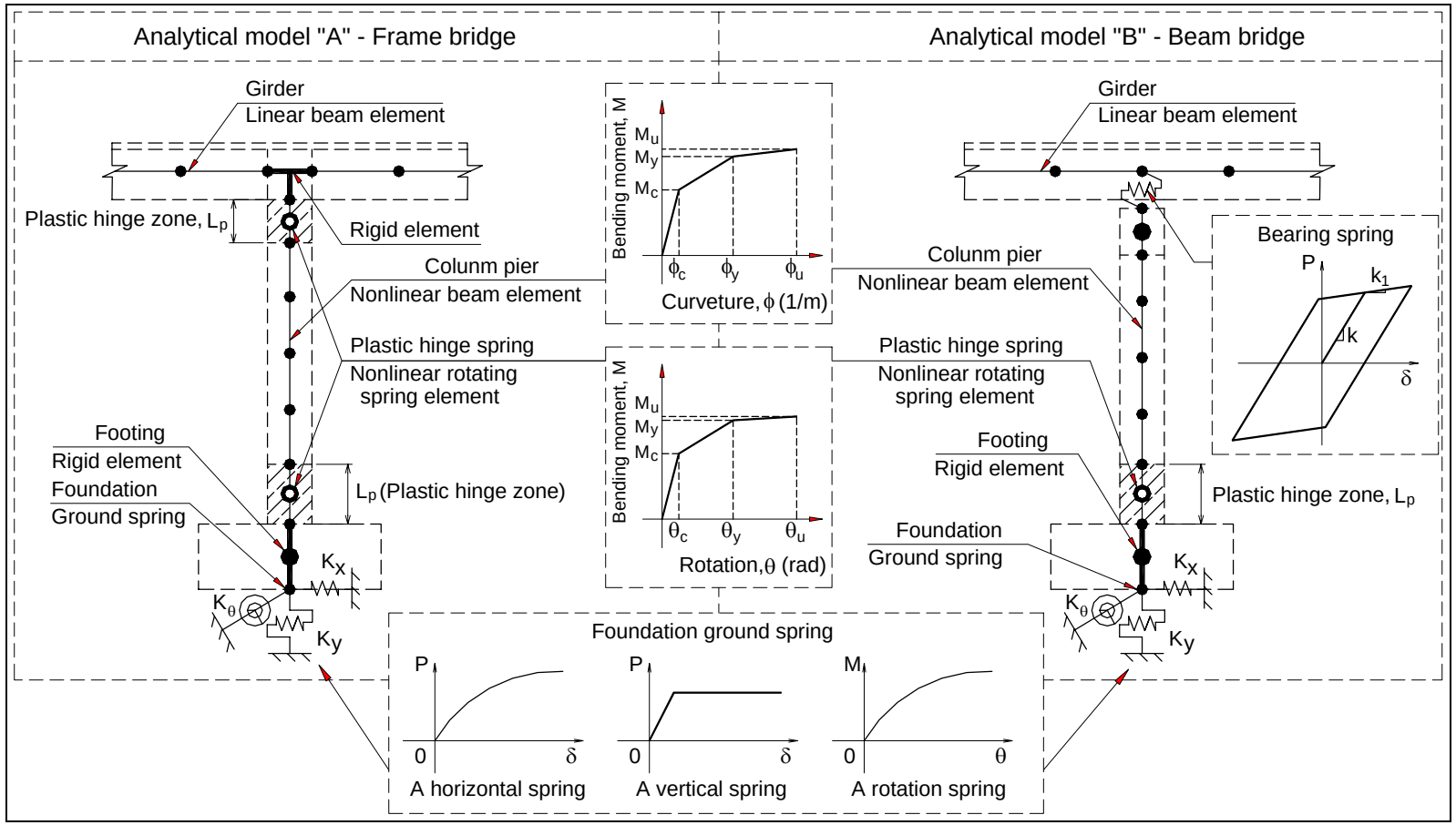

Figure 5.7 Analytical FEM modeling for bridge pier.

5.3 DYNAMIC RESPONSE ANALYSIS: AN EXAMPLE

5.3.1 Description of bridge

A multi-span continuous bridge in Vietnam was chosen for an example of dynamic response analysis in this study. The profile of this bridge was shown in **Fig 5.8**. This bridge was designed by static analysis method according to the *22TCN-272-01* (final version is *22TCN-272-05*). The superstructure is a hollow concrete slab beam structure with 8 continuous spans. The total length of the bridge is 250 m. The substructure system consists of 3 rigid frame piers (P2, P3, and P4) and 4 bent piers (P0, P1, P5 and P6). The compressive strength of the concrete of all piers is 30 MPa; the diameter of the spiral reinforcement is 16 mm; the diameter of the longitudinal reinforcement is 25 mm and 29 mm, spacing of the spiral is 300 mm and 125 mm for P0, P1, P5, P6 and P2, P3, P4, respectively. The rubber bearing supports (P0, P1, P5 and P6) are installed. The basic components of the rubber bearing are elastomeric and steel plates. All of the pier columns and the abutments are fabricated by reinforced concrete and the bored cast-in-place piles are driven under the footing as shown in **Fig 5.9**. The pier columns are all circular with spiral or circular lateral reinforcement as shown in **Fig 5.10**. The ground layer consists of medium sand, fine sand and gravelly sand. The thickness of the surface layer is about 40 m.

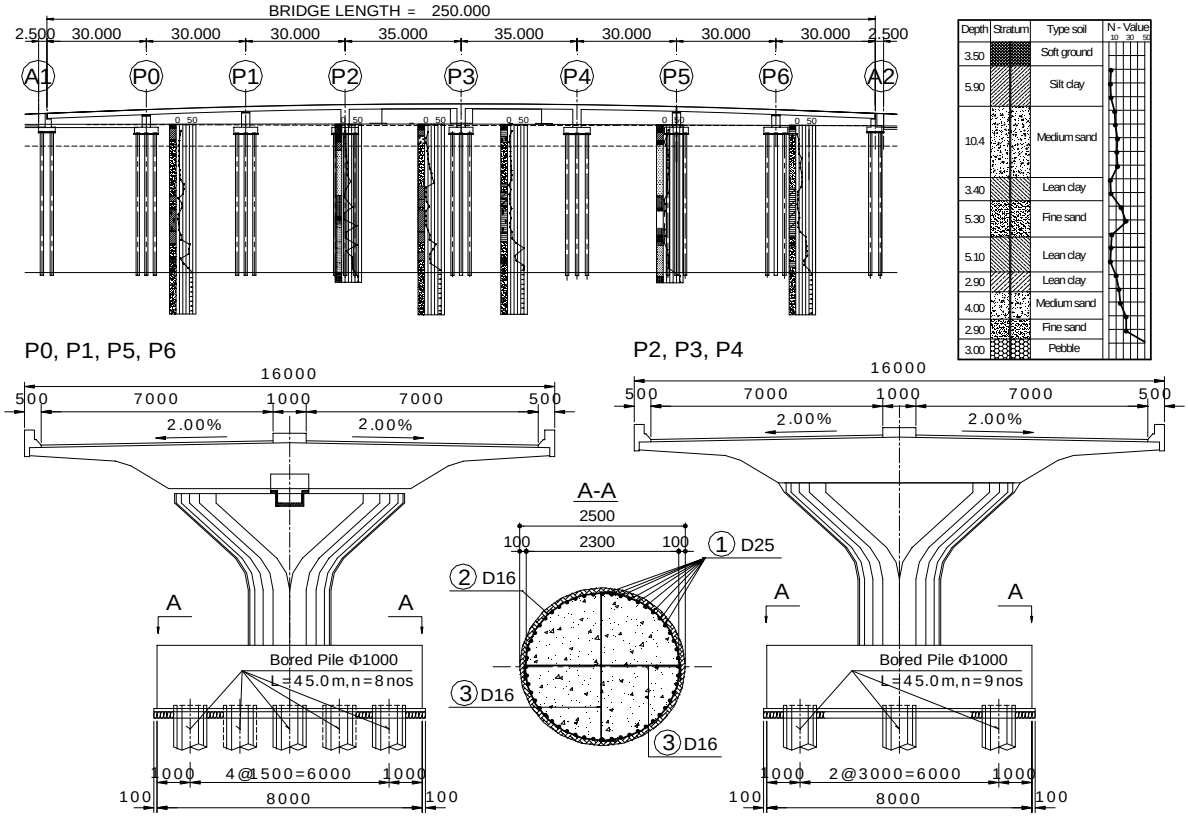

Figure 5.8 The profile of the highway bridge (*unit is mm*).

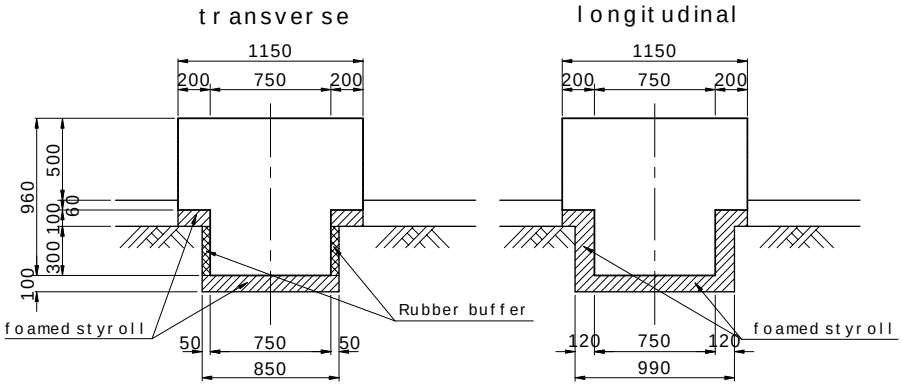

Figure 5.9 Concrete stopper (*unit is mm*).

5.3.2 Analysis procedure

The bridge is designed by the Vietnam design code by static analysis method. The stopper and rubber bearing are also installed to enhance the seismic performance. In this study, the requirements of dynamic response analysis are referred to *JRA-2002*. An analytical model of the bridge is made to estimate seismic performance of the bridge, especially bearing capacity of the members and unseating of the girders. The girders are replaced to linear beam elements. The pile foundation is replaced to the horizontal spring K_x, vertical spring K_y and rotating spring K_θ. The spring values are calculated by Forum 8 software and input into TDAPIII software. Nodal spring element is used to imitate the supported spring. This spring is set to the necessary DOFs of the node that are considered as the elastic suspension and can be added up to three. Element stiffness matrix of this element is given by **Eq. (5.13)** when each spring constant is k_{11}, k_{22} and k_{33} (*TDAP III's manual, 2008*).

$$k = \begin{vmatrix} k_{11} & k_{12} & k_{13} \\ & k_{22} & k_{23} \\ sym. & & k_{33} \end{vmatrix} \tag{5.13}$$

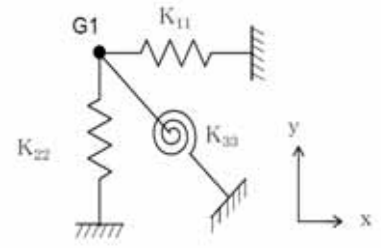

Figure 5.10 Directivity spring elements in TDAP III software.

Table 5.1 Ground type in seismic design (*JRA-2002*).

Ground Type	Characteristic value of ground, T_G(s)
Type I	$T_G < 0.2$
Type II	$0.2 \le T_G < 0.6$
Type III	$0.6 \le T_G$

Table 5.2 Characteristic value of the surface ground.

Soil layers	Thickness, h_i (m)	SPT (N-value)	γ_t (kN/m^3)	V_{si} (m/s)	$T_i = H_i/V_{si}$ (s)
Silt clay	5.9	3	17.4	138.67	0.04
Sand	10.4	10	16.0	218.28	0.05
Lean clay	3.4	3	18.3	135.72	0.03
Fine sand	5.3	21	16.8	273.69	0.02
Lean clay	5.1	3	16.5	144.22	0.04
Lean clay	2.9	12	19.7	228.94	0.01
Sand	4.0	20	16.8	271.44	0.01
Fine sand	2.9	24	16.8	288.45	0.01
Pebble	3.0	50	21.0	368.40	0.01
T_g = 0.82 (s) > 0.60 (s) → Type III ground according to *JRA-2002*.					

The concrete block as a stopper is installed at the top of the pier and replaced to a spring element considering the spacing. The rubber bearing is replaced to a bi-linear spring element in horizontal direction. The pier has circler cross section as shown in **Fig 5.8**. The dominate period of the surface ground is T_G = 0.82 s > 0.60 s i.e. ground type in **Table 5.2** is Type III ground following *JRA-2002*. The dynamic characteristic value of the surface ground is calculated as follow:

$$T_G = 4\sum_{1}^{n} \frac{H_i}{V_{si}} \tag{5.14a}$$

In which, T_G is characteristic value of ground (s), H_i is thickness of the i^{th} soil layer (m), V_{si} is average shear elastic wave velocity of the i^{th} soil layer (m/s). The ground types in seismic design shall be classified following to **Table 5.1**.

For cohesive soil layer:

$$V_{si} = 100N_i^{1/3} \qquad (1 \le N_i \le 25) \tag{5.14b}$$

For sandy soil layer:

$$V_{si} = 80N_i^{1/3} \qquad (1 \le N_i \le 50) \tag{5.14c}$$

Where T is the characteristic value of ground, V_{si} is the average shear elastic wave velocity

of the i^{th} soil layer. It is calculated by using the SPT (N-value) based on the characteristics of the soil layers.

The piers are designed with a compressive strength of concrete is 30MPa, the diameter of the spiral reinforcement is 16mm and spacing of the spiral is 300mm. The column of the pier is replaced to nonlinear beam elements. The nonlinear behavior of the columns is presented by the Takeda model with the potential plastic hinge zone located at bottom of the column. The Takeda hysteresis property is adopted for bending deformation of the pier. Relationship of M - ϕ and M - θ for piers are used for this analysis as shown in **Fig 5.11**.

The stress vs. strain relation of reinforcing bars is idealized by bi-linear model. In the pier column, a plastic hinge modeled by nonlinear rotating spring is arranged at the bottom column zone as shown in **Fig 5.12**. The length of the plastic hinge is calculated according to JRA-2002 as shown in **Eq. 5.11**.

The eigen-value is calculated by subspace method, and until the 30^{th} vibration mode is calculated. As an example, the results of the longitudinal direction are taken up to present. The principal natural modes of vibration and natural frequencies of the bridge of the calculation are shown in **Fig 5.13**. **Fig 5.14** shows the Rayleigh damping coefficients are calculated from the vibration frequencies of the structure. The commercial dynamic analysis program for civil engineering, entitled "Time domain 3-dimensional Dynamic Analysis Program - TDAP III software," is used for the analysis.

Table 5.3 Plastic hinge length of pier, L_p (m).

Pier	P0	P1	P2	P3	P4	P5	P6
h (m)	3.9	4.8	5.7	5.9	5.7	4.8	3.9
L_p m)	0.5	0.7	0.4	0.5	0.4	0.7	0.5

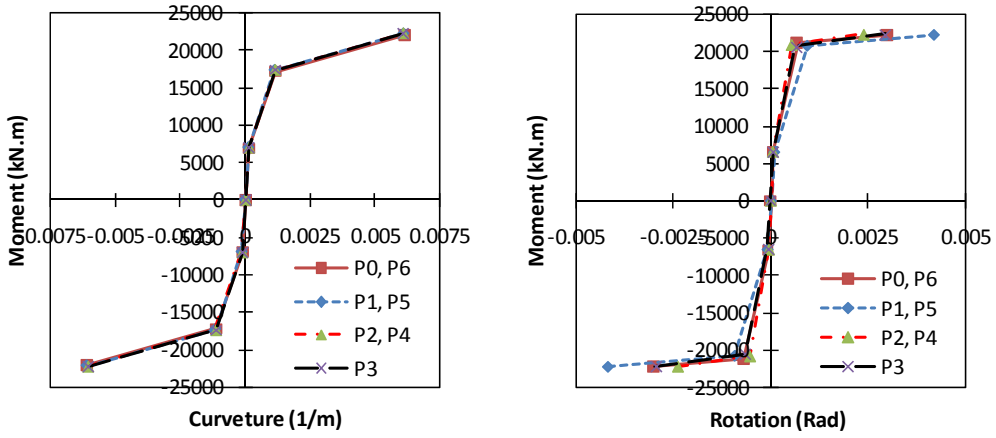

Figure 5.11 Analytical model of a bridge column pier (*left figure*) and plastic hinge spring (*right figure*).

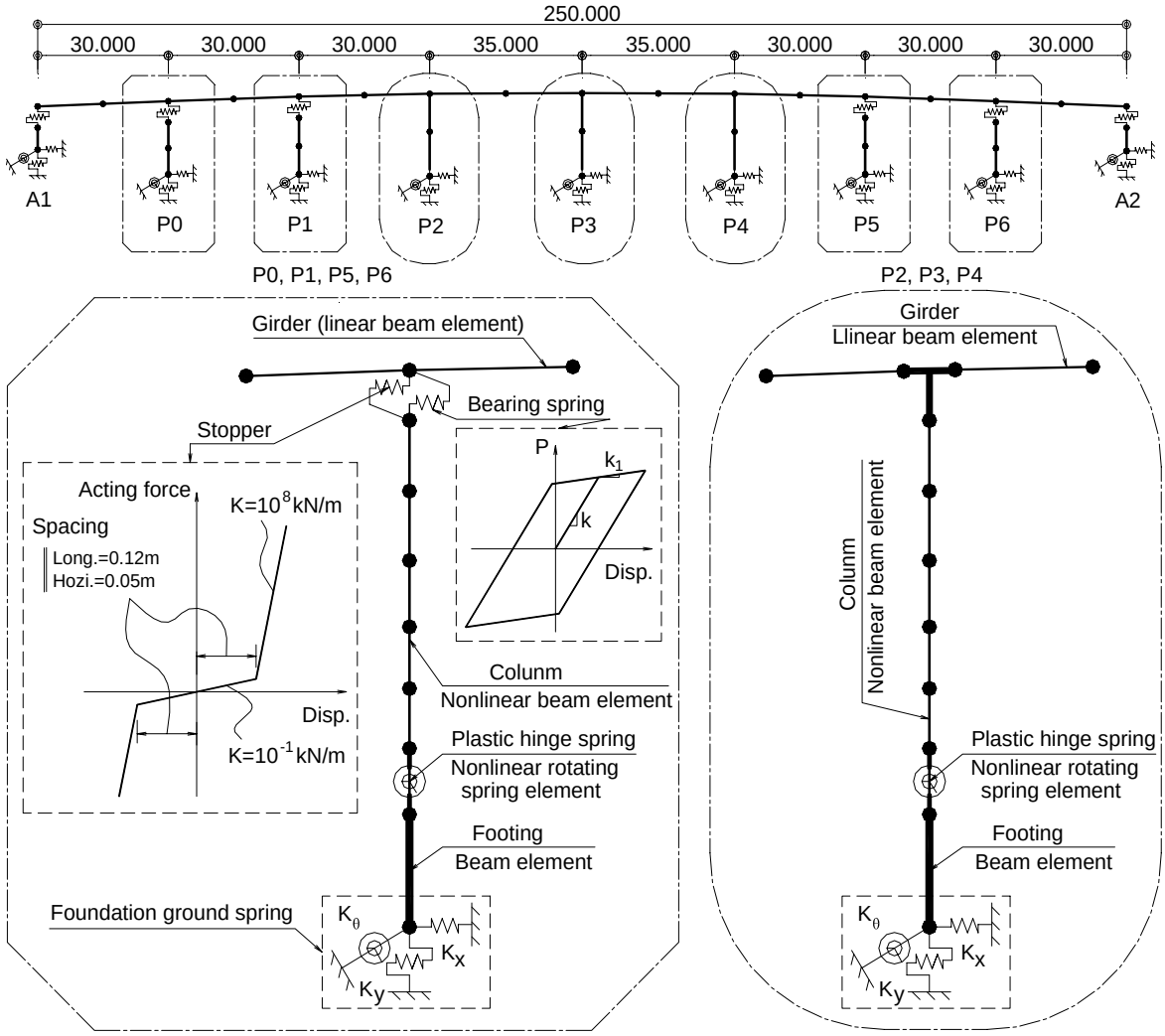

Figure 5.12 Analytical model for the whole bridge (*unit is* mm).

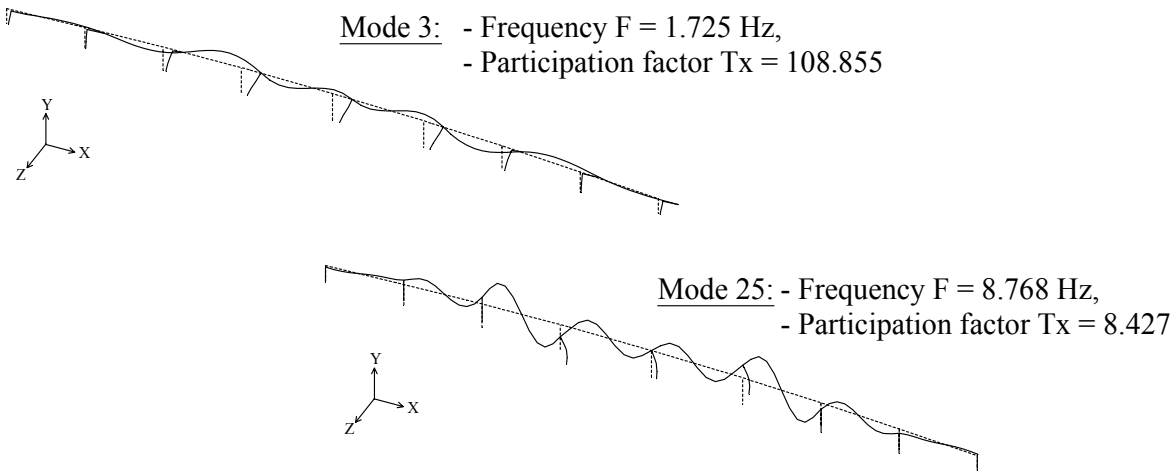

Figure 5.13 Natural modes.

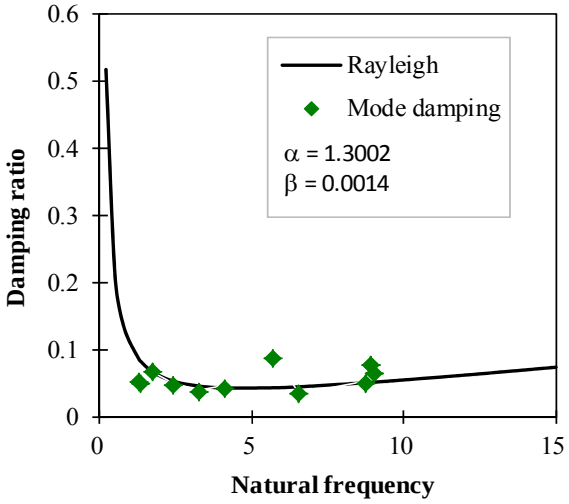

Figure 5.14 Mode damping.

5.3.3 Seismic response

5.3.3.1 Case study and input ground motions

Chapter 4 illustrated that Vietnam was classified to the moderate seismic zone, the maximum magnitude did not exceed a magnitude of 7.0 on the Richter scale. The author was predicted maximum ground motion in Vietnam based on stochastic method through a historical earthquake, observed earthquake records in Vietnam and comparison between prediction values of PSA and the current seismic codes such as *EC 8*, *LRFDSEIS-1*, *JRA-2002*, etc. The current specification of bridge design requires seismic analysis for bridge into 3 seismic zones with acceleration coefficients from 0.00 to 0.29 g. The peak ground acceleration of earthquake wave is 0.18 g and 0.32 g with a return period of 475 years and 2,500 years, respectively. These earthquake waves are adopted on the rock soil corresponds with the soil condition in the North of Vietnam. Thus, predicted ground motion in Vietnam with return period of 475 years (called as VNL1) and return period of 2,500 years (called as VNL2) are adopted as input waves at the ground level in this study as shown in **Figs 4.15** and **4.16**, respectively.

Stopper and non-stopper effect will be considered in this study because of this bridge is designed with stopper in the top of piers of P0, P1, P5 and P6, but most bridges are previously designed not arranged stoppers.

5.3.3.2 Dynamic response of the superstructure

Dynamic response analysis in this study is concentrated on the response displacement and acceleration, and verified by the results of the longitudinal direction. The time-history of the

response horizontal acceleration and displacement of the superstructure at the P3 has calculated by VNL1 and VNL2 waves are shown in **Figs 5.15** and **5.17**, respectively. The response accelerations and displacements with case of stopper at the top pier are smaller than that with case of non-stopper. These figures show the Fourier spectrum of the superstructure horizontal acceleration. It is shown that the vibration of the superstructure is dominated by one vibration mode with the frequency of 1.7 Hz. It is thought because the input wave predominates at short period.

5.3.3.3 Dynamic response of the piers

Figs 5.16 and **5.18** show the time-history of the response horizontal acceleration and displacement at the top of the pier P1. The top of this pier was arranged rubber bearing and stopper. These figures show the Fourier spectrum of the horizontal acceleration. Unlike the superstructure, the vibration of the pier is dominated by three vibration modes with the frequency of 1.75 Hz, 8.59 Hz and 10.15 Hz, and 1.71 Hz, 8.11 Hz and 8.64 Hz for the VNL1 and VNL2 input wave, respectively. However, like the superstructure, a prominent vibration mode of 1.7 Hz is also dominated by seismic input wave.

5.3.3.4 Elastic and plastic response

Figs 5.19 and **5.20** show the hysteristic response at the plastic hinge of the piers, including the rubber bearing is installed at the top of the pier P0, P1, P5 and P6, and rigid jointed between the pier and the girder at the pier P2, P3 and P4.

Comparison between the characteristics of the analytical model and the analytical results of dynamic response of the piers show that all piers are still within the yield strength state, no serious damage is evaluated for proposed ground motions, named VNL1 and VNL2 wave in Vietnam. Although this analysis shows plastic hinge cannot occur in this bridge with predicted ground acceleration in Vietnam. Assuming plastic hinging is possible for this bridge structure, cross section and reinforcement must be changed with the lower section, deflections can be expected to increase markedly.

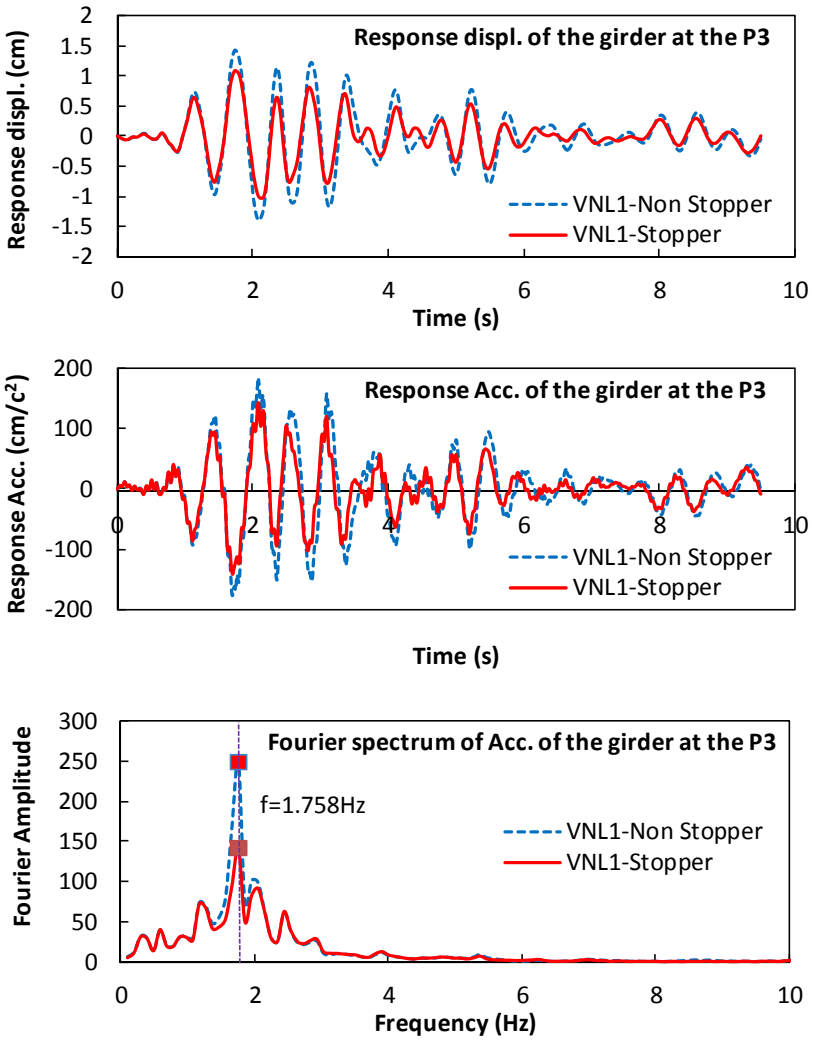

Figure 5.15 Response characteristic of the girder (VNL1 ground motion).

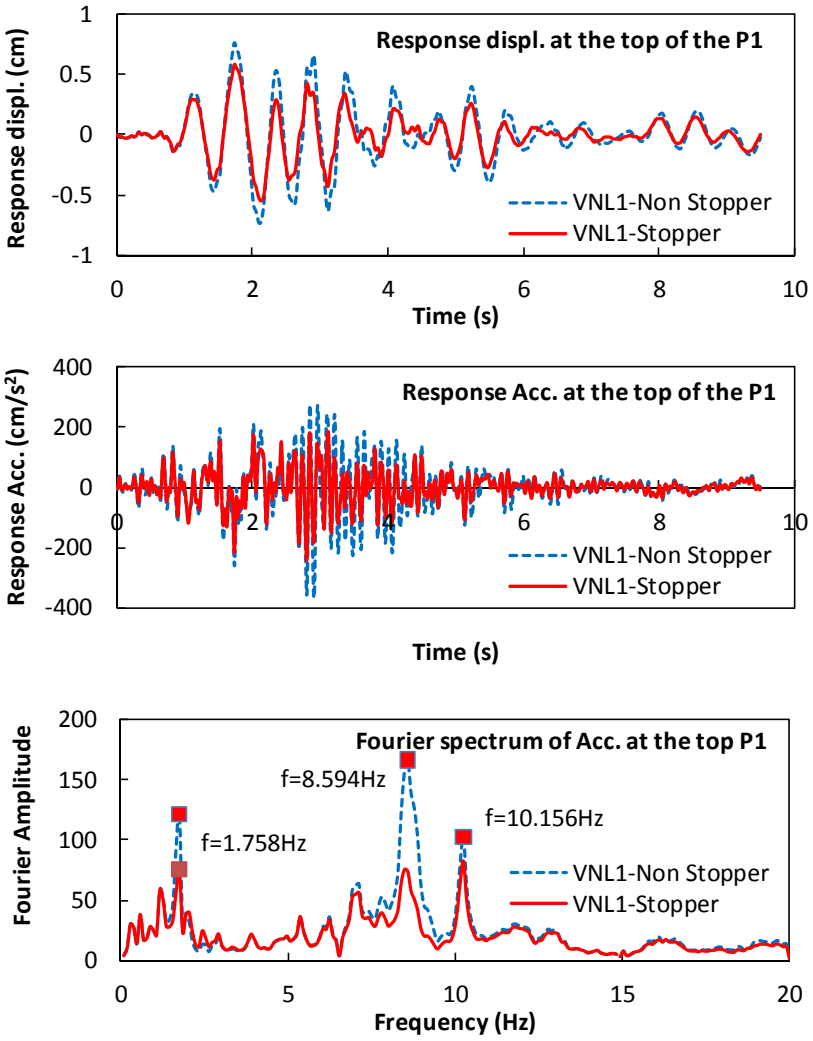

Figure 5.16 Response characteristic at the top of the pier (VNL1 ground motion).

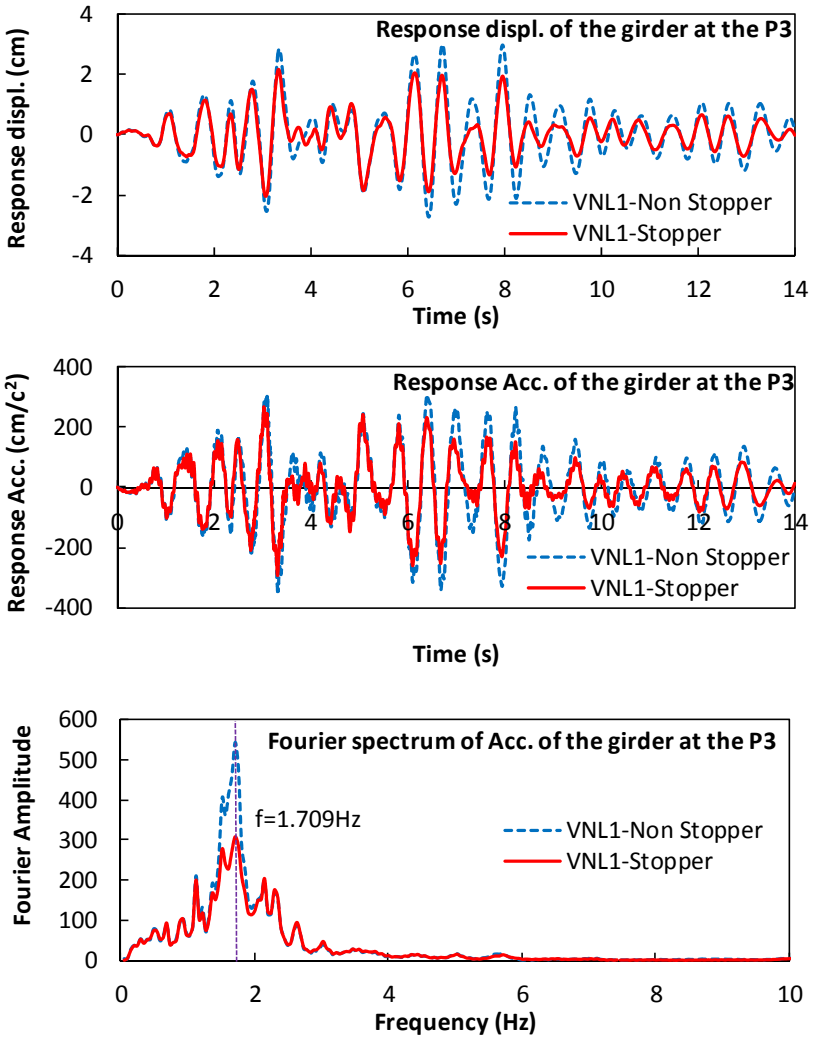

Figure 5.17 Response characteristic of the girder (VNL2 ground motion).

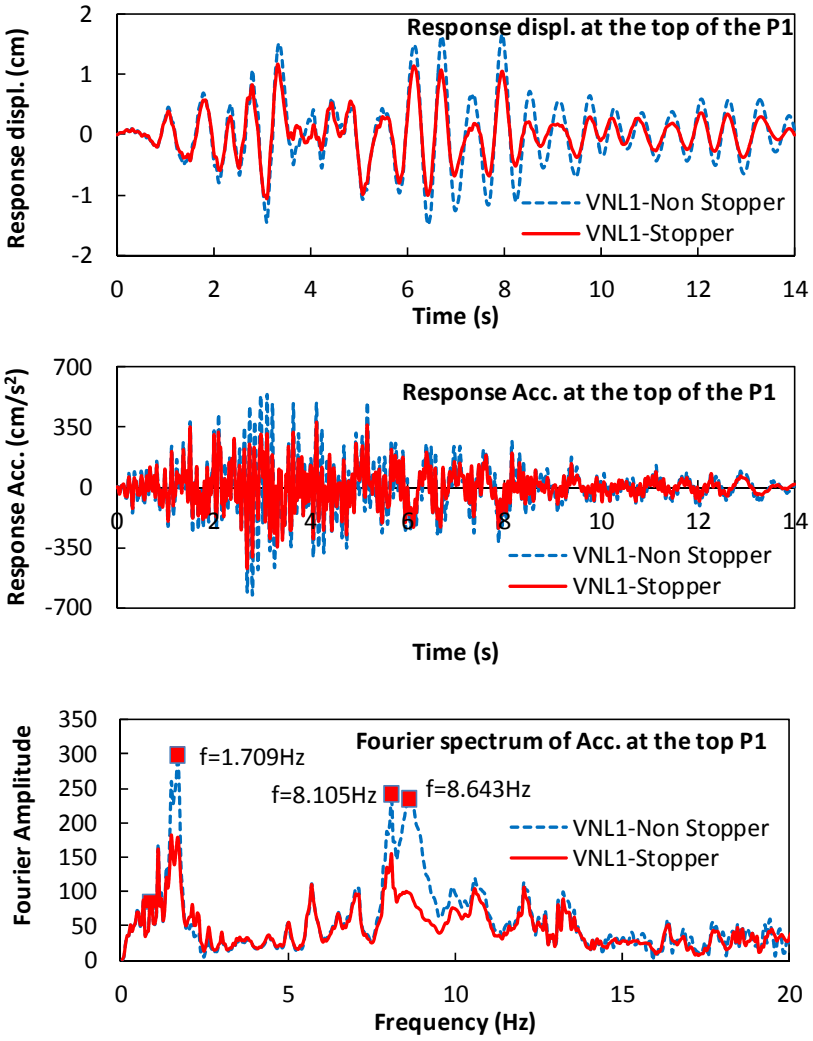

Figure 5.18 Response characteristic at the top of the pier (VNL2 ground motion).

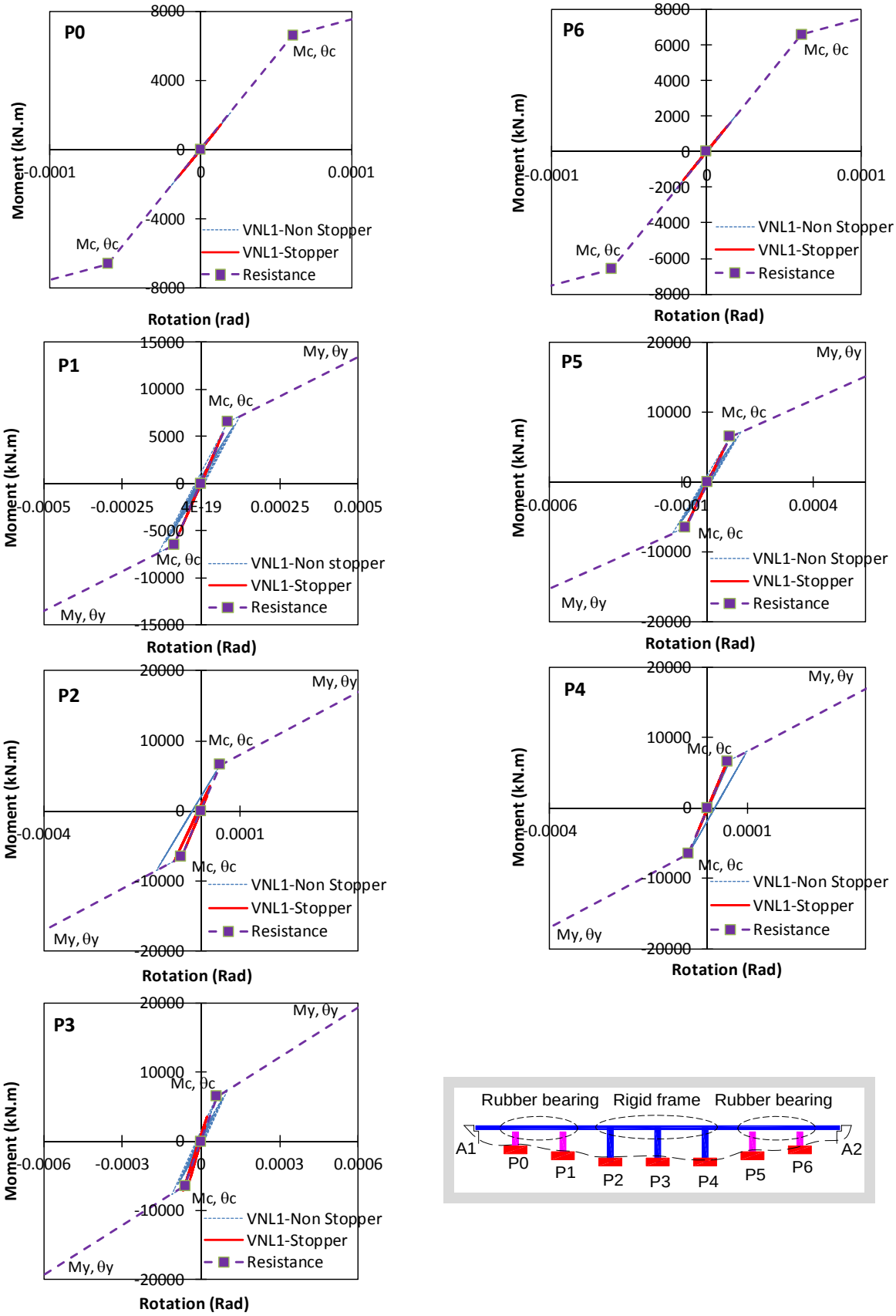

Figure 5.19 Hysteretic response of the piers at the plastic hinge with VNL1 wave in case of stopper and non-stopper.

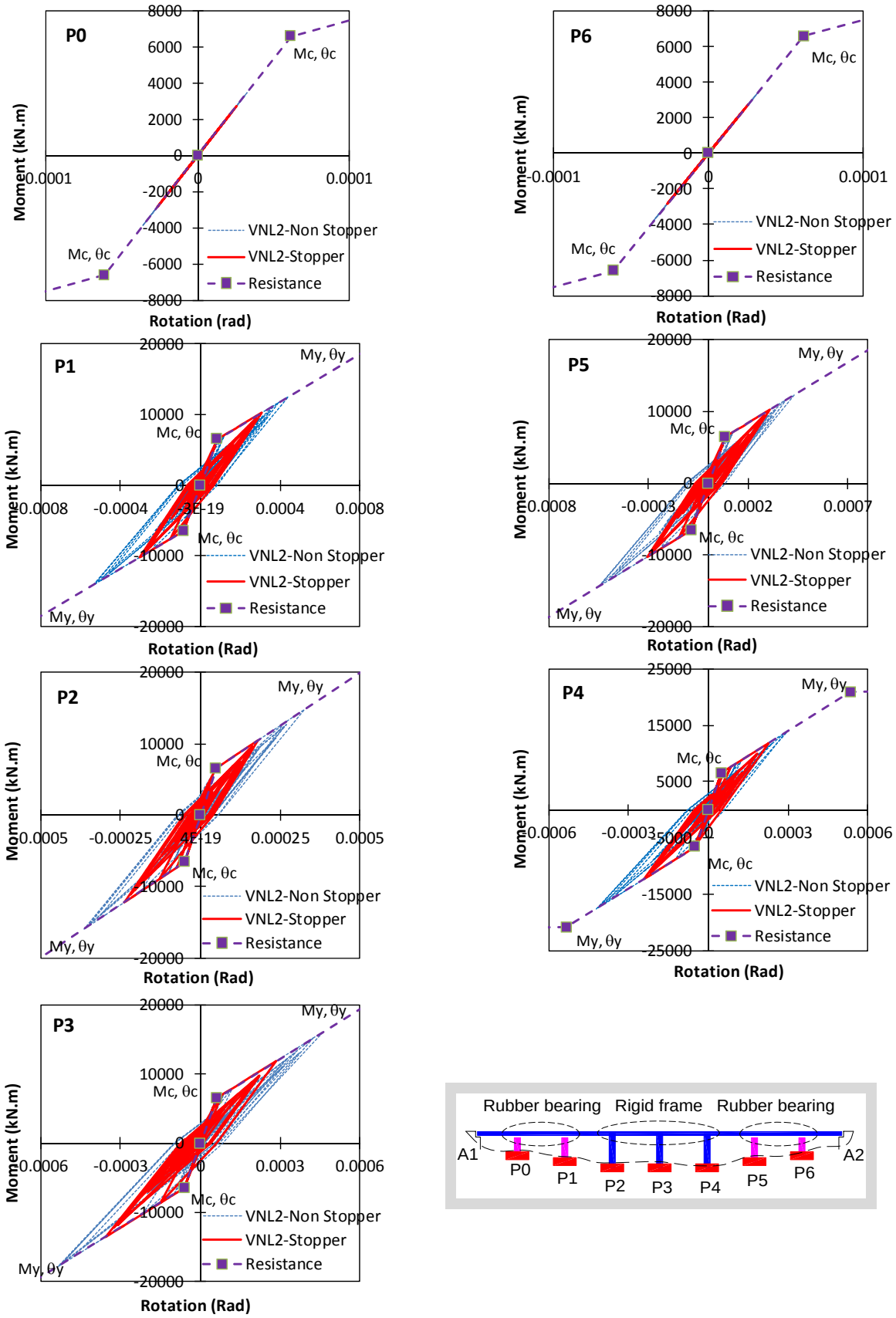

Figure 5.20 Hysteretic response of the piers at the plastic hinge with VNL2 wave in case of stopper and non-stopper.

5.4 CONSIDERATION

The dynamic response of this structure is evaluated in terms of response acceleration, response displacement of the superstructure. Moment distribution in the piers and plastic hinge according to predicted acceleration wave in Vietnam (VNL1 and VNL2 waves).

This bridge structure is determined to be no damage that occurs during earthquakes in both the predicted acceleration wave in Vietnam (VNL1 and VNL2 waves). The bearing capacity of the piers is still within the elastic limit state with both VNL1 and VNL2 waves.

The seismic performance of the bridge designed by the current Vietnam code can be verified by the proposed waves, i.e. the proposed earthquake waves are useful for the seismic design of the bridge in Vietnam. Thus, this typical bridge is also secured from the current earthquake occurring in Vietnam. However, the results calculated by the dynamic method may be different depending on the engineer's choice for boundary conditions even though the same analytical model.

Dynamic response analysis of highway bridges is very complex. Current specification for highway bridge (*22TCN 272-05*) in Vietnam requires that an elastic analysis be performed to estimate design forces within design displacements and seating length. This indicates that the application of hysteristic models to predict the appearance of plasticity in the bridge structure show clearly the ability to appear plastic hinge under earthquake occur such as Takeda model is used in this study.

A plastic zone and plastic hinge should be conducted clearly in Vietnam code like they have been adopted in the current seismic codes such as performance-based seismic design belong to specification for highway bridge in Japan (*JRA-2002*) and guide specifications for LRFD seismic bridge design in the United States (*LRFDSEIS-1, 2009*).

The analysis results in this chapter show the addition of provisions on the dynamic analysis of the current specification for bridge design in Vietnam is very important in determining the dynamic response of bridge structure under earthquake effect through time-history dynamic response analysis. Example of using the predicted seismic waves, the calculation results show the behavior of the bridge within the elastic limit state. That is the main design goals of current standards to ensure safety and service life of the bridge.

5.5 REFERENCES

[1]. 22TCN 272-05, *Specification for Bridge Design*, Ministry of Transport of Vietnam, 2005.

[2]. AASHTO, *Load and resistance factor design (LRFD) specifications for highway bridges*, Washington (DC): American Association of State Highway and Transportation Officials (AASHTO), 1998.

[3]. JRA-2002, *Specification for Japanese Highway Bridges, part V: seismic design*, Japan Road Association, 2002.
[4]. TDAPIII's manual (2008), Theoretical Manual - Version 3.01, Ark Information Systems, Inc.
[5]. Chen, W.F. and Duan, L. (2003-3), "Bridge Engineering", Seismic Design, *Chapter 3. Dynamic Analysis* (R. Bavirisetty and M.Vinayagamoorthy and L. Duan), CRC Press 2003.
[6]. Chen, W.F. and Duan, L. (2003-4), "Bridge Engineering", Seismic Design, *Chapter 4. Nonlinear Analysis of Bridge Structures* (M. Akkari and L. Duan), CRC Press 2003.
[7]. Chen, Y. F. (2004). *Assessment of the current US seismic displacement requirements for bridges in a low-moderate seismic zone*, Engineering Structures, Vol 26, pp. 1365–1379.
[8]. Clough, R.W. and Penzien, J. (2003), *Dynamics of Structures*, Third Edition, Computers & Structures, Inc.
[9]. Hung, T.V., Kiyomiya, O. and An, T.X. (2009). *Assessment of seismic design for bridge in Vietnam – a low moderate seismic zone*, Proceedings of the 30th JSCE Earthquake Engineering Symposium, Japan, Vol. 30, 5/2009.
[10]. Lee, D.H., Choi, E. and Zic, G. (2005). *Evaluation of earthquake deformation and performance for RC bridge piers*, Engineering Structures, Vol. 27, pp. 1451-1464.

This page intentionally left blank

CHAPTER 6

CONCLUSIONS

6.1 SUMMARY AND CONCLUSIONS

In this dissertation, seismic waves and design response spectrum are proposed and discussed based on historical earthquake events and observed earthquakes records in Vietnam. The research work on verification of dynamic response analysis for bridge design has been carried out in this study. The study undertaken has revealed that some further development may be necessary and of interest for seismic design in Vietnam. Dynamic analysis of the bridge is used commonly, which described in **Chapter 1**. The discussion has focused to complement the requirements of the analytical model for time-history dynamic method; **Chapter 1** also reviewed the Vietnam specification for seismic bridge design (*22TCN 272-05*). A comparative study of them with other seismic codes such as *JRA-2002*, *EC 8*, *LRFDSEIS-1 (2009)* has been performed in this chapter.

Chapter 2 shows earthquakes occurred in Vietnam have short duration and period based on observed earthquake's records. **Chapter 3** presented a new attenuation relationship. The data based includes earthquake records in Vietnam, Yunnan and Japan. The selection of this database is limited in the moderate earthquake magnitudes, strike-slip faults and shallow inland earthquakes. This relationship is recommended to use for probabilistic seismic hazard analysis in Vietnam.

Chapter 4 analyzed seismic hazard and presented the maximum peak ground acceleration following to various return periods. This chapter also proposed two-level earthquake ground motions and a new form of the response acceleration spectrum. They are recommended in order to seismic analysis for structure in Vietnam. These are based on the stochastic ground motion prediction model. The study was described in this chapter focuses on stochastic modeling and simulation of ground motion time-histories for dynamic analysis. This employ is performed base on classification of seismic performance (Level 1 and Level 2 earthquake ground motions) in the Japanese specification for highway bridge - Part V: seismic design (*JRA-2002*). In previous studies of earthquakes in Vietnam, those studies, mainly on predicting the magnitude scales and the peak ground acceleration (PGA) for applying into the seismic design for bridge through response spectra acceleration according to foreign

standards such as *AASHTO LRFD 1998* and *EC 8*, but no research on predicting time-histories. The response spectral acceleration and seismic waveforms are proposed in this thesis. The proposed seismic levels are VNL1 and VNL2 corresponding to earthquake of a return period 475 and highest earthquake events (M = 7) with high and low probability of occurrence for the bridge life, respectively. Finally, to understand clearly dynamic analysis method for a bridge, a typical bridge was constructed in Vietnam and calculated by the static method is also verified and discussed with proposed ground motion as shown in **Chapter 5**.

Based on the results of this study, the following conclusions can be made:

6.1.1 Earthquake occurrence rate

This dissertation has summarized many seismic records of historical earthquake events in Vietnam based on previous studies earthquake of the Vietnamese and foreign scientists. After that, the annual earthquake occurrence rates of potential seismic source areas are determined. This rating also shown that Vietnam lies in a low moderate seismicity region.

6.1.2 The new attenuation relationship of earthquake ground motion

The new relation is developed for shallow strike-slip earthquake by a regression technique with the range of magnitudes of $3.0 \leq M_w \leq 6.9$ and source distances up to 300 km. In this relationship, V_{s30} is adopted to estimate of ground motion with linear site effects as shown in **Eq. 3.10**. The PGA values in new attenuation relation in place of old one can be used for earthquake resistant design of various infrastructures in Vietnam.

6.1.3 Ground motion prediction

This study intends to predict earthquake ground motions in Vietnam because of only very few strong ground motion records are available. It was found that Boore's stochastic model can best predict strong ground motions on rock site in the North of Vietnam.

A stochastic model comprising the source factor and various path and local factors characterizing different amplification and attenuation mechanisms has been constructed in Vietnam. This model can be used to simulate artificial ground motions. The simulation requires little more than the generation of standard normal random variables, their multiplication with deterministic time functions, and post-processing through a high-pass filter. Regarding to predicted ground motions, it can generate a library of simulated motions with specified earthquake and site characteristics for use in performance-based earthquake

engineering analysis. These results of predicted time-histories waves can be used for non-linear dynamic analysis to future editions of seismic code in Vietnam.

The stochastic model is a widely used tool to simulate acceleration time series and develop ground motion prediction equations. The stochastic method begins with the specification of the Fourier spectrum of ground motion as a function of magnitude and distance. An overview of the method is presented in this study. Only horizontal component of earthquake motion is generated and the stochastic source model is based on-field observations of the site condition such as shear waves, and the most important source parameter for the simulations is the stress parameter, which controls the spectral amplitudes at high frequencies.

Besides, earthquake ground motions in Vietnam have been predicted by the extreme value distribution based on Weibull distribution theory. The results of simulated ground motion are selected corresponding with the prediction of ground motion.

This research benefits the field of performance-based earthquake engineering by providing synthetic ground motions for specified design scenarios that have characteristics similar to those of real earthquake ground motions.

Two main objectives proposed are fulfilled:

(1) Response spectra acceleration,

(2) Time-history waves for dynamic analysis.

The major developments and findings of this study are summarized as follows:

6.1.3.1 Proposed response spectra acceleration

The response spectra accelerations for rock sites are generated with earthquake of occurrence based on the historical earthquake parameters and observed earthquake records. The skeleton pattern of the response spectrum is to be compared with other seismic codes, and consistent with the earthquake level in Vietnam.

The proposed response spectra obtained on a rock site from this simulation show maximum of response spectra acceleration is ranging of a short period from 0.07 sec. to 0.35 and 0.08 sec. to 0.4 sec for VNL1 and VNL2, respectively. For structures with periods greater than T_S (0.35 sec. for VNL1 and 0.4 sec. for VNL2), the far-field earthquakes will govern the design. For shorter structural periods (less than T_S), the near-field earthquakes should be considered in seismic design.

6.1.3.2 Proposed time-history waves for dynamic analysis

Acceleration time-histories wave obtained by simulating the stochastic model are high-pass filtered. The selected filter is a critically damped oscillator. The oscillator frequency determines the level of high-pass filtering and helps to avoid overestimation of a simulated response spectrum ordinate at long periods.

For a given design scenario with known earthquake and site characteristics, the predictive equations are employed to simulate realizations of the model parameters. Inputting each set of parameter realizations into the stochastic model results in an ensemble of synthetic ground motions that can be used in place of or in conjunction with recorded ground motions.

The earthquake ground motions are simulated by stochastic model according to investigation results on the active faults and earthquake parameters. Based on Japanese code (*JRA-2002*), two levels of earthquake performance also proposed with a return period of 475 and the highest earthquake events (M = 7) corresponding to high and low probability of occurrence in Vietnam, respectively. Two earthquake levels may be more suitable for seismic design according to the design conditions, seismic performances and economic requirements of the projects.

The predicted peak ground acceleration of earthquake wave is 0.18 g and 0.32 g with a return period of 475 years and the highest earthquake events (M = 7), respectively. These earthquake waves are adopted on the rock soil corresponds with the site condition in the North of Vietnam where earthquakes occurred with high intensity and magnitude of large-scale.

6.1.4 Verification of seismic response by dynamic analysis

Methods used for design earthquake ground motions include time-history wave method and response spectra acceleration method. Current specification for highway bridge (*22TCN 272-05*) in Vietnam requires that an elastic analysis be performed to estimate design forces within design displacements. The response spectra acceleration methods were fully presented in *22TCN 272-05*. Dynamic response analysis of highway bridges is very complex. The dynamic time-history analysis method is a common use in a recent year but not yet is verified in *22TCN 272-05* even though dynamic analysis is very importance while the earthquake occurs. The bridge structure should be analyzed by the dynamic method, especially for long-span bridges and complex structures because large-scale earthquakes may occur suddenly and difficulty in early warning of earthquakes.

This study indicates that the application of hysteretic models to predict the appearance of plasticity in the bridge structure show clearly the ability to appear plastic hinge under earthquake occur such as Takeda model is used in this study. An analytical model can be applied in bridge design software are widely used in Vietnam now. In order to evaluate a bearing capacity of a bridge in Vietnam, the existing PC Bridge has been analyzed with proposed seismic waves based on a simple analytical model consistent with applying a material non-linear. The good results obtained in this analysis shown that proposed time-histories can be used to verify seismic design by a dynamic method in Vietnam such as plasticity of pier and unseating length of a girder.

6.2 LIMITATIONS AND FUTURE RESEARCH

The research presented in this dissertation is based on a number of limiting assumptions, limited data and a limited scope. Some of the relevant research areas that should be performed in the future are discussed in the following sub-sections.

This study considered only and predicted seismic ground motion with a rock site conditions. The other soils have not considered in this study. The great limitation of study is research data because earthquake occurrence in Vietnam is low frequency and measurement of seismograph station by digital instruments is arranged within 20 years.

The structural response goes into a non-linear inelastic range, and linear dynamic based methods are likely to give poor response estimates. Thus, non-linear time-history analyses of the structural response may be necessary studied.

When a bridge is designed on an unstable ground such as across a fault, near-fault zone on a lateral spreading ground due to liquefaction, etc., it is necessary to consider the interaction between the ground and the foundation structure.

Further, a performance-based design concept is used for the purpose to respond to the international harmonization of design codes and the flexible employment of new structures and new construction methods.

These are essential issues for further research, and it is related to the performance objectives.

The great limitation of study is the database of earthquake events because strong earthquakes occur with low frequency in Vietnam. Moreover, bridges are designed on an unstable ground such as across a fault, near-fault zone on a lateral spreading ground due to liquefaction, etc. It is necessary to research on ground motion within these conditions and to consider the interaction between the ground and the foundation structure. These are essential issues for further research.

List of research achievements

List of research achievements (1/2)

種類別 (By Type)	題名、　発表・発行掲載誌名、　発表・発行年月、　連名者（申請者含む） (theme, journal name, date & year of publication, name of authors inc. yourself)
Paper	
○1	Ground motion attenuation relationship for shallow strike-slip earthquakes in northern Vietnam based on strong motion records from Japan, Vietnam and adjacent regions. *Journal of JSCE, Division A: Structural Engineering/Earthquake Engineering & Applied Mechanics*, 2012. *TRAN Viet Hung* . Osamu KIYOMIYA (Accepted, In Press).
○2	Evaluation of seismic behavior of a high pier bridge for 2011 Tohoku earthquake. *Proceedings of the 2011 World Congress on Advances in Structural Engineering and Mechanics (ASEM11+)*, Seoul, South Korea, pp. 4384-4397, Sep. 2011. *TRAN Viet Hung*. Osamu KIYOMIYA . Tongxiang AN (In CD Rom).
○3	Nonlinear dynamic analysis of soil-steel pipe pile sheet-structure interaction under seismic excitation. *Proceedings of the 35th International Symposium on Bridge and Structural Engineering, jointly organized by IABSE-IASS*, London, UK, Sep. 2011. Tongxiang AN . Osamu KIYOMIYA . *TRAN Viet Hung* . Ryosuke KOCHI (In CD Rom).
○4	Effect of earthquake-proof reinforcement by ground anchor and damper on an existing bridge with high pier. *Proceedings of the 9th U.S. National and 10th Canadian Conference on Earthquake Engineering (9USN/10CCEE)*, Toronto, Canada, pp. 489-495, Jul. 2010. Tongxiang AN. Osamu KIYOMIYA . *TRAN Viet Hung* (In CD Rom).
○5	Seismic response of the steel pipe pile foundation in the soft ground and the liquefiable soil. *Proceedings of the Joint IABSE-fib Conference*, Dubrovnik, Croatia, pp. 831-838, May 2010. *TRAN Viet Hung* . Osamu KIYOMIYA . Tongxiang AN.
○6	Seismic resistance assessment of multi-span continuous bridge in Vietnam by dynamic response analysis. *Proceedings of the 33rd International Association for Bridge and Structural Engineering (IABSE) Symposium*, Thailand, Sep. 2009. *TRAN Viet Hung* . Osamu KIYOMIYA . Tongxiang AN (In CD Rom).
○7	Evaluation of seismic resistance for PC continuous bridge by dynamic response analysis in Japan specifications, JRA-2002. *Journal of Bridge and Road Engineering*, Vietnam, Vol. 4, pp. 18-24, Apr. 2009. *TRAN Viet Hung* . Osamu KIYOMIYA . Tongxiang AN (in Vietnamese).
○8	Evaluation of seismic resistance for a multi-spans bridge in Vietnam by investigation of earthquake activity and dynamic response analysis. *Journal of Structural Engineering. A (JSCE)*, Vol.55A, pp. 537-549, Mar. 2009. *TRAN Viet Hung* . Osamu KIYOMIYA . Tongxiang AN.

List of research achievements (2/2)

種類別 (By Type)	題名、　発表・発行掲載誌名、　発表・発行年月、　連名者（申請者含む） (theme, journal name, date & year of publication, name of authors inc. yourself)
Others	
○1	Proposal on attenuation relationship for peak horizontal acceleration of inland earthquakes in northern Vietnam region. *Proceedings of the 66 Annual Meeting of JSCE*, Ehime, Japan, I-460, Sep. 2011. *TRAN Viet Hung* . Osamu KIYOMIYA (In CD Rom).
○2	Stochastic ground motion prediction in the north of Vietnam region. *Proceedings of the 65 Annual Meeting of JSCE*, Hokkaido, Japan, I-337, Sep. 2010. *TRAN Viet Hung* . Osamu KIYOMIYA (In CD Rom).
○3	Evaluation of seismic response for RC bridge pier in Vietnam, a low moderate seismic zone. *Proceedings of the 64 Annual Meeting of JSCE*, Fukuoka, Japan, pp. 79-80, Sep. 2009. *TRAN Viet Hung* . Osamu KIYOMIYA . Tongxiang AN. (In CD Rom).
○4	Assessment of seismic design for bridge in Vietnam – a low moderate seismic zone. *Proceedings of the 30th JSCE Earthquake Engineering Symposium*, Japan, Vol. 30, May 2009. *TRAN Viet Hung* . Osamu KIYOMIYA . Tongxiang AN (In CR Rom).
○5	Evaluation on seismic resistance of existing bridge in Vietnam by dynamic response analysis. *Proceedings of the 63 Annual Meeting of JSCE*, Sendai, Japan, pp.219-220, Sep. 2008. *TRAN Viet Hung* . Osamu KIYOMIYA . Tongxiang AN (In CD Rom).
○6	Evaluation on seismic resistance of existing bridge in Vietnam by dynamic response analysis. *Proceedings of the 35 Conference of JSCE*, Kanto Branch, No. 137, Mar. 2008. *TRAN Viet Hung* . Osamu KIYOMIYA . Tongxiang AN (In CD Rom).